



Dong, Li (2021) *hDlg controls the trafficking of gap junction protein Cx43 in normal keratinocytes and human papillomavirus-positive tumour cells*.  
PhD thesis.

<http://theses.gla.ac.uk/82160/>

Copyright and moral rights for this work are retained by the author

A copy can be downloaded for personal non-commercial research or study,  
without prior permission or charge

This work cannot be reproduced or quoted extensively from without first  
obtaining permission in writing from the author

The content must not be changed in any way or sold commercially in any  
format or medium without the formal permission of the author

When referring to this work, full bibliographic details including the author,  
title, awarding institution and date of the thesis must be given

Enlighten: Theses  
<https://theses.gla.ac.uk/>  
[research-enlighten@glasgow.ac.uk](mailto:research-enlighten@glasgow.ac.uk)



University of Glasgow | College of Medical,  
Veterinary & Life Sciences

**hDlg controls the trafficking of gap junction  
protein Cx43 in normal keratinocytes and human  
papillomavirus-positive tumour cells**

Li Dong

BSc, MSc

Submitted in the fulfilment of the requirements for the Degree  
of Doctor of Philosophy

MRC-Centre for Virus Research

Institute of Infection, Immunity and Inflammation

College of Medical, Veterinary & Life Sciences

University of Glasgow

January 2021

## Abstract

Gap junction intercellular channels allow the exchange of ions and small molecules between neighbouring cells. Our laboratory showed previously that tumour suppressor protein and cell polarity regulator hDlg (human homologue of *Drosophila* Discs Large) binds to the wide-spread gap junction protein Connexin 43 (Cx43) in human papillomavirus (HPV) - positive cervical tumour cells. Cx43 relocated together with hDlg to the cytoplasm of these cells, and hDlg knockdown resulted in some Cx43 reappearing on the plasma membrane. This led to our hypothesis that hDlg could control Cx43 trafficking. High-risk HPV oncoprotein E6 via its PDZ-binding domain targets hDlg for proteasome degradation. Previously, co-immunoprecipitation indicated Cx43 binds to hDlg *in vitro* in cervical tumour cell lines and proximity ligation assays indicated their interaction *in vivo* in cervical epithelial tissue from high-grade cervical lesions. Moreover, our protein-protein interaction data indicated that HPV E6 oncoprotein took part in the hDlg/Cx43 interaction. Cx43 and hDlg were observed on the plasma membrane in non-transformed cervical tumour cells (W12G, low level of HPVE6) but appeared in the cytoplasm in fully transformed cervical tumour cells W12GPXY (high level of HPVE6). C33a cells (HPV-negative cervical tumour cells with membranous Cx43) transfected with mutated HPVE6 (loss of ability to bind to hDlg) showed membranous Cx43 while re-location of Cx43 to the cytoplasm was observed in C33a cells transfected with wild-type HPVE6. This indicates that HPVE6 negatively regulates the trafficking of Cx43 through interaction with hDlg. It may be that the ability of hDlg to suppress cell growth relies on correct GJIC communication, and HPVE6 interference with Cx43/hDlg functionality may provide a growth advantage to cells, which would increase viral production.

To determine if the Cx43/hDlg interaction requires HPV E6, Cx43/hDlg interaction was investigated in HPV-negative cervical cancer cell lines (C33a and C33aE6 (C33a cells stably expressing HPV16E6)). Co-immunoprecipitation indicates Cx43 binds hDlg in these cells. Immunofluorescence confocal microscopy shows the co-localisation of Cx43/hDlg on the plasma membrane in C33a cells and in the cytoplasm in C33aE6 cells. To determine if the Cx43/hDlg interaction is dependent on the cancer environment, similar experiments were carried out in non-tumour epithelial cell lines that do not express E6 (HEK293, HaCaT, NIKS) and NIKS16 cells (NIKS cells stably transfected with HPV16 genomes). Co-immunoprecipitation shows that Cx43 forms a complex with hDlg in HEK293, HaCaT, NIKS cells and the presence of HPV E6 at low levels in NIKS16 cells do not affect their interaction. Co-localisation of Cx43 and hDlg was observed on the plasma membrane in these cells. This indicates the Cx43-hDlg interaction is neither HPV-E6-dependent nor cancer-cell-specific.

The role of hDlg in controlling the trafficking of Cx43 has been investigated by siRNA depletion of hDlg in HaCaT, HEK293, NIKS and NIKS16 cells. siRNA depletion of hDlg in these cells led to a reduction in levels and cytoplasmic location of Cx43. HaCaT cells with stable depletion of hDlg (HaCaT shDlg) also displayed a similar pattern of Cx43 rearrangement.

Endolysosomal/lysosomal inhibition by ammonium chloride ( $\text{NH}_4\text{Cl}$ ) and chloroquine (CQ) led to increased levels of Cx43 in HaCaT and HEK293 cells and HaCaT cells with siRNA depletion of hDlg. These data indicate the role of hDlg in maintaining a cytoplasmic pool of Cx43 and suggest that hDlg may play roles in the delivery of Cx43 to the membrane.

To investigate if changes in cell signalling can alter the Cx43/hDlg complex formation, a scrape wound healing model was used since the wound healing process shares many similarities with tumour progression. The changes in

subcellular location and expression levels of the two proteins during scrape wound closure were investigated. The wound closure rates in the non-tumour epithelial cells were also been checked. At the start of wound closure in HaCaT keratinocytes, Cx43 and hDlg colocalised on the plasma membrane but both proteins moved into the cytoplasm 4-16 hours post-wound. After 24 hours, most of the proteins regained a membrane location. A similar phenomenon was also observed in NIKS cells during wound healing. There were significant reductions in Cx43 and hDlg levels during the early stages of wound closure and changes in Cx43 phosphorylation were also observed during the wound closure process.

hDlg is one of the regulators of cell polarity, which is important in cell migration especially in direct migration. In wound closure experiments, hDlg depletion led to cell death and a significantly delayed wound closure rate in HaCaT and NIKS16 cells. The cell monolayer was not repaired after 24 hours (less than 50% closure). Sudden loss of hDlg by siRNA might lead to loss of regulation of cell polarity and affect the wound healing process. Surprisingly, in HaCaT shDlg cells (HaCaT cells stably depleted of hDlg), wound closure was completed at 16h post-wound (faster than control HaCaT cells with 70% closure at 24h) and no cell death was observed. hScrib, a tumour suppressor protein, is involved in the regulation of cell polarity (Dow et al., 2003). Faster wound closure might be due to the role of hScrib in HaCaT shDlg cells to complement the stable loss of hDlg, while the sudden loss of hDlg through siRNA treatment might lead to lower tolerance of cell stresses such as wound healing.

Interestingly, the presence of the HPV16 genome drives faster closure of the wound in NIKS16 cells compared to NIKS cells. Wound closure was complete at 16h post-wound in NIKS16 cells while after 24h post-wound a small gap remained in NIKS cell monolayers. This might be due to the effect of beta-

catenin. Beta-catenin transits to the nucleus and induces gene expression of proteins involved in cell migration, which enhance wound healing. HPVE6 causes beta-catenin to accumulate in the nucleus. However, none of the cervical cancer cell lines (C33a, C33aE6 and HeLa43) were able to close the scrape wound properly (closure of 17%, 33% and 28% respectively). This might be due to a combination of the effect of membranous Cx43 and HPVE6 on the regulation of nuclear beta-catenin. Nuclear transmission of beta-catenin could be prevented by interaction with membranous Cx43, which could explain the loss of membranous Cx43 at the early stage of wound repair. C33a cells (membranous Cx43, no HPVE6) close the wound at the slowest rate (17%) while C33aE6 (cytoplasmic Cx43, HPVE6) and HeLa43 (membranous Cx43, HPVE6) show faster wound closure (33% and 28%). However, whilst no evidence is presented, it is known that HPVE6 induces accumulation of nuclear beta-catenin via its PDZ-binding domain and thus is a good candidate for future studies.

Lastly, through Cx43 C-terminal mutagenesis and co-immunoprecipitation experiments, the Cx43-hDlg binding region has been limited to amino acids 348-382 of the Cx43 C-terminus. Six different serine residues were chosen for the mutation to alanine to mimic un-phosphorylated serine. Four of these were MAPK kinase phosphorylation sites, one was an Akt and one a PKC phosphorylation site. However, these Cx43 C-terminal nonphospho-mutants could still interact with hDlg, suggesting that phosphorylation does not affect Cx43 binding to hDlg.

In conclusion, hDlg binds to regions of amino acids 348 -382 of the Cx43 CT. This Cx43-hDlg interaction is not cancer cell-specific and not HPVE6-dependent. The data in this thesis add to accumulating evidence of a role for hDlg in maintaining a cytoplasmic pool of Cx43 and delivery of Cx43 to the plasma membrane.

# Table of content

Abstract .....	2
Table of content .....	6
List of figures.....	8
List of tables .....	10
Publications.....	11
Acknowledgements .....	12
Abbreviations.....	13
1 Chapter 1 Introduction .....	15
1.1 Connexin 43 (Cx43).....	15
1.1.1 Gap junctions, connexons and connexins .....	15
1.1.2 Connexin protein-protein interactions.....	24
1.1.3 The life cycle of Cx43 .....	29
1.1.4 Connexins and disease .....	34
1.1.5 Connexins and cancer .....	38
1.1.6 Connexin and wound healing.....	43
1.2 hDlg.....	48
1.2.1 MAGUK proteins .....	48
1.2.2 hDlg .....	52
1.3 HPV16 E6 .....	57
1.3.1 HPV .....	57
1.3.2 HPV and cancer .....	61
1.3.3 HPV genome .....	65
1.3.4 HPVE6.....	67
1.4 Hypothesis and aims .....	72
2 Chapter 2 Materials and methods .....	74
2.1 Materials.....	74
2.1.1 Cell culture reagents.....	74
2.1.2 Common chemicals and buffer.....	74
2.1.3 Antibodies.....	75
2.1.4 Bacteria culture.....	77
2.1.5 Cell lines .....	77
2.2 Methods.....	79
2.2.1 Small scale preparation of plasmid DNA (mini preps) .....	79
2.2.2 Large scale preparation of plasmid DNA (midi-preps).....	80
2.2.3 PCR mediated site-directed mutagenesis and recombinant DNA .....	80
2.2.4 RNA extraction .....	82
2.2.5 cDNA synthesis .....	82
2.2.6 qRT-PCR.....	83
2.2.7 Cell culture .....	83
2.2.8 Preparation of cell stocks .....	84

2.2.9	Total cell extract preparation .....	84
2.2.10	Bradford assay.....	85
2.2.11	SDS Polyacrylamide Gel Electrophoresis (SDS-PAGE) .....	85
2.2.12	Western blot.....	85
2.2.13	Co-immunoprecipitation .....	86
2.2.14	GST protein purification .....	87
2.2.15	Coomassie staining .....	88
2.2.16	Transfection of cells with lipofectamine 3000 .....	88
2.2.17	siRNA knockdown of hDlg .....	88
2.2.18	Scratch wound assay .....	89
2.2.19	Immunofluorescence staining and confocal microscopy ....	89
2.2.20	Quantification .....	90
3	Chapter 3 The interaction between Cx43 and hDlg is neither HPVE6-dependent nor tumour cell-specific .....	91
3.1	Cx43/hDlg interaction is not HPVE6-dependent .....	93
3.2	Cx43/hDlg interaction is not tumour-cell specific.....	98
3.3	hDlg is a controller of Cx43 .....	106
3.4	Cx43 and lysosome inhibition.....	114
3.5	Discussion.....	122
4	Chapter 4 Cx43 and the wound healing process .....	126
4.1	Cx43 is internalised during keratinocyte scrape wound closure .	127
4.2	hDlg plays an important role in scrape wound healing .....	140
4.3	Behaviour of tumour cells during the wound healing process ...	150
4.4	Discussion.....	158
5	Chapter 5 Mapping the interaction of Cx43 C-terminal tail with hDlg	163
5.1	The region of Cx43 which binds hDlg is located in the last 33 amino acids of the Cx43 C-terminus.....	166
5.2	Phosphorylation mutation does not affect the interaction between Cx43 and hDlg.....	173
5.3	Discussion.....	180
6	Discussion, conclusion and future work.....	184
7	Reference list.....	193

## List of figures

Figure 1.1: A schematic diagram of a gap junction intracellular channel (GJIC) between neighbouring cells. ....	18
Figure 1.2: A schematic diagram of the C-terminus of Cx43 with phosphorylation sites indicated.....	23
Figure 1.3: A schematic diagram of the Cx43 C-terminal tail from amino acids 234 to 382 with some potential binding partners and binding domains. ....	28
Figure 1.4: The life cycle of connexins. ....	33
Figure 1.5: The expression of Cx43 during the wound healing process. ....	47
Figure 1.6: The structure of proteins of the MAGUK families. ....	51
Figure 1.7: The structure of hDlg and its binding partners. ....	56
Figure 1.8: The phylogenetic tree of the papillomavirus.....	59
Figure 1.9: The classification of HPVs.....	60
Figure 1.10: The life cycle of HPV depends on the differentiation of epithelial. ....	64
Figure 1.11: A schematic diagram of HPV16 genome. ....	66
Figure 1.12: A schematic diagram of the structure of HPVE6 and its binding partners.....	71
Figure 3.1: Cx43 colocalised with hDlg mainly on the plasma membrane in C33a cells but mainly in the cytoplasm in C33aE6 cells.....	96
Figure 3.2: Interaction of Cx43 and hDlg in cervical cancer cells. ....	97
Figure 3.3: Cx43 and hDlg expression in non-tumour cells (HEK293, HaCaT, NIKS and NIKS16). ....	100
Figure 3.4: Cx43 colocalised with hDlg on the plasma membrane in HEK293 and HaCaT cells. ....	101
Figure 3.5: Interaction of Cx43 and hDlg in non-tumour cells (HEK293 and HaCaT). ....	102
Figure 3.6: Cx43 interacted and colocalised with hDlg on the plasma membrane in NIKS and NIKS16 cells. ....	105
Figure 3.7: siRNA depletion of hDlg led to a reduction in levels of Cx43 in non-tumour cells: ....	109
Figure 3.8: siRNA depletion of hDlg led to the cytoplasmic location of Cx43 in non-tumour cells (HEK293, HaCaT). ....	111
Figure 3.9: Reduced level and cytoplasmic location of Cx43 was observed in HaCaT cells with stable depletion of hDlg (HaCaT shDlg). ....	113
Figure 3.10: Increasing levels and accumulated cytoplasmic Cx43 was observed in HaCaT cells with lysosome inhibitor treatment. ....	118
Figure 3.11: Increasing levels and accumulated cytoplasmic Cx43 was observed in HEK293 cells with treatment of lysosome inhibitor. .	120

Figure 3.12: Lysosome inhibitor rescued some level of Cx43 decreased by siRNA depletion of hDlg in HaCaT cells. ....	121
Figure 4.1: Cx43 cycled from the plasma membrane to the cytoplasm during the wound healing process in HaCaT cells. ....	130
Figure 4.2: The levels of Cx43 and hDlg in HaCaT cells are altered during the wound healing process. ....	131
Figure 4.3: The wound closure process in HaCaT cells. ....	132
Figure 4.4: Cx43 cycled from the plasma membrane to the cytoplasm during the wound healing process in NIKS cells. ....	135
Figure 4.5: The levels of Cx43 and hDlg in NIKS cells are altered during the wound healing process. ....	136
Figure 4.6: The levels of Cx43 and hDlg in NISK16 cells are altered during the wound healing process. ....	137
Figure 4.7: The wound closure process in NIKS and NIKS16 cells. ....	139
Figure 4.8: The wound closure process in mock-treated HaCaT and HaCaT cells with siRNA depletion of hDlg. ....	144
Figure 4.9: The wound closure process in mock-treated NIKS16 and NIKS16 cells with siRNA depletion of hDlg. ....	146
Figure 4.10: siRNA depletion of hDlg led to more floating cells in response to wound healing. ....	147
Figure 4.11: The wound closure process in HaCaT cells and HaCaT shDlg cells. ....	149
Figure 4.12: The wound closure process in C33a and C33aE6 cells. ...	153
Figure 4.13: The levels of Cx43 and hDlg in C33a cells are altered during the wound healing process. ....	154
Figure 4.14: The levels of Cx43 and hDlg in C33aE6 cells are altered during the wound healing process. ....	155
Figure 4.15: The wound closure process in HeLa43 cells. ....	156
Figure 4.16: The levels of Cx43 and hDlg in HeLa43 cells altered during the wound healing process. ....	157
Figure 5.1: Sequence information of Cx43 CT with some interaction partners. ....	165
Figure 5.2: A scheme of Cx43 interaction with hDlg. ....	167
Figure 5.3: Generating the flag tagged Cx43 CT deletions. ....	170
Figure 5.4: GST-hDlg is successful induced by IPTG. ....	171
Figure 5.5: The binding region of hDlg is located at the last 100bp of Cx43 CT. ....	172
Figure 5.6: Successful expression of all these un-phosphorylation mimic site mutations of the Cx43 CT. ....	177
Figure 5.7: Non-phosphorylation mimic site mutations at Cx43 CT did not affect/block the Cx43-hDlg interactions. ....	179
Figure 6.1: A schematic diagram of the Cx43 life cycle and the possible stages that hDlg and ZO-1 were involved. ....	192

## List of tables

Table 1: List of 14 inherited diseases associated with human connexin gene mutations.....	37
Table 2.1: Buffers .....	75
Table 2.2: List of antibodies, source and dilution.....	76
Table 2.3: List of primers designed for Cx43 CT phosphorylation site mutations .....	81
Table 2.4: List of primers and probes used in RT-PCR.....	83
Table 4.1: Summary of the location of Cx43 and hDlg in cells during the wound healing process in HaCaT and NIKS cells. ....	161
Table 4.2: Summary of expression of Cx43 and hDlg during the wound healing process in different cell types.....	161
Table 5.1: List of phosphorylation mimic site-mutation at Cx43 CT and the kinase involved in each phosphorylation site. ....	176

## **Publications**

**Dong L., Srinivasan S., MacDonald A.I., Stevenson A. Massimi P., Banks L., Johnstone S.R., and Graham S.V.** The human Discs large protein (Dlg1) alters Connexin 43 (Cx43) trafficking and gap junction signalling in the epithelium. In preparation, 2021.

## Acknowledgements

Firstly, I would like to acknowledge my supervisors, Prof. Sheila Graham, and Dr. Scott Johnstone. Thank you for the great support, guidance and encouragement as well as your patience during these years.

I would like to thank all the members in the Graham group, who helped me physically and emotionally. Particularly, I would like to thank Andy for his technical support and willingness to talk and advise whenever I was facing difficulties. I would like to thank Ilaria, Chris, Megan, Gladys, Josep and Michaela for making each day full of scientific discussions and joys. Thanks to Colon Loney for helping with confocal microscopy.

I would also like to thank my friends who, with caring and encouragement, helped me enormously during this long journey. Special thanks to the McClure family who made me feel at home here in Glasgow.

Finally, I am very grateful to my family, especially my mother and father, for their unconditional support, endless encouragement and love during my study.

## Abbreviations

DAPI	4'6'-diamino-2-phenylindole hydrochloride
DMEM	Dulbecco's Modification of Eagle's Minimal Essential medium
DMSO	Dimethyl sulphoxide
EGF	Epidermal growth factor
ERAD	Endoplasmic-reticulum-associated protein degradation
FBS	Fetal bovine serum
GJ	Gap junction
GJIC	Gap junction intercellular communication
hDlg	Human homologue of <i>Drosophila</i> Discs Large
HPV	Human papillomavirus
HRP	Horseradish peroxidase
IF	Immunofluorescence
IgG	Immunoglobulin G
kDa	Kilodalton
KGM	Keratinocyte growth medium
MAGUK	Membrane-associated guanylate kinase

PBS	Phosphate buffered saline
PCR	Polymerase chain reaction
PDZ	PSD95/Dlg/ZO-1 family
PLA	Proximity Ligation Assay
PKC	Protein kinase C
RT	Reverse transcriptase
SDS	Sodium dodecyl sulphate
WHO	World health organisation

# 1 Chapter 1 Introduction

## 1.1 Connexin 43 (Cx43)

### 1.1.1 Gap junctions, connexons and connexins

Cell-cell communication is a key event to maintain the homeostasis of tissue/organs in living creatures. Through this communication, cells can alter the concentration of different materials within cells to adjust to the changes of different environments. By making the correct response to alterations of the environment, cells send/receive signals to/from neighbouring cells to maintain the integrity of tissues. Gap junction intercellular channel communication (GJIC) is one of the key communication types, which allows direct connection between the cytoplasm of adjacent cells. The observation of gap junctions can be traced back to the year 1958 when Sjostrand and co-workers (Sjostrand et al., 1958) observed specific regions between plasma membranes of neighbouring cardiac muscle cells using electron microscopy (EM). Later the tight apposition (nexus) that they described was also observed in smooth and striated muscle cells (Karrer, 1960, Dewey and Barr, 1962). These nexus sites were then found to contain hexagonal array structures with defined “gaps” of 2 nm between apposed cell membranes in mouse heart cells (Revel and Karnovsky, 1967). In a key experiment, yellow dye M4RS (molecular weight approximately 500 Da) was able to spread from one cytoplasm to another cytoplasm via gap junctions of synapses but did not enter the cytoplasm from the extracellular space. This increased the understanding of gap junctions in allowing the direct interaction between cells (Payton et al., 1969). Gap junctions of hepatocyte from mice were isolated and characterised by X-ray diffraction assay

(Goodenough and Stoeckenius, 1972). Two years later, bulk isolation of gap junctions from the same mouse tissue led to the isolation of structural protein subunits of gap junctions, which were named “connexons”(Goodenough, 1974). GJIC provides direct interaction between opposing cells by allowing the exchange of small molecules (<1 kDa), including metabolites and second messengers (Alexander and Goldberg, 2003b). Gap junctions are thought to be involved in many cellular activities such as proliferation, differentiation and apoptosis (Vinken et al., 2006). For example, GJIC inhibitors 18 $\alpha$ -glycyrrhetic acid (AGA) and octanol (OcOH) blocked GJIC and induced the reduction of cell proliferation and initiation of cell apoptosis in human endometrial stromal cells (Yu et al., 2014). GJIC is found in all multicellular animals and the majority of vertebrate cell types (Saez et al., 2003).

Gap junctions on the plasma membrane can be regulated in several ways: 1) regulation of connexin gene transcription; 2) regulation of connexin protein synthesis; 3) the building of subunits of gap junctions; 4) regulation in the delivery of gap junction proteins to the plasma membrane; 5) regulation of gap junction protein recycling from the plasma membrane; 6) regulation in the degradation of gap junction proteins; 7) functional regulation of opening and closing of gap junction intracellular channels. These regulation events could be summarised as regulation in the life cycle of gap junction proteins that affect the function of gap junctions and gating of gap junctions. Due to GJIC functions at the plasma membrane, any factors that affect the formation of gap junctions at the cell membrane will affect their function (this will be reviewed in detail in 1.3). In terms of gating of gap junctions, any factors that affect the opening/closing of gap junctions will be counted such as phosphorylation of connexins or changes in

response to calcium concentration (Nielsen et al., 2012a). For example, phosphorylation at serine368 at Cx43 C-terminus led to a decrease in gap junctional communication (Lampe et al., 2000), while increasing calcium concentrations led to a block in dye transfer between HeLa cells stably transfected Cx43 and expressing functional gap junctions (Lurtz and Louis, 2007).

Gap junction intracellular channels are structurally formed of two connexons (also called hemichannels) with head-to-head docked formation (Figure 1.1 A). Each connexon is formed of six connexins, which could be the same connexins (homologous connexon) or combinations of different connexins (heterologous connexon) (Figure 1.1 B). Each connexin contains two extracellular loops (E1 and E2), which are the most conserved domains among connexins. Three cysteine residues in the E1 and E2 domains form disulphide bonds that are contained by all connexins able to form functional GJs. Hydrogen bonds at the docking interface act like “glue” to help the docking of two connexons and form functional GJs between neighbouring cells (Bai et al., 2018).

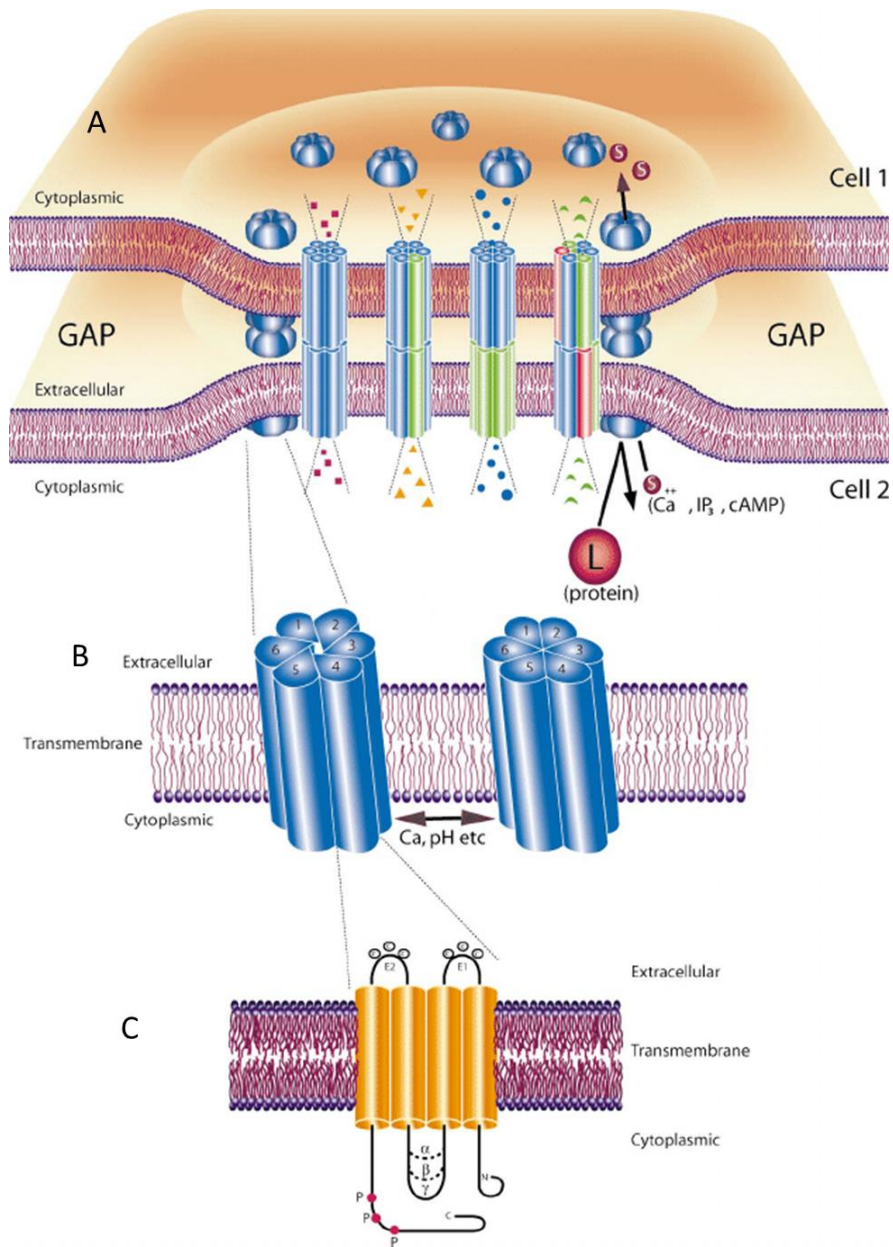


**Figure 1.1: A schematic diagram of a gap junction intracellular channel (GJIC) between neighbouring cells.**

(A) Gap junction intercellular channels (GJIC), formed by two docked connexons, allow the exchanges of ions and small molecules that are less than 1kDa. (B) Each connexon is formed by six connexins, either the same connexin (homologous connexon) or combinations of different connexins (heterologous connexon). (C) Each connexin contains an N-terminus, four trans-membrane domains which are linked with two extracellular loops (EL) and one intracellular loop (IL) and a C-terminal tail which normally contains protein-protein interaction sites or post-translation modification sites such as phosphorylation. The figure is taken from (El-Sabban et al., 2003).

The gap junction proteins, connexins, traverse the cell membrane four times with amino and carboxyl termini staying in the cytoplasmic intracellular environment. A schematic diagram of a general connexin is shown in Figure 1.1. This generates the following structure: four trans-membrane domains (TM) that contain helices anchored into the lipid bilayer of the plasma membrane; two extracellular loops that allow the connexons of neighbouring cells to couple; one cytoplasmic loop; and an N- and C-terminal region located on the cytoplasmic membrane face (Figure 1.1 C). The amino acid sequence of the extracellular loops and trans-membrane domains are highly conserved between different connexins. Therefore, the connexins are different from each other, mainly in the amino acid differences in the intracellular loop and the variable length of the carboxyl-terminal tail (Evans and Martin, 2002). Research has been done to investigate the function of different domains in the connexins. The amino terminus acts as a calmodulin-binding domain that may affect the oligomerisation (Ahmad et al., 2001, Torok et al., 1997). This region also plays an important role in membrane insertion and trafficking. Site-specific mutation at position 12 led to an accumulation of the protein in the cytoplasm, and it was mainly located in the Golgi apparatus (Martin et al., 2000).

All the trans-membrane domains act as membrane anchors. Deletion of TM1 blocked overall membrane insertion (Martin et al., 2000). Mutation of Cx32 TM1 (I28L) resulted in Cx26-like trafficking and post-translation insertion properties. This suggested the TM1 plays key roles in regulating trafficking pathways of individual connexins (Martin et al., 2001). The TM3 is thought to contribute to the formation of the channel wall (Skerrett et al., 2002). The extracellular loops, as mentioned above, function in the docking of connexons between neighbouring cells. Genetic mutations leading to disordered function and trafficking

emphasised the importance of these loops in docking (Marziano, 2003, Bakirtzis et al., 2003). It has been reported that the C-terminal tail of connexins interacts with the intracellular loop like a “ball and chain” model, which monitors the chemical gating of the channel (Stergiopoulos et al., 1999). Cx32 with truncation of the carboxyl tail showed little effect on the assembly of gap junctions (Yum et al., 2002). Cx26 with the addition of the C-terminus of Cx43 maintained the original trafficking pathway, which indicted the carboxyl tail was not involved in the trafficking of connexins (George et al., 1999). However, in most connexins (apart from Cx26), C-terminal tails contain multiple post-translation modification sites. For example, the C-terminal tail of Cx43 contains 33 phosphorylation sites phosphorylated by more than one protein kinases (Chen et al., 2013a). Its C-terminus also contains many protein-protein interaction regions allowing it to interact with other associated proteins such as microtubules and ZO-1 (Giepmans et al., 2001b, Toyofuku et al., 1998).

Since the first gap junction protein was cloned and sequenced from rat heart in 1986, there are now 21 connexin genes identified in the human genome and 20 in the mouse genome. Connexins can be divided into five subgroups ( $\alpha$ ,  $\beta$ ,  $\gamma$ ,  $\delta$ , or  $\epsilon$ ) based on their sequence similarities and the length of their cytoplasmic loop. Their names depend on their predicted molecular weight (e.g. Cx43 is about 43 kDa in size) (Beyer et al., 1987, Nielsen et al., 2012b). This project focuses on Cx43 because it is the most widespread connexin, and its long C-terminus contains many phosphorylation sites and protein-protein interaction domains.

As the first gap junction protein being cloned and sequenced, Cx43 is well-studied compared to other connexins. Cx43, with the molecular weight of 43 kDa, is the major building unit of gap junctions that can be

found in many mammalian cell types, and especially epithelial cells (Laird, 2010). These post-translation modification sites on the Cx43 CT makes it different from most other connexins (Leithe et al., 2017a). The carboxyl-terminal domain of Cx43 is 17 kDa and reported to contain many sites phosphorylated on serine or tyrosine residues by different kinases (Lampe and Lau, 2004). This CT domain is also reported to be associated with the stabilisation of Cx43 anchoring in plasma membranes. Investigation of Cx43 CT truncated mutants indicates the important role of 235 - 242 amino acid (aa) of Cx43 CT in GJ formation in the plasma membrane; the amino acid region of 271 - 302 in the CT of Cx43 is associated with controlling the size of GJ plaques; 325-342 aa region plays an important role in the control of internalisation of GJ plaques (Wayakanon et al., 2012). There are in total 66 S/T/Y sites in Cx43, and 32 of them are in the CT domain (Chen et al., 2013b). Monomeric Cx43 molecules are found in phosphorylated form, which indicates that Cx43 receives phosphorylation before insertion into the plasma membrane (Musil and Goodenough, 1993). Phosphorylation of Cx43 influences many aspects of gap junctions: gap junctions formed by Cx43 with mutations after 239aa are still functional but inhibited in the opening of the hemichannel, which indicates that phosphorylation sites in this region are important for opening the channel (Johnstone et al., 2012). Connexins phosphorylated by PKC and MAPK maintain hemichannels in a closed state. PKC directed phosphorylation of S368 in Cx43 reduces the opening of hemichannels. Therefore, the opening/closing state of hemichannels is controlled by the balance of phosphorylation/ de-phosphorylation at the C terminus of Cx43 (Contreras et al., 2002, De Vuyst et al., 2007). Phosphorylation of S364 by PKA and S325/S328/S330 by CK1 is thought to increase the assembly and stability of gap junctions. Generally, Cx43 is positively phosphorylated by CK1 (and PKA) while PKC, MAPK, v-SRC and CDC2 reduce gap junction activity. De-phosphorylation

of Cx43 at S365 may result in intracellular redistribution and removal from gap junction plaques (Johnstone et al., 2012).

**Main PTMs in  
Cx43 CT**

- 244 CaMKII
- 247 Src
- 255 MAPK/CaMKII
- 257 PKG/CaMKII
- 262 PKC
- 265 Src
- 279 MAPK
- 282 MAPK
- 296 CaMKII
- 297 CaMKII
- 306 CaMKII
- 314 CaMKII
- 325 CK1/CaMKII
- 328 CK1/CaMKII
- 330 CK1/CaMKII
- 364 PKA/CaMKII
- 365 PKC/PKA/CaMKII
- 368 PKC
- 369 PKC/CaMKII/Akt
- 372 PKC/CaMKII
- 373 PKC/CaMKII/Akt

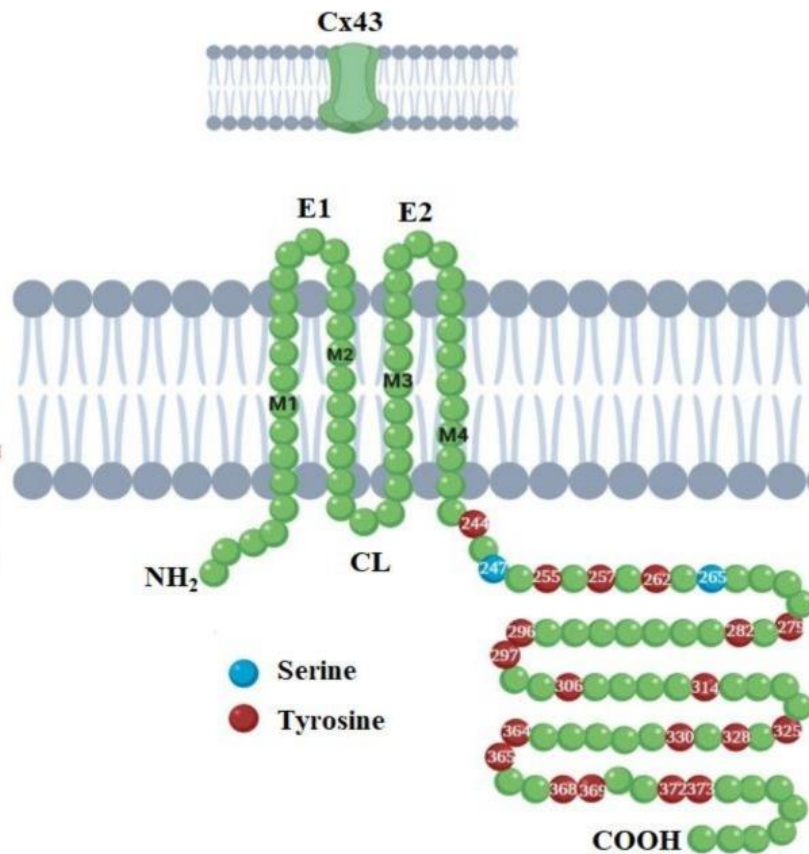


**Figure 1.2: A schematic diagram of the C-terminus of Cx43 with phosphorylation sites indicated.**

Cx43 CT contains many phosphorylation sites phosphorylated by many kinases such as PKA, PKC, and MAPK. Phosphorylation at tyrosine residues is coloured in brown, and phosphorylation at serine residues is coloured in blue. The phosphorylation sites and kinases involved are indicated at the left. The figure is taken from (Sánchez et al., 2020).

### 1.1.2 Connexin protein-protein interactions

In the beginning, connexins were thought only as the building blocks of gap junctions, but more and more evidence has been found that connexins are able to interact with other proteins and regulate cell functions or cell activities. Such interactions can regulate connexins at different levels, including biosynthesis, trafficking, and degradation of connexins and the formation of GJIC. As mentioned above, sequences of connexins are conserved from the N-terminus to the fourth trans-membrane region, but there is variation in C-terminal tails. Peptides correlated to the N-terminus (residues 1-21) and C-terminus (residues 216-230) of Cx32 have been found to bind to fluorescently-tagged Calmodulin (a  $\text{Ca}^{2+}$ -binding protein) in a  $\text{Ca}^{2+}$ -dependent manner. The third amino acid at the N-terminal of Cx32 (Trp3) is critical in this interaction (Torok et al., 1997). However, the Calmodulin-binding motif has been identified differently in Cx43, which is located at the intracellular loop (residues 136-158) in a  $\text{Ca}^{2+}$ -dependent manner (Zhou et al., 2007). Cx43, the most widespread connexin, contains SH2, SH3 and PDZ binding domains at its C-terminus facilitating the interactions between Cx43 and its binding partners. A diagram with potential binding partners of Cx43 CT and some binding domains is shown in Figure 2. It has been shown that many proteins can interact with the C-terminal tail of Cx43 and other connexins. These include tight-junction proteins, cytoskeletal proteins and some protein kinases. The examples have been listed below.

Zonula occludens-1 (ZO-1), the first identified tight junction protein (Stevenson et al., 1986), belongs to the membrane-associated guanylate kinase (MAGUK) family that contains Postsynaptic density/Discs large/ZO-1 (PDZ) domains and has a role in maintaining epithelial cell polarity (Van Itallie and Anderson, 2014). ZO-1, with its second PDZ domain, has been found to directly interact with Cx46, Cx50 and Cx43 (Giepmans and

Moolenaar, 1998, Toyofuku et al., 1998, Nicholson, 2003). The extreme C-terminus (amino acids DLEI) of Cx43 was identified as the binding sites for ZO-1 PDZ2 domain (Giepmans and Moolenaar, 1998). Phosphorylation of Cx43 at Ser373 negatively affects the Cx43-ZO-1 interaction. A mimetic peptide representing the last 12 amino acids of the Cx43 C-terminal tail with the phosphorylated mimic substitution at Ser373 site displays a 7-fold lower affinity of binding to the second PDZ domain of ZO-1 compared with wild-type peptide (Chen et al., 2008). Elimination of the Cx43-ZO-1 interaction by Akt-dependent phosphorylation at Ser373 in the C-terminus of Cx43 led to enlarged gap junction size (Dunn and Lampe, 2014). This rapid increase in GJ communication may potentially let cell signalling molecules enter the cells and initiate the activation and migration of keratinocytes in response to a wound or ischemic injury (Dunn and Lampe, 2014). HeLa cells stably transfected with Cx43-GFP expressing abnormal large size and this could be normalised by transfection of native Cx43. This was due to Cx43-GFP block the Cx43-ZO-1 interaction since peptide inhibition of Cx43-ZO-1 interaction led to enlarged gap junction (Hunter et al., 2005). This enlarged gap junction was due to the incorporation of non-junctional connexons to gap junctions (Hunter et al., 2005). This enlarged size of gap junctions may decrease the non-junctional pool of Cx43 on the plasma membrane since they incorporation into gap junctions and may also allow internalisation of annular junctions more efficiently (Solan and Lampe, 2014). Phosphorylation at S368 has been observed increasing with the blocking of Cx43-ZO-1, followed by internalisation of Cx43 (Palatinus et al., 2011).

Cx43 has been reported to interact with cytoskeleton proteins. The Cx43 CT binds to tubulin directly through its juxtamembrane region with 35 amino acids (residues 228-263). This tubulin-binding motif is not found in other connexins, therefore it is Cx43-specific (Giepmans et al., 2001a). A mimetic peptide correlated to residues 234-259 at Cx43 CT has been shown to

interact with tubulin, and it could compete with Cx43 CT to limit tubulin-binding. This Cx43-tubulin interaction is prevented by Src kinase-mediated phosphorylation on Cx43 CT Y247 (Saidi Brikci-Nigassa et al., 2012) Cx43 CT binds to both alpha-tubulin and beta-tubulin equally (Giepmans et al., 2001b). Cx43 can bind to ZO-1 (which can bind to actin), tubulin and drebrin (an actin-binding protein) with different non-overlapping binding domains located at its C-terminus to form a supramolecular complex, which indicates the important role of this protein complex in the regulation of cytoskeleton rearrangement and further regulating cell migration (Ambrosi et al., 2016).

Cx43 CT binds to 14-3-3 theta and zeta at the 14-3-3-binding motif (370-376), which requires Akt induced phosphorylation of Cx43 CT-S373 (Park et al., 2006, Park et al., 2009). The interaction between Cx43 and 14-3-3 theta was associated with the internalisation of gap junctions (Smyth et al., 2014). There are seven isoforms of 14-3-3 protein (beta, epsilon, gamma, eta, tau/theta, zeta and sigma), involved in many biological processes such as cell proliferation and cell migration (Moreira et al., 2008). Overexpression of 14-3-3 tau was observed in breast cancer, through activation of Rho GTPase and ROCK2. This led to increased cell migration and invasion of breast cancer cells, and reduced adhesion within each other (Xiao et al., 2014). An increasing level of 14-3-3 zeta was observed in chronic wounds and mice with deficiency of 14-3-3 zeta exhibited faster wound healing associated with increasing signalling downstream of ROCK (Kular et al., 2015).

There are a number of other proteins which bind to Cx43 CT. Caveolin-1 directly binds to Cx43 CT via its caveolin-scaffolding domain (residues 82-101) and the C-terminal domain (135-178) (Schubert et al., 2002). Cx43 was targeted to lipid rafts where it interacted with caveolin-1 (Schubert et al., 2002). The specific binding region of caveolin-1 on Cx43 CT remains unclear.

CIP75 (Cx43-interacting protein of 75kDa) binds to Cx43 CT with its C-terminal UBA (ubiquitin-associated) domain. The Cx43-CIP75 interaction region is between amino acids 264 and 302 within Cx43 CT. Its role was suggested to be involved in the turnover of Cx43 since overexpression of CIP75 increased the degradation of Cx43, possibly through the proteasome (Li et al., 2008). NEDD4 (neural precursor cell-expressed developmentally downregulated gene 4) binds to the PY motif (XPPXY, where P is proline, X is any amino acid, and Y is tyrosine) on the Cx43 CT, specifically at 283-286. The role of NEDD4 was also thought to be involved in the degradation of Cx43 since downregulation of NEDD4 led to an increasing number of gap junction plaques on the plasma membrane (Spagnol et al., 2016). Drebrin, an actin-binding protein, directly binds to three regions of Cx43 CT, residues 264-275 being critical for this interaction. Src phosphorylation at Y265 negatively regulated Cx43-drebrin interaction (Ambrosi et al., 2016). Specifically, another MAGUK family protein hDlg is found to bind to the C-terminal of Cx43 via its N-terminal and C-terminal. However, the last four amino acids of Cx43 CT (required to bind ZO-1) were not required for hDlg binding (Macdonald et al., 2012b).

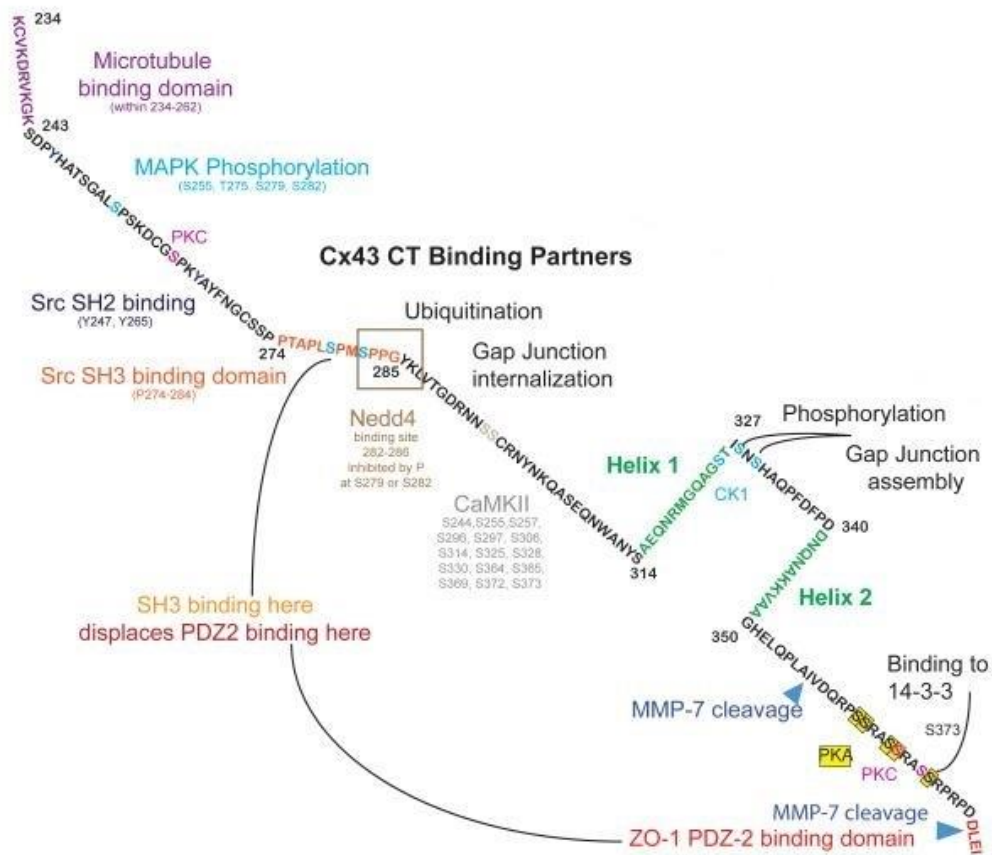


**Figure 1.3: A schematic diagram of the Cx43 C-terminal tail from amino acids 234 to 382 with some potential binding partners and binding domains.**

Cx43 interacts with many other proteins through its binding domain located at its C-terminus. Different colours indicate different binding partners, and the location of the interaction region at Cx43 CT is also displayed. The figure is taken from (Palatinus et al., 2012).

### 1.1.3 The life cycle of Cx43

Fully functional GJIC requires the correct levels of properly folded connexins (the building blocks of gap junctions) to be structured in gap junction plaques on the cell membrane. In this case, tissues regulate the number of connexins forming the gap junctions on the plasma membrane by regulating the expression of connexins, trafficking, recycling and degradation of connexins. Like many secreted proteins, connexins are transcribed to mRNA in the nucleus and translated into protein in the ribosome, followed by post-translation modification in the endoplasmic reticulum (ER) and Golgi complex and then are delivered to the plasma membrane.

The gene, named GJA1, that encodes Cx43, contains two exons and one intron located in the 5' untranslated region (5'-UTR) (Sullivan et al., 1993). Genes encoding different connexins are located in different chromosomes. For example, GJA1 (encoding Cx43) was mapped to human chromosome 6, while GJB1 (encoding Cx32) was located on the X chromosome (Fishman et al., 1991). The expression of different connexins is cell-/tissue-specific. For example, in the basal cell layer of human epidermis, the expression of Cx26 is predominant, while Cx43 is found only in small amounts. But in the spinous cell layer and granular cell layer of human epidermis, the expression of Cx43 is predominant (Oyamada et al., 2005). DNA methylation might be one of the modulators of transcription that cause variation in connexin expression. Methylation was found in the Cx32 promoter in rat liver epithelial cells that expressed Cx43 but not Cx32, whereas in rat hepatocytes, it was the promoter of Cx43, not Cx32, which was methylated leading to the totally opposite expression of these two connexins (Piechocki et al., 1999).

Gap junction connexins have been reported to have a short half-life of 1.5 - 5 hours. This short lifespan allows the GJIC formed by connexins to respond to alteration of the surrounding environment rapidly via either up-regulated or down-regulated gap junction coupling (Laird, 2006). For example, in the myometrium, the total number of gap junctions dramatically increases just before labour onset and following labour, reduces back to a steady state of GJIC levels in the uterus (Hendrix et al., 1992, Risek and Gilula, 1996). Connexins are believed to insert into the ER (endoplasmic reticulum) co-translationally. *In vitro* experiments have shown that both Cx26 and Cx32 can co-translationally insert ER membranes. Cx26 but not Cx32 can also insert ER membranes post-translationally (Zhang et al., 1996). Connexins folding into mature states and the formation of disulfide bonds between cysteine residues at extracellular loops occurs in the ER (John and Revel, 1991, Rahman and Evans, 1991).

Connexins are transported from the ER to the Golgi complex, where the oligomerization occurs. Monomers formed of Cx43 or Cx46 are found in the Golgi apparatus while oligomerizations of these two connexins were found in the trans-Golgi network (Musil and Goodenough, 1993, Koval et al., 1997). Fractionation studies have shown connexons consisting of Cx26 and Cx32 were found in the Golgi apparatus in the guinea-pig liver (Diez et al., 1999). In general, connexins exist as monomer forms in the ER and become oligomerized in the trans-Golgi network. However, oligomerization of connexins could be induced by a high level of connexins in the ER (VanSlyke et al., 2009) because in baby-hamster kidney (BHK) cells, gap junction-like structures consisting of Cx32 were observed in the ER (Kumar et al., 1995). The chaperone ER-localized, 29-kDa thioredoxin-family protein (ERp29) has been suggested to stabilize monomeric Cx43 in the ER and enable the oligomerization occurring in the Golgi apparatus (Das et al., 2009).

After being properly folded and oligomerized in the trans-Golgi network, connexins in the form of connexons are transported to the cell surface. Microtubules are thought to be involved in this trafficking of connexins. Microtubules, act as a high-way in the cytoplasm connecting the Golgi and membrane-anchored proteins (e.g. Adherens junction proteins). Connexons leaving the Golgi in vesicles can traffic to the membrane along the microtubules (Shaw et al., 2007). In cells treated with Brefeldin A (a drug that disrupts the Golgi compartment), the majority of Cx32 and Cx43 was trapped and unable to traffic to the cell membrane and gap junction communication was largely inhibited while Cx26 was minimally affected (George et al., 1999, E. et al., 2001). This indicates that Cx26 can traffic to the membrane independent of Golgi trafficking. In the cells treated with nocodazole (a drug that disrupts microtubules), assembly of Cx26 gap junctions was abolished while there was little effect on Cx43 gap junction assembly (George et al., 1999, E. et al., 2001). This indicates that Cx43 can traffic to the membrane by alternative pathways to microtubules. Non-sarcomeric actin has been thought to be involved in the delivery of Cx43, in addition to microtubules, via regulating vesicular transport. The dependence of GJ formation and maintenance has been identified to involve actin (Theiss, 2002, Qu et al., 2009, Thomas et al., 2001). Apart from direct binding to actin, Cx43 can interact with actin indirectly via binding to ZO-1 and drebrin (both can interact with actin) (Ambrosi et al., 2016). Live cell imaging with different colour labels distinguishing older and younger protein molecules of Cx43 indicated that newly synthesis Cx43 trafficked in vesicles with the size between 10 - 150 nm to the plasma membrane at the edge of gap junction plaques while older Cx43 located at the centre of the plaques (Gaietta et al., 2002).

Older Cx43 connexons have been shown to be removed from the centre of the gap junction plaques (Gaietta et al., 2002). Co-culture of NRK cells

expressing GFP -labelled Cx43 and cells with endogenous expression of Cx43 resulted in fluorescently tagged Cx43 being internalised into the non-fluorescent cells (Naus et al., 1993). Combined with the observation of double-membrane annular gap junctions internalised in cells (Gaietta et al., 2002), this suggests that older Cx43 from the centre of gap junction plaques as annular gap junctions (connexosomes) can be internalised into one of the neighbouring cells. Annular gap junctions removed from the centre of gap junction plaques can sometimes be recycled to the membrane regenerating the gap junction instead of newly synthesised connexins. This can occur after mitosis is completed in cell lines such as SW-13 adrenocortical tumour cells and normal rat kidney (NRK) cells (Boassa et al., 2010, Vanderpuye et al., 2016). The internalisation of Cx43 occurs after ubiquitination prior to lysosomal or proteasomal degradation. These events can be triggered by post-translation modification, such as phosphorylation. Phosphorylation at Ser373 in the Cx43 CT led to the binding of 14-3-3 theta and subsequently phosphorylation at Ser368 that resulted in gap junction ubiquitination, internalisation and degradation in the event of acute cardiac ischemia (Smyth et al., 2014).

Cx43 can be degraded through the proteasome and lysosome but mainly the latter. Degradation of Cx43 was delayed in the presence of proteasome inhibitor, and Cx43 was also found to be a substrate for ubiquitin, which is normally a target to the proteasome. But mono-ubiquitination was found for Cx43, which is thought to act as a trigger for internalisation while proteins with poly-ubiquitination are normally the target to the proteasome. Accumulated evidence has revealed that the degradation of Cxs is mostly via the lysosomes. For instance, immunofluorescence assay indicates that intracellular Cx43 is located in the lysosome and lysosome inhibitor-treated breast cancer cells shows increasing levels of Cx43 (Qin et al., 2003).

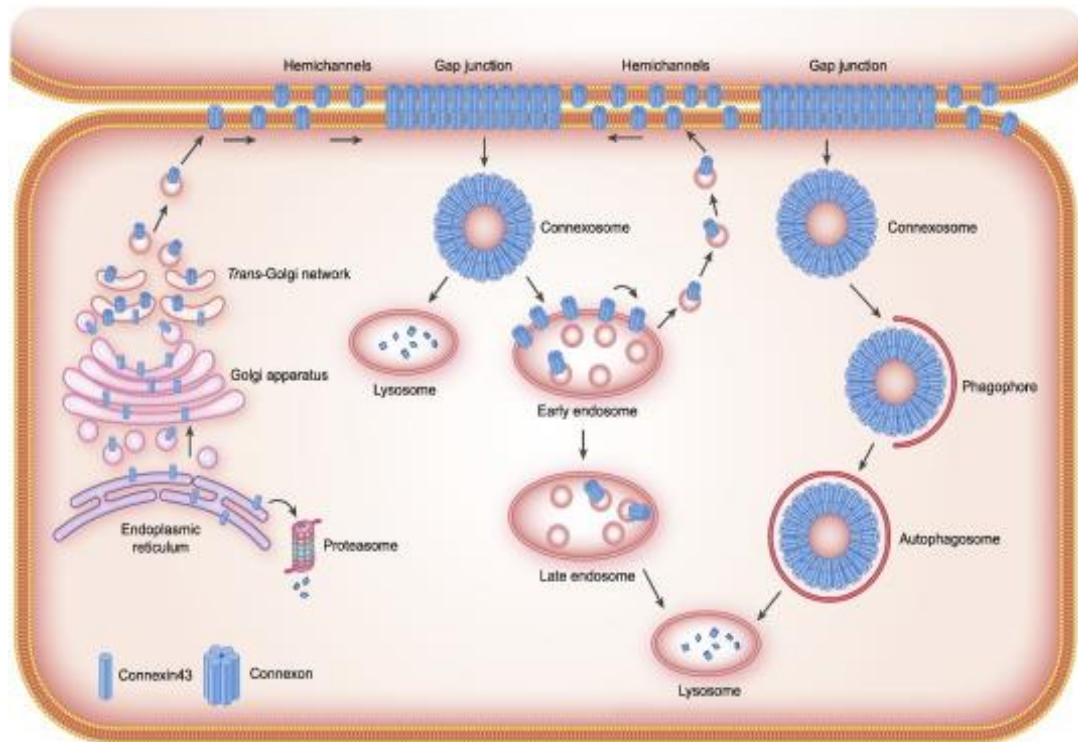


**Figure 1.4: The life cycle of connexins.**

Properly folded connexins are delivered to the Golgi apparatus through the trans-Golgi network (TGN). Improperly folded connexin may be targeted for endoplasmic-reticulum-associated protein degradation (ERAD). Connexins, in the form of connexons, are delivered to the cell surface in vesicles. Microtubules facilitate this process. New gap junction channels are delivered to the margins of gap junction plaques while older channels are found in the centre of the plaques. Older channels are internalized as annual junctions (connexosomes). Connexins may also be internalized through classical endocytic pathways. Internalized connexins are targeted to lysosome degradation. The figure is taken from (Leithe et al., 2018).

### 1.1.4 Connexins and disease

Gap junction intercellular channels, as a bridge connecting cells to neighbouring cells allowing the exchange of small molecules or signals between cells and their surrounding environment, act as a maintainer of homeostasis that ensures that cellular physiological activities occur properly. As building blocks of gap junctions, connexins behaving abnormally will affect the function of gap junctions. Fourteen inherited human diseases have been linked to connexin mutations. These include myelin-related diseases, deafness and skin diseases, cataracts and oculodentodigital dysplasia (ODDD) (Table 1)(Kelly et al., 2014). X-linked Charcot-Marie-Tooth disease (CMTX), a genetic neuropathy in the peripheral nerves resulting in muscle weakness, especially in the limbs (Wang and Yin, 2016), was the first identified connexin-linked human disease for which seven different mutations were found in the Cx32 gene in patients from eight CMTX families (Bergoffen et al., 1993). There have been over 400 mutations found in the gene GJB1 (encoding Cx32) in CMTX patients, most of which lead to the unsuccessful formation of gap junctions, or gap junctions with abnormal properties (Kleopa et al., 2012). Transgenic mice with point-mutation in the Cx32 gene resulted in loss-of-function of Cx32 in Schwann cells and oligodendrocytes (Sargiannidou et al., 2009). In addition, mice with knockout Cx32 showed more susceptibility to chemically induced liver carcinogenesis (Temme et al., 1997).

More than 220 different Cx26 mutations have been linked to non-syndromic hearing loss (Hilgert et al., 2009). In the inner ear, gap junctions predominantly formed by Cx26 are thought to be critical in recycling potassium to maintain the high endolymphatic potassium concentration (Xu and Nicholson, 2013). Apart from Cx26 mutations, many hearing loss cases are also associated with mutations in the Cx30 gene (Common et al., 2005).

Apart from Cx26 and Cx30 mutations, the linkage has also been reported between mutations in another three connexins (Cx30.3, Cx31, and Cx43) and hearing loss (Xu and Nicholson, 2013, Hong et al., 2010, Scott and Kelsell, 2011).

In humans, Cx43 is the predominant connexin expressed in the epidermis. Cx43 is mainly confined to the basal epithelial layers, whereas other connexins like Cx26 and Cx30 are expressed in the spinous layer (Martin et al., 2014). Mutations occurring in the genes encoding these connexins can cause various skin diseases including Erythrokeratoderma Variabilis (EKV), which is associated with short-lasting red patches and thickened skin (hyperkeratosis); and Bart-Pumphrey syndrome, which is characterized by white discolouration of the nails and knuckle pads on the knuckles of the fingers and toes (Kelly et al., 2014). EKV was linked to the mutations in the genes encoding Cx31 and Cx30.3 (Richard et al., 1998, Richard, 2003). Gene mutations of Cx46 and Cx50 have been linked to cataracts (Pal et al., 2000). The first Cx43 gene mutations were associated with the inherited disease, Oculodentodigital Dysplasia (ODDD), which leads to congenital craniofacial deformities (Paznekas et al., 2003). Over 73 mutations of Cx43 have been found associated with ODDD (Laird, 2014). As a widespread connexin that is expressed in most cell types in humans, Cx43 is critical. This is supported with experimental data where homozygous Cx43-knockout mice (-/-) died shortly after birth due to failure of gas exchange in the lung while in heterozygous Cx43-knockout mice (+/-), the majority of cells were coupled and membrane Cx43 were observed. Importantly, the morphology of the heart appeared normal in heterozygous mice while in homozygous mice enlarged conus region were observed in the right ventricle (Reaume et al., 1995).

Gap junctions are abundant in the normal cervix but dramatically decreased in severe dysplasia and deficient in cervical carcinomas (McNutt and Weinstein, 1969b, McNutt et al., 1971). Immunohistochemistry on cervical biopsies showed strong expressing of Cx43 in the normal epithelium but a dramatic reduction in Cx43 in dysplasia regions (King et al., 2000, Aasen et al., 2005). GJIC was lost, and Cx43 relocated from the membrane into the cytoplasm, in HPV-positive cervical cells (Aasen et al., 2003a). Co-localisation of Cx43 and hDlg were observed on the plasma membrane of W12G cells (immortal but non-transformed cervical epithelial cells) but moved into the cytoplasm of W12GPXY cells (fully transformed cervical epithelial cells derived from W12G cells) and co-immunoprecipitation indicated the direct interaction between Cx43 and hDlg in cervical epithelial cells W12 and W12GPXY cells (Macdonald et al., 2012b). Later HPVE6 was indicated involved in this Cx43/hDlg interaction since co-immunoprecipitation of Cx43/hDlg, hDlg/E6 and E6/Cx43 was observed in cervical tumour cells W12GPXY. Transfection of HPVE6 in C33a cells (HPV-negative cervical tumour cells) led to the relocation of Cx43/hDlg from the plasma membrane (in C33a cells) into the cytoplasm (in C33aE6 cells). This relocation of Cx43 could be due to interaction between HPVE6 and hDlg since transfection of mutated HPVE6 (loss ability to bind hDlg) in C33a cells did not lead to the cytoplasmic location of Cx43 and hDlg. This Cx43/hDlg interaction was also observed in cervical tumour cells *in vivo* (Sun et al., 2015).

**Table 1: List of 14 inherited diseases associated with human connexin gene mutations.**

Taken from (Kelly et al., 2014).

<b>Inherited disease</b>	<b>Connexin gene (protein)</b>
<b>Syndromic and non-syndromic hearing loss</b>	
Most common	GJB2 (Cx26) GJB6 (Cx30)
Less common	GJA1 (Cx43), pGJA1(pCx43)/GJB3 (Cx31)/GJB4 (Cx30.3)
Auditory-linked neuropathies	GJB1 (Cx32)/GJB3 (Cx30.2/Cx29)
<b>Myelin-related disease</b>	
X-linked Charcot-Marie-Tooth disease	GJB1 (Cx32)
Pelizaeus-Merzbacher-like disease	GJC2 (Cx47)
Oculodentodigital and craniometaphyseal dysplasias	GJA1 (Cx43)
Cataracts	GJA3 (Cx46)/GJA8 (Cx50)
<b>Skin diseases</b>	
Bart-Pumphrey syndrome	GJB2 (Cx26)/GJB6 (Cx30)
Clouston syndrome	GJB6 (Cx30)
Erythrokeratoderma Variabilis (EKV)	GJB3 (Cx31)/GJB4 (Cx30.3)/GJB6 (Cx30)
Hystrix-like ichthyosis with deafness	GJB2 (Cx26)
Keratitis ichthyosis deafness syndrome	GJB2 (Cx26)/GJB6 (Cx30)
Vohwinkel syndrome	GJB2 (Cx26)/GJB6 (Cx30)
<b>Cardiovascular diseases</b>	
Atrial fibrillation	GJA5 (Cx40)/GJA1 (Cx43)
Sudden infant death syndrome	GJA1 (Cx43)

### 1.1.5 Connexins and cancer

Apart from the many diseases mentioned above, connexins are also thought to be linked to tumour progression since gap junctions are involved in controlling cell growth (growth factors passing through gap junctions or independent from the formation of gap junctions) (Moorby and Patel, 2001) and cells becoming lack of growth control, which is one of the main characteristics in cancer. In 1966, Loewenstein and colleges observed that electrical communication in healthy rat liver cells was lost in liver cancer cells. Cancer formation induced the reduction of communication in cells around and between cancer cells (Loewenstein and Kanno, 1966). Similar phenomena of the loss of intercellular communication in rat liver cancer cells, rat and hamster thyroid cancer cells were also observed (Loewenstein and Kanno, 1967, Jamakosmanovic and Loewenstein, 1968), which indicated that the loss of cellular communication is one of the identifying characteristics in cancer cells. Later in 1969, deficiencies in gap junction ultrastructure (nexuses intracellular junction) were demonstrated in human invasive cervical squamous cell carcinoma (SCC) (McNutt and Weinstein, 1969a).

Metabolic cooperation, a transferring of metabolites (hypoxanthine in their experiment) to adjacent cells, was found to be mediated by cell-cell contacts (H et al., 1969) that were identified with electron microscopy as gap junctions (Gilula et al., 1972). Metabolic cooperation between HPRT<sup>+</sup> (hypoxanthine phosphoribosyltransferase) and HPRT<sup>-</sup> cells rescued HPRT<sup>-</sup> cells from dying in HAT medium, which provided a way of measuring metabolic cooperation by measuring the release of radioactivity during co-culture of labelled HPRT<sup>-</sup> cells and unlabelled HPRT<sup>+</sup> cells in HAT medium. Metabolic cooperation was dysregulated between mouse embryonal carcinoma (EC) cells (resemble multipotential embryonic cells lacking of

HPRT) and human teratocarcinoma-derived cell lines (Nicolas et al., 1978). Tumour promoters (chemical agents with weakly carcinogenic or non-carcinogenic activity themselves that require other agents to initiate tumours), especially 12-O-tetradecanoyl-phorbol-13-acetate (TPA), blocked such metabolic cooperation in Chinese hamster cells (Yotti et al., 1979), in cocultured epidermal and 3T3 cells (Murray and Fitzgerald, 1979) and gap junctions in mouse epidermal cells (Kalimi and Sirsat, 1984). Apart from tumour promoters, tumour-associated viruses such as the avian sarcoma virus negatively affected gap junction intracellular channel permeability (Atkinson et al., 1981). This further supports the hypothesis that loss or alteration in gap junctions is a hallmark of cancer.

On the one hand, the loss of gap junctions in cancer cells could be due to the abnormal expression of gap junction proteins. For example, Cx43 levels were reduced in cervical dysplastic cells and colorectal carcinomas compared to normal epithelial cells (TJ et al., 2000, Sirnes et al., 2015). In human bladder cancer cells, Cx26 expression was reduced by upregulation of KDM5B (a demethylase at H3K4) (Li et al., 2013). However, up-regulated expression of connexins has also been observed in some cancer cells such as Cx26 in pancreatic carcinomas and colorectal cancer (Kyo et al., 2008, Ezumi et al., 2008). On the other hand, the loss of GJIC in cancer cells could be also due to the alteration of the subcellular location of gap junction proteins. For example, in cancer cells connexins located in the cytoplasm instead of on the plasma membrane. Alterations in subcellular location of connexins from the plasma membrane into the cytoplasm have been demonstrated in many cancers (for example, Cx26 in colorectal cancer cells and pancreas carcinoma (Kyo et al., 2008, Ezumi et al., 2008), Cx32 in liver cancers (Krutovskikh et al., 1994), and Cx43 in cervical cancer cells (Aasen et al., 2003b).

Since the loss of gap junction intracellular channels has been observed in many cancers, it is interesting to investigate whether the restoration of gap junctions could reverse or delay the carcinoma process in these cells. In transformed mouse embryo cells, transfection of an expression plasmid containing the Cx43 coding region led to the restoration of gap junctions and inhibited the growth of the transformed cells (Mehta et al., 1991). Expression of a gene encoding Cx43 in rat glioma cells enhanced gap junction intracellular channels and slowed their growth in vitro and in vivo (Zhu et al., 1991, Naus et al., 1992). It was hypothesised that this was accomplished possibly by the interaction between Cx43 and CCN3, which belongs to a family of Cyr61/connective tissue growth factors overexpressed in neuroblastomas (Fu et al., 2004). Small interfering RNA (siRNA) knockdown of Cx43 in breast cancer cells led to faster growth and increasing migration ability of the cells (Shao et al., 2005). Mouse models have shown that downregulation of Cx43 caused by deletion of one allele of the Cx43 gene resulted in increased susceptibility to urethane-induced lung tumours (Avanzo et al., 2004). Cx32-deficient mice showed high susceptibility to spontaneous and chemically-induced lung tumours (Temme et al., 1997), and the increasing prevalence of radiation-induced lung tumours in Cx32-knockout mice was associated with the increased activation of mitogen-activated protein kinase (MAPK) (King and Lampe, 2004). Taken together, these data demonstrate that some, but not all connexins, could act as tumour suppressors in some cancers.

The ability of connexins as tumour suppressors can vary among different tissue types and different stages of cancer and different connexin isoforms (Aasen et al., 2016). However, dye transfer has been observed between metastatic melanoma cells and bovine aortic endothelial cells that were prevented by gap junction communication blockers. The expression of Cx43 was found in metastatic melanoma cells (el-Sabban and Pauli, 1991). Since

then, increasing evidence has demonstrated the relationship between connexin expression and cancer cell migration into the blood vessels, and metastases of cancer cells, which indicates the role of connexins in helping cancer cell invasion and metastasis that is one of the hallmarks of cancer (Kotini and Mayor, 2015). Cx26 may enhance the metastasis of human melanoma cells by facilitating their communication with surrounding cells (Saito-Katsuragi et al., 2007). Increased levels of Cx43 and Cx26 and membrane location of both proteins were found in lymph node metastatic breast cancer cells (Kanczuga-Koda et al., 2006). Alternatively, the expression of Cx26 was significant linked with lymphatic vessel invasion in tumour samples from patients with breast cancer (Naoi et al., 2007). Expression of Cx43 in GJIC-deficient breast tumour cells (HBL100) showed the membrane location and connection between tumour cells and endothelial cells and an increase in diapedesis, a process involved in metastasis (Pollmann et al., 2005). Increasing expression of Cx43 was observed in the cell contact area between mouse breast tumour cells and pulmonary microvascular endothelial cells in vitro and in vivo (Elzarrad et al., 2008). Overexpression of Cx43 in mouse breast tumour cells led to their increasing attachment to lung endothelium, which required the involvement of functional gap junctions (Elzarrad et al., 2008). Injection of mouse breast tumour cells with a knockout of Cx43 (4T-1KNCx43) led to decreasing formation of microtumour, less extravasation and invasion in the brain of zebrafish compared to control (4T-1) (Stoletov et al., 2013). Injection with 4T-1KNCx43 led to decreased brain colonization and less co-option with brain vasculature in chicken compared to control (4T-1) (Stoletov et al., 2013). The metastatic gene Twist induced tumour cell extravasation and metastasis in the brain by inducing the expression of Cx43 (Stoletov et al., 2013). cGAMP transfer utilizing Cx43 gap junctions was thought to involve in brain metastasis (Chen et al., 2016). In 2017, after reviewing related studies using human tissue samples, Phillips observed the loss of GJIC in breast

cancer due to the cytoplasmic relocation of Cx43 but the increased expression and membrane localization of Cx43 in breast cancer metastasis, which indicates different roles of Cx43 in different stages of breast cancer (Phillips et al., 2017). Also, connexin expression could increase the resistance of cancer cells to chemotherapy and radiotherapy (Munoz et al., 2014, Artesi et al., 2015). The expression of Cx30 in human glioblastoma cells reduced their growth and decreased radiation-induced DNA damage and cell death (Artesi et al., 2015). Cx43 expression was observed in glioblastoma cells that showed the resistance to Temozolomide (TMZ), a frontline chemotherapeutic agent that induces cell apoptosis of Glioblastoma Multiforme (GBM) (Munoz et al., 2014). siRNA knockdown of Cx43 in GBM cells led to more cell death under the treatment with TMZ (Munoz et al., 2014). Tumour microtubes (extend ultra-long membrane or membrane connections in astrocytoma) mediated by Cx43 in brain tumour cells was demonstrated to be involved in tumour cell invasion and resistance to radiotherapy (Osswald et al., 2015). Furthermore, some connexins (e.g. Cx43) can act as oncogenes by establishing metastasis of cancer cells, but this depends on the cancer type and stage (Aasen et al., 2019).

### 1.1.6 Connexin and wound healing

Skin is the first barrier for human to prevent the invasion of bacteria and virus. Any damage to the skin will lead to wound healing as a result of lesion closure (Gantwerker and Hom, 2011). Wound healing is a complex, dynamic process that generally can be divided into four phases: Haemostasis, inflammation, proliferation and maturation/remodelling (Gantwerker and Hom, 2011). Haemostasis is a necessary step to stop bleeding immediately after onset of the lesion. This achieved by aggregation of platelet as a result of the formation of a fibrin clot (Shaw and Martin, 2009). The involvement of leukocytes and cytokines is essential in the inflammation step to prevent skin from infections from bacteria (Eming et al., 2007). Then newly formed cells are needed to fill the lesion and restore the wound, which involves many cellular processes such as cell proliferation and cell migration (Gonzalez et al., 2016). These are the sorts of processes that often involve connexins.

Growth factors synthesized by fibroblasts were stimulated by keratinocytes and can induce the proliferation of keratinocytes. Moreover, keratinocytes can modulate the differentiation of fibroblasts (Werner et al., 2007). Skin keratinocytes and fibroblasts express different types of connexins but the predominant connexin expressed is Cx43, which is normally expressed in the suprabasal layers. In a human cutaneous wound healing model generated from biopsies taken from patients and cultured in laboratory condition, first alterations were observed at 6h post-wounding when Cx43 was down-regulated at the wound edge and the protein level was continually reduced until Cx43 was virtually non-detectable within the first 1-2 days after wounding (Brandner et al., 2004). These events are regulated through a “kinase program”, where specific Cx43 CT-phosphorylation events (especially phosphorylated at S368) occur in a time-dependent manner

during wound closure (Figure 1.5) (Solan and Lampe, 2016). Solan and co-workers (Solan and Lampe, 2016) found that in response to wound, Cx43 was first phosphorylated at S373 by Akt at 5-30min, which enlarges GJ size and blocks Cx43-ZO-1 interaction (Dunn and Lampe, 2014); followed by PKC that phosphorylated at S368 at 15-60min that induced the ubiquitination and internalization of Cx43 (Richards et al., 2004).

Although Cx43 is dramatically reduced in actively migrating leading edge keratinocytes, it has been found at relatively high levels a few cell rows back from the wound edge where there are actively proliferating cells. Interestingly, in wound edge keratinocytes Cx43 is reduced as early as 5h post-wound and nearly undetectable by 24h while Cx26 and Cx30 which are normally expressed at low levels were found to be greatly increased in cells at the edge of wounds (Brandner et al., 2004). This indicates that gap junction communication might be still required for keratinocyte migration but the loss of Cx43 is a key event (Coutinho et al., 2003). However, in most non-healing wounds, instead of decreasing but abnormal increasing in level for Cx43 in the wound margin (Sutcliffe et al., 2015). Peptides targeting Cx43 has been researched and utilized to improve healing the wound (Montgomery et al., 2018a).

Factors that affect the normal wound healing process such as infection or hypoxia might lead to chronic wounds (Gantwerker and Hom, 2011). Body state of humans such as age and diabetes will also affect the wound healing process and cause chronic wound (Gantwerker and Hom, 2011). Patients suffered from chronic wounds become more prevalent due to more people with older ages and increasing incidence of diabetes. Chronic wounds severely affect the quality of life (Goodridge et al., 2005). Abnormal expressions of Cx43 were observed at the wound edge of keratinocytes in a human chronic wound, which was thought to be the response for a slow

healing in diabetes patients (Brandner et al., 2004). However, antisense of Cx43 reduced the level of Cx43 and increased the healing rate (Qiu et al., 2003). The effect of Cx43 antisense oligodeoxynucleotide (Cx43asODN) on acute wound healing has been reviewed in Becker 2012 (Becker et al., 2012). The main findings are: 1. Increasing levels of Cx43 normally occurs in the blood vessels around wound sites, and this upregulation is reduced by Cx43asODN, which reduces the leakiness of blood vessels; 2. Rapidly reduced levels of Cx43 by Cx43asODN at the wound edge in keratinocytes and fibroblasts leads to increased proliferation and migration rate of keratinocytes and fibroblasts. This results in faster wound closure resulting in faster reepithelialisation and smaller scars. There are a few antisense or Cx43 mimetic peptides that have been investigated for their therapeutic potential for the treatment of chronic wound and some of them have been developed as drugs and tested in clinical trial for example Nexagon (Lorraine et al., 2015). A peptide mimetic of Cx43 the C-terminal (alpha CT1) has shown a significant effect in increasing healing in chronic wounds and is now in Phase III clinical trials (Montgomery et al., 2018b). Mimetic peptide Gap27 inhibited Cx43-GJIC and increased the cell migration rate of both keratinocytes and fibroblasts to the wound area (Wright et al., 2009).

Chronic wounds might be treated with keratin-based treatment and after treatment, 64% (29 out of 45) of chronic wounds from patients were healed completely and over 50% reduction in wound size was observed in 8 samples (Batzler et al., 2016). Keratins are typical intermediate filament proteins that compose the cytoskeleton in epithelial cells. Their major function is maintaining the integrity of cells in response to mechanical stress such as wound healing (Moll et al., 2008). The role of keratins in epithelial cell migration has been review (Yoon et al, 2019) and might depend on interaction with actin (Kölsch et al., 2009). Keratins 6 (K6) and 16 (K16) were observed to increase at the wound edge within 6h after injury of

human epidermis (Paladini et al., 1996). Activated keratinocytes exhibit upregulated K6/16 at the onset of migration to the wound region and the expression of K6 and K16 persists until complete closure of the wound (DePianto and Coulombe, 2004). Delayed wound healing was observed in mice with knockout of keratin 6a (Wojcik et al., 2000). There is no evidence showing that Cx43 interacts with keratins, but they might interact through intermediate proteins such as beta-catenin since keratin 19 interacts with beta-catenin and enhances nuclear translocation of beta-catenin in breast cancer cells (Saha et al., 2017).

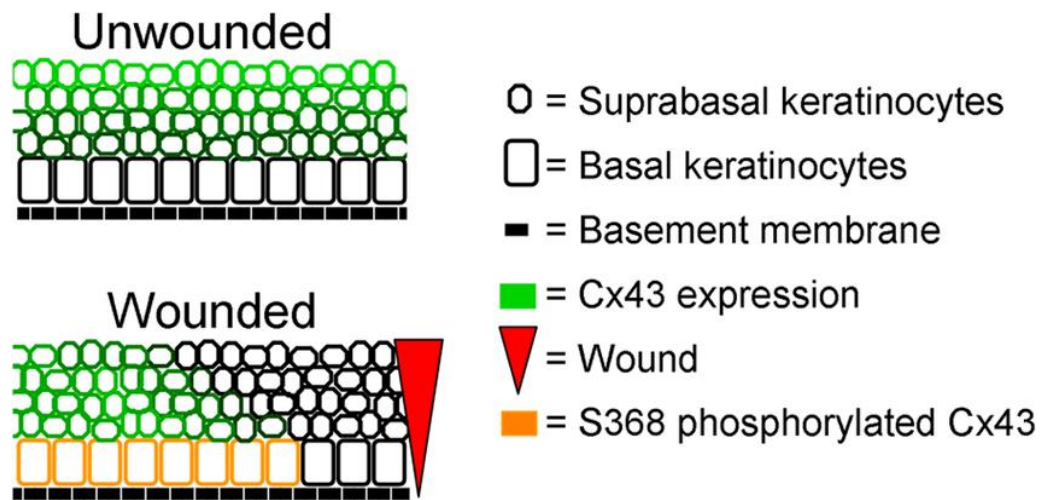


**Figure 1.5: The expression of Cx43 during the wound healing process.**

In unwounded skin, Cx43 expression (labelled in green) is mainly in the differentiated suprabasal layers. In wounded skin, the expression of Cx43 reduced at the very near the wound and redistributed into lower layers in the cells behind the wound. phosphorylated Cx43 at S368 (labelled in orange) is found in basal keratinocytes. The figure is taken from (Solan and Lampe, 2009).

## 1.2 hDlg

### 1.2.1 MAGUK proteins

Proteins belonging to the membrane-associated guanylate kinases (MAGUKs) family serve as scaffold proteins. They are enriched at cell-cell junctions and play important roles in many cellular processes including maintaining cell polarity (Ye et al., 2018). All MAGUK proteins have a distinctive domain structure: one or more PDZ domains, an SH3 domain and a guanylate kinase (GK) region. In addition to these core domains, some MAGUKs contain other motifs such as homologous to CaM kinase domain and the HOOK domain (Dimitratos et al., 1999). These protein-protein domains make MAGUK proteins recruit many other proteins such as cytoskeleton protein and signalling molecules to form a large complex, which can speed up signal transmission within some cellular processes (Dimitratos et al., 1999). MAGUKs can cluster these proteins recruited in the large complex at the plasma membrane. For example, PSD-95 protein binds directly to subunits of the K<sup>+</sup> channel and anchors it at the plasma membrane (Kim et al., 1995).

MAGUKs can be divided into several subfamilies depended on their difference of domain structure: Discs large (DLGs), zonula occludens (ZOs), palmitoylated membrane proteins (MPPs), caspase recruitment domain family (CARMA), calcium/calmodulin-dependent protein kinase (CaMK), calcium channel beta subunit (CACNB) and inverted repeated membrane-associated guanylate kinase (MAGI) (Figure 4) (de Mendoza et al., 2010). The product of *Drosophila* tumour suppressor gene Discs-large (*dlg*) was the first identified MAGUK proteins, which is located at septate junctions. Neoplastic overgrowth with loss of apical-basal polarity was observed in the imaginal discs of flies carrying a loss-function mutation in the *DLG* gene (Woods and Bryant, 1993, Woods et al., 1996a). The *Dlg* subfamily contains SAP97

(DLG1), PSD93 (DLG2), SAP102 (DLG3) and PSD95 (DLG4). All share similar domain structures with three PDZ domains, an SH3 domain and a GK domain (Figure 3)(Nithianantharajah et al., 2012). These proteins are essential in the regulation of glutamate receptors in synapses (Elias and Nicoll, 2007).

Zonula occludens made up the second MAGUK subfamily, containing ZO-1, ZO-2 and ZO-3. All of them contain three PDZ domains, an SH3 domain and a GK domain (Figure 4). They constitute the tight junctions and act as a linker between tight junction proteins and the cytoskeleton built with actin (González-Mariscal et al., 2000). CASK proteins contain one PDZ domain, an SH3 domain, a GK domain and two L27 domains (target Lin-2 and Lin-7 proteins) (Figure 4). CASK is concentrated in synapses and modulates the trafficking of synaptic vesicles and is involved in synaptic signalling transmission (Butz et al., 1998, Sheng et al., 1998). MPPs are p55-like proteins containing a single PDZ domain, an SH3 domain, and a GK domain (Figure 4). They are essential in the maintenance of the apical junction complex and involved in neuronal migration (Dudok et al., 2013). MAGIs contain several PDZ domains and an inverted GUK domain (instead of being located at the C-terminal of protein, it is located at the N-terminal) with no SH3 domain. Additionally, it contains two WW domains (Figure 4). MAGIs, enriched in the brain, modulate the trafficking of AMPA receptors in synapses and act as tumour suppressor maintaining the integrity of non-neuronal cells (Danielson et al., 2012, Nagashima et al., 2015).

Despite the variety of protein-protein domains in the proteins belonging to the different subfamily of MAGUKs, all MAGUKs share a distinct structure (except for MAGI) with one or more PDZ domains, an SH3 domain, and a GK domain (Figure 3). PDZ domains, originally named as GLGF (relatively conserved sequence of Gly-Leu-Gly-Phe) or DHR motifs (Discs-large homologous region), now are named after the name of the protein in which

they were originally identified: post-synaptic density protein with molecular weight 95kDa (PSD-95), *Drosophila* tumour suppressor (Dlg) and tight junction protein Zonula occluden-1 (ZO-1) (Ponting et al., 1997) and they are the best-characterized binding domain in all the MAGUK proteins. PDZ domains are found in many proteins other than MAGUKs from many species such as mammal, fish, flies, and even in bacteria (Ponting et al., 1997). PDZ domains are normally 80-90 amino acid regions with GLGF motifs that forming a 'pocket' for binding activity (Subbaiah et al., 2011). Data from X-ray crystallography and from specificity binding assays utilizing oriented peptide library techniques indicated that PDZ domains can bind to specific motifs with S/TXV at the C-terminal, and to other PDZ domains (Doyle et al., 1996, Cabral et al., 1996, Songyang, 1997). Src homology 3 (SH3) domains, containing approximately 60 amino acids with a proline-rich sequence, are involved in regulation of many cellular pathways such as cell migration and cytoskeletal modification (Kurochkina and Guha, 2012).

The GUK domain evolved from an ancient enzyme guanylate kinase, which catalyses the conversion of ATP-dependent GMP to GDP. However, the catalytic activity of GUK in MAGUKs has been lost and has evolved to support specific protein-protein interactions (Olsen and Brecht, 2003, Zhu et al., 2011). The crystal structure of SH3-GUK revealed that these two domains can form an integrated unit and respond to specific phosphorylated protein binding (McGee et al., 2001, Zhu et al., 2011). Besides the core domains of PDZ, SH3 and GUK, MAGUKs may also contain other domains such as a HOOK domain, a CaM kinase domain and a Lin-7-binding domain (Dimitratos et al., 1999).

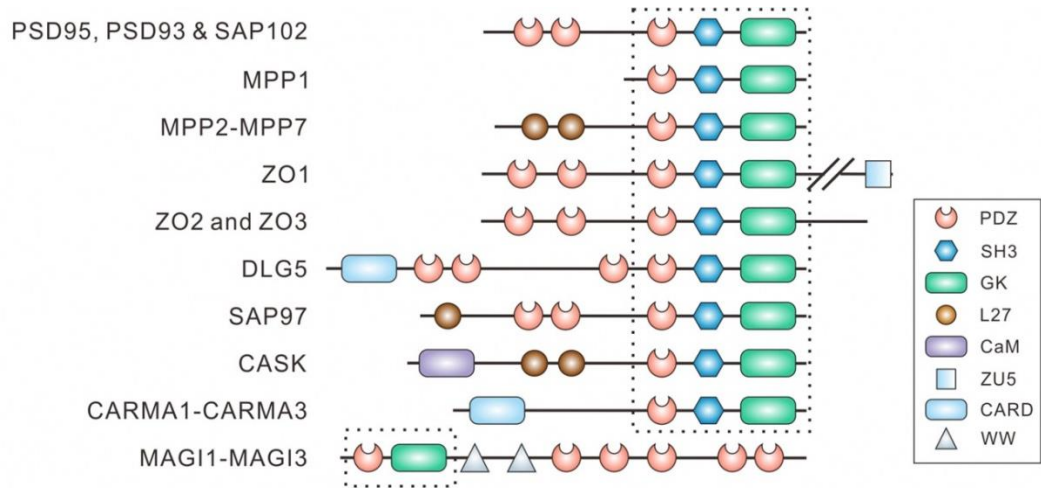


**Figure 1.6: The structure of proteins of the MAGUK families.**

Each protein belongs to membrane-associated guanylate kinase (MAGUK) contains the PDZ domains and GK domains. They also contain other functional domains such as the L27 domain in SAP97 and WW domain in MAGI 1. The figure is taken from (Ye et al., 2018).

### 1.2.2 hDlg

hDlg (human homologue of the *Drosophila* discs large protein) belongs to the MAGUK (membrane-associated guanylate kinase) family (Subbaiah et al., 2011). It contains several protein-interaction domains that can form protein scaffolds that assemble for signal transduction networks. Similar in structure to the tight junction protein ZO-1, hDlg contains an SH3 domain, a HOOK domain, a GUK domain, three PDZ domains and also an N-terminal protein-interaction domain (Matsumine et al., 1996a). Flies with a mutation in the SH3 domain lost septate junctions and there was over proliferation in the imaginal discs. This suggested that the SH3 domain in hDlg is crucial for the control of normal cell proliferation (Woods et al., 1996a). Flies with mutated Dlg such that the GUK domain was lost led to overgrowth of imaginal discs that were unable to differentiate to adult cuticle without affecting epithelial structures (Woods et al., 1996a). In transgenic flies expressing altered Dlg with loss of one or more functional domains, showed that the HOOK domain is important for membrane targeting because HOOK-mutated proteins stayed in the nucleus (Hough et al., 1997). The second PDZ domain is required for septate junction location, without which, the proteins become localised through the entire membrane (Hough et al., 1997).

Similar to Dlg in *Drosophila*, its human homologue (hDlg) is found broadly expressed in epithelial tissues and plays role in maintaining cell polarity and controlling cell proliferation (Bilder, 2004). Mutation of *Drosophila* Dlg leads to disorganized epithelial structure, therefore perturbation of intercellular junctions and loss of cell polarity (Roberts et al., 2012b). The actin and tubulin cytoskeleton were both distributed throughout the cell by loss of Dlg protein (Woods et al., 1996b). Overexpression of hDlg in mouse fibroblast

3T3 cells led to suppressed cell proliferation by blocking cell cycle progression from G0/G1 to S phase (Ishidate et al., 2000).

Loss of cellular polarity, as one of the hallmarks of cancer, leads to disruption of cell structure and increasing invasion ability to surrounding tissues (Hanahan and Weinberg, 2011). hDlg, as a regulator of cell polarity, is believed to be involved in the process of tumorigenesis (Humbert et al., 2008). Loss of membrane hDlg has been reported during cancer development such as cervical cancer, colon cancer and endometrial cancer (Watson, 2002, Gardiol et al., 2006, Sugihara et al., 2016). Patients with endometrial cancer with loss of expression of hDlg showed poor overall survival than those with membrane-expression of hDlg (Sugihara et al., 2016).

Endometrial cancer cells KLE with stable depletion of hDlg showed increased ability in both migration and invasion than control KLE cells (Sugihara et al., 2016). Cancer-causing human papillomavirus (HPV) oncoprotein E6 has a PDZ-binding motif (X-T/S-x-L/V) at its C-terminal, through which, HPV E6 can bind a large number of proteins containing PDZ domain such as hDlg (Thomas et al., 2008).

The second PDZ domain of hDlg is the target for HPV E6 and HPV18E6 bound to hDlg about 5-times stronger than HPV16-bound (Liu et al., 2007). Through this interaction, HPV E6 targets hDlg for proteasome-mediated degradation (Gardiol et al., 1999, Pim et al., 2000). In addition to HPV E6, other viral oncoproteins can also bind to hDlg. For example, adenovirus type 9 oncoprotein encoded by E4 region ORF1 binds to the second PDZ domain of hDlg (Lee et al., 1997). In human T-cell leukaemia virus type 1 (HTLV-1)-infected T-cells, oncoprotein Tax, utilizing its C-terminus, binds to hDlg and prevents hDlg-APC binding (Suzuki et al., 1999). Somatic point mutations were observed in the gene encoding the second PDZ domain of hDlg in

mammary ductal carcinoma (Fuja et al., 2004), which is the binding domain for APC (Matsumine, Ogai et al. 1996).

hDlg, as a PDZ-domain containing protein, interacts with many other proteins that contain the PDZ-binding domain. For instance, hDlg can bind to a PDZ-binding motif located at the C-terminal of APC (adenomatous polyposis coli), another tumour suppressor protein involved in the Wnt signalling pathway (Goode and Perrimon, 1997, Matsumine et al., 1996a). The APC-hDlg interaction is important in the negative regulation of the cell cycle (Ishidate et al., 2000). hDlg with its second PDZ domain binds to PTEN, a tumour suppressor phosphatase, at its C terminus that contains a PDZ-binding motif, which stabilizes PTEN (Valiente et al., 2005). hDlg (SAP97) binds to PBM of aquaporin-2 (AQP2) with its second PDZ domain. This interaction regulates PKA-mediated phosphorylation at Ser256 of AQP2 in response to arginine-vasopressin (AVP), which induces the AQP2 translocation from storage vesicles to the membrane in kidney-derived LLC-PK1 cells (Nooh et al., 2019).

Loss of Dlg led to the disruption of the network of actin and tubulin (Woods et al., 1996b). hDlg (SAP97) colocalised with F-actin at the plasma membrane in CACO-2 cells (a colon epithelial cell line), which is redistributed to the cytoplasm under the reduction in levels and cytoplasmic relocated F-actin caused by drug treatment (Reuver and Garner, 1998). E-cadherin mediated the localisation of hDlg at cell-cell adhesion sites attached to the cortical cytoskeleton (Reuver and Garner, 1998). Although hDlg is unable to bind to E-cadherin and beta-catenin directly, hDlg seems to form a supermolecular complex since E-cadherin interacts with alpha- and beta-catenin and APC, beta-catenin bound to actin (Reuver and Garner, 1998, Subbaiah et al., 2012, Matsumine et al., 1996b). Overexpression of beta-catenin led to an increase in proteasome-degradation of hDlg, while

siRNA depletion of beta-catenin enhances the stability of hDlg (Subbaiah et al., 2012). Protein 4.1R, a family of cytoskeletal proteins, is reported to bind to the HOOK domain of hDlg, which is important for hDlg membrane targeting (Hanada et al., 2003, Hough et al., 1997). There is another domain, named as L27 (lin-2 Lin-7) domain, located at the N-terminus of hDlg, which mediates the membrane targeting of hDlg in epithelial cells (Wu et al., 1998, Doerks et al., 2000, Lee et al., 2002).

hDlg has been reported to interact with gap junction proteins. hDlg interacts with Cx32 Ct with its GUK domain (Stauch et al., 2012), and was originally identified as a binding partner for Cx43 in a tandem mass spectrometry analysis of normal rat kidney cell lysates (Singh and Lampe, 2009). Previously we demonstrated the interaction between Cx43 and hDlg in HPV-positive cervical tumour cells. Due to the fact that HPVE6 binds to hDlg, we proposed that the trafficking of Cx43 to the plasma membrane is controlled by the HPVE6-hDlg interaction (Macdonald et al., 2012b).

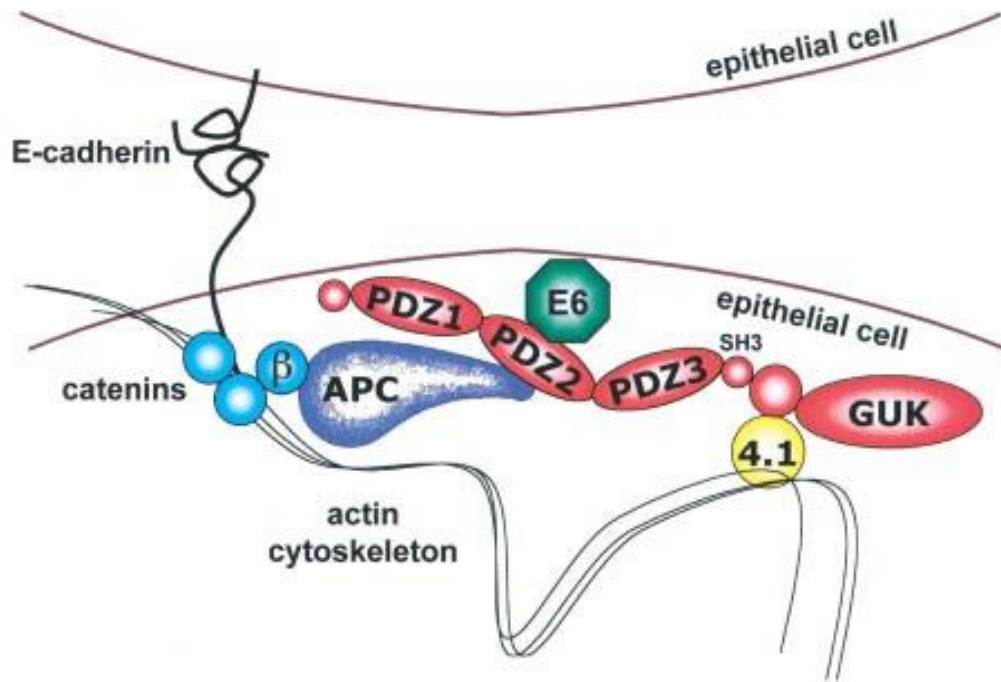


**Figure 1.7: The structure of hDlg and its binding partners.**

hDlg (indicated in red) contains three PDZ domains, one SH3 domain and one Guanylate kinase (GUK) homology domain, which allows it to bind to other proteins. HPVE6 binds to the second PDZ domain of hDlg. APC also binds to the same PDZ domain as HPVE6. Protein 4.1 connected hDlg to actin. The figure is taken from (Mantovani and Banks, 2001).

## 1.3 HPV16 E6

### 1.3.1 HPV

Papillomaviruses (PVs) together with polyomaviruses were thought previously to belong to the Papoviridae family but later were identified as individual taxonomic families (papillomaviridae and polyomaviridae) in the 7th report of the International Committee on Taxonomy of Viruses (ICTV) (Fauquet and Mayo, 2001). The family of papillomaviridae was officially nominated in the 8th report of the ICTV and the PV research community in 2005 (Fauquet et al., 2005). The more research carried on them, the more PV subtypes have been widely identified throughout the animal kingdom such as in birds, mammals and humans. There are over 240 subtypes of papillomavirus classified in 37 genera and the number keeps increasing (Van Doorslaer, 2013). The classification of the papillomaviridae family is defined based on the homology of the L1 nucleotide sequence (Bernard et al., 2010). The L1 gene is the most conserved gene within all the PVs genomes, therefore it is used to identify novel PV types and construct the phylogenetic trees (de Villiers et al., 2004) (Figure 1.8). In this classification, the PV types, subtypes and variants are dependent on the dissimilarity in the L1 gene region such that dissimilarity over 10% is identified as a new PV type; the dissimilarity between 2 - 10% is identified as a new subtype and when it less than 2% is thought to be a variant (de Villiers et al., 2004). In this classification, different genera are named utilizing Greek letters. After all the Greek alphabet was used, the prefix “dys” was employed and to restart the Greek alphabet, but omitting Alpha, Beta and Gamma letters due to these PV genera contain the most medically significant HPVs (Bernard et al., 2010). For nomenclature, the abbreviation of the host as initial letter followed by PV (refer to papillomavirus) and the number for the reference

sequence published. For example, HPV stands for the papillomavirus from the host of human or Homo sapiens (Bernard et al., 2010).

The taxonomy history of HPV dates back to the 1970s when isolating papillomavirus from human tissue started. With the development of isolating technology and cell biology, more and more HPV types were found (de Villiers, 2013). Currently, there are now 226 HPV types established in PaVE (<https://pave.niaid.nih.gov/>) where the highest number is HPV225 due to the withdrawn of four previous categorised HPV types (HPV46, HPV55, HPV64 and HPV79) in PaVE. These four HPV types were withdrawn because they are thought to be a subtype of other HPV types. For example, the genome of HPV55 shares 95% homology to that of HPV44 (between 2 - 10%), therefore HPV55 is thought to be a subtype of HPV44 (de Villiers et al., 2004). Phylogenetically, HPV can be divided into five evolutionary genera: alpha, beta, gamma, mu and nu. There are 14 groups of HPV in the alpha-papillomavirus, 5 groups of HPV in the beta-papillomavirus and 17 groups of HPV in the gamma-papillomavirus while just one group of HPV in either mu- and nu-papillomavirus (Figure 1.9) (de Villiers, 2013).

Apart from this classification, HPV, based on the tissues where it comes from, can be divided into cutaneous or mucosal-infective (de Villiers, 2013). According to whether they cause cancer or not, HPVs can also be divided into low-risk types and high-risk types. Where high-risk HPV such as HPV16 and HPV18 are the cause for cervical cancers and low-risk HPV such as HPV6 and HPV11 causes genital warts (Burd, 2003). HPV type 16 and 18 are responsible for 70% of all cervical cancers. In particular, HPV 16 causes around 55% of all HPV infections of women depending on geographical location and economic status (Crosbie et al., 2013).

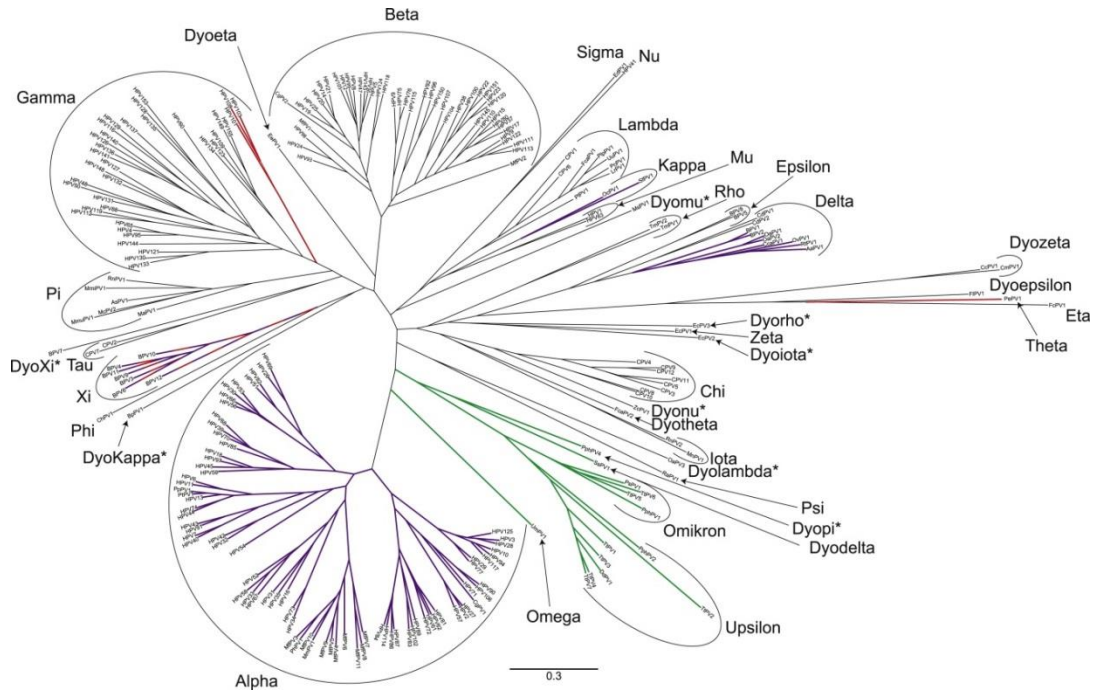


**Figure 1.8: The phylogenetic tree of the papillomavirus.**

The phylogenetic tree is generated based on the sequence of the L1 gene of papillomaviruses, obtained from 241 papillomaviruses on the PaVE website. The tree is coloured based on the presence/absence of the E5, E6 and E7 proteins. The red clades indicate the lack of E6, and the green indicate the lack of E7. The purple clades indicate these viruses contain E5. The figure is taken from (Van Doorslaer, 2013).

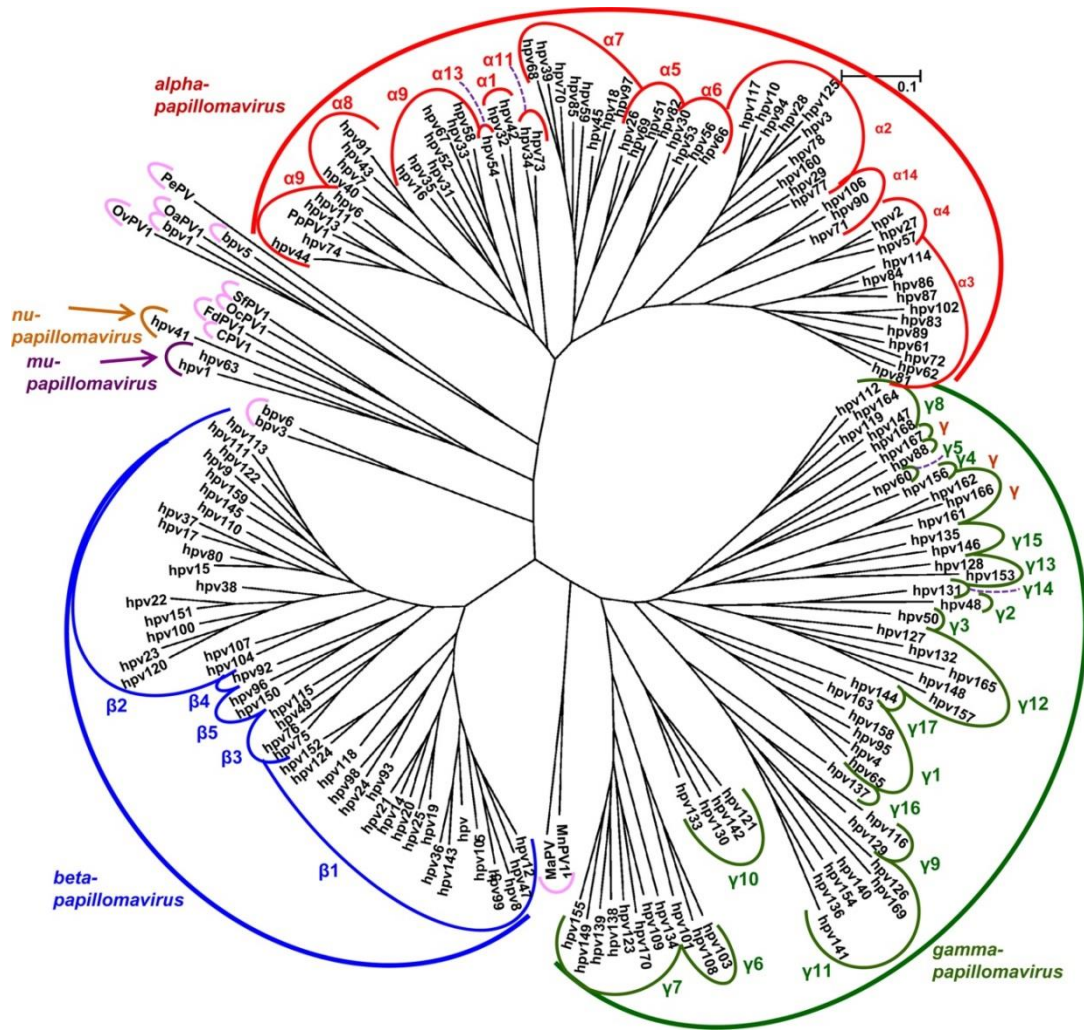


**Figure 1.9: The classification of HPVs.**

The phylogenetic tree is generated based on the L1 ORF sequences of 170 HPV types. HPV can be divided into five evolutionary genera: alpha (red), beta (blue), gamma (green), mu (purple) and nu (Ai et al.). The figure is taken from (de Villiers, 2013).

### 1.3.2 HPV and cancer

The DNA of HPV was firstly isolated from common warts of human skin (Gissmann and Hausen, 1976, Gissmann et al., 1977). The isolation of HPV16 and HPV18 from cervical cancer biopsy samples supports the hypothesis of German researcher Harold Zur Hausen that HPV is strongly associated with cervical cancer (zur Hausen et al., 1976, Durst et al., 1983, Boshart et al., 1984). This discovery led to him receiving the Nobel Prize in Physiology or Medicine in 2008. With deeper research, HPV is also been demonstrated in association with other cancers such as anal cancer, penile cancer and head and neck cancer (HNC) (Burd and Dean, 2016).

Cervical cancer is ranked as the fourth leading cause of cancer death in women with an estimated 570,000 cases and 311,000 deaths in 2018 worldwide, which occupied 6.6% in the incidence and 7.5% in the mortality in 10 most common cancer in women in 2018 (Bray et al., 2018). It is the most frequent cancer in 28 countries mainly in the south and west of Africa and the leading cancer cause of death in 42 countries mainly in Africa (Bray et al., 2018). In the UK, it is estimated that there are 3430 women diagnosed with cervical cancer and 1033 die from it each year and 79% of invasive cervical cancers are contributed to HPV16/18. It is the second most common diagnosed cancer among women in the UK with the age ranged from 15 to 44. In China, every year it is estimated that there are 106430 women diagnosed with cervical cancer and 47739 died from it and 69.1% of invasive cervical cancers are contributed to HPV16/18. It is the 3<sup>rd</sup> most frequent cancer in women in China with the age ranged from 15 - 44 (HPV information centre, <https://www.hpvcentre.net/datastatistics.php>).

Although most HPV infections will be cleared by the immune system, the antibodies produced by natural infections are normally not enough for

protection against reinfections (Schwarz et al., 2010). Therefore, vaccines are required to ensure high and sustained antibody levels to provide protection from HPV infections. Currently, three HPV vaccines are licensed: Cervarix®, a bivalent HPV vaccine targeting HPV16 and HPV18, which are responsible for most cervical cancer cases; Gardasil®, a quadrivalent vaccine targeting HPV16 and HPV18 and additionally HPV6, HPV11; and Gardasil 9, a nonavalent vaccine targeting HPV31, HPV33, HPV45, HPV52, and HPV58 in addition to those targeted by the Gardasil quadrivalent vaccine (Wang et al., 2020). These vaccines have been utilized and significantly reduces cervical HPV infections (Harper and DeMars, 2017) and cervical diseases (Palmer et al., 2019).

Normally, high-risk HPVs infections will be eventually cleared by the immune system over a period of time. However, about 10-15% of infected women failed to mount a successful immune response and the persistent viral infection will lead to the development of cervical cancer (Stanley, 2010). Cancer progression is not the ideal outcome for the virus because the carcinoma progression abrogates the viral replication cycle in the infected cells and no virions are produced (Graham, 2017). The cervical disease can be divided into a three-stage system (cervical intraepithelial neoplasia (CIN)) or a two-stage system (squamous intraepithelial lesion (SIL)) with the increased expression of oncoprotein HPV E6 and E7 from CIN1 to CIN3 (Baldwin et al., 2003, Doorbar et al., 2015).

Human papillomavirus can only infect epithelial cells and reproduce itself through the differentiation of host cells (Figure 10). The initial infection starts from an entry of viral particles into cells of the basal layer of the epithelium presumably via micro-wounds. Following infection, the viral episomal genome is maintained in a low copy number in the basal epithelium with a low expression level of early proteins E6, E7, E2 and E1

(Doorbar, 2005). For normal epithelial basal cells when they undergo proliferation they can undergo migration to the suprabasal layers and terminal differentiation (Graham, 2017). With the proliferation of basal cells, HPV genomes are also replicated and once these cells begin to differentiate, they carry the HPV genomes to the suprabasal layer of the epithelium. E1 and E2 bind to the origin of the replication region in the Upstream Regulatory Region (URR) in the viral genome (McBride, 2013). They replicate the viral genome utilizing the host DNA replication machinery. E6 and E7 from high-risk HPVs interact with p53 and pRb respectively so that they modulate the cell cycle: abolish the restraints on cell cycle progression, degrade p53 so that abnormally dividing cells do not die and retard terminal differentiation (Pol and Klingelutz, 2013, Roman and Munger, 2013). L1 and L2 are structural proteins that form the viral capsid. They are synthesised in the uppermost epithelial layers that support the assembly of viral particles (Graham, 2017). Expression of these HPV antigens is delayed until they reach the surface of the epithelium so that the immune system is unable to detect HPV replication in the lower epithelial layers (Stanley, 2012).

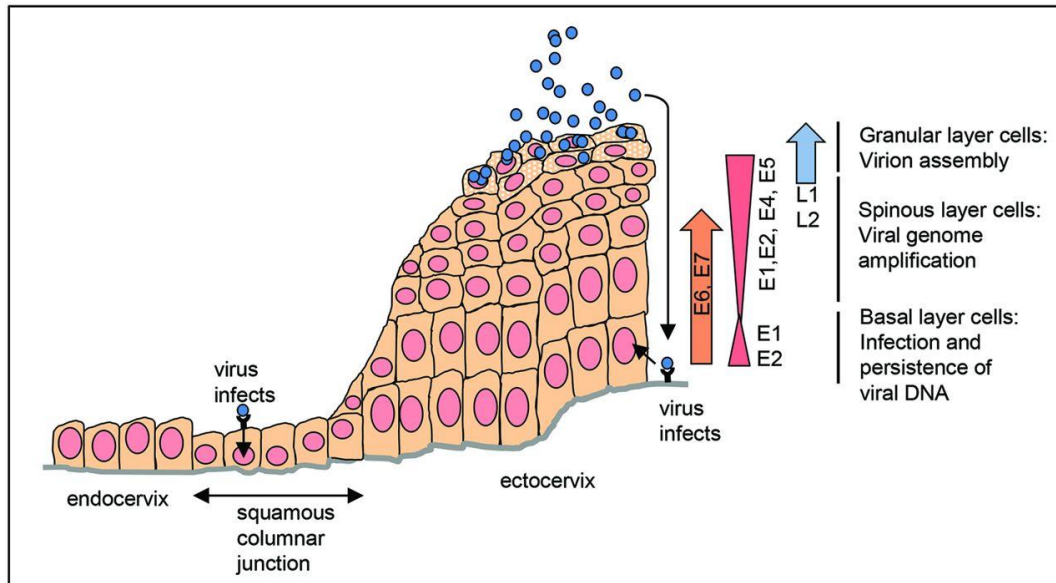


**Figure 1.10: The life cycle of HPV depends on the differentiation of epithelial.**

HPV infects the basal layer cells of the epithelium. With the division and differentiation of infected basal layer cells, viral genomes are segregated into daughter cells and carried into upper differentiated layers. The viral expression during the differentiation of keratinocyte is indicated on the right-hand side. Nuclei are shown in pink. The figure is taken from (Graham, 2017).

### 1.3.3 HPV genome

HPV is a circular double-stranded DNA virus with a genome length of around 8000bp. The genome of HPV can be divided into three parts: 1) the early (E) region encoding viral proteins (E1, E2, E4, E5, E6 and E7) that regulate the cellular function in infected cells, within which high-risk HPV E6 and E7 are defined as oncoproteins (Roman and Munger, 2013, Pol and Klingelutz, 2013). 2) The late (L) region that encodes late proteins (L1 and L2) which are the structural proteins responsible for the formation of the virus capsid (Buck and Trus, 2012). 3) The LCR (long control region), also called the upstream regulatory region (URR) that is located between L1 and E6 (Van Doorslaer et al., 2017)(Figure 11 ). The LCR contains no open reading frames (ORF) but the transcription start site of E6 promoter (P97) in HPV16, transcriptional enhancers or activators, silencers or repressors and other cis-regulatory sequences (Bernard, 2013).

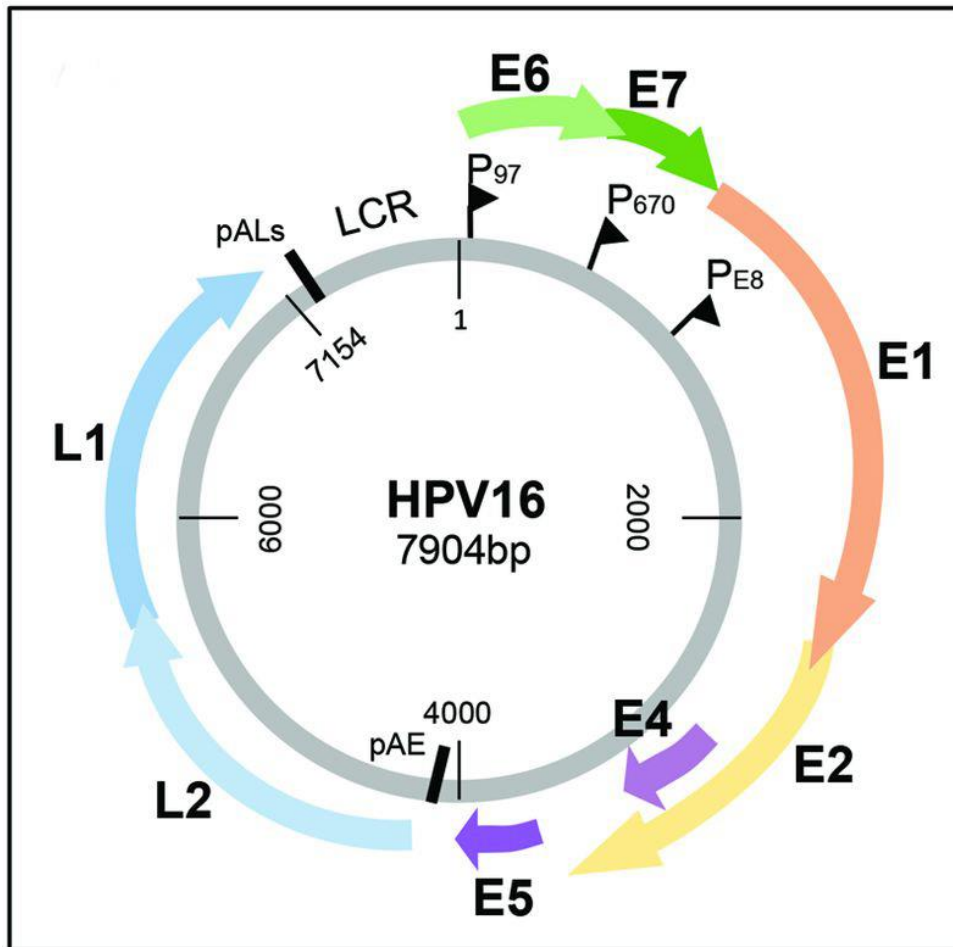


**Figure 1.11: A schematic diagram of HPV16 genome.**

HPV16 encodes six early proteins (E1, E2, E4, E5, E6 and E7) and two late proteins (L1 and L2). Promoters are indicated with P (e.g. P97). HPV16 also contains a long control region (LCR). The figure is taken from (Graham, 2017).

### 1.3.4 HPVE6

E6 and E7 proteins from high-risk HPVs (such as HPV16/18) act as oncoproteins and are important for the stimulation of cell growth and cell transformation. Utilizing this property, HPVE6 and E7 can immortalize several human cell types (Münger and Howley, 2002). Low levels of E6 and E7 is observed in CIN I (mild dysplasia) and CIN II (moderate dysplasia) lesions in which the viral genomes replicate episomally, but in CIN III (severe dysplasia, carcinoma in situ) where the viral genome is often intergraded into the host genome, the high levels of E6 and E7 are observed. In a word, during the carcinoma progression, the high-risk HPV genome integrates into the host genome leading to the overexpression of viral oncoprotein E6 and E7 (Narisawa-Saito and Kiyono, 2007).

HPV16 E6 is a basic nuclear protein with a molecular weight of 18 kDa and 151 amino acids. It contains four Cys-X-X-Cys motifs forming two zinc finger domains that directly bind to zinc and a PDZ-binding domain at its very end of the C-terminus (Thomas et al., 2008, Kanda et al., 1991). A schematic representation of high-risk HPV E6 and its binding proteins is shown in Figure 12. Although E6 is a small protein, as one of the HPV oncoproteins, it has effects on many cellular progress that are involved in the HPV viral life cycle, inhibition of immune-response, immortalization and transformation of cells, inhibition of cell apoptosis and differentiation and further leading to cancer (Narisawa-Saito and Kiyono, 2007). For oncogenic function of E6, the first insight is its interaction with p53. p53 is a well-known tumour suppressor protein that regulates the expression of proteins involved in the control of the cell cycle or the apoptosis process when the cell is facing cellular stress or DNA damage. In response to DNA damage, p53 is activated and arrests the cell cycle at G1 by inducing the expression of p21WAF1 (senescent cell-derived inhibitor) and at G2/M, as well as leading to

apoptosis (Ozaki and Nakagawara, 2011). In cervical cancer and head-and-neck cancers caused by high-risk HPV, degradation of p53 by viral oncoprotein E6 is observed (Pol and Klingelhutz, 2013). E6 binds to ubiquitin ligase E6AP at a short leucine (L)-rich sequence LxxLL through its zinc-binding domains. The E6/E6AP complex then results in recruitment and ubiquitination and subsequent degradation of p53 (Martinez-Zapien et al., 2016). Appropriate nuclear distribution of p53 is important for the expression of proteins regulated by p53. Therefore, abnormal cytoplasmic location leads to loss-of-function of p53 (Ozaki and Nakagawara, 2011). In cervical cell lines, blocking the E6-induced degradation of p53 led to an increasing level of p53 but the p53 was located in the perinuclear area and not in the correct nuclear location (Mantovani and Banks, 1999). Only high-risk HPV E6 can induce the ubiquitin degradation of p53, low-risk HPV E6 is able to bind to p53 with relatively low affinity but unable to induce the degradation of p53. Only high-risk HPV E6 binds to the core domain of p53, while both high-risk and low-risk HPV E6 bind to the C-terminal domain of p53 (Pietsch and Murphy, 2014).

HPV E6 is important for immortalizing several human cell types. However, the immortalization ability is not p53-dependent. HPV16 E6 mutants that were unable to induce the degradation of p53 retained the ability to immortalize human mammary epithelial cells (Liu et al., 1999). One of the important onco-functions is that E6, only from high-risk HPV but not low-risk HPV, contains a PDZ (PSD-95/Dlg/ZO-1) binding domain allowing its association with the proteins of the PDZ-containing family such as hDlg, Scrib, MAGI (Ganti et al., 2015). Through this PDZ-binding domain, HPV E6 targets many PDZ-containing proteins for proteasome-mediated degradation, the majority of which are related to the regulation of cell polarity (Nagasaka et al., 2013a). The PDZ-binding motif (PBM) (sequence x-S/T-x-V/I/L) of HPV16 E6 is located at the extreme end of the C-terminus. This

interaction between HPVE6 and PDZ-containing proteins is important in the viral life cycle and is thought to stabilize HPVE6 protein in a PBM-dependent manner during the early stage of the viral life cycle (Nagasaka et al., 2013b). The importance of this interaction is confirmed by transgenic mice experiments where mutated HPV16 E6 lacking the PDZ-binding motif retained the ability to inactivate p53 but failed to display epithelial hyperplasia which is normally seen in wild-type E6 transgenic mice (Nguyen et al., 2003).

Another important role of HPV E6 is its contribution to cellular transformation, of which telomerase is involved. Human telomerase is a ribonucleoprotein enzyme that is composed of at least two parts: a template RNA component hTR (human telomerase RNA) and a catalytic subunit hTERT (the telomerase reverse transcriptase). As a cellular reverse transcriptase, it synthesises and elongates the telomeric DNA (Pendino et al., 2006). Telomerase is normally expressed in germ-line cells and its absence in somatic cells results in telomere shortening and somatic cell ageing. However, in many cancer cells, the activity of telomerase is reconstituted (Pendino et al., 2006). hTERT gene transfected into normal human somatic cells led to the reconstitution of the telomerase activity, elongated telomere and extended life span of cells (Bodnar, 1998). HPVE6 activates the activity of telomerase in human keratinocytes (Klingelhutz et al., 1996). This activation of telomerase is achieved by HPV E6 induced expression of hTERT, in which Myc and Sp-1 are thought to be involved (Oh et al., 2001). In the presence of HPVE6, Myc binds to the promoter of hTERT and replaces the repressors USF1 and USF2, as a result of increasing levels of hTERT and furthermore the activation of telomerase (McMurray and McCance, 2003, Veldman et al., 2003). NFX1-91, a novel repressor of the hTERT promoter, is degraded in the presence of E6/E6-AP so that Myc is able to bind the promoter of hTERT and further increase the telomerase activity (Gewin,

2004). Besides these interactions, HPVE6 has many other binding partners that are involved in many cellular pathways such as CBP/p300 involved in down-regulation of p53 activity; and Bak involved in the apoptosis process (Narisawa-Saito and Kiyono, 2007).

Specifically, for this project, HPV16 E6, via its PDZ-binding domain, targets hDlg (human discs large protein; a protein containing PDZ domains (Subbaiah et al., 2011) for proteasome degradation. The forms of hDlg in the nucleus and cytoplasm are mainly targeted while membrane-bound forms are unaffected (Ganti et al., 2015). hDlg is a tumour suppressor. For example, it could prevent the transformation of primary baby rat kidney (BRK) cells induced by HPV E7/ras (Massimi et al., 2004). This ability of hDlg to suppress cell growth could be overcome by HPVE6 that targets hDlg and for degradation (Massimi et al., 2004). In terms of Cx43, a building block of gap junctions, was observed to a dramatic reduction in level in dysplasia regions of cervical biopsies while it strongly expressed in the normal epithelium (King et al., 2000, Aasen et al., 2005). Overexpression of Cx43 in HeLa cells (HPV-positive cervical cancer cells) led to decreased saturation density and reduced cell growth rate (Aasen et al., 2003a, J.King et al., 2000). It may be that the ability of hDlg to suppress cell growth relies on correct GJIC communication, and HPVE6 interference with Cx43/hDlg functionality may give a growth advantage to increase keratinocyte proliferation. This could lead to increased viral replication that might result in cellular transformation following increased HPV E6 and E7 expression.

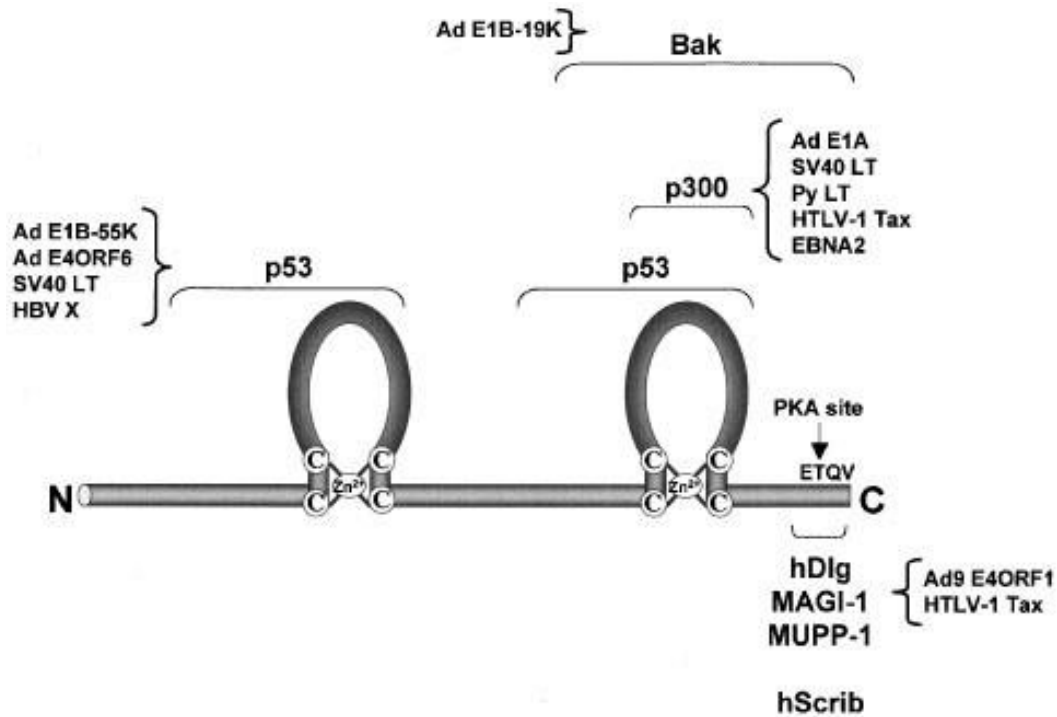


**Figure 1.12: A schematic diagram of the structure of HPVE6 and its binding partners.**

HPVE6 contains two zinc fingers and the regions interacted with cellular proteins targeted by other viral oncoproteins. There is a PDZ binding motif located at the C-terminus of HPVE6 that allows its binding to PDZ-containing proteins such as hDlg and hScrib. The figure is taken from (Mantovani and Banks, 2001).

## 1.4 Hypothesis and aims

The hypothesis that this study addresses is that hDlg controls the trafficking of gap junction protein Cx43 and maintains its cellular levels.

Aim 1: To investigate the interaction of Cx43/hDlg in normal epithelial cells.

- a. To identify the subcellular location of Cx43 and hDlg in normal epithelial cells.
- b. To investigate the alteration in protein level and subcellular location of Cx43 in normal epithelial cells with the siRNA knockdown of hDlg.
- c. To investigate Cx43 trafficking by examining the effect of lysosomal inhibition in the protein level of Cx43 in HaCaT cells.

Aim 2: To investigate the alteration of Cx43 during the wound closure process in HPVE6 positive and negative cells.

- a. To identify the subcellular location of Cx43 and hDlg in HaCaT and NIKS cells.
- b. To identify the alteration in protein levels of Cx43/hDlg in normal epithelial cells during wound closure.
- c. To investigate the wound healing speed in normal epithelial cells with or without siRNA knockdown of hDlg.
- d. To investigate the behaviour of HPV-positive cells during the wound healing process.

Aim 3: To investigate the region of the Cx43 CT that interacts with hDlg and whether selected phosphorylation site point mutations on Cx43 CT affect its interaction with hDlg.

## **2 Chapter 2 Materials and methods**

### **2.1 Materials**

#### **2.1.1 Cell culture reagents**

Dulbecco's Modified Eagle Medium (DMEM), fetal bovine serum (FBS), L-glutamine, penicillin and streptomycin (P/S) and trypsin were purchased from Gibco™ by life Technologies, Renfrew, UK. Keratinocyte basal medium (KGM) was purchased from Lonza, Slough, UK.

#### **2.1.2 Common chemicals and buffer**

All chemicals were purchased from Sigma Chemical Co., Irvine, UK except the following:

Protease inhibitor cocktail tablets and phosphatase inhibitor cocktail tablets were purchased from Roche, Welwyn Garden city, UK.

High-performance chemiluminescence film was purchased from GE Healthcare, Hatfield, UK.

Trizol reagent was purchased from Ambion, Renfrew, UK.

All the buffers were prepared or purchased following the comments in Table 2.1.

**Table 2.1: Buffers**

solution	comment
Coomassie stain solution	0.02% (w/v) Coomassie Brilliant Blue TM, 50% (v/v) methanol, 7% (v/v) acetic acid
Destain solution	5% (v/v) methanol, 10% (v/v) acetic acid
PBS	170mM NaCl, 3.4mM KCl, 10mM Na <sub>2</sub> HPO <sub>4</sub> , 1.8mM KH <sub>2</sub> PO <sub>4</sub> , pH7.2
PBS-Tween	PBS containing 0.1% (v/v) Tween 20
0.5% NP40 lysis buffer	50mM Tris-HCl pH 8.0, 150mM NaCl, 0.5% (v/v) NP40 (TGPAL CA-630), protease and phosphatase inhibitor cocktail (one tablet of each inhibitor in 10 ml NP40 lysis buffer)
MES SDS running buffer (20X)	Invitrogen, Renfrew, UK, ref no B0002

### 2.1.3 Antibodies

The antibodies used in western blotting and immunofluorescence experiments are list in Table 2.2 along with the dilution they were used and their source.

**Table 2.2: List of antibodies, source and dilution.**

Antibody	Species	Dilution	Source	Reference Number
Cx43	Rabbit	1:2000 (WB)	Sigma	C6219
Cx43	Rabbit	1:2000 (IF)	Gift from Dr Leithe	Institute for Cancer Research, The Norwegian Radium Hospital, Montebello, N-0310 Oslo, Norway.
hDlg	Mouse	1:1000 (WB)  1:200 (IF)	Santa Cruz	Sc-9961
HPV18E6	Mouse	1:500 (WB)	Santa Cruz	Sc-365089
GAPDH	Mouse	1:1000 (WB)		
Anti-mouse IgG HRP	Donkey	1:1000 (WB)	Thermo scientific	SA1-100
Anti-rabbit IgG HRP	Donkey	1:1000 (WB)	Thermo scientific	SA1-200
Anti-rabbit IgG	Goat	1:5000 (WB)	Thermo scientific	35568
Anti-mouse IgG	Goat	1:5000 (WB)	Thermo scientific	35521
Alex488 anti- mouse IgG	Donkey	1:1000 (IF)	Life technology	A21202
Alex555 anti- rabbit IgG	Donkey	1:1000 (IF)	Invitrogen	A31572

## 2.1.4 Bacteria culture

The BL21 *E. coli* strain (gift from Dr. Li Ping, Centre for virus research, Glasgow) was used for plasmid transformation and GST-protein purification. L-broth (10g NaCl, 16g Bactopeptone, 5g yeast extract in 1 litre H<sub>2</sub>O, pH 7.5) was used to grow bacteria. Agar plates made of 1.5% (w/v) agar in L-Broth was used to grow bacteria. When necessary, 100 µg/ml ampicillin or 0.5 M IPTG (SIGMA, Irvine, UK, ref no 16758) were added to the bacteria culture.

## 2.1.5 Cell lines

C33a: HPV negative but p53 mutated cervical carcinoma cell line (Crook T, 1991).

C33aE6: C33a cells with stable transfection of a plasmid expressing HPV16E6 (Sun et al., 2015)

HeLa43: HeLa cells (transformed cervical epithelial adenocarcinoma cell line) with stable expression of Cx43 (Johnstone et al., 2010)

HaCaT: HPV negative spontaneously immortalized aneuploid human keratinocytes cell line (Boukamp et al., 1988).

HEK293: human embryonic kidney 293 cell line (ATCC, [https://www.lgcstandards-atcc.org/products/all/crl-1573.aspx?geo\\_country=gb](https://www.lgcstandards-atcc.org/products/all/crl-1573.aspx?geo_country=gb))

NIKS: spontaneously immortalized human keratinocyte cell line (Allen-Hoffmann et al., 2000)

NIKS16: NIKS cells stable transfected with the HPV16 genome (Isaacson Wechsler et al., 2012)

J2-3T3 cells (3T3 cells): Fibroblast J clone cell line from random-bred swiss mouse.

HaCaT shDlg: HaCaT cells with stable knockdown of hDlg (Massimi et al., 2012)

## **2.2 Methods**

### **2.2.1 Small scale preparation of plasmid DNA (mini preps)**

The small-scale extraction of plasmid DNA prepared from bacterial culture was carried out using the QIAprep® spin miniprep kit (Qiagen, Manchester, UK, cat no 27104) following the manufacturer's instruction. Briefly, a single colony of transformed bacteria was selected and dipped into 5 ml of L-broth containing 100µg/ml ampicillin shaking incubation overnight at 37°C. Overnight-incubated bacterial solution was then pelleted at 14000 rpm for 4 minutes at room temperature. The supernatant was discarded, and the pellet was re-suspended in 250µl buffer P1 (containing 100µg/ml RNase A) followed with gentle mixing with 250µl buffer P2 (lysis buffer). After 5 minutes of incubation at room temperature, 350µl buffer N3 (neutralization solution) was added to the lysate. Cell debris was removed by centrifugation at 14000 rpm for 10 minutes at room temperature. The supernatant containing the plasmid DNA was transferred to a QIAprep spin column and centrifuged at 14000 rpm for 1 minute at room temperature. After two washes with wash buffer, the column was further centrifuged for 1 minute at 14000 rpm at room temperature to ensure no residual wash buffer was left. Buffer EB (elute buffer) was added to the column, incubated at room temperature for 1 minute and followed with 1-minute centrifugation at 14000 rpm at room temperature. After concentration was measured by nano-drop, the DNA solution was stored at -20°C.

### **2.2.2 Large scale preparation of plasmid DNA (midi-preps)**

Larger amounts of plasmid DNA were obtained from bacterial culture using the QIAGEN plasmid midiprep kit (Qiagen, Manchester, UK, cat no. 12943) following the manufacture's instruction.

### **2.2.3 PCR mediated site-directed mutagenesis and recombinant DNA**

The GST-tagged human Cx43 plasmid pGEX2T-Cx43 was used as the template to carry out PCR-mediated site-directed mutagenesis. The primers were designed to allow mutation of Ser residues to Alanine (Table 2.3). The PCR reactions were carried out according to the manufacturer's protocol. The PCR product was treated with a cloning enhancer (Takara Clontech, Saint-Germain-en-Laye, France) and the plasmids were cloned using the mutagenesis protocol with the In-Fusion kit (Takara Clontech, Saint-Germain-en-Laye, France).

Reactions were transformed into *E. coli* Stellar Competent Cells and transformants selected on L-agar plates containing 100 µg/ml ampicillin (Sigma, Irvine, UK). Plasmid DNA was prepared (Qiagen QIAprep Spin Midiprep Kit) and the clones and mutations were verified by DNA sequencing (Eurofins, Livingston, UK). Mutant plasmids created were transformed into *E. coli* BL21 for expression studies.

**Table 2.3: List of primers designed for Cx43 CT phosphorylation site mutations**

mutation	Primers (5' - 3')
S255A	Fw: TGGTGCGCTGGCCCCTGCCAAAGACTGTGGGTCTC Rv: AGGGGCCAGCGCACCCTGGTCGCATGGTAAGGGTCG
S262A	Fw: TGCCAAAGACTGTGGGGCCCAAAAATATGCTTATTTCAATGGC Rv: TTGGGCCCCACAGTCTTTGGCAGGGCTCAGCGCACCCTG
S279A	Fw: AACCGCTCCCCTCGCCCCTATGTCTCCTCCTGGGTACAA Rv: ATAGGGGCGAGGGGAGCGGTTGGTGAGGAGCAGCCATTG
S282A	Fw:AACCGCTCCCCTCTCGCCTATGGCCCCTCCTGGGTACAAGCTGGTTACTGGCGACAGAAACAA TTC Rv: AGGGGCCATAGGCGAGAGGGGAGCGGTTGGTGAGGAGCAGCCATTGAAATAAGC
S373A	Fw: AGCAGTCGTGCCGCCAGCAGACCTCGGCCTGATGACCTGGAGATC Rv: TGCTGGCGGCACGACTGCTGGCTCTGCTTGAAGGTCGCTGG
S368A	Fw: TTCAAGCAGAGCCGCCAGTCGTGCCAGCAGCAGACCTCGG Rv: ACGACTGGCGGCTCTGCTTGAAGGTCGCTGGTCCACAATGG

#### **2.2.4 RNA extraction**

RNA was extracted using Trizol according to the manufacturer's instructions (Invitrogen, Renfrew, UK). Briefly, cells were washed with ice-cold PBS two times. 500µl Trizol (Ambion, Renfrew, UK, ref no 15596026) was added into each well of a 6-well culture plate and cells were scraped using a cell scraper and transferred into 1.5ml screw-capped Eppendorf tubes. 100µl chloroform (CHCl<sub>3</sub>) was added into each sample followed by shaking by inversion for 20 seconds. The mixed solution was incubated at room temperature for 3 minutes followed by centrifugation at 10,000g for 15 minutes at 4°C. The aqueous phase was taken and transferred into a new tube and mixed with 250µl isopropanol. After 10 minutes of incubation at room temperature, the mixed solution was centrifuged at 10,000g for 10 minutes at room temperature to precipitate the RNA. The supernatant was removed, and the small blueish pellet was washed with 500µl 70% ethanol. Ethanol was removed by centrifugation at 10,000g for 10 minutes at 4°C. Further centrifugation for 1 minute was required to remove residual ethanol. RNA was re-suspended in RNase-free water. RNA concentration was measured by a Nano-Drop 2000 Spectrophotometer (a machine used to quantify and assess the purity of DNA, RNA and proteins; ThermoFisher Scientific, Renfrew, UK) and stored at -20°C.

#### **2.2.5 cDNA synthesis**

cDNA was generated using the Maxima First Strand cDNA Synthesis kit according to the manufacturer's instructions (ThermoFisher Scientific, Renfrew, UK). Briefly, for each reaction, 500 ng RNA templates were mixed with 0.5µl DNase buffer, 0.5µl DNase and ddH<sub>2</sub>O to make the total volume of 5µl. After incubation in a water bath at 37°C for 2 minutes, the reaction solution was mixed with 2µl Reaction mix, 1µl Maxima enzyme mix and 2µl ddH<sub>2</sub>O to make a total volume of 10µl. After incubation at room temperature for 10 minutes, the reaction was incubated at 50°C for 30 minutes and subsequently incubated at 85°C for 15 minutes to stop the reaction. The cDNA samples were then stored at -20°C.

## 2.2.6 qRT-PCR

The qRT-PCR reactions were carried out using a Takyon™ qPCR kits (Eurogentec, Seraing, Belgium, cat no. UF-RPMT-B0701) according to the manufacturer's instructions. Briefly for each reaction, 1µl cDNA was mixed with 10µl 2X Master Mix, forward and reverse primers (final concentration for GAPDH was 300nM, for HPV16E6 was 900nM), probes (final concentrations for both were 100nM) and nuclease-free water to make a final volume of 20µl. The reaction was performed on an ABI Biosystems 7500 machine. Analysis was carried out using the 7500 v2.3 ThermoFisher software (ThermoFisher Scientific, Renfrew, UK) and the Ct value relative to GAPDH as the reference target gene was quantified.

**Table 2.4: List of primers and probes used in RT-PCR**

	GAPDH	HPV16E6
Forward	5' -GAAGGTGAAGGTCGGAGT -3'	5' -CAATGTTTCAGGACCCACAG -3'
Reverse	5' -GAAGATGGTGATGGGATTC -3'	5' -CTGTTGCTTGCAGTACACACATTC -3'
probe	5' FAM- CAAGCTTCCCGTTCTCAGCC-TAMRA -3'	5' -CCACAGTTATGCACAGAGCTGC -3'

## 2.2.7 Cell culture

HEK293, HaCaT and C33a cells were cultured in Dulbecco's modified Eagle's medium (DMEM) (Gibco, Renfrew, UK, ref no 31966-021), supplied with 1% (v/v) Penicillin Streptomycin (P/S) (Gibco, Renfrew, UK, ref no 15140-122) and 10% (v/v) Fetal bovine serum (FBS) (Gibco, Renfrew, UK, ref no 10270-106). C33aE6 cell was cultured as above but with the addition of 0.5 mg/ml G418 (Gibco, Renfrew, UK, ref no 10131-035).

HaCaT shDlg and HeLa43 were cultured as above but supplemented with 10 mg/ml puromycin (Gibco, Renfrew, UK, ref no A11138-03) instead of G418.

3T3 cells were cultured in DMEM supplied with 10% (v/v) Donor Bovine Serum (DBS) (Gibco, Renfrew, UK, ref no 16030-074), 1% (v/v) Penicillin/Streptomycin (P/S) (Gibco, Renfrew, UK, ref no 15140-122) and 1% (v/v) L-Glutamine 200Mm

(Gibco, Renfrew, UK, ref no 25030-024)). 3T3 cells were treated with 4 µg/ml mitomycin C (Sigma, Irvine, UK, cat no M0503-2MG) for 2-5 hours to inhibit cell division. After two times wash with PBS, cells were harvested by incubation with 0.05% trypsin-EDTA (Gibco, Renfrew, UK, ref no 25300-054) until all cells were detached. Media containing FBS was added to inactivate trypsin.

NIKS and NIKS16 cells were cultured in DMEM supplied with 1% (v/v) Penicillin Streptomycin, 10% (v/v) FBS, 0.5 µg/ml hydrocortisone (SIGMA, Irvine, UK, ref no H0888-1G) and 8.4 ng/ml cholera toxin and 10 ng/ml epidermal growth factor (EGF) cocultured with 4µg/ml mitomycin C-treated J2-3T3 cells. NIKS and NIKS16 cells were also cultured in Keratinocyte Basal Medium (Lonza, Slough, UK, cat no cc-3101) supplemented with KGM SingleQuots (Lonza, Slough, UK, cat no cc-4131). All cells were maintained under humidified conditions in 5% CO<sub>2</sub> at 37°C.

### **2.2.8 Preparation of cell stocks**

After trypsinisation and counting, the confluent cells were resuspended into an appropriate growth medium containing 10% DMSO at 1X10<sup>6</sup> cells/ml. The cells suspensions were aliquot into 1 ml/vial and frozen at -80°C overnight before transferring into a liquid nitrogen freezer in vapour-phase.

### **2.2.9 Total cell extract preparation**

Confluent monolayer cells were washed twice with ice-cold PBS and lysed in appropriate amounts of LDS sample buffer (Noves, ref no B0007). The cell lysates were scraped into Eppendorf tubes and passed through an 18-20-gauge needle 8-10 times to shear the chromosomal DNA. The cell lysate was centrifuged to pellet the cell debris. If cells were lysed in NP40 lysis buffer (0.5% NP-40, 150 mM NaCl, 50 mM TrisOHCl pH8) containing PhosphoSTOP (Roche, ref no 04906845001) and complete mini protease inhibitor cocktail (Roche, ref no 04693159001), similar lysis steps to lysis using LDS sample buffer were followed but without the syringe passing step. Protein concentration was determined by Bradford assay. Cell lysates were stored at -20°C.

### **2.2.10 Bradford assay**

Bradford assay was used to measure the concentration of protein extracts according to the manufacturer's protocol. Briefly, Bradford reagent (Bio-Rad, Perth, UK) was diluted at 1:5 with distilled water. 10 µl protein extract and 1 ml diluted reagent were mixed and put into the Nanodrop machine for measurement. Diluted reagent was used as blank and different concentration of BSA (2mg/ml, 1mg/ml, 0.4mg/ml, 0.2mg/ml and 0.1mg/ml) were used to prepare a standard curve.

### **2.2.11 SDS Polyacrylamide Gel Electrophoresis (SDS-PAGE)**

Proteins were separated in pre-made Bolt™ 4-12% Bis-Tris plus 12-well gel (Invitrogen, Renfrew, UK, ref no NW04122BOX) in 1X MES SDS running buffer (Invitrogen, Renfrew, UK, ref no B0002) in a Bolt mini gel tank (Invitrogen, Renfrew, UK). 10µl of protein lysate in NP40 lysis buffer (about 10µg) was mixed with 4µl LDS sample buffer and 1.6µl reducing reagent. No further treatment was used for samples lysed with LDS sample buffer. Protein samples were then boiled at 100°C for 5 minutes. All the samples were loaded into the pre-made Bolt™ 4-12% Bis-Tris plus 12-well gel with 5µl of SeeBlue®Plus prestained standard (Invitrogen, Renfrew, UK, cat no LC5925) loading in the first lane. The gel was run at 150V until the dye front reached the bottom of the gel.

### **2.2.12 Western blot**

Separated proteins were transferred to a nitrocellulose membrane using iBlot® gel transfer nitrocellulose stacks (Invitrogen, Renfrew, UK, ref no IB301001) in an I-blot dry blotting system model P3 (ThermoFisher, Renfrew, UK), following the manufacturer's instructions. After 7 minutes of electrotransfer, the proteins were completely transferred from the gel to the membrane. The transferred membrane was blocked with 5% (w/v) dry milk powder in PBS-0.1% tween(v/v) at

room temperature for 1 hour followed by overnight incubation with primary antibody diluted in blocking solution at 4 °C on a rotating shaker. After washing with PBS-tween for 5 minutes three times, the membrane was incubated on a rotating shaker at room temperature for 1 hour with horseradish peroxidase (HRP)-conjugated secondary antibodies (1:1000) diluted in blocking solution. The membranes were subsequently washed for 3 times 5 minutes with PBS-Tween followed by the development of the signal with enhanced chemiluminescence (ThermoFisher, Renfrew, UK, ref no 32106) for 1min or with ECL plus (ThermoFisher, Renfrew, UK, ref no 32132) for 5 minutes and exposed to high-performance chemiluminescence film (GE health, ref no 28906835).

Alternatively, after incubation with primary antibody and 3 PBST washes, the membranes were incubated with fluorescent IRdye® secondary antibodies (detail in table 2.2) diluted in blocking solution for 1hr at RT. The membranes were washed with PBS-tween for 10 minutes three times and one final wash with PBS (no Tween) for 10 minutes. The membranes were kept in the dark during the wash steps due to the light sensitivity of IRdye® secondary antibodies. The membranes were subsequently imaged and analysed with the two-colour fluorescent western blotting on the Odyssey infrared imaging system (Odyssey® CLx scanner, LI-COR® Biosciences, Cambridge, UK) and the image studio® software (LI-COR® Biosciences, Cambridge, UK).

### **2.2.13 Co-immunoprecipitation**

Cells were washed with ice-cold PBS twice followed by scraping into ice-cold 0.5% NP40 lysis buffer containing protease and phosphatase inhibitors. After 30min incubation on ice, the cell lysate was centrifuged at 12000 g for 5min at 4 °C. Protein concentrations were determined by Bradford assay. Protein Sepharose beads (Sigma, Irvine, UK, ref no P3296-5ml) were washed three times with 500 µl NP40 lysis buffer by centrifugation at 4 °C at full-speed for 30 seconds. 200 ng proteins were incubated with rotation with pre-cleared ProteinG Sepharose beads at 4 °C for 1h. This step is to remove the non-specific binding proteins from the cell extracts. The supernatant was evenly distributed into two tubes

and the volume was made up to 200 $\mu$ l with NP40 lysis buffer and incubated with rotation with either antibody (hDlg H-60) or control (Rabbit IgG (Abcam, Cambridge, UK, ref no ab37415)) at 4 $^{\circ}$ C for 1h. Then 20 $\mu$ l pre-cleared beads were added into each tube and incubated with rotation at 4 $^{\circ}$ C overnight. The beads were washed 5 times with ice-cold NP40 lysis buffer by centrifugation at 4 $^{\circ}$ C at full speed for 30 seconds before the addition of 10 $\mu$ l LDS loading buffer. The input was one-tenth of the protein volume used in Co-IP. The beads and inputs were heated at 100 $^{\circ}$ C for 5 min and followed by gel electrophoresis and western blot analysis.

### **2.2.14 GST protein purification**

One colony of bacteria BL21 transformed with GST-fusion protein expression plasmids was incubated at 37 $^{\circ}$ C in a shaker overnight. Bacteria cultures were diluted 1 in 10 and cultured for 2h at 37 $^{\circ}$ C in a shaker until the OD600 reached 0.4 - 0.6 followed by induction with 1mM IPTG (SIGMA, ref no 16758) for 3h at 30 $^{\circ}$ C. Cells were pelleted by centrifugation at 5500 g for 5 min at 4 $^{\circ}$ C. The supernatant was decanted, and the pellet was re-suspended in 2ml PBS/ 1% Triton X-100 containing protease and phosphatase inhibitors and suspensions were sonicated for three times 20 seconds on ice. The cell debris was removed by centrifugation at 1200 g at 4 $^{\circ}$ C for 15min. The supernatant was transferred to a fresh tube and stored at -20 $^{\circ}$ C. The protein concentration was determined by the Bradford assay. 5  $\mu$ g of bacterial lysate with GST only or GST-Dlg were incubated with 20 $\mu$ l of pre-cleared Glutathione Sepharose 4B (GE Healthcare, ref no 17075601) at 4 $^{\circ}$ C for 1h on a rotating shaker. Samples were made up to 100 $\mu$ l with NP40 lysis buffer. This step was to allow the GST-fused protein to bind to the beads. Then the beads were washed twice with 500 $\mu$ l NP40 lysis buffer by centrifugation at 4 $^{\circ}$ C at full speed for 30 seconds. This step was to remove the unbounded GST-fused proteins. Then the beads were incubated with rotation with 50  $\mu$ g extracts from cells expressing Cx43 C-terminal mutations/deletions at 4 $^{\circ}$ C overnight (samples were made up to 150 $\mu$ l with NP40 lysis buffer). After overnight incubation, the beads were washed with NP40 lysis buffer three times followed by resuspending with loading buffer. After boiling at 100 $^{\circ}$ C for 5 minutes, the samples were analysed by SDS-PAGE and western blot.

### **2.2.15 Coomassie staining**

To ensure the success of IPTG induction, the lysed bacterial solution was run on an SDS-PAGE gel. The gel was stained in Coomassie blue staining solution for 1 hour at room temperature with shaking. Then the gel was incubated with destain solution with shaking overnight.

### **2.2.16 Transfection of cells with lipofectamine 3000**

HEK293 cells at a confluence of 80% were used for transfection utilizing the lipofectamine®3000 transfection kit (Invitrogen, ref no L3000-008) according to the manufacturer's instructions. Briefly, cells were seeded on 12-well plates. Lipofectamine 3000 reagent was diluted in Opti-MEM medium (Gibco, ref no 31985-047) and mixed well. A master mix of DNA was prepared through diluting the amount of plasmid into Opti-MEM medium and lipofectamine 3000 reagent was then added and mix by inversion. The diluted lipofectamine 3000 reagent was mixed with the DNA master mix and incubated at RT for 10 - 15 min. After incubation, the required amount of DNA-lipid complexes was added to each well (125 µl/well in a 12-well plate and 250 µl/well in a 6-well plate). Then the cells were incubated at 37° C for 48h. Co-transfection of a GFP expression plasmid was used to determine the efficiency of transfection by visualizing the cell population under microscopy and counting the percentage of GFP-positive cells (transfection efficiency was around 90%).

### **2.2.17 siRNA knockdown of hDlg**

Cells were plated in a normal culture medium at 200,000 - 500,000 cells/well in a 6-well plate one day before transfection. siRNAs against hDlg (5'GAUGAUGAAUAGUAGUAUUTT3', Ambion, cat no 4390824) or control siRNA (siGLO, Dharmacon, cat no D-001630-01-05) were transfected using Lipofectamine RNAiMAX (Invitrogen, ref no 13778-150) according to the

manufacturer's instructions. The final concentration of siDlg was 0.2 $\mu$ M. Cells were harvest for protein extraction or used for further wound healing assay at 48h post-transfection.

### **2.2.18 Scratch wound assay**

Cells were seeded in a 6-well or 12-well plate and grown until they reached 100% confluence. A 20 $\mu$ l yellow tip was used for creating wounds, which were three lines in each well in the 6-well plate for protein extraction or one line in the 12-well plate for gap closure photography and immunofluorescence microscopy. The culture medium was changed after scratching. Protein was extracted from cells for Western Blot or fixed for immunofluorescence microscopy at 0h, 4h, 8h, 16h, 24h post-wound. Un-wounded cell layers were used as a control in all experiments and harvested at 0h. The wound closure was measured in terms of area employing ImageJ (<https://imagej.net/Fiji>).

### **2.2.19 Immunofluorescence staining and confocal microscopy**

Cells were seeded on sterile 13 X 13 mm coverslips and grown until they reached the required confluence for the designed experiment (90% confluence for the location of Cx43; 100% for wound healing). Cells were washed three times with PBS and fixed with 100% ice-cold methanol at -20 $^{\circ}$ C for 20min. Then cells were permeabilized with acetone for 1min at room temperature followed by three washes with PBS, each time for 5 minutes. Coverslips were blocked in 10% (v/v) donkey serum (Sigma, ref no D9663-10ml) in PBS for 1h at room temperature, followed by 1h incubation with primary antibodies diluted in 5% (v/v) donkey serum in PBS at room temperature. After washing with PBS three times, coverslips were then incubated with secondary antibody labelled with fluorescence (details in table 2.2) diluted 1:1000 in 5% (v/v) donkey serum in PBS. After washing three times with PBS and one time with distilled water, coverslips were mounted with ProLong<sup>®</sup> Gold antifade reagent with DAPI (Invitrogen, ref no P36935). Incubation with no primary antibody as a negative

control was applied in all the experiments. Images were taken using a Zeiss LSM880 Meta confocal microscope. Images were analysed using ImageJ (<https://imagej.net/Fiji>).

### **2.2.20 Quantification**

All the experiments were repeated three times (N = 3) and analysed using ImageJ (<https://imagej.net/Fiji>).

Briefly, the intensity of western blot bands was measured by ImageJ with the equation:

the real intensity of bands = band intensity measured - the intensity of the background.

The expression of Cx43 and hDlg was normalised with the expression of GAPDH in each cell lines.

For the wound healing process, bands intensity was measured as above and normalised to un-wound for each cell line. The area of a gap was measured by ImageJ delineating the edges of the wound. The wound area was normalised to that at 0h of each cell line. Significant of data were indicated by student T-test (\* indicates  $p < 0.05$ ; \*\* indicates  $p < 0.005$ ; \*\*\* indicates  $p < 0.0005$ ).

### **3 Chapter 3**

## **The interaction between Cx43 and hDlg is neither HPVE6-dependent nor tumour cell-specific**

There are a predicted 570,000 new cases of cervical cancer per annum, the fourth most frequent cancer in woman worldwide, which accounted for 6.6% of all female cancers in 2018 (WHO). Averages of 3200 new cervical cancer cases were found every year in the UK between 2014 and 2016. Human papillomavirus (HPV) shows a strong connection with cervical cancers especially HPV16 and 18, which are responsible for 70% of all cervical cancers (Crosbie et al., 2013). HPVE6, one of the oncoproteins synthesized by HPV, is known to be the key driver in cervical tumour progression. Together with E6-associated protein (E6-AP), it can target and degrade tumour suppress protein p53. Cellular ubiquitin ligase E6-AP is known to participate in the degradation of the p53 tumour suppressor protein by E6 and the crystal structure of the ternary complex has been solved (Martinez-Zapien et al., 2016). Besides this p53 degradation activity, HPVE6 is known to target the PDZ tumour suppressor protein hDlg for ubiquitin-proteasome degradation. It is uncertain whether E6-AP is involved in hDlg degradation. (Grm and Banks, 2004) used an *in vitro* E6-AP immunodepletion assay to indicate that the degradation of hDlg by HPVE6 is E6-AP-independent. However, a different conclusion was made two years later. *In vitro* binding assays indicated the complex formation of hDlg, E6 and E6-AP. The degradation ability of E6 to hDlg correlated with its ability to interact with E6-AP. Therefore, the authors concluded that E6-AP is involved in the degradation process of hDlg by HPVE6 (Matsumoto et al., 2006). Aside from the involvement of E6-AP in the degradation of hDlg by HPVE6, hDlg can be degraded via the proteasome both in the presence or absence of HPVE6 (Mantovani et al., 2001).

Cx43, a widespread building block of gap junction intercellular channels (GJIC), was observed to be lost from the plasma membrane in HPV-E6-positive cervical tumour cells. Experiments carried out by our group firstly found that Cx43 can form typical gap junction plaques (accumulation of many gap junctions) in HPV-positive non-transformed W12G cervical epithelial cells, but Cx43 relocates to the cytoplasm of full-transformed W12GPXY cervical cancer cells with loss of

GJIC (Aasen et al., 2003b). Ectopic expression of HPVE6 in C33a cells (HPV-negative cervical cancer cells) leads to Cx43 being relocated from the plasma membrane into the cytoplasm (Sun et al., 2015). siRNA depletion of HPVE6 in HPV16-positive W12GPXY cervical cancer cells leads to restoration of membrane Cx43 (Sun et al., 2015). HPVE6-mediated relocation of Cx43 from the plasma membrane into the cytoplasm is due to its interaction with hDlg because membrane Cx43 is observed in C33a cells transfected with mutated HPV18E6 that has lost the ability of binding to hDlg, while in C33a wild-type HPV18E6 Cx43 is in the cytoplasm (Sun et al., 2015). Cx43 colocalised with hDlg on the membrane in W12G cells but in the cytoplasm in W12GPXY cells (Macdonald et al., 2012b). Pull-down-assays indicate Cx43 interacts with hDlg in both W12G and W12GXY cells. More specifically, GST pull-down assay using bacterially produced hDlg and W12GPXY cell extracts indicate that Cx43 binds directly to both N- and C-terminal of hDlg through its C-terminus (Macdonald et al., 2012b).

Based on the relationship between Cx43-hDlg and hDlg-HPVE6, it would be interesting to investigate whether the interaction between Cx43 and hDlg requires the involvement of HPVE6.

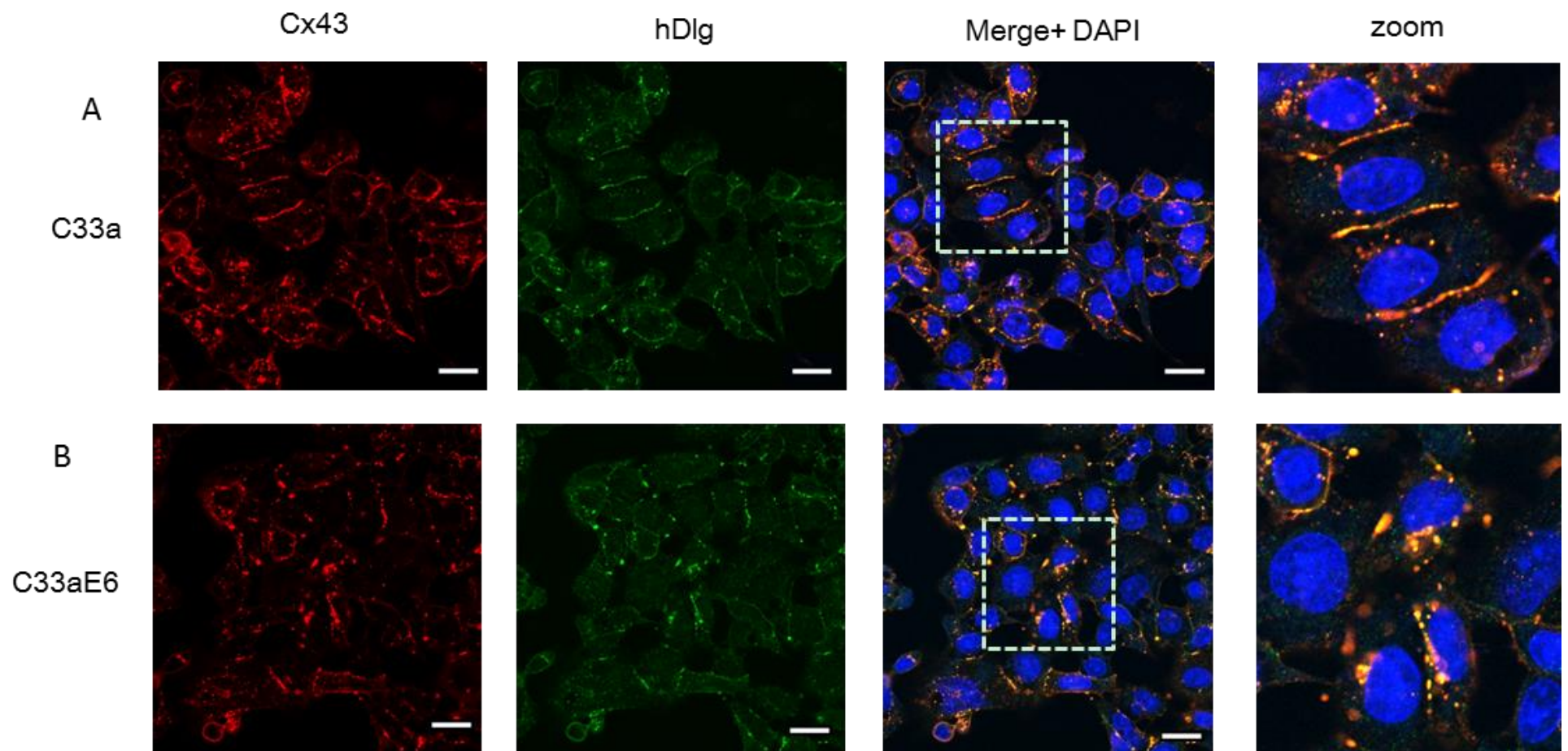
### 3.1 Cx43/hDlg interaction is not HPVE6-dependent

Previously Cx43 and hDlg interaction was found both in vitro by pull-down assay and in vivo by Proximity Ligation Assay in high-grade cervical lesions (Sun et al., 2015). However, HPVE6 is expressed in both W12G cells (in the nucleus) and W12GPXY cells (in the cytoplasm) (Sun et al., 2015). HPVE6 has a PDZ binding domain and binds to the second PDZ domain of hDlg, which might affect the interaction between hDlg and other proteins such as Cx43. To investigate whether HPVE6 is essential for the Cx43/hDlg interaction, we used C33a (HPV-negative cervical cancer cells) and C33aE6 cells (C33a cells stably transfected with an HPVE6 expression plasmid).

First, immunofluorescence confocal microscopy was used to investigate the subcellular location of Cx43 and hDlg in the presence and absence of HPVE6 in C33aE6 and C33a cells. In the absence of HPVE6 in C33a cells, Cx43 was mainly found on the plasma membrane, displaying the long and continued line pattern of staining that is consistent with the presence of gap junction plaques. Very little cytoplasmic Cx43 was observed in C33a cells (Figure 3.1 A). In contrast, in C33aE6 cells with the presence of HPVE6, Cx43 accumulated in the cytoplasm and particularly in the peri-nuclear area with less staining found on the plasma membrane (Figure 3.1 B). This was consistent with our previous observation in W12GPXY cells (Sun et al., 2015). A similar staining pattern was observed for hDlg in both C33a and C33aE6 cells: in C33a cells, hDlg was mainly observed on the plasma membrane and little cytoplasmic hDlg was observed (Figure 3.1 A). However, in C33aE6 cells, accumulated hDlg was found in the cytoplasm and less membrane staining was observed (Figure 3.1 B). Strong co-staining of Cx43 and hDlg was observed in C33a cells on the plasma membrane indicating that hDlg co-localised with Cx43 in the gap junction plaques (Figure 3.1 A). Strong co-staining of Cx43 and hDlg was observed in the cytoplasm in C33aE6 cells (Figure 3.1 B). This was consistent with the observation that HPVE6 restricted the Cx43 and hDlg from the plasma membrane into the cytoplasm in W12GPXY cells (Sun et al., 2015). HPVE6 relocation of Cx43 from the plasma membrane into the cytoplasm was due to its interaction with hDlg (Sun et al., 2015). HPV16 targeted and degraded hDlg less efficient than HPV18 (Pim et al., 2000). This could be an explanation of membranous Cx43 and hDlg observed in C33aE6 cells (HPV16E6).

Then qRT-PCR was used to ensure that there was reduced HPVE6 in C33a cells, confirming that the Cx43/hDlg interaction in C33a cells is not due to HPVE6. RNA was extracted from each cell line using the Trizol/chloroform method, followed by qRT-PCR analysis. The expression of HPV16E6 was detected in C33aE6 cells but not in C33a cells, while GAPDH was expressed in both cell lines as expected (Figure 3.1 C). Thus, it appeared that the interaction between Cx43 and hDlg in cervical cancer cells was not due to the effect of HPV16E6.

Next, Cx43/hDlg interaction was investigated through immunoprecipitation, using cell extracts of C33a and C33aE6. Beads incubated with rabbit anti-hDlg antibody immunoprecipitated Cx43, which was clearly observed in C33aE6 cells expressing HPVE6 (Figure 3.2 line 5) while no bands were detected in beads bound with rabbit IgG control (Figure 3.2 line 6). This is consistent with the previous observation in co-immunoprecipitation in W12GPXY cell extracts (Macdonald et al., 2012b). Importantly, there is a clear observation of interaction between Cx43 and hDlg in the absence of HPVE6 in C33a cells, compared to rabbit IgG control (Figure 3.2 line 2 and 3). The additional bands in the co-immunoprecipitation western blots are the heavy and light chains of the antibody (Figure 3.2). This indicates that the Cx43/hDlg interaction is not HPVE6-dependent.



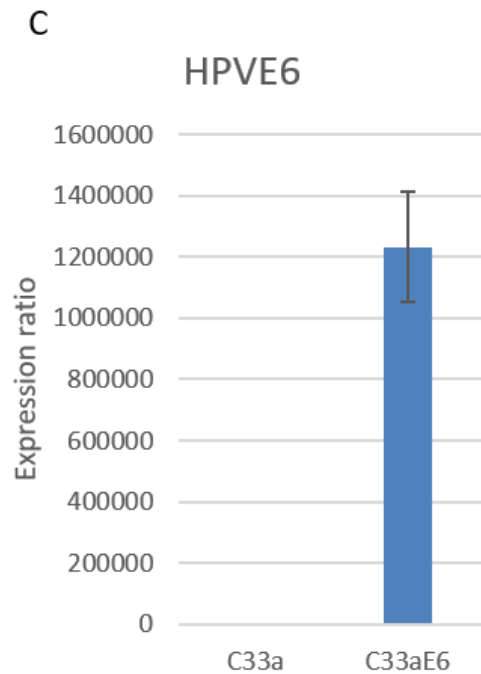


**Figure 3.1: Cx43 colocalised with hDlg mainly on the plasma membrane in C33a cells but mainly in the cytoplasm in C33aE6 cells.**

Confocal immunofluorescence microscopy showing the location of Cx43 and hDlg in (A) C33a (HPV-negative cervical cancer cells) and (B) C33aE6 (C33a cells transfected with HPV16E6). The image shows Cx43 (red) and hDlg (green) colocalised mainly on the plasma membrane in C33a cells but mainly in the cytoplasm in C33aE6 cells. Large merged images of typical colocalisation of each cell line are shown on the right-hand side. Nuclei were stained with DAPI (blue). The scale bar is 20µm. (C) qRT-PCR analysis ensures the expression of HPV16E6 in C33aE6 but not in C33a cells. RNA extraction of each cell line was done with Trizol/chloroform methods followed by qRT-PCR analysis with primers for GAPDH and HPV16E6.

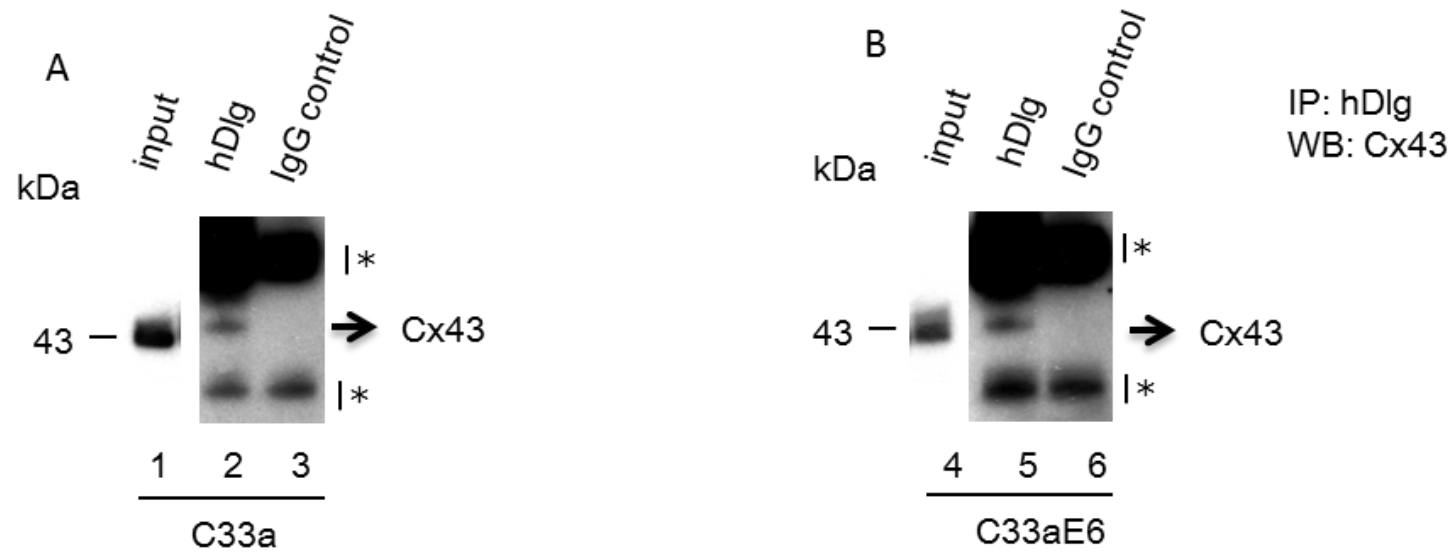


**Figure 3.2: Interaction of Cx43 and hDlG in cervical cancer cells.**

Co-immunoprecipitation of endogenous Cx43 from C33a and C33aE6 cervical cancer cells using an anti-hDlG antibody. Rabbit antibody against hDlG (H-60) was used in Co-IP. Rabbit IgG was used as a negative control in Co-IP. The blot was probed with an anti-Cx43 antibody and checked by X-ray film. Asterisks indicate antibody heavy and light chains that trapped Cx43 antibody. One-tenth volume of supernatants from the Co-IP experiments was used as input.

### 3.2 Cx43/hDlg interaction is not tumour-cell specific

Given the evidence that Cx43-hDlg interaction is not HPVE6-dependent, it was important to investigate whether the interaction only happens in a tumour situation. The results so far about this interaction are either in cancer cells (C33a, C33aE6, W12GPXY, and cervical lesion) or W12G (HPV16E6-positive cervical epithelial cells). Cancer has some major characteristics such as unlimited multiplication, invasion and resisting cell death (Hanahan and Weinberg, 2011), which are different from normal cells. During carcinoma progression or virus infection, the micro-environment within cells is changed. For example, p53 is a well-known tumour suppressor protein that can arrest the cell cycle, or induce apoptosis of infected cells. In cervical cancer cells, HPVE6 targets p53 for degradation. Cx43 has been known to have many functions in many cellular activities, apart from forming a gap junction channel, such as involvement in cell migration (Kameritsch et al., 2012). hDlg, as a tumour suppressor protein, maintains cell polarity, and cytoskeleton structure. It would be interesting to know whether Cx43 and hDlg interact in non-tumour cells. If this interaction is tumour cell-specific, it could suggest that the cell carcinoma process is strongly connected with Cx43/hDlg interaction, and this might provide a biomarker for some cancer diagnostic tests. Four non-tumour cell lines were used to investigate this interaction: HEK293 (human embryonic kidney cells), HaCaT (human keratinocyte cells), NIKS (normal immortalized keratinocyte cells) and NIKS16 (NIKS cells stably transfected with the HPV16 genome).

Western blot, using rabbit polyclonal Cx43 antibody and mouse monoclonal hDlg antibody, demonstrated that all four cell lines expressed Cx43 and hDlg. HEK293 and NIKS cells expressed the highest level of Cx43 compared to HaCaT and NIKS16 cells. HaCaT expressed the greatest level of hDlg in all these cells. The level of hDlg in HEK293 was slightly higher than that in NIKS cells. For NIKS16 cells, more than one band was observed for hDlg, which might be partial degradation or isoforms for hDlg (Figure 3.3). The low level of Cx43 in HaCaT cells might be due to these cells being cultured in high

calcium concentration that trigger cell differentiation and the low levels of Cx43 expressed in differentiated keratinocytes.

Then the subcellular location of Cx43 and hDlg was investigated in HEK293 and HaCaT cells. Cx43 was located on the plasma membrane between neighbouring cells in HEK293 and HaCaT with a staining pattern that was consistent with gap junction plaques. Some peri-nuclear location of Cx43 was observed in HaCaT cells. hDlg was also located on the plasma membrane in both cells with a staining pattern similar to that was observed with Cx43. Cx43 co-stained with hDlg on the plasma membrane in both non-tumour cells (Figure 3.4). Then interaction between Cx43 and hDlg was investigated using cell extracts from HEK293 and HaCaT. Beads bound with rabbit anti-hDlg antibody pulled-down Cx43 clearly compared to rabbit IgG control in HEK293 and HaCaT cells. Light and heavy chains of antibody were detected in the co-immunoprecipitation experiment (Figure 3.5) as observed before. Even if the level of Cx43 in HaCaT is lower than that in HEK293, the pulled-down Cx43 band in HaCaT cells is stronger than that in HEK293 cells (Figure 3.5 line 1, 2 and 4, 5). This might due to higher levels of hDlg in HaCaT cells and the use of an anti-hDlg antibody in immunoprecipitation experiments. These results suggested that Cx43 interacts with hDlg in non-tumour cells.

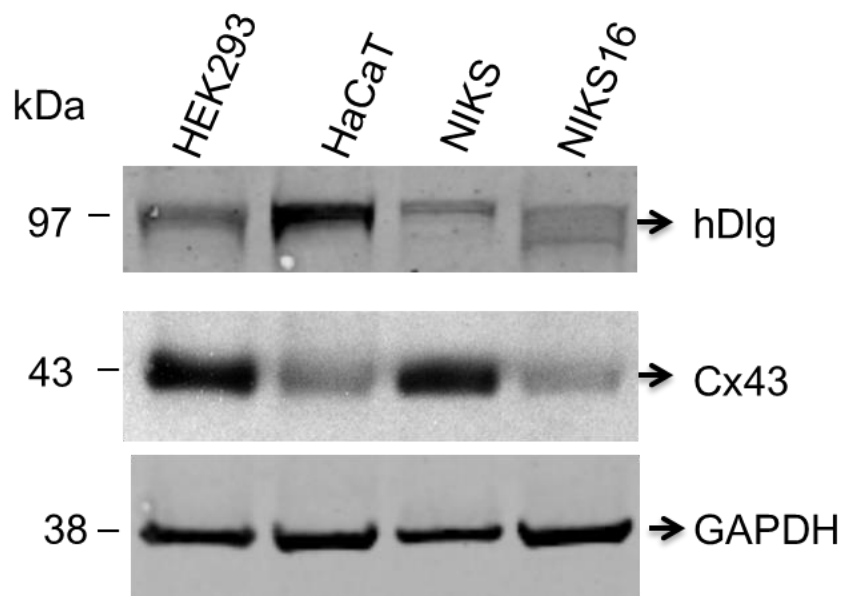


**Figure 3.3: Cx43 and hDlg expression in non-tumour cells (HEK293, HaCaT, NIKS and NIKS16).**

Western blot showed the expression of Cx43 and hDlg in cell extracts from non-tumour cell lines (HEK293, HaCaT, NIKS and NIKS16). The image of hDlg and GAPDH were obtained from Licor and the image of Cx43 was exposed with X-ray film.

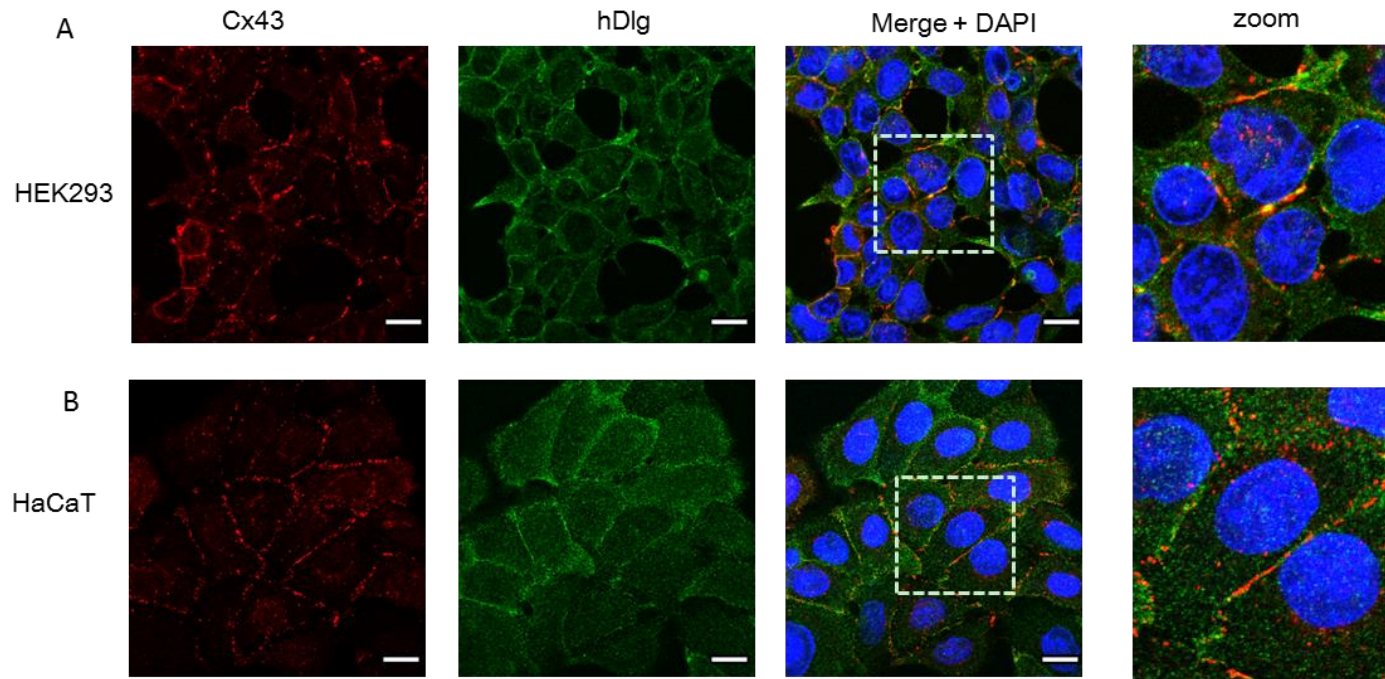


**Figure 3.4: Cx43 colocalised with hDlg on the plasma membrane in HEK293 and HaCaT cells.**

Confocal immunofluorescence microscopy shows the location of Cx43 and hDlg in HEK293 (human embryonic kidney cells) and HaCaT (human keratinocyte cells). The image shows Cx43 (red) and hDlg (green) colocalised on the plasma membrane in HEK293 and HaCaT cells. Large merged images of typical colocalisation of each cell line are shown on the right-hand side (zoom). Nuclei were stained with DAPI (blue). The scale bar is 20 $\mu$ m.

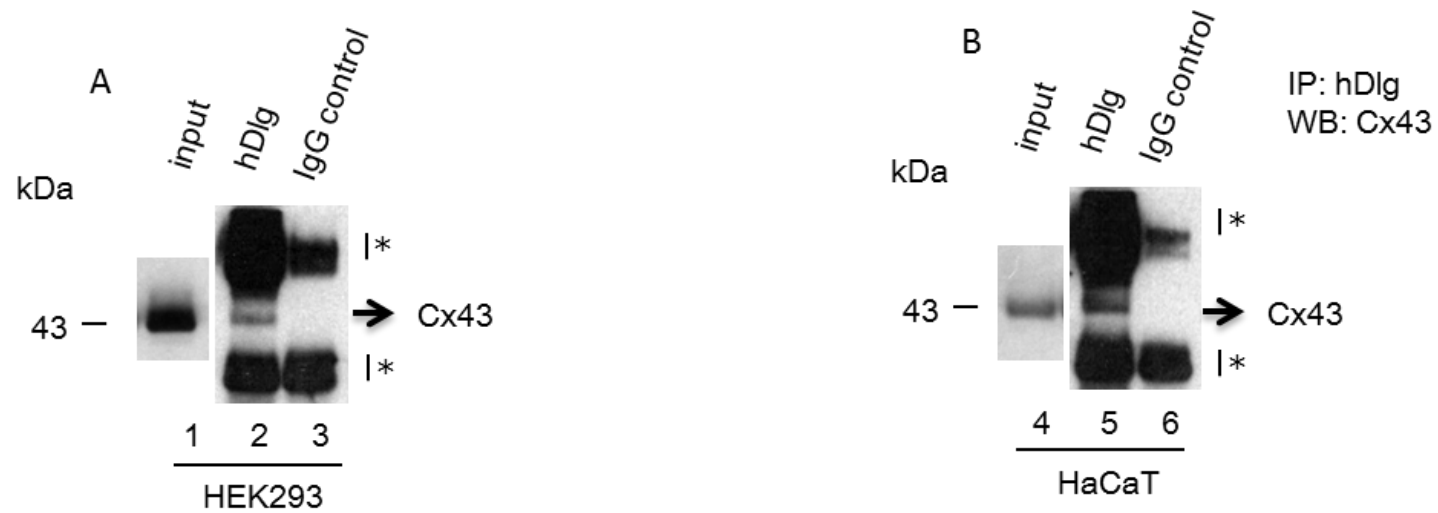
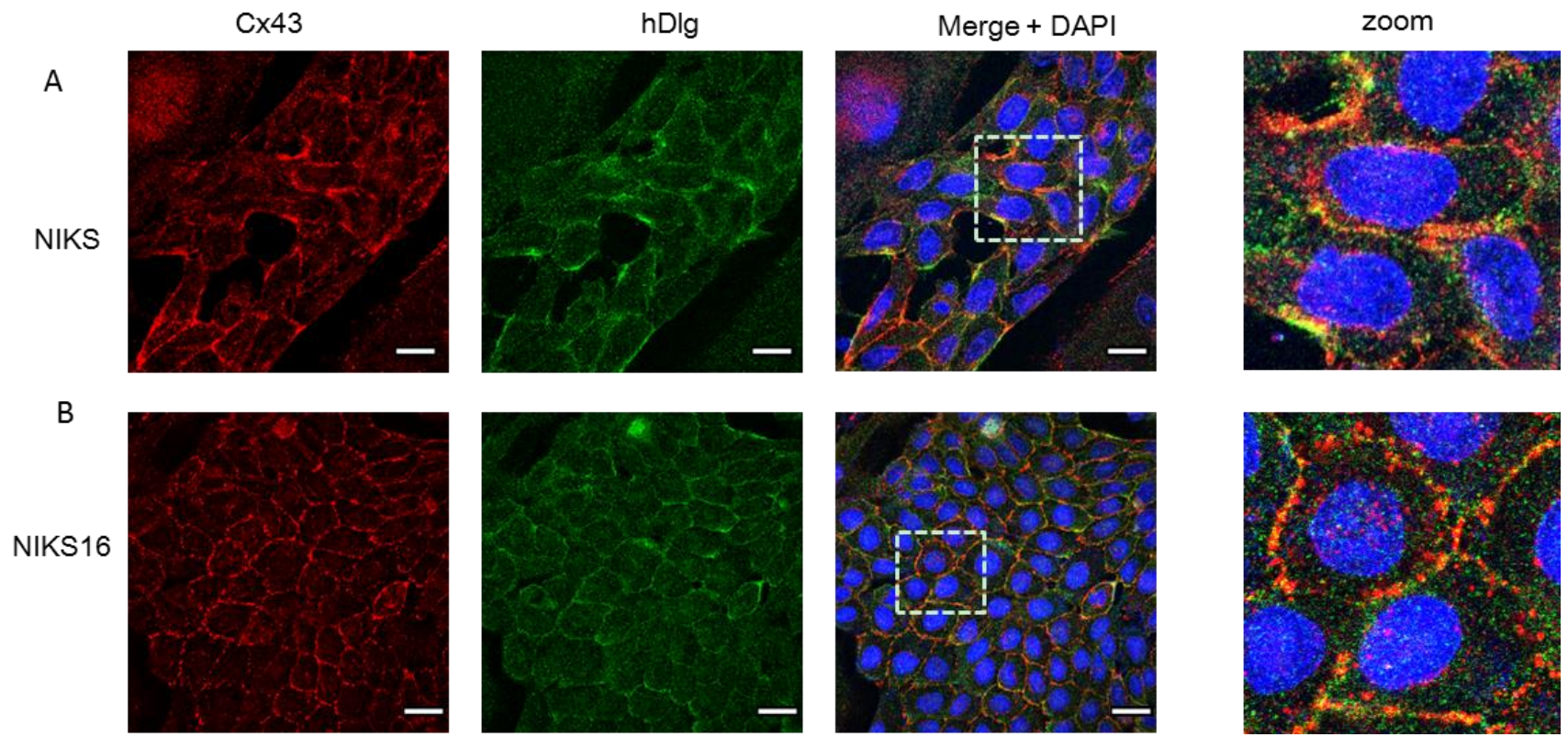


**Figure 3.5: Interaction of Cx43 and hDlg in non-tumour cells (HEK293 and HaCaT).**

Co-immunoprecipitation of endogenous Cx43 from HEK293 and HaCaT cells using an anti-hDlg antibody. Rabbit antibody against hDlg (H-60) was used in Co-IP. Rabbit IgG was used as a negative control in Co-IP. The blot was probed with an anti-Cx43 antibody and developed by X-ray film. Asterisks indicate antibody heavy and light chains that trapped Cx43 antibody. One-tenth volume of supernatants from the Co-IP experiments was used as input.

Very similar experiments were carried out in NIKS and NIKS16 cells. NIKS (normal immortal keratinocytes) is derived from BC-1-Ep normal keratinocytes that were isolated from newborn human foreskin (Allen-Hoffmann et al., 2000). NIKS16 are NIKS cells that are stably transfected with the episomal HPV16 genome. NIKS and NIKS16 cells require co-culture with mitomycin C-treated mouse fibroblasts 3T3 cells as a feeder layer, which mimics the situation of epithelial cell growth on the dermis. There are gaps observed between NIKS/NIK16 cells and 3T3 cells, suggesting that they might not have proper cell to cell communication, including gap junctional communication. Comparison between NIKS and NIKS16 can provide more information on whether infection with HPV16, as opposed to HPV16-associated tumour progression, will affect the Cx43/hDlg interaction.

NIK1S and NIK16 were co-cultured with 3T3 cells until day 7 before fixation for immunofluorescence staining. Cx43 located on the plasma membrane in NIK1S cells with strong gap junction plaques visible while some cytoplasmic Cx43 was also observed (Figure 3.6 A). Similar to NIK1S cells, Cx43 was observed in both the membrane and cytoplasm in NIK16 cells (Figure 3.6 B). hDlg was mainly located on the plasma membrane in both cell types. Strong co-staining between Cx43 and hDlg was observed on the cell margin in both NIK1S and NIK16 cells (Figure 3.6 A & B). Co-immunoprecipitation also showed Cx43 and hDlg could interact in both NIK1S and NIK16 cells. Beads incubated with rabbit anti-hDlg antibody showed a clear pull-down Cx43 band compared to rabbit IgG control beads (Figure 3.6 C & D). These results indicated that the low level of HPV16 in NIK16 cells not affected the interaction between Cx43 and hDlg.



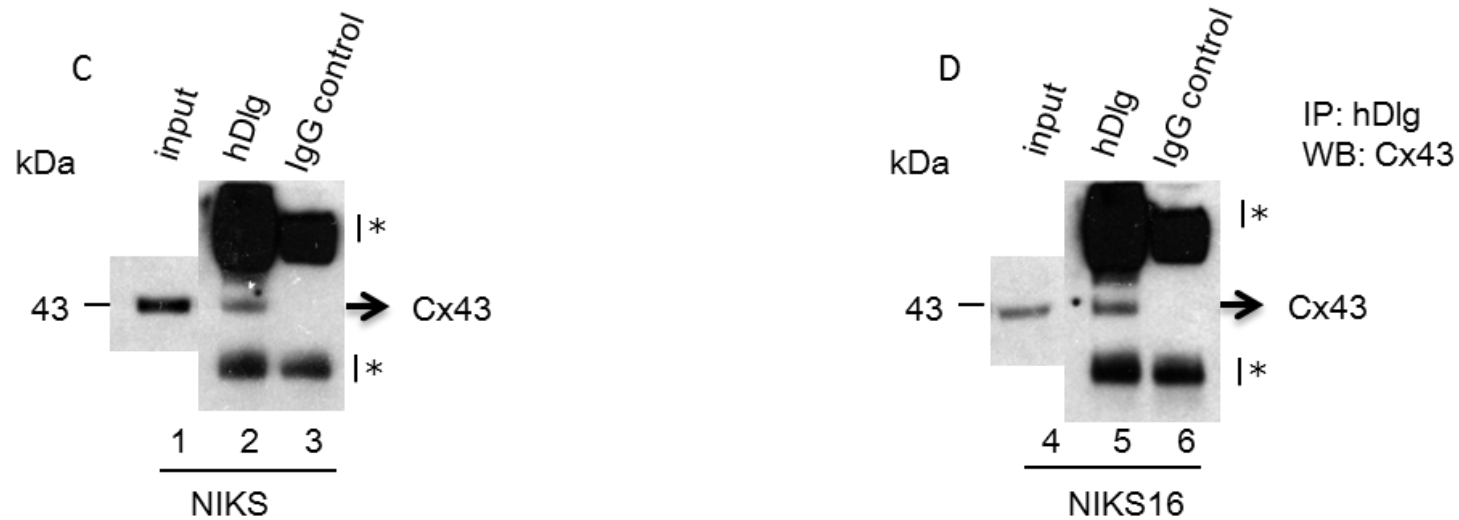


**Figure 3.6: Cx43 interacted and colocalised with hDIg on the plasma membrane in NIKS and NIKS16 cells.**

Confocal immunofluorescence microscopy shows the location of Cx43 and hDIg in (A) NIKS (normal immortalized keratinocyte cells) and (B) NIKS16 (NIKS cells stably transfected with HPV16 genome). The image shows Cx43 (red) and hDIg (green) colocalised on the plasma membrane in NIKS and NIKS16 cells. Large merged images of typical colocalisation of each cell line are shown on the right-hand side. Nuclei were stained with DAPI (blue). The scale bar is 20 $\mu$ m. Interaction of Cx43 and hDIg in (C) NIKS and (D) NIKS16 cells. Co-immunoprecipitation of endogenous Cx43 from NIKS and NIKS16 cells using an anti-hDIg antibody. Rabbit antibody against hDIg (H-60) was used in Co-IP. Rabbit IgG was used as a negative control in Co-IP. The blot was probed with an anti-Cx43 antibody and checked by X-ray film. Asterisks indicate antibody heavy and light chains that trapped Cx43 antibody. One-tenth volume of supernatants from the Co-IP experiments was used as input.

### 3.3 hDlg is a controller of Cx43

Data above show that Cx43-hDlg interaction is neither HPVE6-dependent nor tumour cell-specific. Previous experiments showed that siRNA depletion of hDlg in W12GPXY cells leads to a reduction in the levels of Cx43 (Macdonald et al., 2012b). Then Sun and co-workers (Sun et al., 2015) found that HPVE6 was responsible for reducing the level of Cx43 in W12GPXY cells, compared to the parental non-tumour W12G cells. Moreover, Cx43 stayed on the plasma membrane in C33a cells transfected with an expression construct encoding mutated HPV18E6 with the loss of its ability to binding hDlg. This suggested that HPVE6 controls the trafficking and reduces the level of Cx43 via binding to hDlg. On the other hand, Cx43 can bind hDlg directly, in the absence of HPVE6 in *in vitro* binding assays (Macdonald et al., 2012b). Based on this, it is important to investigate the role of hDlg in its regulation of Cx43 in general. For this reason, the level of Cx43 was first checked in the four non-tumour cell lines, mentioned above, upon the siRNA depletion of hDlg.

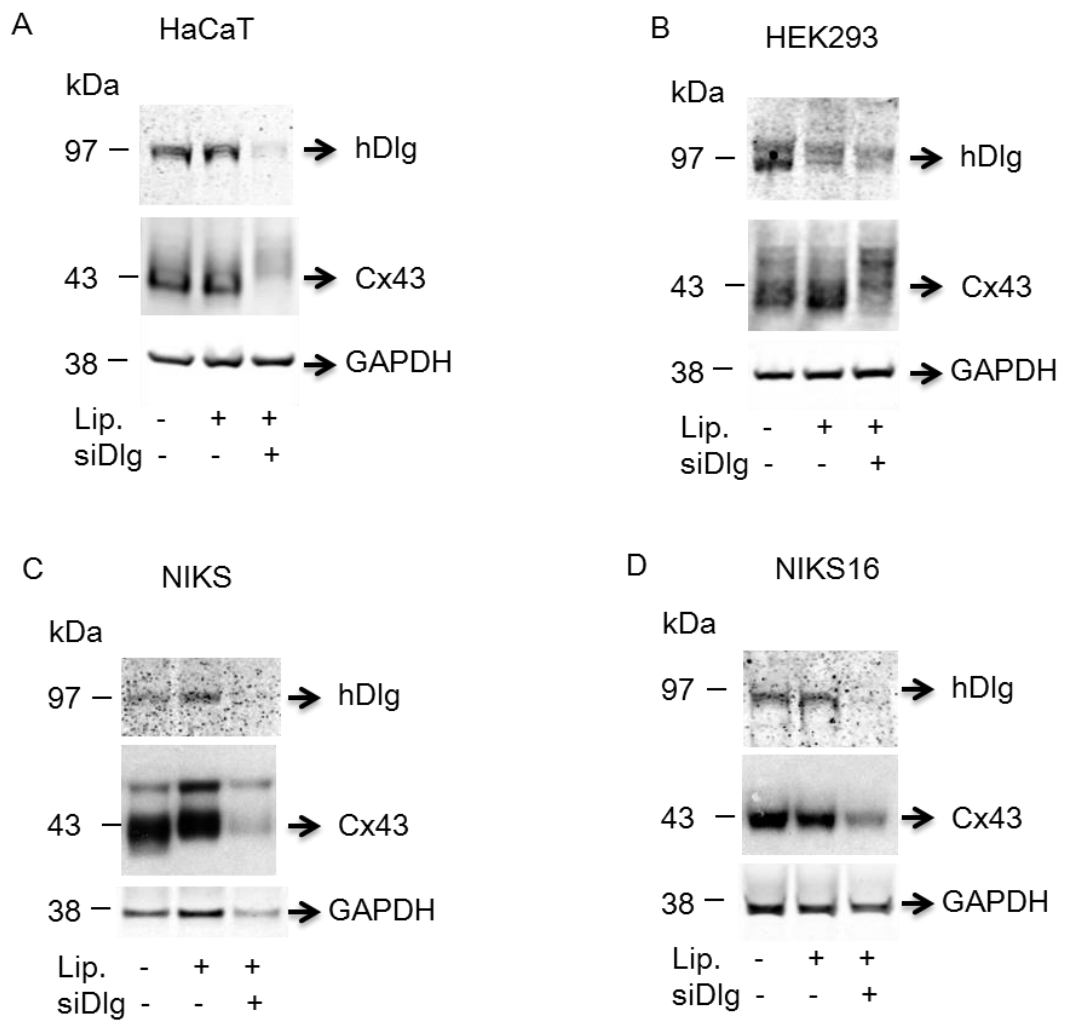
As expected, good depletion of hDlg was observed in HaCaT, NIKS and NIKS16 cells but there was less of an effect in HEK293 cells compared to mock-treated cells. A reduction in the levels of Cx43 was observed upon siRNA depletion of hDlg in all the non-tumour cells, compared to mock-treated and lipofectamine treated control cells (Figure 3.7). Interestingly, in HEK293 cells upon siRNA depletion of hDlg, the Cx43 main band is weaker but upper bands appear stronger than mock and control bands (Figure 3.7 B). Upper bands were also observed in HaCaT siDlg treated cells compared to mock-treated cells (Figure 3.7 A). These upper bands might be phosphorylated or ubiquitinated forms of Cx43. This could be confirmed in the future with antibodies for phosphorylated forms of Cx43. NIKS and NIKS16 cells in these experiments (and also for the confocal experiments below) were cultured in KGM without co-culture with 3T3 cells. Because western blots display the protein level of whole cultured cells, NIKS and NIKS16 were cultured in KGM to avoid the effect of 3T3 cells. In NIKS cells, besides the main band of Cx43, an upper band (might be a phosphorylation form) was also observed (Figure 3.7 C) while in NIKS16 cells only the main bands were observed (Figure 3.7 D). These results show the reduction in levels of Cx43 along with the siRNA

depletion of hDlg, which suggested the role of hDlg in maintaining levels of Cx43 in non-tumour cell lines, which is consistent with what was reported for HPV E6-positive tumour cells by MacDonald (Macdonald et al., 2012b).

Next, whether the subcellular location of Cx43 is altered upon the siRNA depletion of hDlg was investigated in HaCaT and HEK293 cells. In HaCaT cells, Cx43 was located on the plasma membrane with a discontinuous staining pattern. hDlg was found at the outer edges of the cell. Some co-localisation of Cx43 and hDlg was observed on the plasma membrane (Figure 3.8 A). In contrast, in HaCaT cells with siRNA depletion of hDlg, the amount of Cx43 observed was much less and particularly Cx43 lost its membrane location and relocated into the cytoplasm (Figure 3.8 B). The staining of hDlg was hard to see, which is consistent with the western blot results (Figure 3.7 A; 3.8 B). Similar results were observed in HEK293 cells where Cx43 was located on the plasma membrane and hDlg was also located on the plasma membrane (Figure 3.8 C). In HEK293 cells with siRNA depletion of hDlg, Cx43 was relocated from the plasma membrane into the cytoplasm (Figure 3.8 D). Upon siRNA depletion of hDlg, Cx43 was distributed in a more scattered fashion in the cytoplasm in HaCaT cells compared to that in HEK293 cells (Figure 3.8 B & D). This suggested that hDlg was involved in controlling the trafficking or maintaining the membrane location of Cx43.

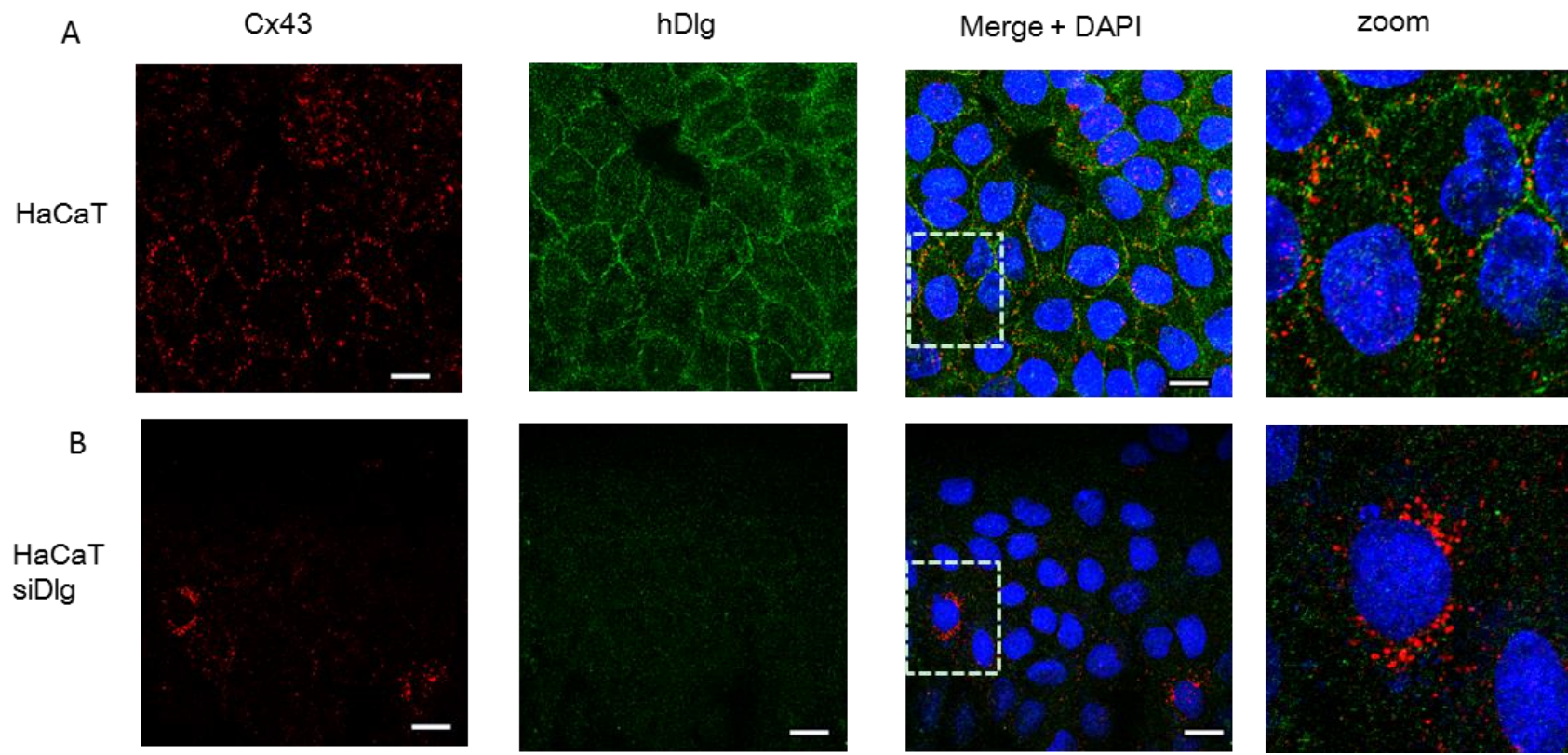
HaCaT cells with a stable knockdown of hDlg (named HaCaT shDlg cells) were kindly provided by Dr. Lawrence Bank (ICGEB, Trieste, Italy). A reduced level of Cx43 and low levels of hDlg were found in HaCaT shDlg cells compared to the normal HaCaT cells, similar to what has been observed in HaCaT cells with siRNA depletion of hDlg (Figure 3.9 A). Interestingly, the 20kDa Cx43 isoform was observed in HaCaT shDlg cells but neither in HaCaT cells nor in the HaCaT cells upon siRNA depletion of hDlg (Figure 3.9 A). Similar to what was shown in Figure 3.8 A, Cx43 displayed a gap junction staining pattern on the plasma membrane while hDlg located on the plasma membrane outlining the cell in HaCaT cells. Co-staining of Cx43 and hDlg was observed on the plasma membrane (Figure 3.9 B). In HaCaT shDlg cells, hDlg was hard to be seen as expected. Cx43 was relocated from the plasma membrane into the cytoplasm (Figure 3.9 C), which is consistent with the previous observation

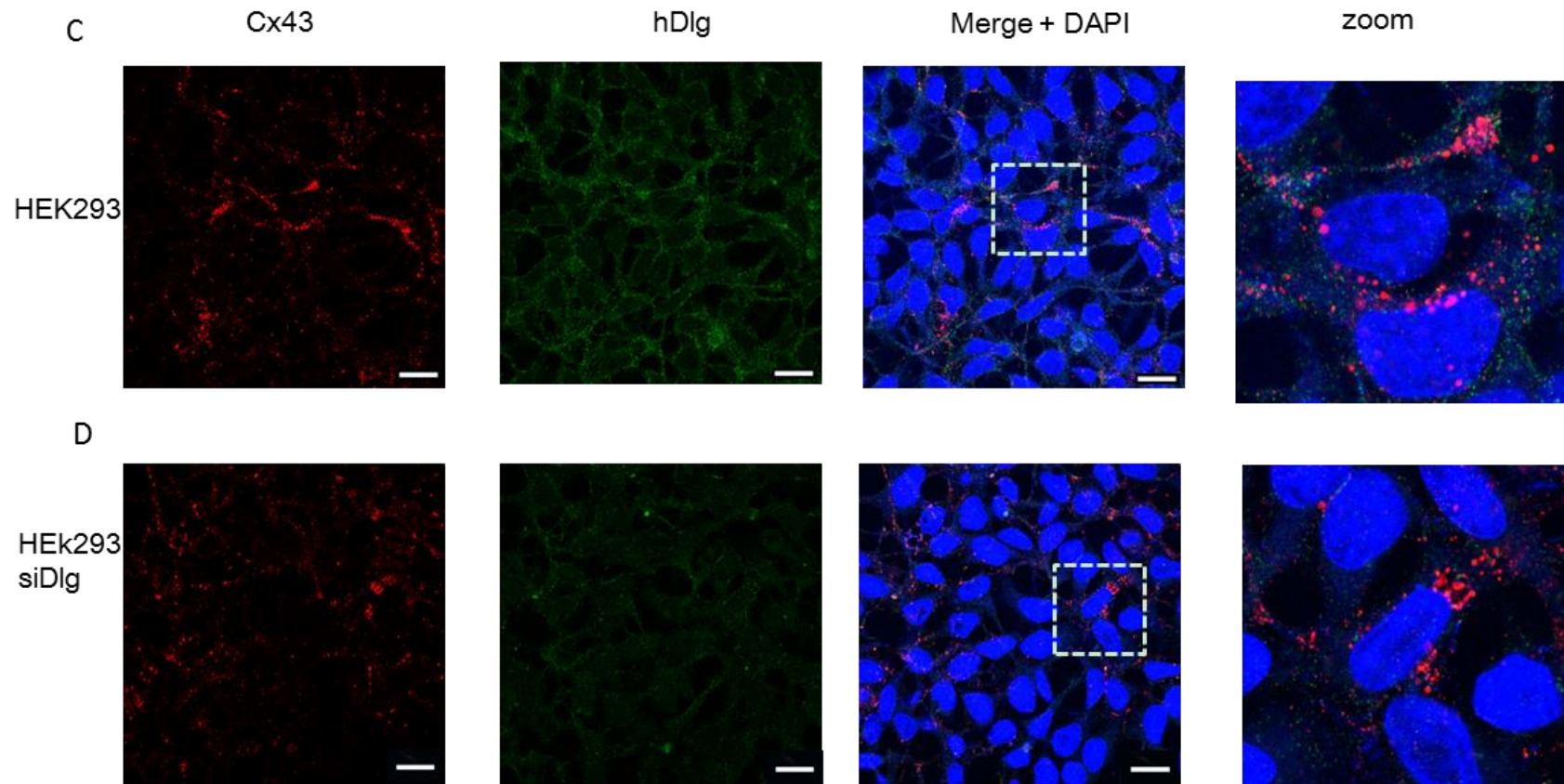
upon siRNA depletion of hDlg. Taken together, these results indicate that hDlg is a regulator of Cx43.



**Figure 3.7: siRNA depletion of hDlg led to a reduction in levels of Cx43 in non-tumour cells:**

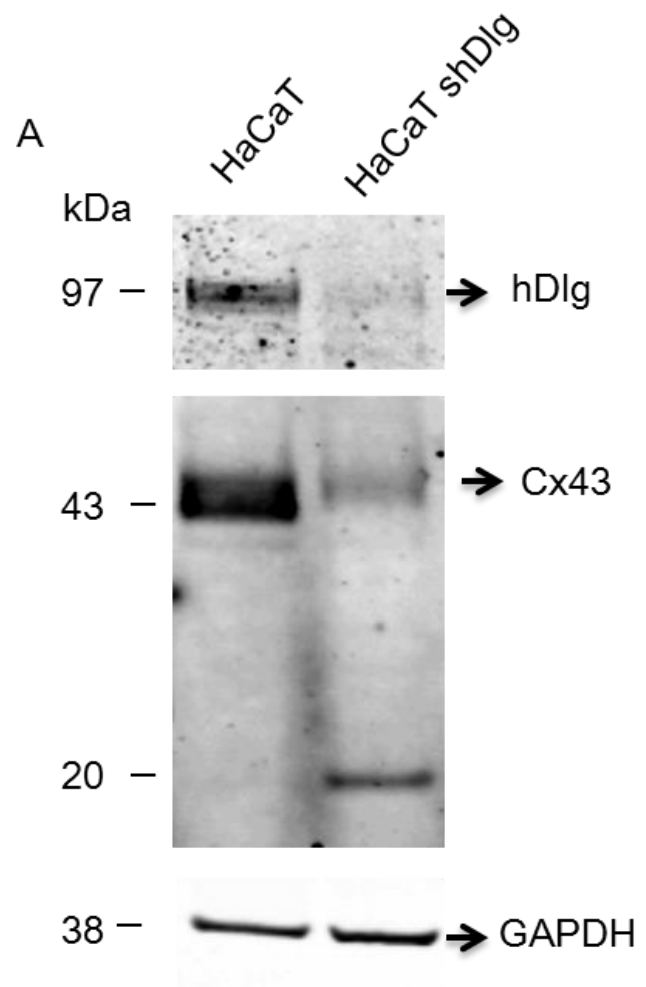
(A) HaCaT, (B) HEK293, (C) NIKS, (D) NIKS16. HaCaT (A) and HEK293 (B) cells were treated with mock, control siRNA or siRNA for hDlg for 48h before checking with western blotting. NIKS (C) and NIKS16 (D) cells were cultured in KGM and with the same siRNA treatment.





**Figure 3.8: siRNA depletion of hDlg led to the cytoplasmic location of Cx43 in non-tumour cells (HEK293, HaCaT).**

Confocal immunofluorescence microscopy shows the location of Cx43 and hDlg in HaCaT cells with/without siRNA depletion of hDlg (A and B) and in HEK293 cells with/without siRNA depletion of hDlg (C and D). These images show Cx43 (red) and hDlg (green) on the plasma membrane in the mock-treated HaCaT and HEK293 cells (A and C) but Cx43 is in the cytoplasm in HaCaT and HEK293 with siRNA depletion of hDlg (B and D). Large merged images of each cell line are shown on the right-hand side. Nuclei were stained with DAPI (blue). The scale bar is 20 $\mu$ m.



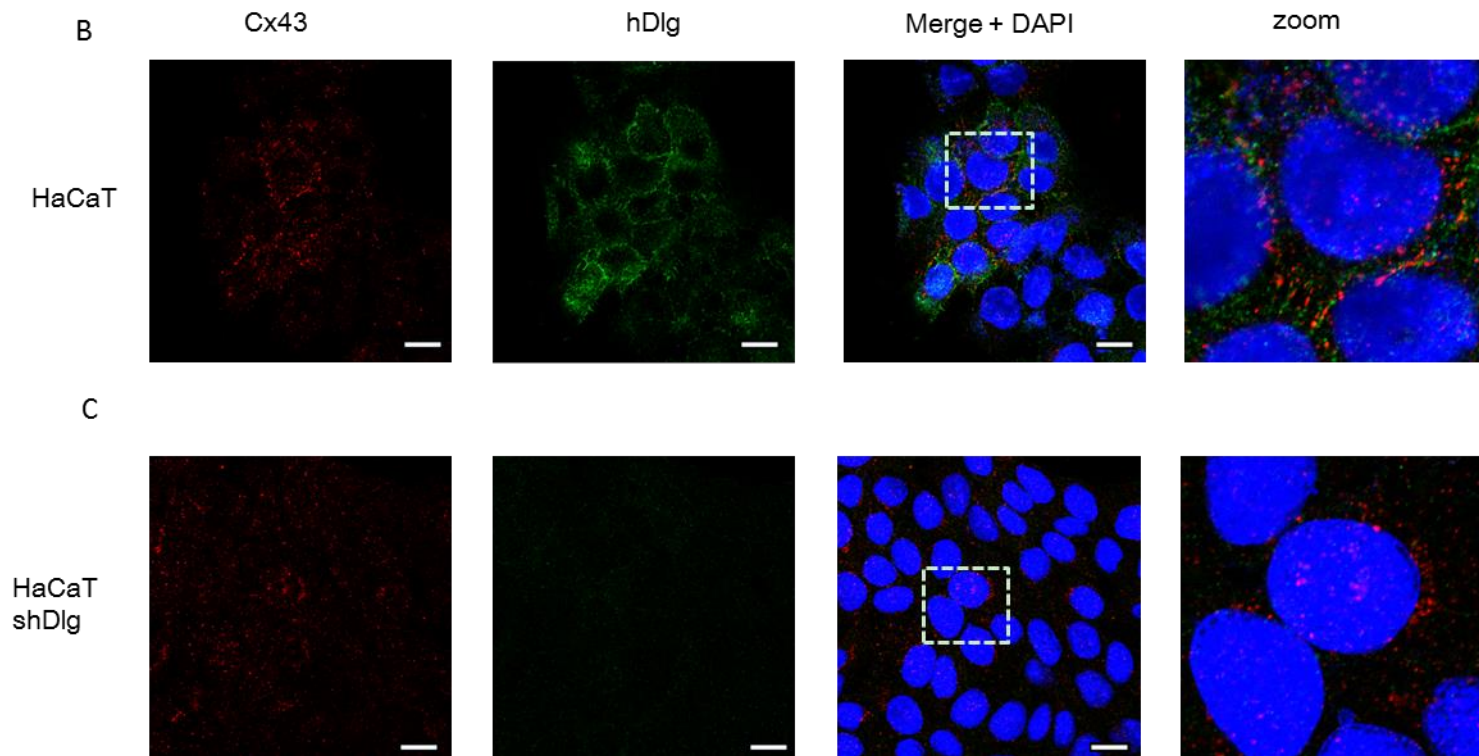


**Figure 3.9: Reduced level and cytoplasmic location of Cx43 was observed in HaCaT cells with stable depletion of hDlg (HaCaT shDlg).**

(A) Reduced level of Cx43 was observed in HaCaT shDlg cells compared to HaCaT cells. The 20kDa Cx43 band was observed in HaCaT shDlg cells but not in HaCaT cells. Confocal immunofluorescence microscopy shows the location of Cx43 and hDlg in (B) HaCaT cells and (C) HaCaT shDlg. These images show Cx43 (red) and hDlg (green) on the plasma membrane in the HaCaT cells (B) but cytoplasmic Cx43 is observed in HaCaT shDlg (C). Large merged images of each cell line are shown on the right-hand side. Nuclei were stained with DAPI (blue). The scale bar is 20 $\mu$ m.

### 3.4 Cx43 and lysosome inhibition

Cx43 is a building block of gap junction channels with a half-life of 1.5 - 5h (Laird, 2006). Cx43 can be degraded through proteasome and lysosome but mainly the latter. Degradation of Cx43 was delayed in the presence of proteasome inhibitor, and Cx43 was also found to be a substrate for ubiquitin, which is normally a target to the proteasome. But mono-ubiquitination was found for Cx43, which is thought to act as a trigger for internalisation while proteins with poly-ubiquitination are the target to the proteasome (Qin et al., 2003). Accumulated evidence has shown the degradation of Connexins is mainly via the lysosomes. For instance, immunofluorescence assay indicates that intracellular Cx43 is located in the lysosomes and lysosome inhibitor-treated breast cancer cells show increasing levels of Cx43 (Qin et al., 2003). Upon treatment with the lysosome inhibitor ammonium chloride ( $\text{NH}_4\text{Cl}$ ), the level of both Cx43 and hDlg increased in W12GPXY cervical cancer cells but less so in the parental non-tumour W12G cells.  $\text{NH}_4\text{Cl}$  also sustained the level of Cx43, which was decreased upon siRNA depletion of hDlg in W12GPXY cells (Macdonald et al., 2012b). For this reason, whether  $\text{NH}_4\text{Cl}$  and another endosome/lysosome inhibitor, chloroquine, sustained the level of Cx43 reduced by siRNA depletion of hDlg was investigated in non-tumour cells. HaCaT and HEK293 cells were treated with mock or lysosome inhibitor ( $\text{NH}_4\text{Cl}$  and chloroquine) for 8h at  $37^\circ\text{C}$  before fixation or protein extraction. As expected, lysosome inhibitors  $\text{NH}_4\text{Cl}$  and chloroquine significantly increased the level of Cx43 in HaCaT cells compared to the mock treatment. But less effect was observed in the level of hDlg in lysosome-inhibitor-treated HaCaT cells (Figure 3.10 A). Two bands of Cx43 were observed in both mock-treated and lysosome inhibitor-treated HaCaT cells, which might be phosphorylated or ubiquitinated forms of Cx43. Interestingly, the 20kDa isoform of Cx43 was observed in  $\text{NH}_4\text{Cl}$  treated HaCaT cells, but not in chloroquine treated cells (Figure 3.10 A).

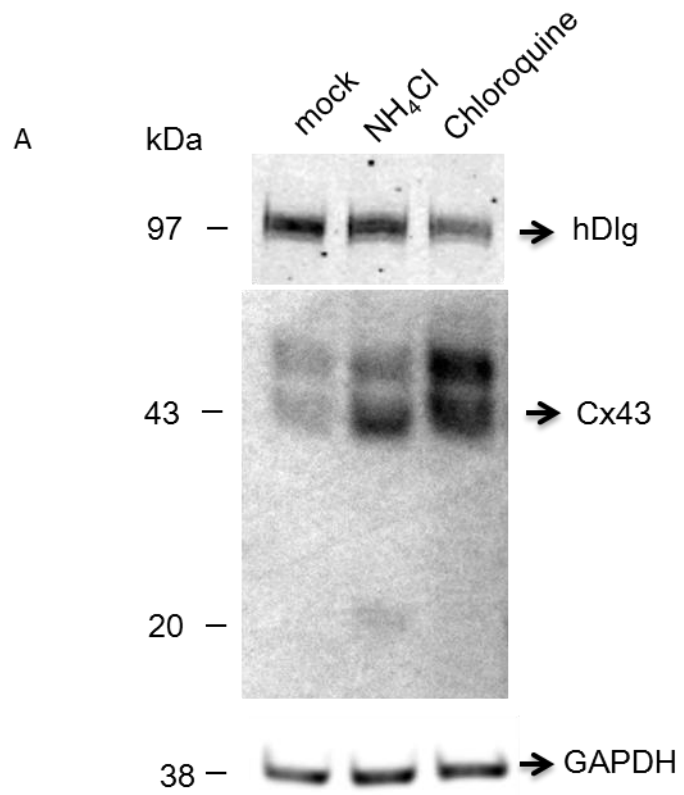
Then the subcellular location of Cx43 and hDlg in HaCaT cells treated with lysosome inhibitors was investigated. With mock-treated HaCaT cells, Cx43 and hDlg were on the plasma membrane with some colocalisation (Figure 3.10 B) as observed previously. In  $\text{NH}_4\text{Cl}$ -treated HaCaT cells, Cx43

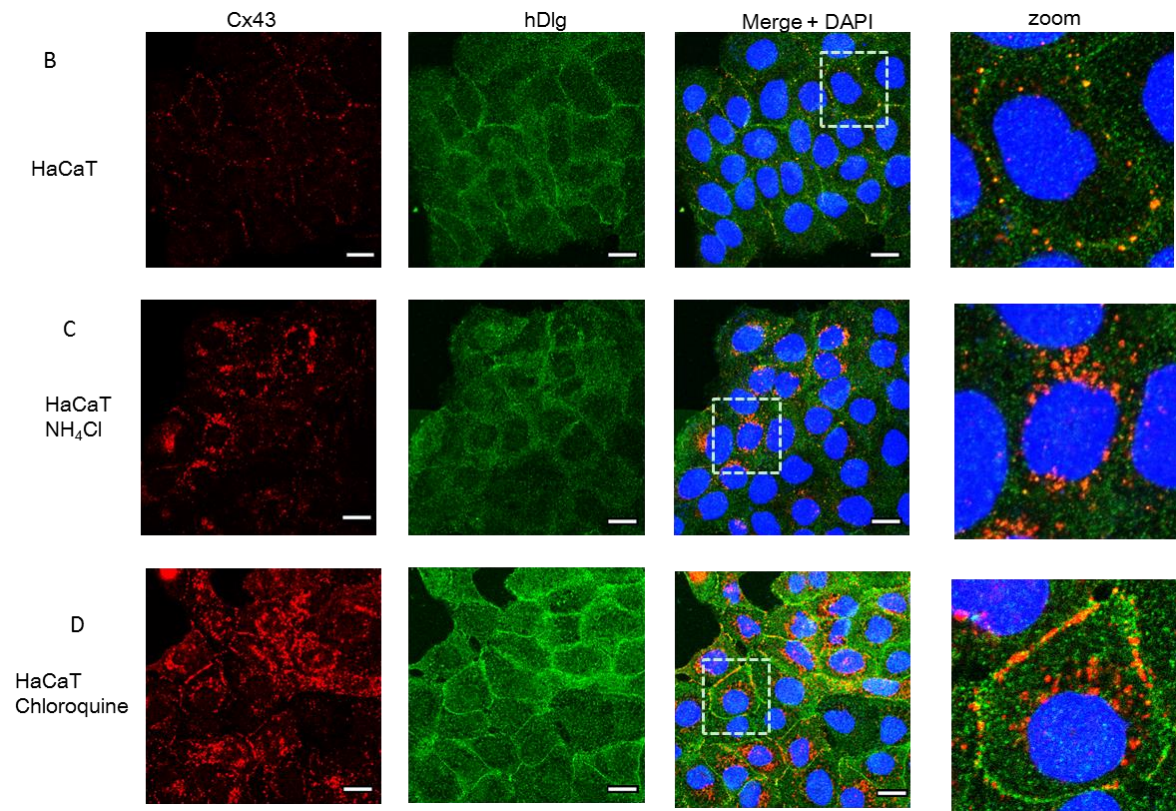
accumulated in the cytoplasm with very little membrane Cx43 (Figure 3.10 C). In chloroquine-treated HaCaT cells, accumulated cytoplasmic Cx43 was observed, while some Cx43 stayed on the membrane with larger gap junction plaques compared to mock-treated HaCaT (Figure 3.10 D). Both  $\text{NH}_4\text{Cl}$  and chloroquine seem to have no effects on the location of hDlg that stayed on the plasma membrane (Figure 3.10 C and D). The same experiments were repeated in HEK293 cells. Similar to the results in HaCaT cells, HEK293 cells treated with  $\text{NH}_4\text{Cl}$  and chloroquine showed an increasing level of Cx43 and no difference in the level of hDlg compared to mock-treated cells. Only one band of Cx43 was observed in HEK293 cells whether mock-treated or lysosomal inhibitor-treated. The 20kDa Cx43 band was only observed in  $\text{NH}_4\text{Cl}$ -treated HEK293 cells (Figure 3.11 A), which is consistent with the observation in  $\text{NH}_4\text{Cl}$ -treated HaCaT cells. Accumulated cytoplasmic Cx43 was observed in both  $\text{NH}_4\text{Cl}$  and chloroquine-treated HEK293 cells while some membrane Cx43 was observed. This is a similar observation to that in HaCaT cells, where lysosome inhibitors seemed to have no effect on the location of hDlg, which stayed on the plasma membrane (Figure 3.11 C and D). These results indicated that the major degradation pathway of Cx43 is via the lysosome degradation pathway.

Next, lysosome inhibitors were used to investigate whether the reduced level of Cx43 caused by siRNA depletion of hDlg in HaCaT cells could be rescued. HaCaT cells underwent siRNA depletion of hDlg for 48h followed by 8h treatment with mock treatment or endosome/lysosome inhibitors  $\text{NH}_4\text{Cl}$  and chloroquine. Both  $\text{NH}_4\text{Cl}$  and chloroquine increased the level of Cx43 in HaCaT cells with siRNA depletion of hDlg compared to mock-treated cells (Figure 3.12).

The 20kDa Cx43 band was observed in both mock-treated and  $\text{NH}_4\text{Cl}$ -treated siDlg HaCaT cells but hardly seen in Chloroquine-treated siDlg HaCaT cells. However, this 20kDa Cx43 band was not observed in previously siDlg HaCaT experiments. In the previous siDlg experiment, HaCaT cell proteins were extracted as soon as 48h treatment was completed with siRNA of hDlg. But in this experiment, the HaCaT cell grew 8h more before extraction (lysosome inhibition treatment is 8h). Since Cx43 has a short half-life, 8h might allow

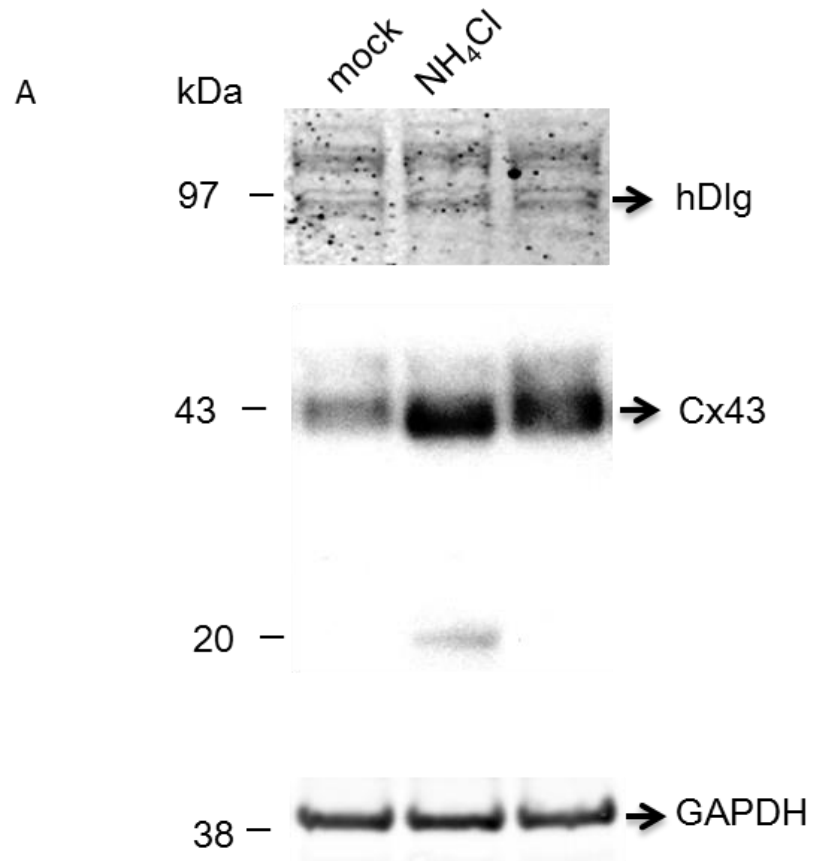
new synthesis of Cx43 which was unable to traffic to the plasma membrane, due to the lack of hDlg, and was delivered to the lysosome for degradation. This suggests a role for hDlg in maintaining the stability of Cx43 in antagonism to lysosome degradation. 20kDa form of Cx43 was only observed in NH<sub>4</sub>Cl treated but not chloroquine treated cells (HaCaT, HEK293, HaCaT siDlg). This indicates that lysosome inhibitor NH<sub>4</sub>Cl might prevent the degradation of 20kDa Cx43.





**Figure 3.10: Increasing levels and accumulated cytoplasmic Cx43 was observed in HaCaT cells with lysosome inhibitor treatment.**

(A) Lysosome inhibitor increases the level of Cx43 in HaCaT cells compared to mock-treated cells. Confocal immunofluorescence microscopy shows the location of Cx43 and hDlg in HaCaT cells with (B) mock-treated, (C) NH<sub>4</sub>Cl treated and (D) chloroquine treated. Cx43 (red) is in the cytoplasm in NH<sub>4</sub>Cl treated HaCaT cells (C) and on both the membrane and cytoplasm in chloroquine treated HaCaT cells (D), hDlg (green) stayed on the plasma membrane with no effect by lysosome inhibitors treatment. Large merged images of each cell line are shown on the right-hand side. Nuclei were stained with DAPI (blue). The scale bar is 20µm.



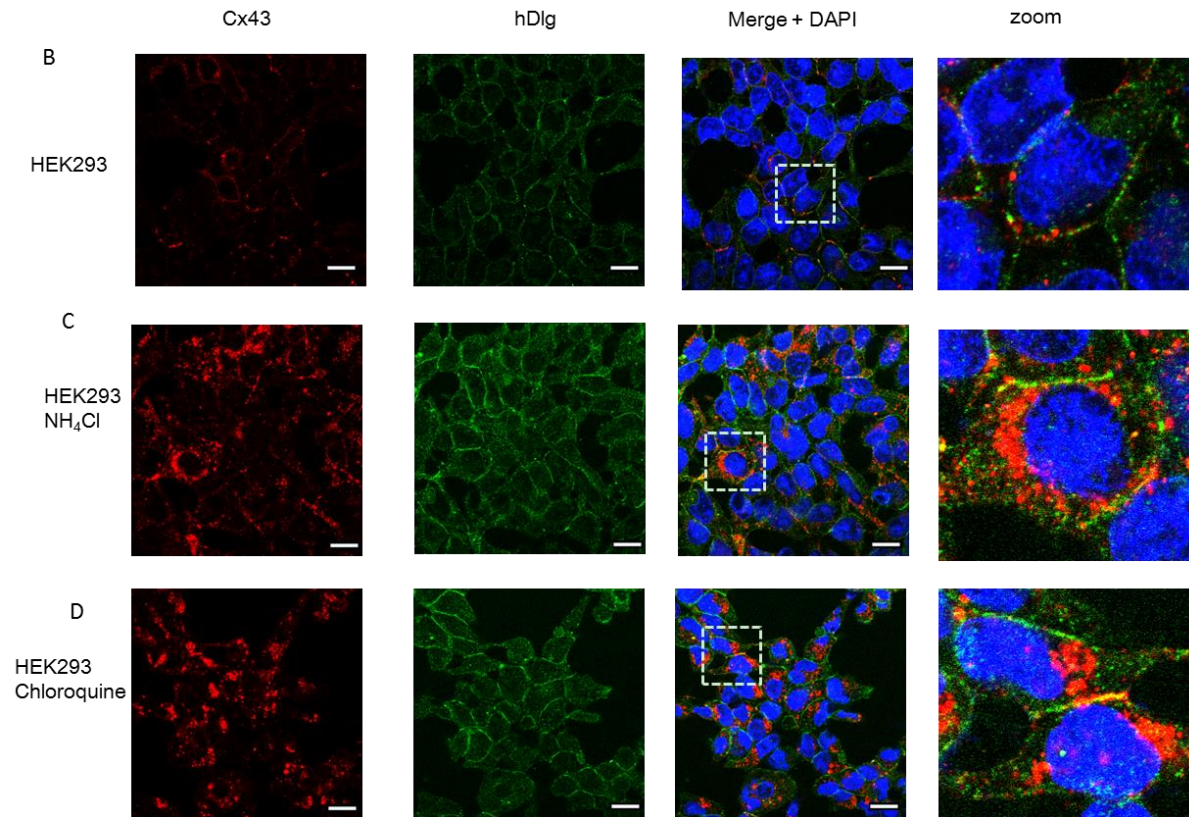


**Figure 3.11: Increasing levels and accumulated cytoplasmic Cx43 was observed in HEK293 cells with treatment of lysosome inhibitor.**

(A) Lysosome inhibitor increases the level of Cx43 in HaCaT cells compared to mock-treated cells. Confocal immunofluorescence microscopy shows the location of Cx43 and hDlg in HEK293 cells with (B) mock-treated, (C) NH<sub>4</sub>Cl treated and (D) chloroquine treated. Cx43 (red) is in the cytoplasm in NH<sub>4</sub>Cl treated HEK293 cells (C) and on both the membrane and cytoplasm in chloroquine treated HEK293 cells (D), hDlg (green) stayed on the plasma membrane with no effect by lysosome inhibitors treatment. Large merged images of each cell line are shown on the right-hand side. Nuclei were stained with DAPI (blue). The scale bar is 20µm.

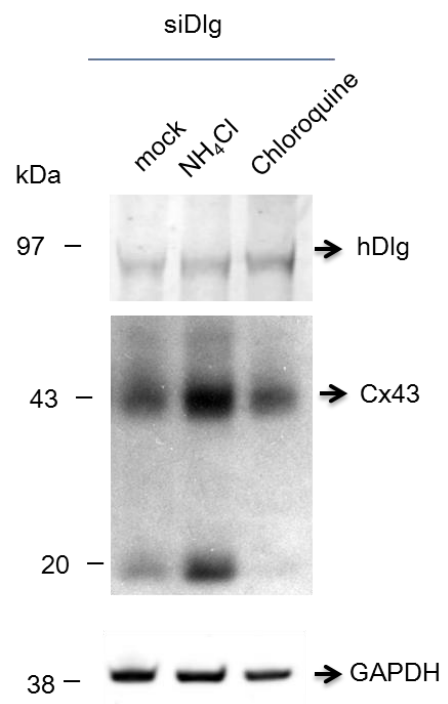


**Figure 3.12: Lysosome inhibitor rescued some level of Cx43 decreased by siRNA depletion of hDlg in HaCaT cells.**

HaCaT cells were treated with mock, NH<sub>4</sub>Cl, and chloroquine after 48h siRNA depletion of hDlg.

### 3.5 Discussion

Gap junction intracellular channels (GJIC) provide direct communication between the cytoplasm from neighbouring cells, allowing the exchange of ions, small molecules, and some secondary messengers, and maintaining homeostasis. Cx43, a widespread building block of gap junctions, has been found associated with many disorders like skin diseases, cardiovascular disease, and cancers. A reduced level and relocation of Cx43 from the plasma membrane to the cytoplasm is observed *in vitro* and *in vivo* in cervical cancers. Nearly all cervical cancer is HPV-positive and HPV16 acts as an oncoprotein and has been found to be involved in controlling the trafficking of Cx43 by targeting hDlg (Macdonald et al., 2012b).

Data here suggest that Cx43 colocalised with hDlg in the cytoplasm in C33a expressing HPV16E6 but mainly on the plasma membrane in C33a (HPV-negative) cells. The colocalisation was also observed on the plasma membrane in non-tumour cells (HEK293, HaCaT, NIKS, and NIKS16). Protein-protein interaction of Cx43 and hDlg is found in these non-tumour cells and HPV-negative cervical cancer cells (C33a and C33aE6). These data suggest the interaction between Cx43 and hDlg is neither HPV16- dependent nor cancer cell-specific.

Heavy chain (HC, 55kDa) and light chain (LC, 25kDa) of the antibody were observed in the co-immunoprecipitation experiments. This is because the traditional secondary antibody, horse radish peroxidase (HRP)-conjugated secondary antibody, and Cx43 antibody (Macdonald et al., 2012b), recognises denatured HC/LC which are eluted from the beads together with antigen. The rabbit polyclonal antibody used in IP and also in Western blot might also be part of the reason. In future experiments, specific secondary antibodies (e.g. RP-conjugated Protein A or Protein G) could be used to remove the background (Lal et al., 2005).

More than one band of hDlg was observed in NIKS16 cells (Figure 3.3). A similar pattern of hDlg has been observed in CaSki and HeLa cells (Kranjec and Banks, 2010). CaSki cells are HPV16-positive while HeLa cells are HPV18-positive. HPV18E6 has a greater targeting and degradation efficiency for hDlg rather than HPV16E6 (Thomas et al., 2005). Therefore, the second band of hDlg in NIKS16

cells (Figure 3.3) could be a partially degraded form of hDlg due to the low level of E6 expressed from the HPV16 genome in NIKS16 cells.

siRNA depletion of hDlg in HaCaT and HEK293 cells led to a reduction in the levels and cytoplasmic location of Cx43. Reduced levels of Cx43 were also observed in NIKS and NIKS16 cells with siRNA depletion of hDlg. Similar results were observed in HaCaT cells with stable depletion of hDlg. These data suggest the role of hDlg in maintaining the level of Cx43 and trafficking of Cx43 in non-tumour cells.

In cervical cancer cells, Cx43 was not located at the plasma membrane but was found in a perinuclear location. This was consistent with the loss of GJIC in these cells (Macdonald et al., 2012b). hDlg was found to colocalise with Cx43 in the cytoplasm in these HPVE6-positive cells. siRNA depletion of HPVE6 in W12GPXY, and in C33a cells of a mutated HPV18E6 that could no longer bind hDlg, led to the restoration of membrane Cx43 (Sun et al., 2015). Data here further confirm that HPVE6 controls the trafficking of Cx43 via its targeting of hDlg in cervical cancer cells. The re-establishment of GJIC between neighbour cells in the presence of inhibitors of protein synthesis, suggests the existence of a cytoplasmic pool of Cx43 allowing the re-building of the gap junction communication. siRNA depletion of hDlg in W12GPXY cells led to a reduced level of Cx43, suggesting the role of hDlg in maintaining a cytoplasmic pool of Cx43 in cervical tumour cells (Macdonald et al., 2012b). Combined with results here, this indicates the general role of hDlg in maintaining a cytoplasmic pool of Cx43. A recycling of Cx43 from this type of cytoplasmic pool to re-establish gap junctions in daughter cells, rather than newly synthesized Cx43, during mitosis has been observed. This recycling of Cx43 might play an essential role in cytokinesis (Boassa et al., 2010). Therefore, it could be interesting to examine the role of hDlg in Cx43 membrane insertion during mitosis.

MAGUK proteins such as hDlg might function in the localisation and recruitment of other proteins to the membrane or as molecular scaffolds allowing interactions of proteins/signals (Dimitratos et al., 1999). hDlg, as a member of the MAGUK protein family, might localise and recruit Cx43 onto the membrane and thus be involved in the control of Cx43 trafficking. The upper stronger bands of Cx43 are observed in HEK293 and HaCaT cells with siRNA depletion of hDlg

compared to mock-treated cells (Figure 3.7 A and B). These might represent Cx43 undergoing post-translation modifications such as phosphorylation or ubiquitination. Phosphorylation plays an important role in GJIC. For example, phosphorylation of Cx43 at site S368 results in a reduction of the hemichannel opening (Bao et al., 2004). Phosphorylation might cause a conformational change that alters the interaction between Cx43 and other proteins. For example, phosphorylation of Cx43 at the site Y265 disrupts the binding between Cx43 and ZO-1 (Toyofuku et al., 2001). hDlg and ZO-1 both belong to the MAGUK protein family, but each has a different interaction region with Cx43 (Macdonald et al., 2012b). It is still interesting to investigate whether phosphorylation affects the interaction between Cx43 and hDlg (this will be discussed in Chapter 5). Cx43 can be a substrate for ubiquitin and mono-ubiquitination as a trigger for internalisation and further degradation via the lysosome.

Previous data have indicated that most intracellular Cx43 and hDlg are targeted to the lysosomal degradation pathway in W12GPXY and C33aE6 cells (Peng Sun, PhD thesis, 2005). Lysosome inhibitor  $\text{NH}_4\text{Cl}$  increases the level of Cx43 and hDlg in W12GPXY cells (Macdonald et al., 2012b), and in the presence of lysosome inhibitor, a notable increase of cellular Cx43 is observed in breast tumour cells (Qin et al., 2003). Both lysosome inhibitor  $\text{NH}_4\text{Cl}$  and chloroquine increase the level and cytoplasmic accumulation of Cx43 in HaCaT and HEK293 cells compared to mock-treated cells. Lysosome inhibitors seem to have no effect on the alteration of both protein levels and the location of hDlg. This might suggest the degradation of Cx43 is mainly through the lysosome degradation pathway while hDlg might utilize another degradation pathway.

20kDa Cx43 is a predominant truncated Ct isoform of Cx43 produced by translation reinitiation (Leithe et al., 2017b). It is only observed in  $\text{NH}_4\text{Cl}$ -treated but not chloroquine-treated HEK293 and HaCaT (Figure 3.10 A and Figure 3.11 A). The majority of Cx43 was located in the cytoplasm and almost no membrane Cx43 was observed in HaCaT cells treated with  $\text{NH}_4\text{Cl}$ , while some membrane Cx43 was observed in chloroquine-treated HaCaT cells (Figure 3.10 C and D). 20kDa Cx43 can interact with full-length Cx43 as a protein-chaperone, which helps the trafficking of Cx43 to the border of cells (Epifantseva and Shaw, 2017). It might also be involved in Cx43 trafficking to the cytoplasm, which could explain why less membrane Cx43 is observed in  $\text{NH}_4\text{Cl}$  treated HaCaT cells

but not in chloroquine treated cells.  $\text{NH}_4\text{Cl}$  and chloroquine work as weak bases that neutralize the pH in the lysosomes (lysosomes require a highly acidic environment for proper function). Chloroquine prevents acidification of endosomes and lysosomes and prevents endosome-lysosome fusion.  $\text{NH}_4\text{Cl}$  can inhibit lysosome movements and phagosome-lysosome fusion. Similar to Cx43, 20kDa Cx43 is degraded via the lysosome and results here suggested that might be through phagosome-lysosome fusion but not endosome-lysosome fusion. 20kDa Cx43 isoform was observed in HaCaT shDlg cells and HaCaT with 8h more growth after siDlg treatment (Figure 3.9 A and Figure 3.12). The 20kDa Cx43 could help full-length Cx43 traffic to the membrane (Smyth and Shaw, 2013). Therefore, the expression of 20kDa Cx43 in HaCaT shDlg and HaCaT with 8h more growth after siDlg treatment might be triggered by Cx43 waiting to be trafficked to the plasma membrane.

In conclusion, in this chapter, it is now shown that Cx43-hDlg interaction is neither HPVE6-dependent nor tumour cell-specific. Cx43 and hDlg colocalised on the plasma membrane in non-tumour cells, HEK293, HaCaT, NIKS, and NIKS16 cells. Interaction between Cx43 and hDlg was also proved with co-immunoprecipitation in these cell extractions. siRNA depletion of hDlg led to a reduction in levels of Cx43 in all these four cells, and cytoplasmic relocation in HaCaT and HEK293 cells. Further, a reduced level and cytoplasmic location of Cx43 was also observed in HaCaT cells with stable depletion of hDlg. Lysosome inhibitor-treated HaCaT and HEK293 cells showed increased levels of Cx43 and accumulation of cytoplasmic Cx43. Furthermore, treatment with lysosome inhibitor led to an increasing level of Cx43 in HaCaT cells with siRNA depletion of hDlg compared to mock cells. These results suggested widespread interaction between Cx43 and hDlg in cells and also indicates the role of hDlg in regulating the trafficking of Cx43 and maintaining the stability of Cx43 from degradation via lysosome.

## **4 Chapter 4**

### **Cx43 and the wound healing process**

Skin is the first protection for humans against any infections. Any wound to the skin will lead to the wound healing process, which includes four stages: haemostasis, inflammation, proliferation, and migration, followed by scar tissue remodelling. This, as a result, closes the wound and restores the protective function of the skin (Gantwerker and Hom, 2011). Previously, data from several laboratories showed that protein levels of Cx43 changed during wound healing (Kretz, 2003, Coutinho, 2003). In human cutaneous wound healing, the first alterations were observed at 6h post-wounding when Cx43 was downregulated at the wound edge and the protein level was continually reduced until Cx43 was virtually undetectable within the first 1-2 days after wounding (Brandner et al., 2004). These events are regulated through a “kinase program”, where specific Cx43 CT-phosphorylation events occur in a time-dependent manner during wound closure (Solan and Lampe, 2016). Although Cx43 is dramatically reduced in actively migrating leading edge keratinocytes, it has been found at relatively high levels a few cell rows back from the wound edge where there are actively proliferating cells. Interestingly, at the wound edge in keratinocytes Cx43 is reduced as early as 5h post-wound and nearly undetectable by 24h while Cx26 and Cx30 which are normally expressed at low levels are found to be greatly increased in cells at the edge of wounds (Brandner et al., 2004). Cx26 and Cx30 can form gap junctions with each other but not with Cx43 and they have very different coupling and dye transfer properties (Brandner et al., 2004). Therefore, cell migration requires gap junctional communication and is associated with less membranous Cx43 since a dramatic reduction in levels of Cx43 is observed in cells along the wound edge.

## 4.1 Cx43 is internalised during keratinocyte scrape wound closure

The previous chapter has indicated that the interaction between Cx43 and hDlg occurs in non-tumour keratinocytes. siRNA depletion of hDlg led to the cytoplasmic location of Cx43 in normal keratinocytes. Sun and co-workers (Sun et al., 2015) demonstrated that deletion of the last four amino acids of E6, which are the site for Dlg binding, resulted in Cx43 membrane location in W12GPXY cells. This suggests that HPVE6 controlled the trafficking of Cx43 via its interaction with hDlg. However, HPVE6 together with HPVE7, the second viral oncoprotein, can alter several signalling pathways in infected cells leading to tumour progression (Gupta and Mania-Pramanik, 2019). Tumour progression is a complex process that includes alterations in many signalling pathways so E6 could affect Cx43 location through the changes it induces in intracellular signalling equally as much as through its physical interaction with hDlg. The wound healing process and the process of cancer progression shares some signalling pathway changes: Sustaining proliferative signalling is one of the cancer hallmarks, while proliferation is one of the phases in wound healing process (Gantwerker and Hom, 2011, Hanahan and Weinberg, 2011). Understanding the role of Cx43 in wound healing process can provide an inspiration on how Cx43 in cancer progression.

It has been reported previously that in keratinocytes Cx43 relocated from the plasma membrane into the cytoplasm during the early stages of the wound healing process (Wright et al., 2009), and this relocation is similar to what has been observed in HPVE6-positive tumour cells. To investigate whether hDlg is involved in controlling the trafficking of Cx43 during the wound healing process, we used a wound healing model in which a 20  $\mu$ l yellow tip was utilized to create the wounds on a monolayer fully confluent cells, and the cells were harvested at certain time points after wounds at 0h, 4h, 8h, 16h, and 24h.

First, immunofluorescence confocal microscopy was used to investigate the subcellular location of Cx43 and hDlg in HaCaT cells undergoing wound healing as a model for normal keratinocytes. As expected, Cx43 was located on the plasma membrane at 0h, which cells were fixed immediately after the wound created so that cellular changes in response to the wound have not occurred and the Cx43

stayed on the plasma membrane just as in an un-wounded state (Figure 4.1 A, white arrow). At 4h, Cx43 at the wound edge was moved into the cytoplasm, while the membrane Cx43 was still observed in cells away from the wound edges (Figure 4.1 B, white arrows). At 8h, Cx43 was observed in the cytoplasm and perinuclear areas in the cells along the wound edges. Cx43 was located in the cytoplasm in the cells away from the wound margin, while some membrane Cx43 was observed in the cells behind the wound edge (Figure 4.1 C, white arrows). At 16h, Cx43 was still observed in the cytoplasm in the cells even behind the wound edge. No membrane Cx43 was observed (Figure 4.1 D, white arrows). The wound was closed at 24h and membrane Cx43 was observed again. Some cytoplasmic Cx43 was also observed (Figure 4.1 E, white arrows). This indicates that the movement of Cx43 during the wound healing process is from the membrane to the cytoplasm and back to the membrane.

Then, the subcellular location of hDlg, as a potential controller of Cx43, was also investigated during the wound healing process. As can be seen in Figure 4.1 A, hDlg was located on the cell membrane that co-localised with Cx43 at 0h. At 4h, hDlg was not on the plasma membrane and might co-localised with Cx43 in the cells along the wound edge but remained and co-localised with Cx43 on the plasma membrane in the cells behind the wound (Figure 4.1 B, white arrows). hDlg was lost from the plasma membrane and co-localised with Cx43 in the cytoplasm and perinuclear area in the cells along the wound edge at 8h. Some hDlg was still observed co-localised on the plasma membrane and in the cytoplasm in the cells behind the wound margin (Figure 4.1 C, white arrows). At 16h, hDlg was mainly located in the cytoplasm in the cells along and behind the wound edge where some co-localisation with Cx43 was observed. Still some membranous hDlg was observed in the cells behind the wound edge (Figure 4.1 D). The wound was closed at 24h, hDlg was mainly located on the plasma membrane where it co-localised with Cx43 (Figure 4.1 E, white arrows). This indicates that at least some hDlg share a similar movement pattern and co-localised with Cx43 during the wound healing process.

It has been reported that the cellular level of Cx43 is reduced at the early stage of wound healing and then it recovers to a normal level after wound closure (Brandner et al., 2004). Therefore, western blotting, using a rabbit polyclonal Cx43 antibody and a mouse monoclonal hDlg antibody, was used to investigate

the alteration in levels of Cx43 and hDlg during the wound healing process. Samples were harvested from the entire cell population (therefore most of the cells are not at the wound edges) according to the time points as previously stated. Mitomycin C was not employed to stop proliferation therefore the phenomenon is due to cell migration and proliferation. Figure 4.2 B shows a drop in Cx43 levels at 4h post wound and a peak of Cx43 protein levels at 16h. The trend for Cx43 levels during the wound healing process was a reduction in levels from 0h to 4h then an increase in Cx43 levels from 4h to 16h followed by a slight reduction at 24h. A hyperphosphorylated band of Cx43 was observed in the protein samples harvested at 4h and 8h compared to mock, 16h and 24h (Figure 4.2 A, arrows). For hDlg, a similar trend to that with Cx43 was observed (Figure 4.2 C). The protein level of hDlg reduced from 0h to 4h, and then increased until a peak at 16h followed by a slight decrease at 24h.

In order to investigate the wound repair process at a cellular level, photographs were taken at each time point at the same wound area during the time course experiment of wound closure in HaCaT keratinocytes. Figure 4.3 shows that between 0h to 8h, the area of the wound seemed not to change. The scrape wound gap started to close between 8h and 16h and then the gap closed much more rapidly between 16h and 24h. The gap closure was almost complete at 24h. This indicates that the reduced levels of Cx43 and hDlg observed in Figure 4.2 were before the start of cell migration/wound closure (0h -4h), and the increased level of these two proteins correlated with rapid wound closure (8-16h). When the closure was nearly finished, the protein levels dropped towards the unwounded state. These data indicated that hDlg might regulate Cx43 during the wound healing process.

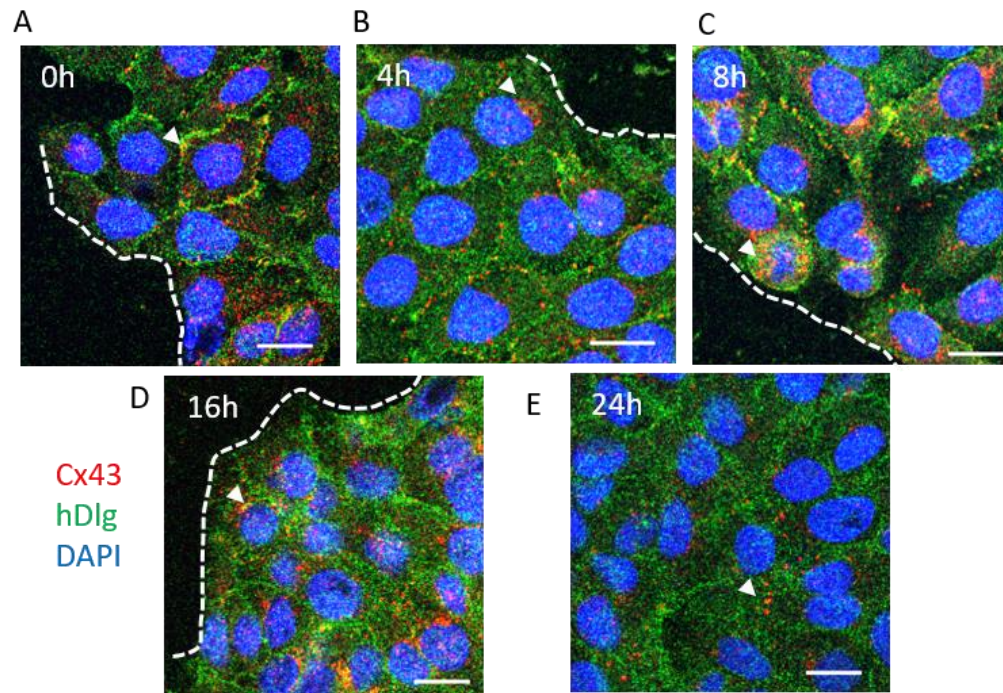


**Figure 4.1: Cx43 cycled from the plasma membrane to the cytoplasm during the wound healing process in HaCaT cells.**

Confocal immunofluorescence microscopy shows the location of Cx43 and hDlg in HaCaT (human keratinocyte cells) according to the wound healing time points: (A) 0h, (B) 4h, (C) 8h, (D) 16h, and (E) 24h. Cx43 (red) and hDlg (green) were co-localised on the plasma membrane at 0h post-wound. White dotted lines indicate the wound edges. The white arrowheads indicate the locations of Cx43. Nuclei were stained with DAPI (blue). The scale bar is 20µm.

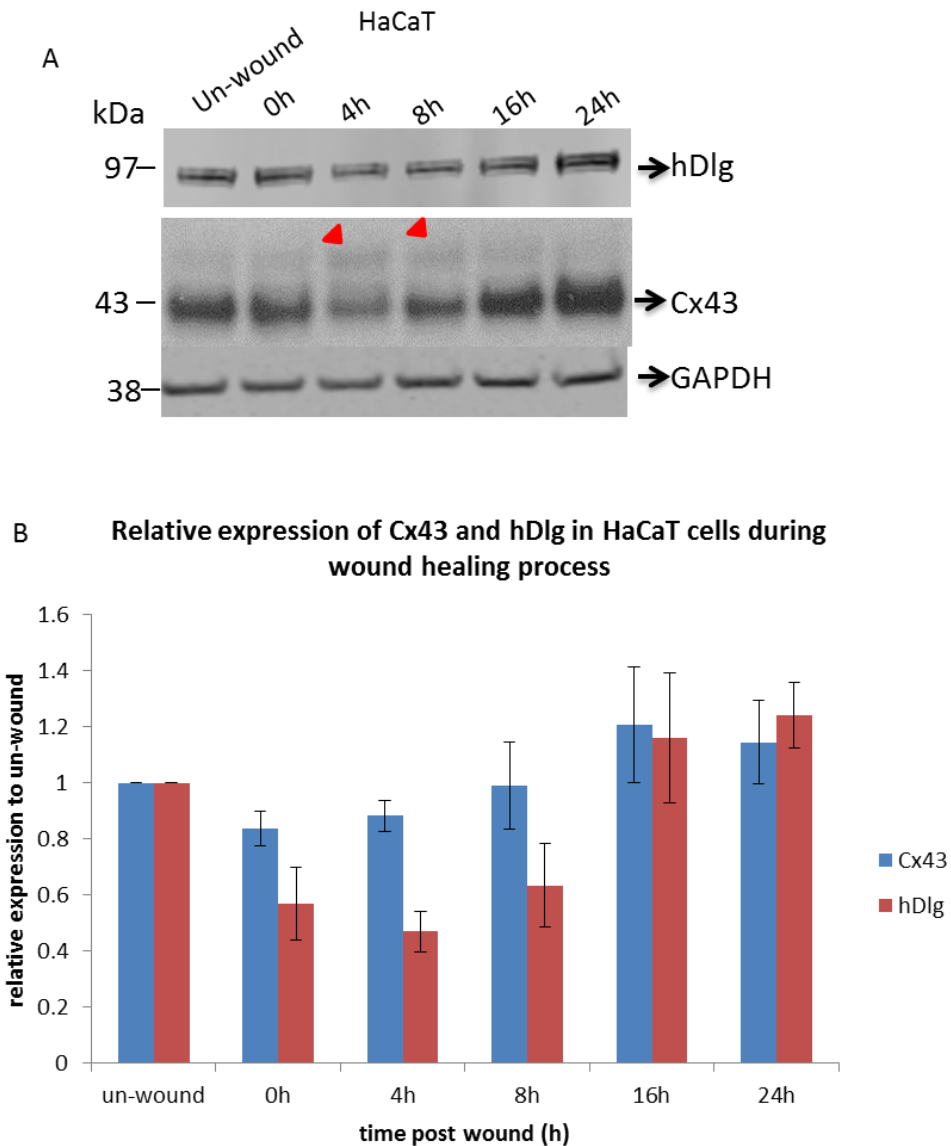


**Figure 4.2: The levels of Cx43 and hDlg in HaCaT cells are altered during the wound healing process.**

(A) Western blot showing the expression of Cx43 and hDlg in cell extracts from HaCaT cells according to the wound healing time points. Red arrows indicate the hyperphosphorylated forms of Cx43. Images of hDlg and GAPDH were obtained from Licor imaging and image of Cx43 were exposed with X-ray film. (B) Quantification of Cx43 and hDlg levels during the wound healing process. The intensity of Cx43 and hDlg bands was measured by ImageJ and normalised to un-wounded cell layers. This experiment has been repeated three times.

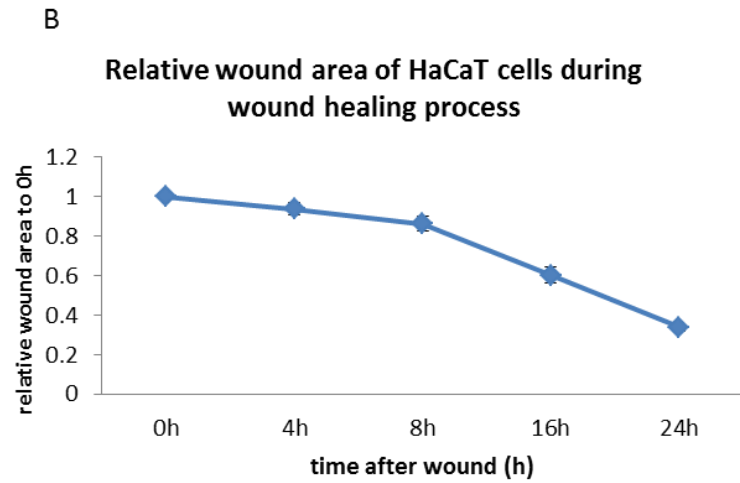
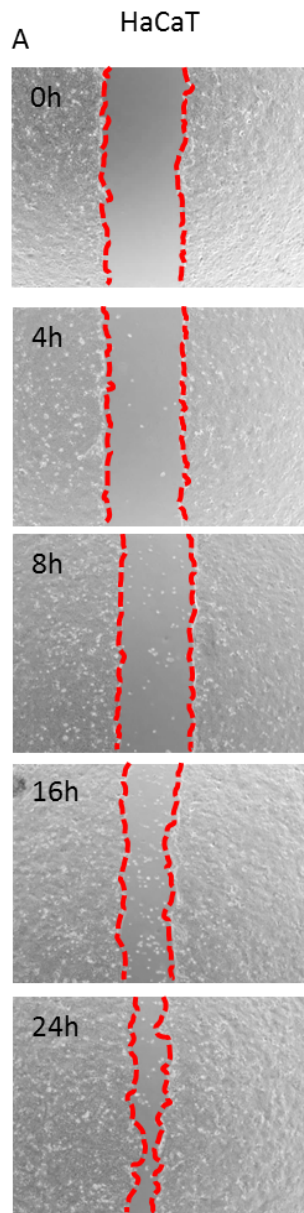


**Figure 4.3: The wound closure process in HaCaT cells.**

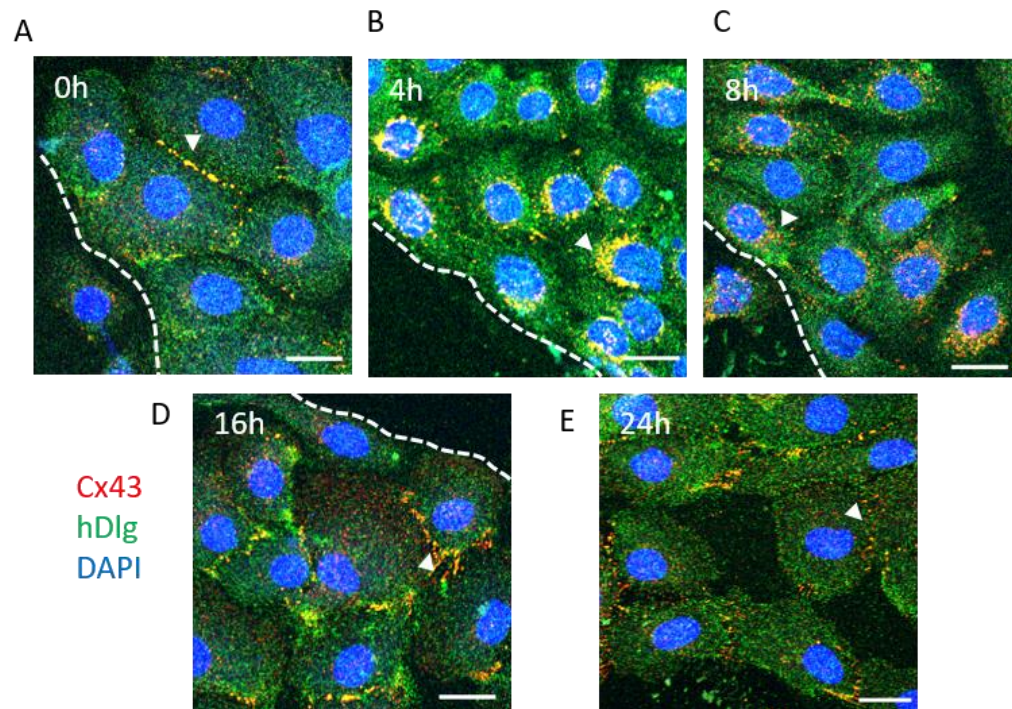
(A) Photos were taken according to the wound healing time points (0h, 4h, 8h, 16h, and 24h). The red dotted lines indicate the wound edges. (B) Quantification of the wound area was normalized to 0h according to wound healing time points. This experiment has been repeated three times.

These experiments were repeated in NIKS (normal immortalized keratinocyte cells) and NIKS16 cells (NIKS cells stably transfected with the HPV16 genome) in order to investigate whether HPV16 genome or low level of HPV E6 will affect cell behaviour in response to wound healing. Here, keratinocyte growth in KGM was used to avoid any influence of the 3T3 feeder layer that was normally used to support NIKS cell growth. Similar to what was observed in HaCaT cells, Cx43 in NIKS cells was located on the plasma membrane at 0h (Figure 4.4 A) and moved to the cytoplasm/peri-nuclear area at 4h (Figure 4.4 B), and stayed in the cytoplasm at 8h (Figure 4.4 C). At 16h, Cx43 was partially back on the plasma membrane and was located mainly on the membrane at 24h (Figure 4.4 D and E). These alterations were not only occurring in the cells along the wound edges but in the cells behind the wound edges as well, which might indicate a rapid spread of cell signalling in NIKS cells compared with HaCaT cells. hDlg co-stained with Cx43 on the plasma membrane at 0h (Figure 4.4 A), while co-staining was observed in the cytoplasm at 4h (Figure 4.4 B) and 8h (Figure 4.4 C) while some membrane hDlg was observed in the cells behind the wound at 4h (Figure 4.4 B). However, due to slow growth in KGM without feeder layers, NIKS cells were not fully confluent before the wound healing assay (Figure 4.4). There were some gaps between cells at 8h, 16h, and 24h (Figure 4.4 C, D, and E). This might explain the relative lack of gap junction plaques observed in Figure 4.4 compared to those of the NIKS cells in the previous chapter.

Regarding the protein levels, Cx43 levels in NIKS cells seemed not to change between 4h and 8h, they increased at 16h (peak) followed by a slight decrease at 24h (Figure 4.5 B). There were only low levels of Cx43 observed at 0h (Figure 4.5 A), this might be due to low cell density at this time point compared to the mock-treated control (the GAPDH band at 0h is less intense than the others at later time points). There are increasing levels of hDlg between 0h to 16h and followed by a decrease at 24h (Figure 4.5 B). The trend of changes in Cx43 and hDlg levels in NIKS cells was similar to what is observed in HaCaT cells except for the decrease of Cx43 level at 4h that was observed in HaCaT cells (Figure 4.2 B and Figure 4.5 B).

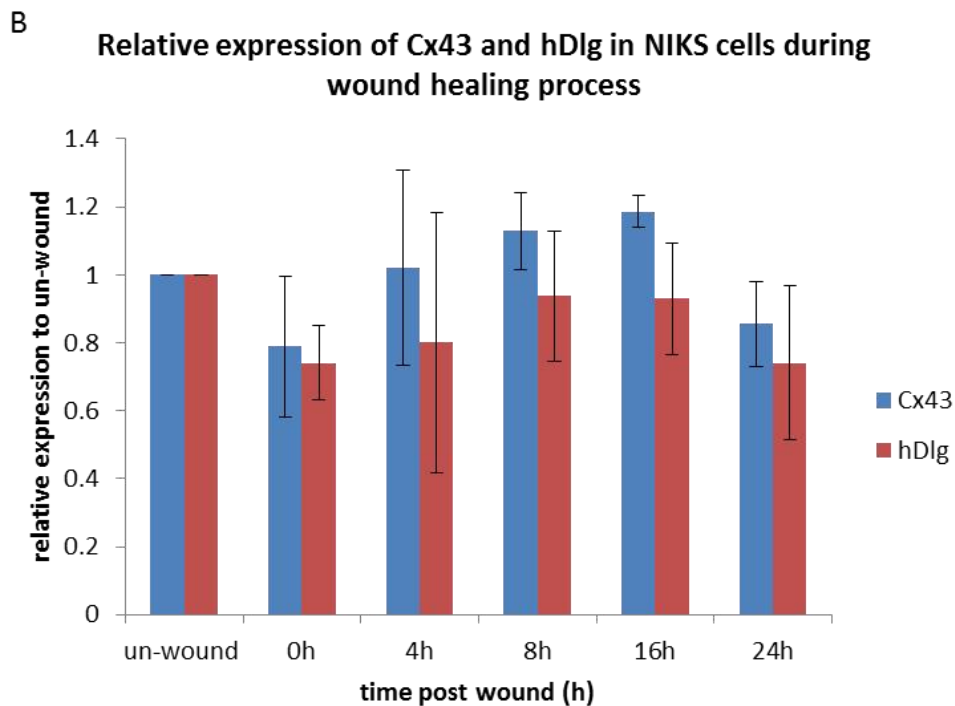
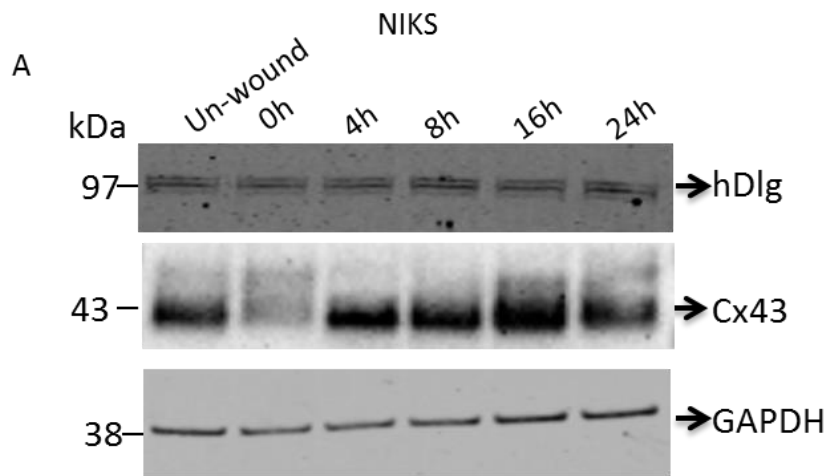
In NIKS16 cells, Cx43 levels were very similar for the first 8 hours following scrape wounding. There was a clear peak of protein levels at 16h followed by a slight decrease at 24h (Figure 4.6 B). The levels of hDlg followed a similar pattern but there was no decrease at 24h (Figure 4.6 C). The protein level alteration between NIKS and NIKS16 cells during the wound healing process was quite different (Figure 4.5 and 4.6).

Then the wound closure speed of NIKS and NIKS16 cells was checked using photographs of phase contract images according to the time points. For NIKS cells, the scrape wound area seemed not to change between 0h to 4h and started to close between 4h to 8h. There was a rapid closure phase between 8h and 16h, but the scrape wounds were not fully closed at 24h (Figure 4. 7 A). However, for NIKS16 cells, the process was much speedier. The wound closure seemed to start between 0h and 4h, rapid closure was observed between 4h and 8h, and the wound was fully closed at 16h (Figure 4.7B). This indicates that the HPV16 genome increases the speed of wound closure in NIKS16 cells compared to NIKS cells.



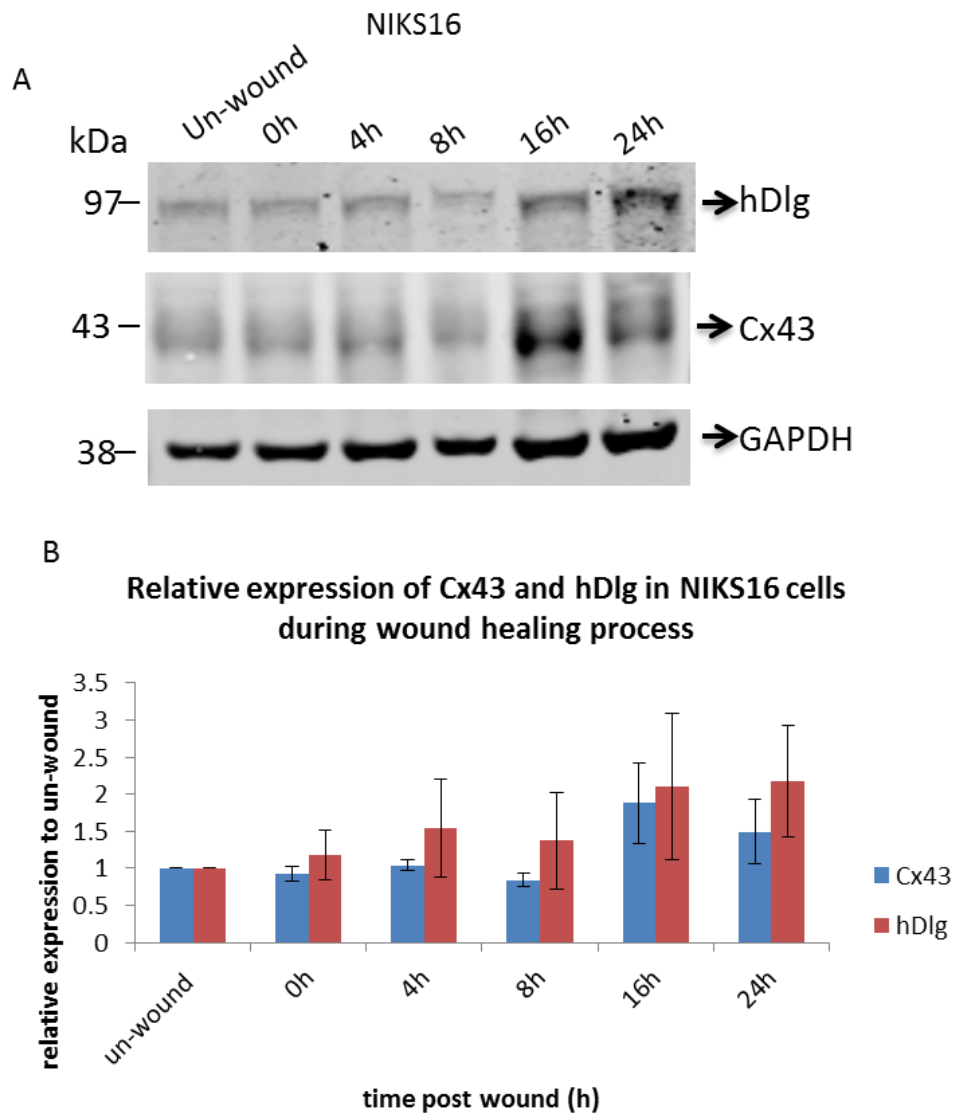
**Figure 4.4: Cx43 cycled from the plasma membrane to the cytoplasm during the wound healing process in NIKS cells.**

Confocal immunofluorescence microscopy shows the location of Cx43 and hDlg in NIKS cells according to the wound healing time points: (A) 0h, (B) 4h, (C) 8h, (D) 16h and (E) 24h. Cx43 (red) and hDlg (green) were co-localised on the plasma membrane at 0h post-wound. White dotted lines indicate the wound edges. The white arrowheads indicate the locations of Cx43. Nuclei were stained with DAPI (blue). The scale bar is 20µm.



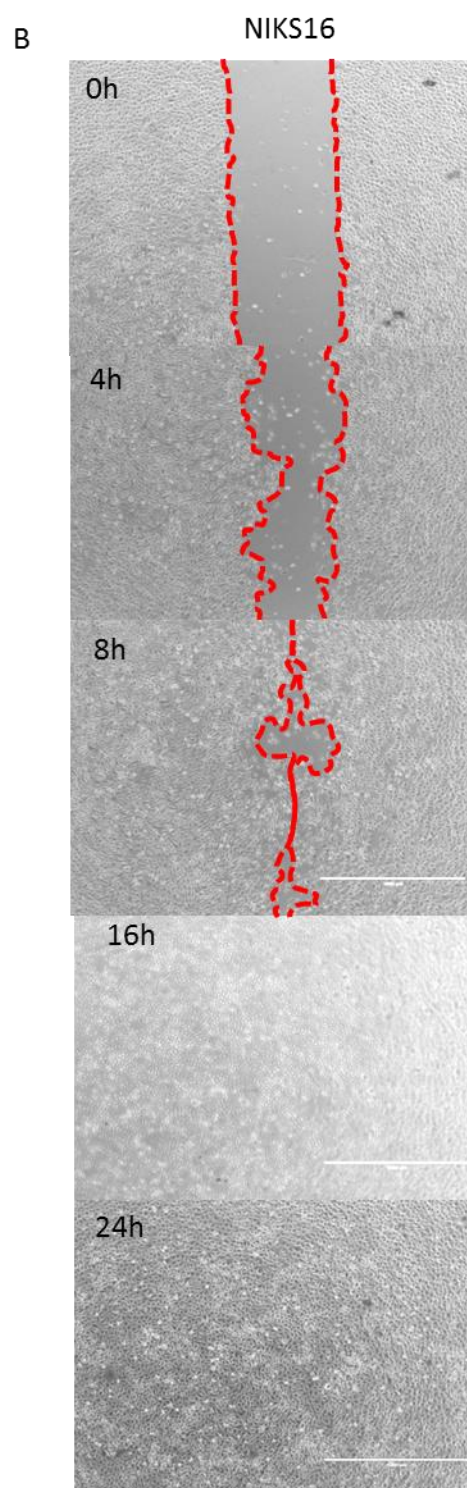
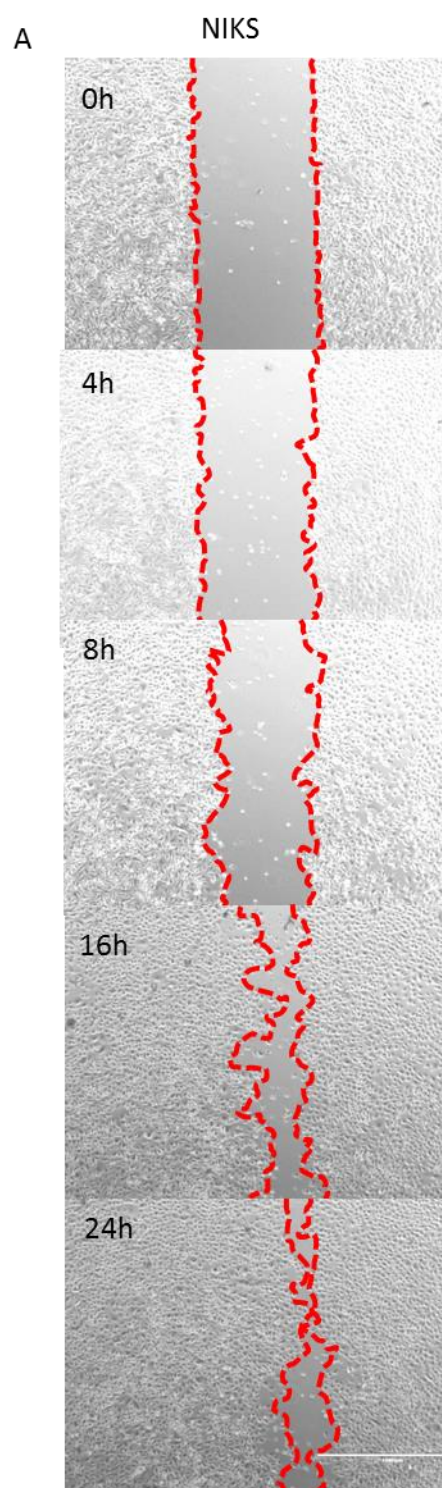
**Figure 4.5: The levels of Cx43 and hDlg in NIKS cells are altered during the wound healing process.**

(A) Western blot showing the expression of Cx43 and hDlg in NIKS cell extracts according to wound healing time points. Images of hDlg and GAPDH were obtained from Licor imaging and the image of Cx43 was exposed with X-ray film. (B) Quantification of Cx43 and hDlg levels during the wound healing process. The intensity of Cx43 and hDlg bands was measured by ImageJ and normalised to un-wounded cell layers. This experiment has been repeated three times.



**Figure 4.6: The levels of Cx43 and hDlg in NISK16 cells are altered during the wound healing process.**

(A) Western blot showing the expression of Cx43 and hDlg in NIKS16 cell extracts according to wound healing time points. Images of hDlg and GAPDH were obtained from Licor imaging and the image of Cx43 was exposed with X-ray film. (B) Quantification of Cx43 and hDlg levels during the wound healing process. The intensity of Cx43 and hDlg bands was measure by ImageJ and normalised to un-wound cell layers. This experiment has been repeated three times.



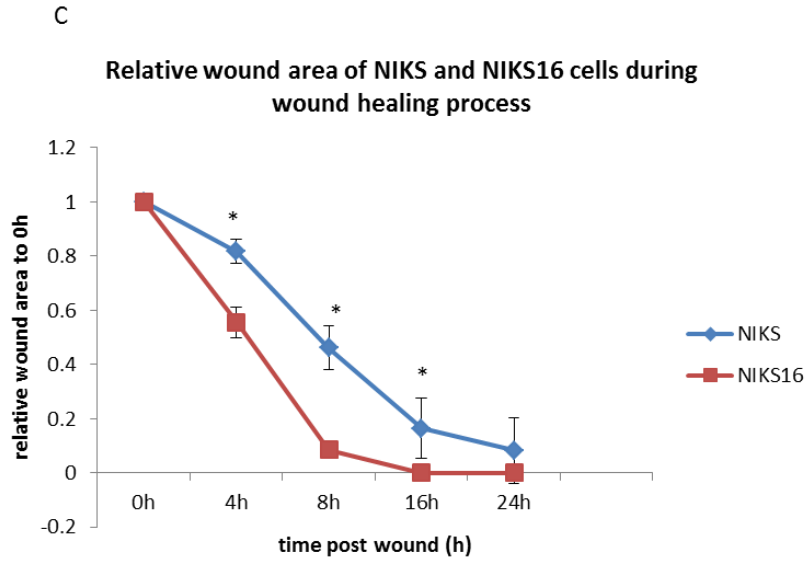


**Figure 4.7: The wound closure process in NIKS and NIKS16 cells.**

Photos of wound area in (A) NIKS and (B) NIKS16 cells were taken according to wound healing time points (0h, 4h, 8h, 16h, and 24h). The red dotted lines indicate the wound edges. (C) Quantification of the wound area changes (normalized to 0h) according to wound healing time points (\* indicates  $p < 0.05$ ). This experiment has been repeated three times.

## 4.2 hDlg plays an important role in scrape wound healing

hDlg has been thought to play roles in cell migration and cell proliferation (Stephens et al., 2018), both processes are included in the wound healing process. Together with the evidence that hDlg is a controller of Cx43 in keratinocytes, it would be worthwhile to investigate the location of hDlg with respect to Cx43 during the wound closure process. Some hDlg co-stained with Cx43 as it changed its location from the plasma membrane to the cytoplasm during scrape wound healing in HaCaT and NIKS cells (Figure 4.1 and 4.4). Reduced levels of Cx43 are required at the early stage of wound healing. Decreased Cx43 caused by Cx43-antisense resulted in increased ability of proliferation and migration of keratinocyte and fibroblast at wound sites (Mori et al., 2006). Since siRNA depletion of hDlg led to a reduction in the level of Cx43 (Chapter 3), it would be interesting to investigate whether siRNA depletion of hDlg altered the closure of scrape wounds due to reduced Cx43 levels. To investigate this, mock or siDlg-treated HaCaT cells prior to scraping wounding were used and analysis of wound closure was carried out. Figure 4.8 shows phase-contrast images of HaCaT cells over a time course of wound closure for the same wound area. In mock-treated HaCaT cells, the wound closure process was very similar to that as previously described, and the wound was nearly closed at 24h (Figure 4.8 A). However, in HaCaT cells with siRNA depletion of hDlg, the area of the wound did not change between 0h to 8h. The wound started to close between 8h to 16h followed by a slight reduction in closure rate at 24h (Figure 4.8 B). This data indicated that siRNA depletion of hDlg in HaCaT cells significantly delayed the wound healing process.

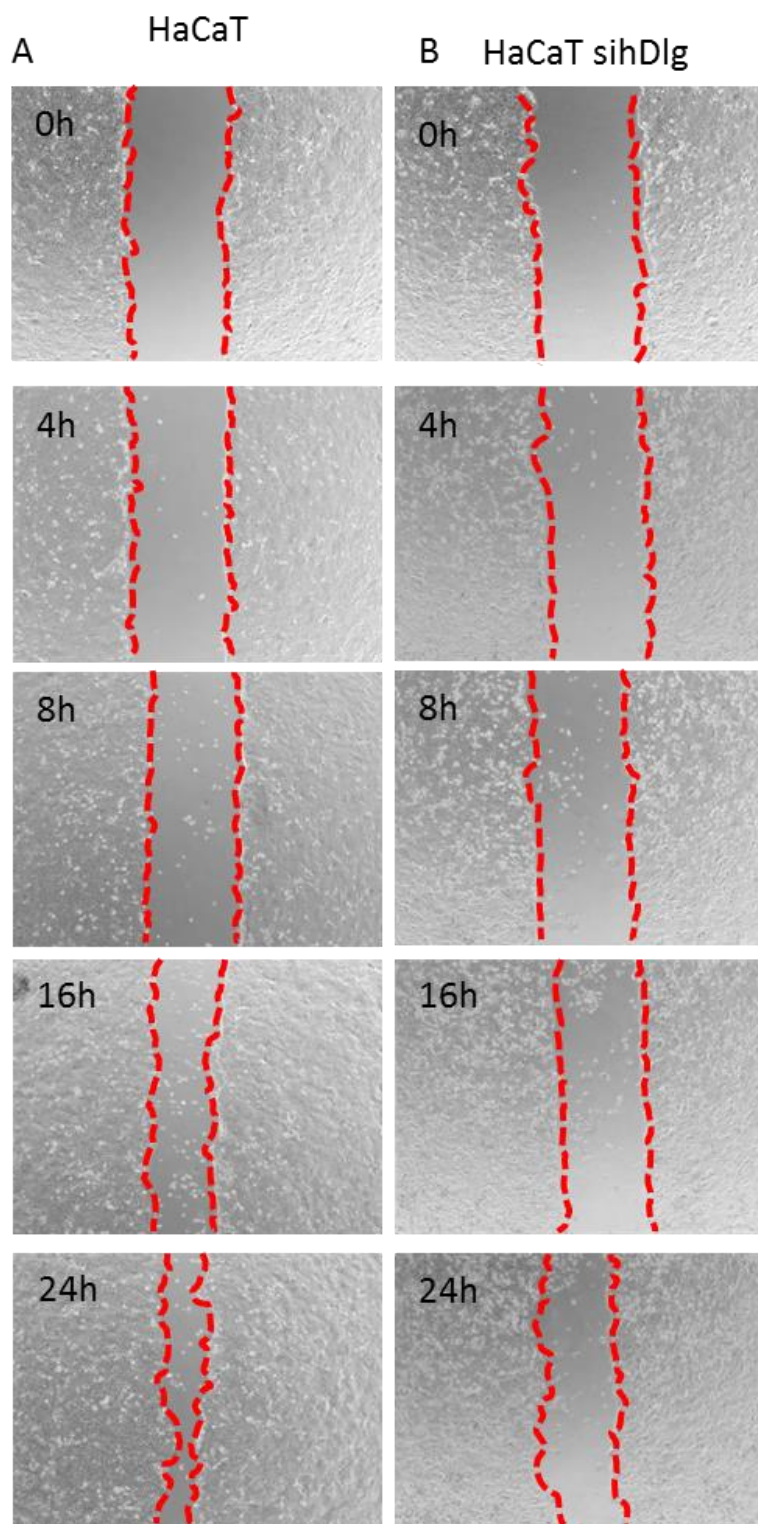
This experiment was repeated in NIKS16 cells to investigate the delayed wound healing by siRNA depletion since NIKS16 cells close the wound fast (complete closure at 16h in Figure 4.7). The results are shown in Figure 4.8. Significant delay of wound closure was observed in NIKS16 cells with siRNA depletion of hDlg. The wound only closed to around 50% after 24h while in mock-treated NIKS16 cells the wound was fully closed at 16h (Figure 4.9). This further supports the role of hDlg in the wound healing process.

From these images, more dead cells were observed in the HaCaT and NIKS16 cell populations with siRNA depletion of hDlg compared to mock-treated cells. The

culture medium was changed after creating the wound. Therefore, the cell death during wound closure was not caused by siRNA transfection. Moreover, no significant cell death was observed in unwounded HaCaT and NIKS16 cells with siRNA depletion of hDlg compared to mock-treated cells in the previous chapter. Therefore, cell death must be due to the wounding process. To investigate this further, at the end of the 24h time course, supernatant in each well from the scrape wound assay was used to count live versus dead cells and the results are shown in Figure 4.10. More floating cells/dead cells were counted in HaCaT and NIKS16 cells with siRNA depletion of hDlg compared to mock-treated and negative control HaCaT cells. This indicated that during wound closure, cells with reduced hDlg levels led to a higher ratio of cell death than cells with normal hDlg levels. However, the cell death caused by siRNA depletion of hDlg in response to wounding should be further investigated maybe through the use of cell apoptosis markers.

To understand more regarding hDlg in the wound healing process, HaCaT cells with a stable knockdown of hDlg (named HaCaT shDlg cells) were used to repeat the experiments. This cell line was used to avoid the possible effects of siRNA depletion of hDlg that might kill the cells in response to wound (Figure 4.10). For unwounded cells, HaCaT shDlg cells showed results consistent with HaCaT cells upon siRNA depletion of hDlg. There was a reduced level of Cx43 and the observation of the cytoplasmic location of Cx43 (as in the previous chapter). Whether the reaction to wounding in HaCaT shDlg is the same as that in HaCaT cells upon siRNA depletion of hDlg is worth checking. The reaction to wounding in both HaCaT cell lines was investigated as above. In HaCaT cells, the wound closure process was very similar to that previously described, and the scrape wound was nearly closed at 24h (Figure 4.11 A). However, in HaCaT shDlg cells, surprisingly the wound was found to be fully closed at 16h, which was very different from the observation in HaCaT cells with siRNA depletion of hDlg that seemed to start to close at 24h (Figure 4.11 B). No significant cell death was observed in these experiments between HaCaT and HaCaT shDlg cells. This indicated that siRNA depletion of hDlg might weaken the cell's adaptability in response to wound healing. Comparing the repair speed of these HaCaT cells in response to the wound, it is easy to see that there is still a relative gap in HaCaT cells with siRNA depletion of hDlg after 24h while the gap was quite small in

HaCaT cells after 24h (Figure 4.8). However, the HaCaT shDlg cells repaired the gap fastest that the gap was completely closed at 16h (Figure 4.11).



C

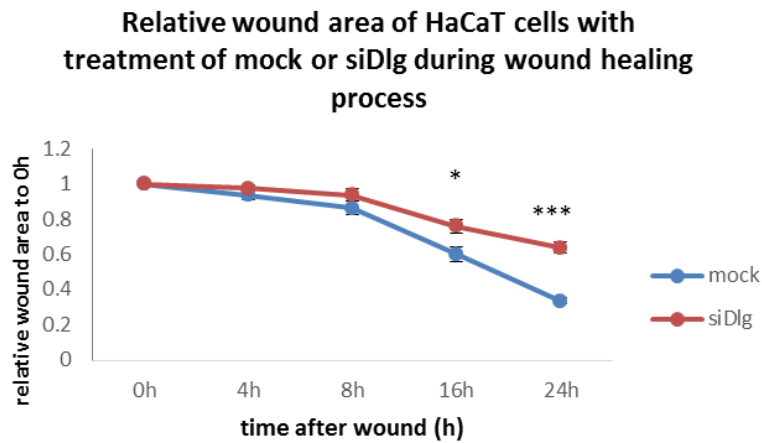
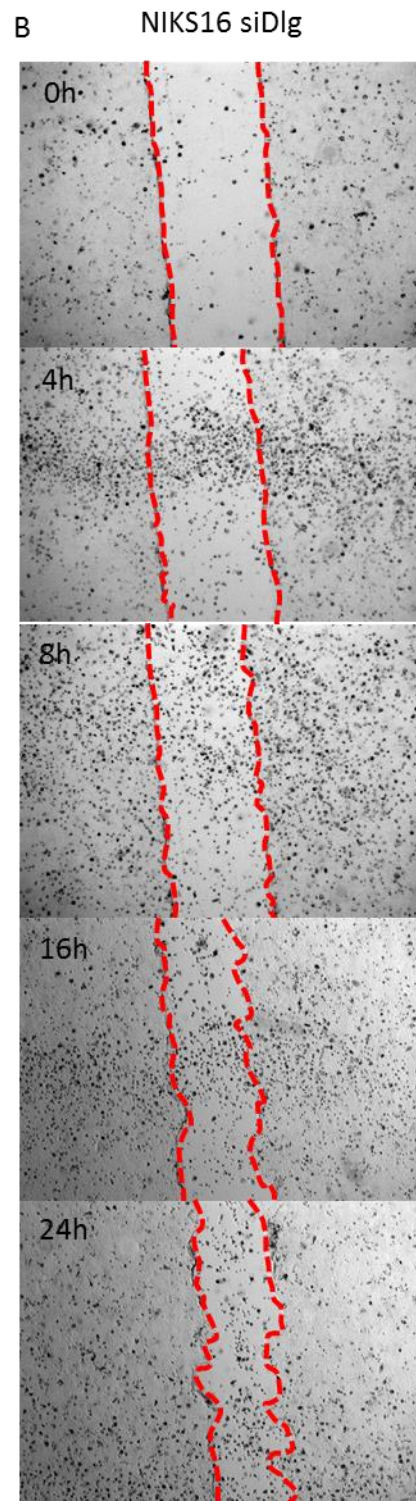
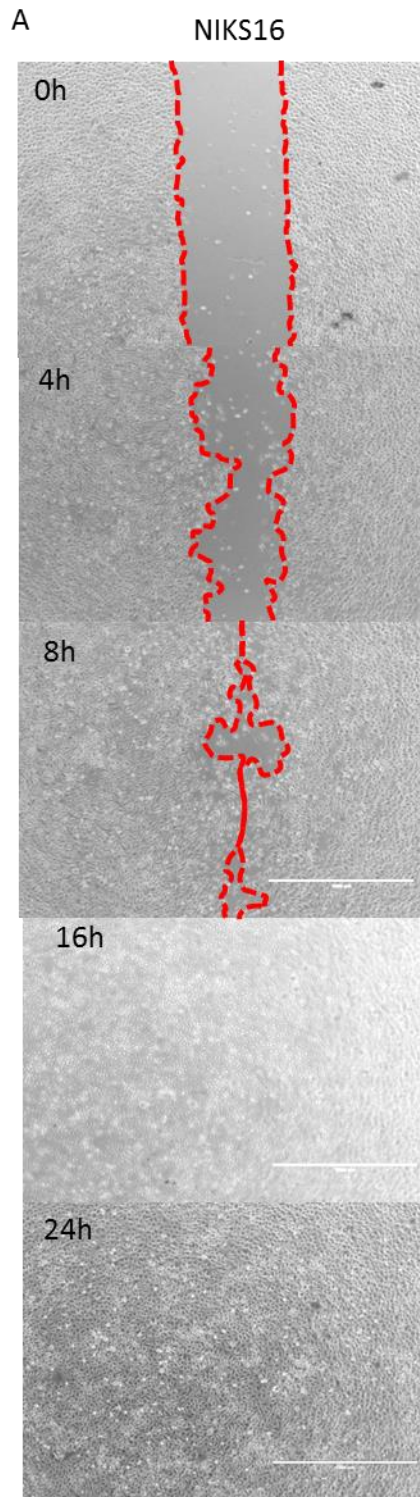


**Figure 4.8: The wound closure process in mock-treated HaCaT and HaCaT cells with siRNA depletion of hDlg.**

Photos of wound area in (A) mock-treated HaCaT and (B) siDlg-treated HaCaT cells were taken according to wound healing time points (0h, 4h, 8h, 16h, and 24h). The red dotted lines indicate the wound edges. (C) Quantification of the wound area (normalized to 0h) changes according to wound healing time points (\* indicates  $p < 0.05$ ; \*\* indicates  $p < 0.005$ ; \*\*\* indicates  $p < 0.0005$ ). This experiment has been repeated three times.



C

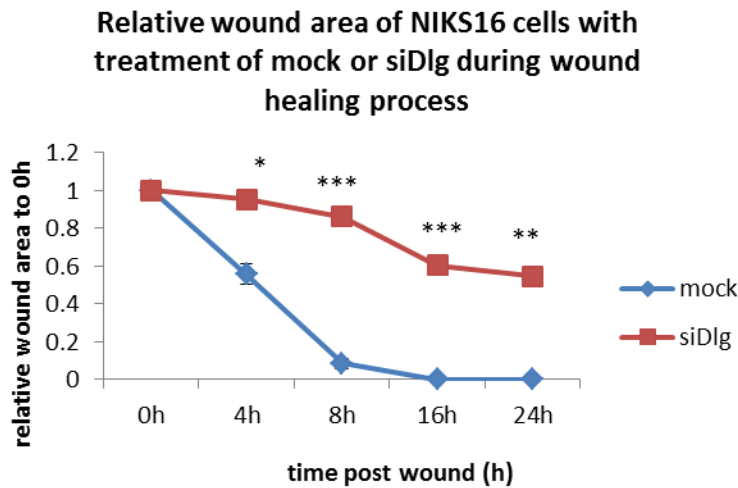


**Figure 4.9: The wound closure process in mock-treated NIKS16 and NIKS16 cells with siRNA depletion of hDlg.**

Photos of wound area in (A) mock-treated NIKS16 and (B) siDlg-treated NIKS16 cells were taken according to wound healing time points (0h, 4h, 8h, 16h, and 24h). The red dotted lines indicate the wound edges. (C) Quantification of the wound area changes (normalized to 0h) according to wound healing time points (\* indicates  $p < 0.05$ ; \*\* indicates  $p < 0.005$ ; \*\*\* indicates  $p < 0.0005$ ). This experiment has been repeated three times.

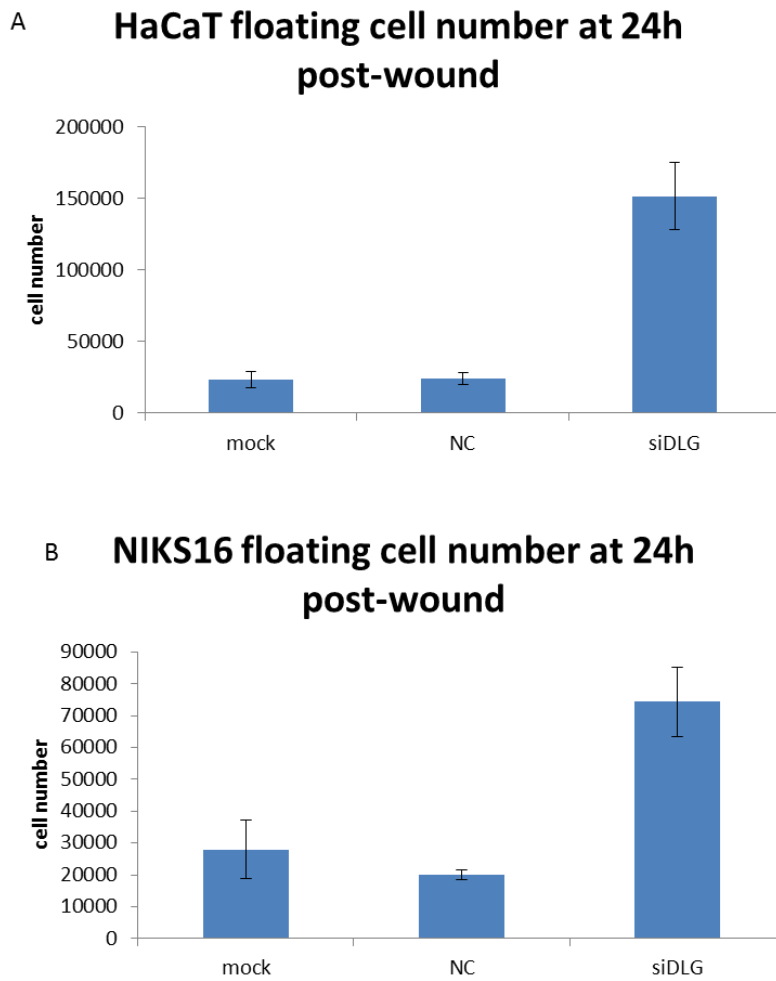
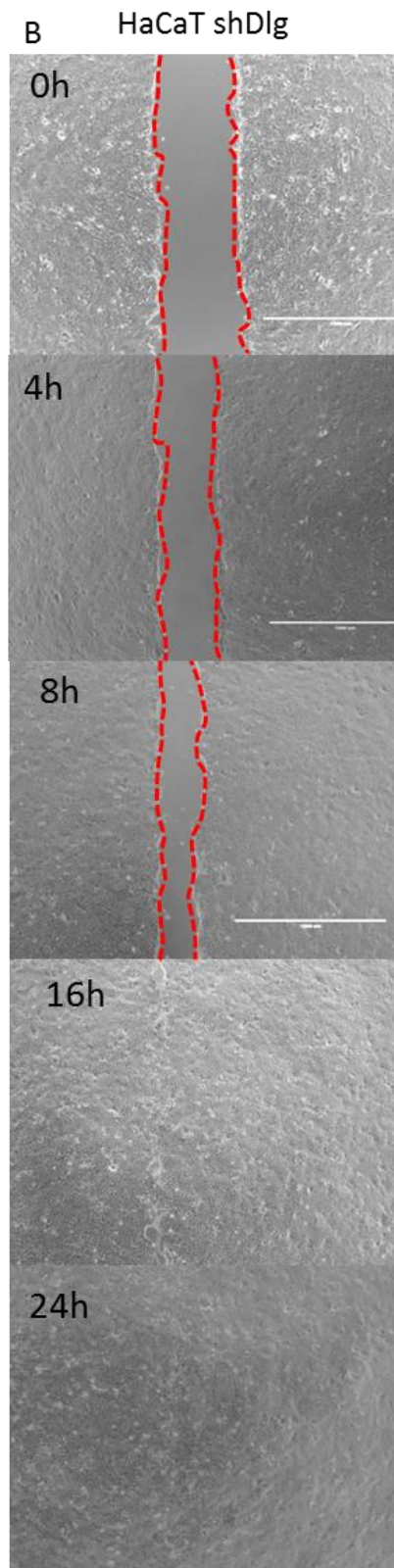
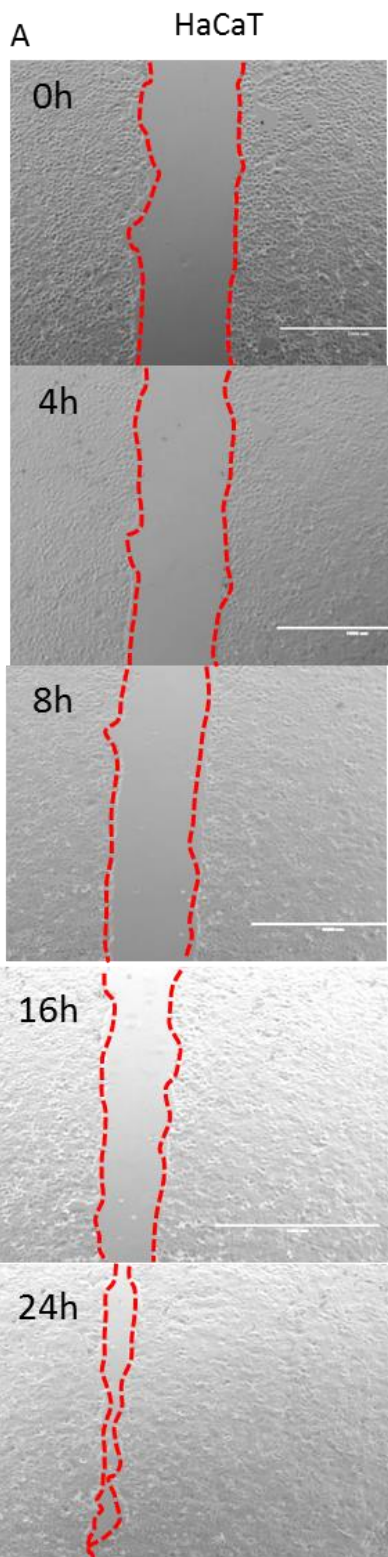


**Figure 4.10: siRNA depletion of hDlg led to more floating cells in response to wound healing.**

Quantification of the cells counted from the supernatant in (A) HaCaT cells and (B) NIKS16 cells after 24h post wound with different treatment: mock-treated (mock), non-target siRNA control-treated (NC) and siRNA target hDlg (siDLg). This experiment has been repeated three times.



C

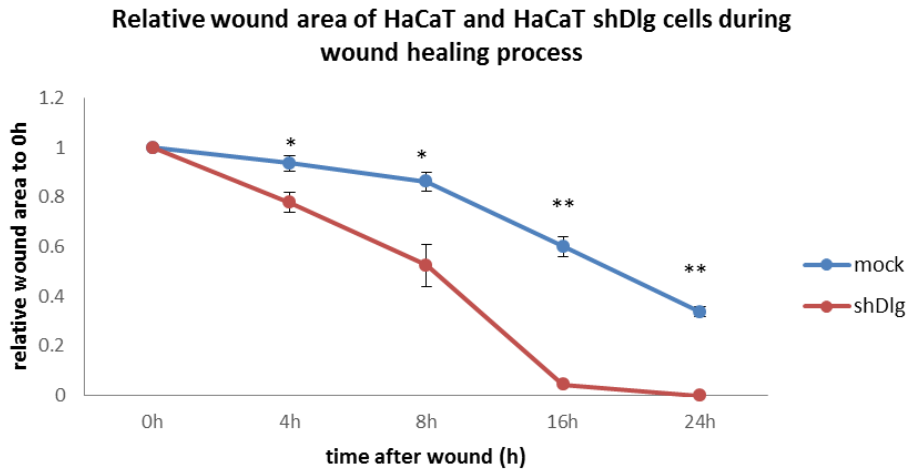


**Figure 4.11: The wound closure process in HaCaT cells and HaCaT shDlg cells.**

Photos of wound area in (A) mock-treated HaCaT and (B) shDlg-treated HaCaT cells were taken according to wound healing time points (0h, 4h, 8h, 16h, and 24h). The red dotted lines indicate the wound edges. (C) Quantification of the wound area changes (normalized to 0h) according to wound healing time points (\* indicates  $p < 0.05$ ; \*\* indicates  $p < 0.005$ ; \*\*\* indicates  $p < 0.0005$ ). This experiment has been repeated three times.

### 4.3 Behaviour of tumour cells during the wound healing process

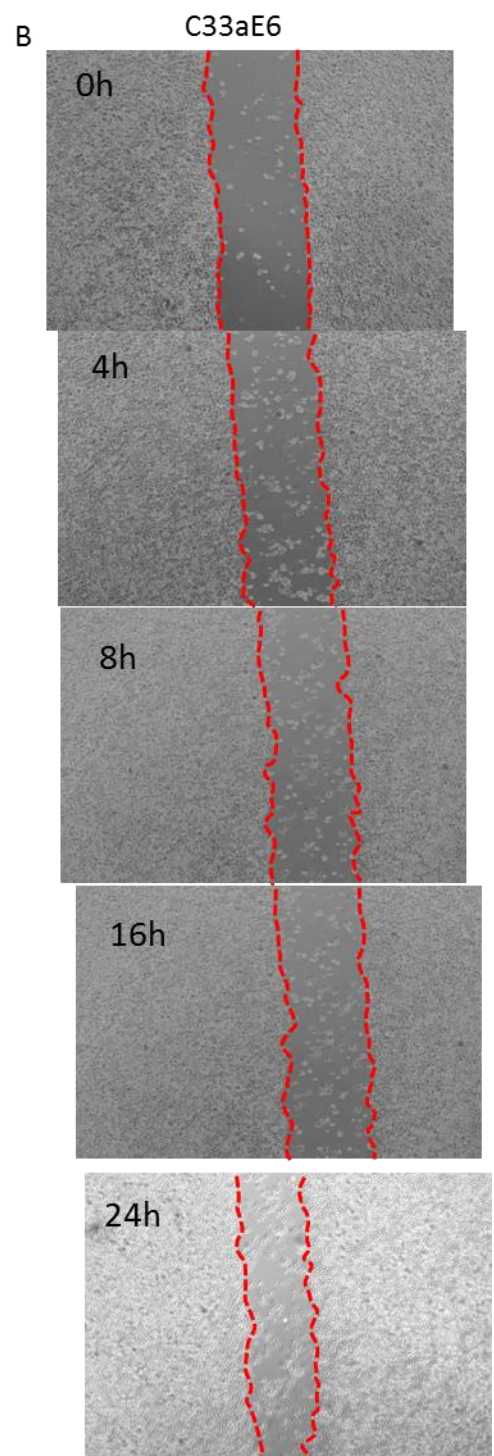
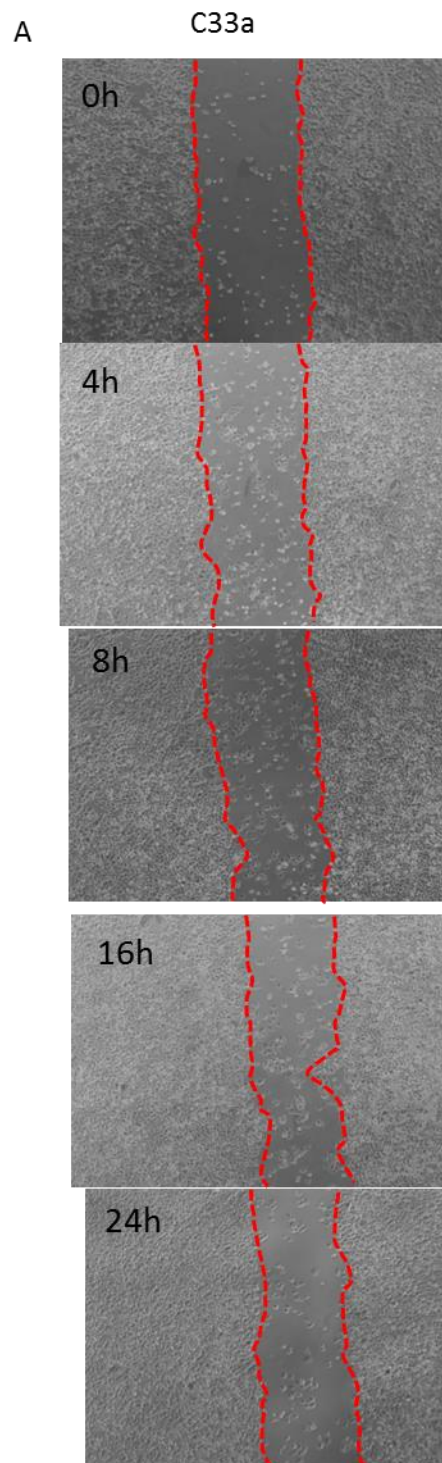
HPV E6 targets and leads to degradation of p53 resulting in uncontrolled cell proliferation (Martinez-Zapien et al., 2016). Recently HPV16 E6 was observed to increase the migration of cervical cancer cells by the down-regulation of PDZ-domain-containing protein Na<sup>+</sup>/H<sup>+</sup> exchanger regulatory factor (NHERF1) (Wang et al., 2018). HPV16 might increase wound healing speed in infected cells as NIKS16 cells close the wound much faster than NIKS cells (Figure 4.7), while stable loss of hDlg could lead to some cell alterations such as cell shape and motility which might speed up the wound healing process (Figure 4.11). HPV E6 targets hDlg for degradation. Because of this known effect of E6, whether the wound healing process is enhanced in cervical cancer cells that express HPV E6 was tested. Therefore, the wound healing process was repeated in C33a (HPV-negative cervical tumour cells), C33aE6 (C33a cells stably transfected with an expression construct for HPV16E6), and HeLa43 cells (HPV18-positive cervical tumour cells transfected with an expression construct for Cx43). C33a cells, which express mainly membrane Cx43 and hDlg, showed no significant amount of wound closure during the scrape wound healing process (closed 17% of the gap at 24h) (Figure 4.12 A). For C33aE6 cells, which contained mainly cytoplasmic Cx43 and hDlg, the wound area seemed unchanged between 0h and 8h (similar to the observation in C33a cells) but the gap began to close between 8h to 24h and finally, the gap was closed to 33% at 24h (Figure 4.12 B). This experiment indicates that the expression of HPV E6, or the presence of less membranous Cx43, was associated with better wound healing.

Next, how the levels of Cx43 and hDlg were changed during wound healing was investigated in C33a and C33aE6 cells. Figure 4.13 shows that in C33a cells, Cx43 levels reached their lowest level at 4h, then reached a peak at 8h followed by a slight drop at 16h and 24h. Following a similar pattern to Cx43 levels, hDlg levels also dipped at 4h, but the peak of expression appeared at 16h followed by a reduction at 24h. However, in C33aE6 cells (Figure 4.14), the time of reduction in Cx43 levels was shifted from 0h to 4h after which it showed a slight increase at 8h followed by a significant increase at 16h and 24h. For hDlg, the level slightly dropped from 0h to 4h and then kept increasing from 4h to 24h. The lower band that is present in the hDlg panel in Figure 4.14 B, is likely to be

partial degradation of hDlg, an unstable protein, which was observed at all the time points during wound healing, but the upper band, which is likely the phosphorylated form of hDlg was observed only at 16h and 24h. This suggests that hDlg can undergo post-translational modification in response to wound closure.

To investigate whether HPVE6 or less membranous Cx43 or both is associated with faster wound healing, these experiments were repeated in HeLa43 cells (HPV-positive cervical cancer cells with ectopic expression of Cx43). Since HeLa43 containing membranous Cx43 and expression of HPVE6, the wound closure rate of HeLa43 should be between that of C33a and C33aE6. As expected, HeLa43 did not close the wound after 24h and the closure rate (30% closure at 24h) is between that measured for C33a and C33aE6 (17% and 33% respectively) (Figure 4.15).

At the protein level, in HeLa43 cells, Cx43 levels kept increasing between 0h to 8h followed by a slight decrease at 16h and another increase at 24h (Figure 4.16 B). For hDlg, the trend of alteration in protein levels was similar to what has been observed for Cx43: increased between 0h to 8h followed by a slight decrease at 16h. However, instead of increasing, the level of hDlg decreased at 24h (Figure 4.16 B). More time-points were chosen to further investigate this alteration of Cx43 and hDlg levels in HeLa43 together with changes in HPV18E6 protein levels (Figure 4.16 A). It seems there a little reduction between 0h to 2h for Cx43 levels. The HPV18E6 level seemed to increase between 0h to 8h and decreased to un-wound levels at 24h (Figure 4.16 A). This might be associated with the increasing levels of hDlg between 0h to 8h, then decreasing levels between 8h to 24h (Figure 4.16 B). The increase in hDlg might suggest that wound healing triggered a pathway that counteracted the ability of HPV18E6 in degradation of hDlg.



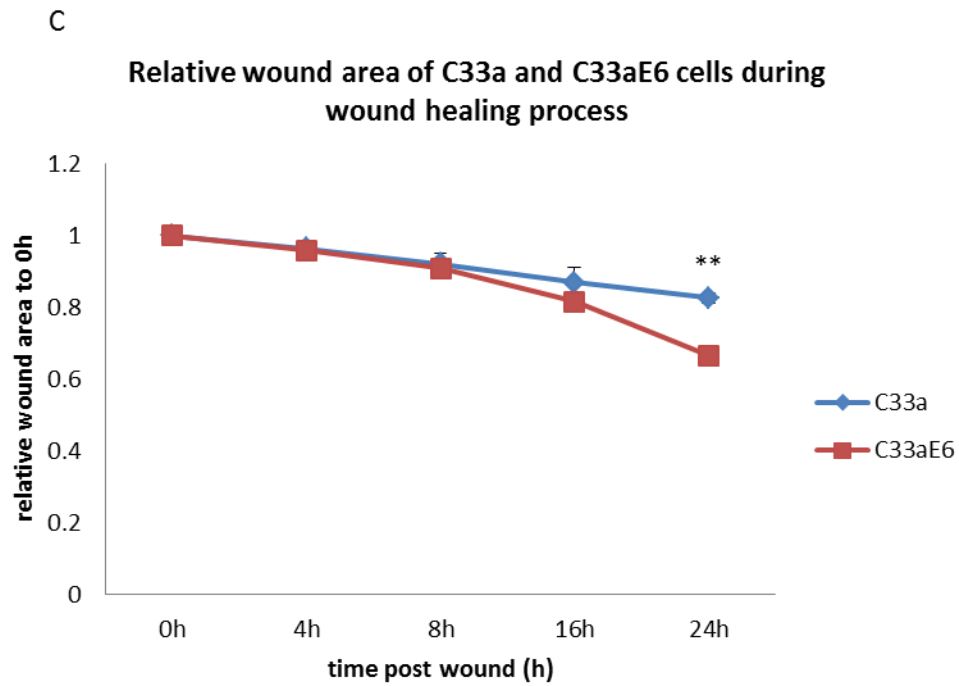
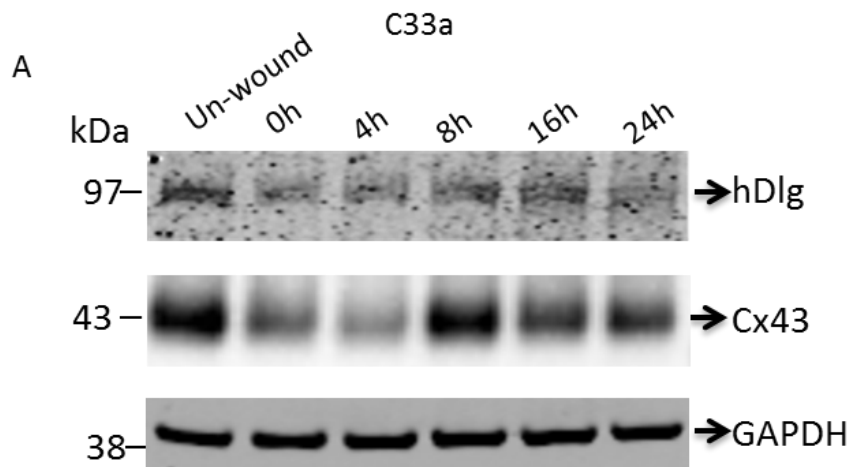


**Figure 4.12: The wound closure process in C33a and C33aE6 cells.**

Photos of wound area in (A) C33a and (B) C33aE6 cells were taken according to wound healing time points (0h, 4h, 8h, 16h, and 24h). The red dotted lines indicate the wound edges. (C) Quantification of the wound area changes (normalized to 0h) according to wound healing time points (\*\* indicates  $p < 0.005$ ). This experiment has been repeated three times.



**B** Relative expression of Cx43 and hDlg in C33a cells during wound healing process

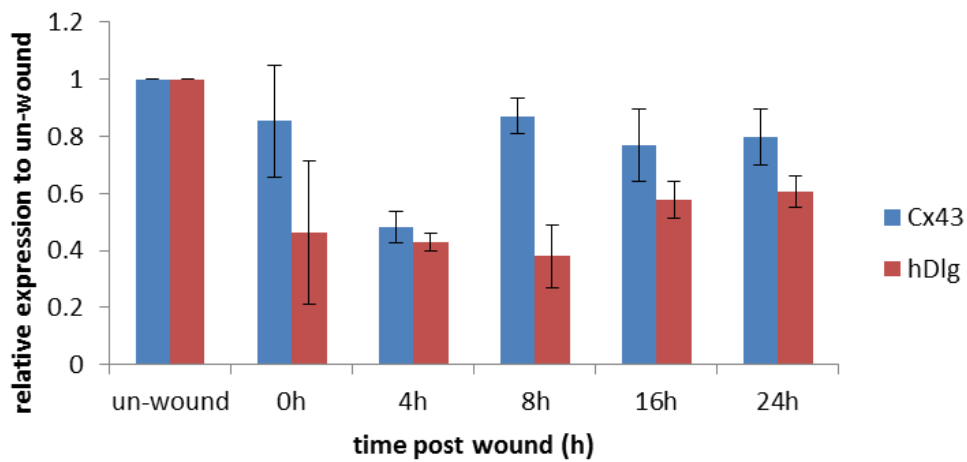


**Figure 4.13: The levels of Cx43 and hDlg in C33a cells are altered during the wound healing process.**

(A) Western blot showing the expression of Cx43 and hDlg in C33a cell extracts according to wound healing time points. Images of hDlg and GAPDH were obtained from Licor imaging and the image of Cx43 was exposed with X-ray film. (B) Quantification of Cx43 and hDlg levels during the wound healing process. The intensity of Cx43 and hDlg bands was measure by ImageJ and normalised to un-wounded cell layers. This experiment has been repeated three times.

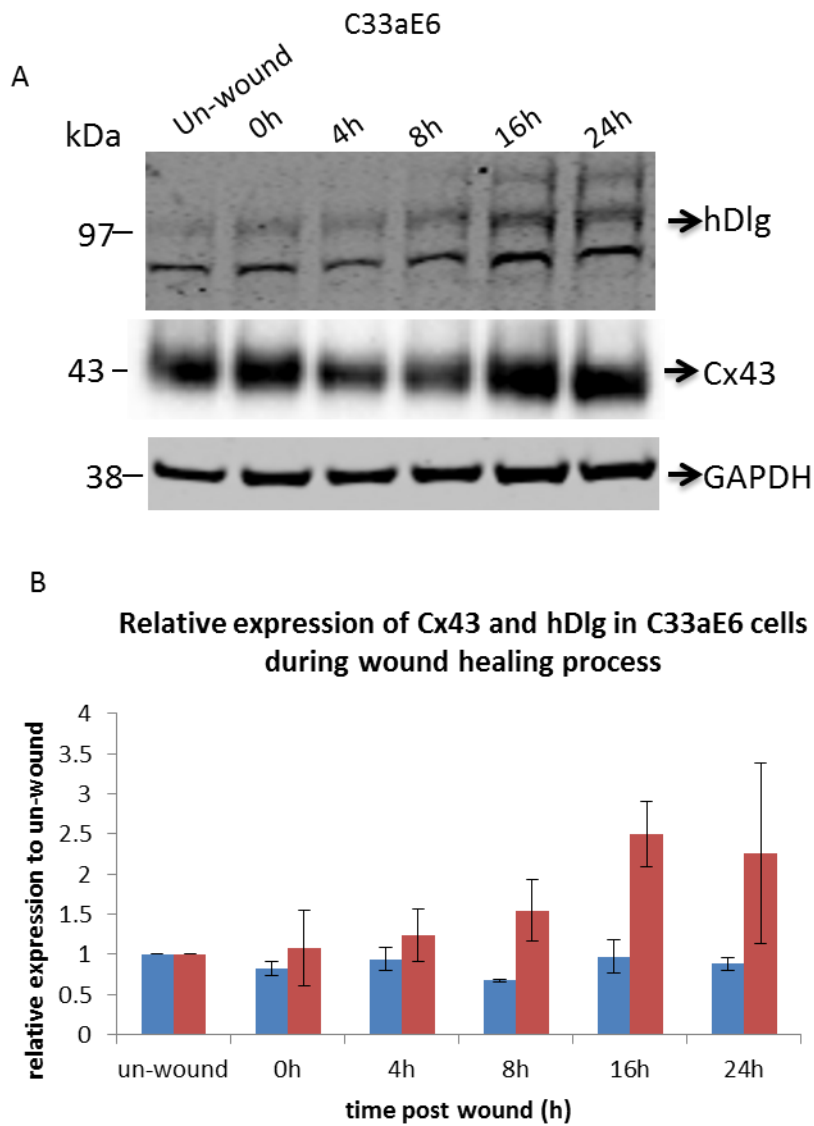


**Figure 4.14: The levels of Cx43 and hDlg in C33aE6 cells are altered during the wound healing process.**

(A) Western blot showing the expression of Cx43 and hDlg in C33aE6 cell extracts according to wound healing time points. Images of hDlg and GAPDH were obtained from Licor imaging and the image of Cx43 was exposed with X-ray film. (B) Quantification of Cx43 and hDlg levels during the wound healing process. The intensity of Cx43 and hDlg bands was measured by ImageJ and normalised to un-wounded cell layers. This experiment has been repeated three times.

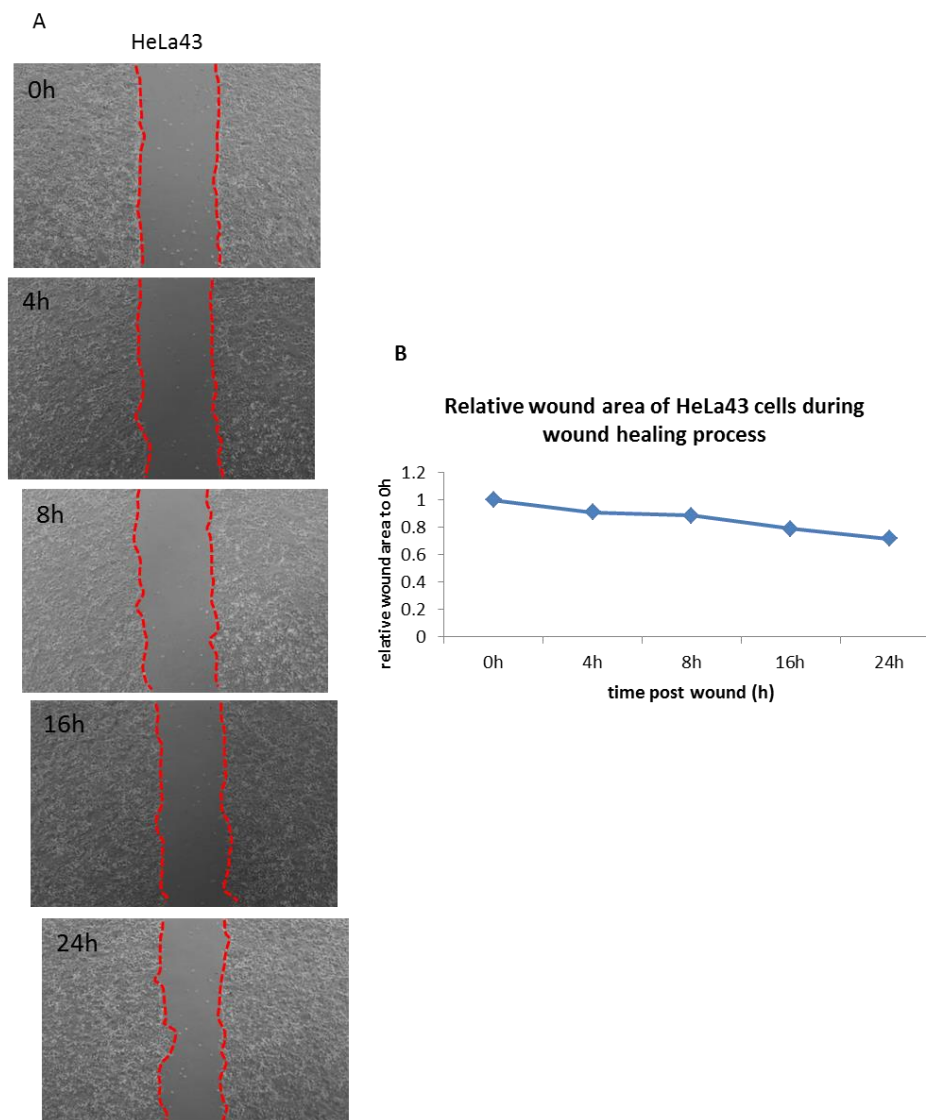


**Figure 4.15: The wound closure process in HeLa43 cells.**

(A) Photos were taken according to the wound healing time points (0h, 4h, 8h, 16h, and 24h). The red dotted lines indicate the wound edges. (B) Quantification of the wound area (normalized to 0h) according to wound healing time points. This experiment has been repeated three times.

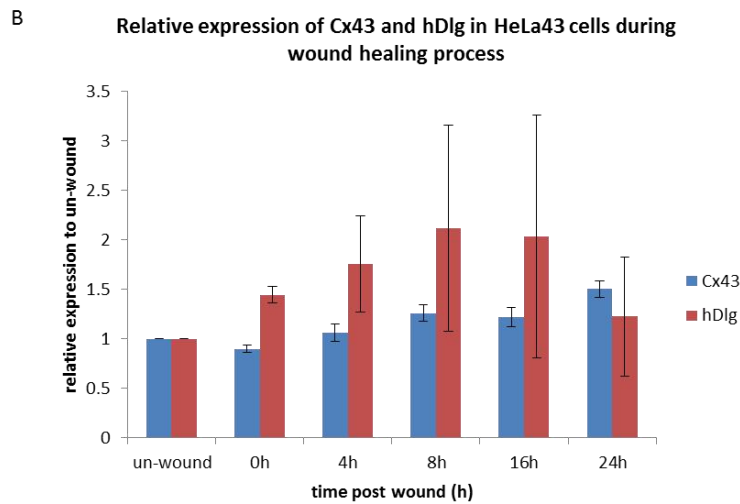
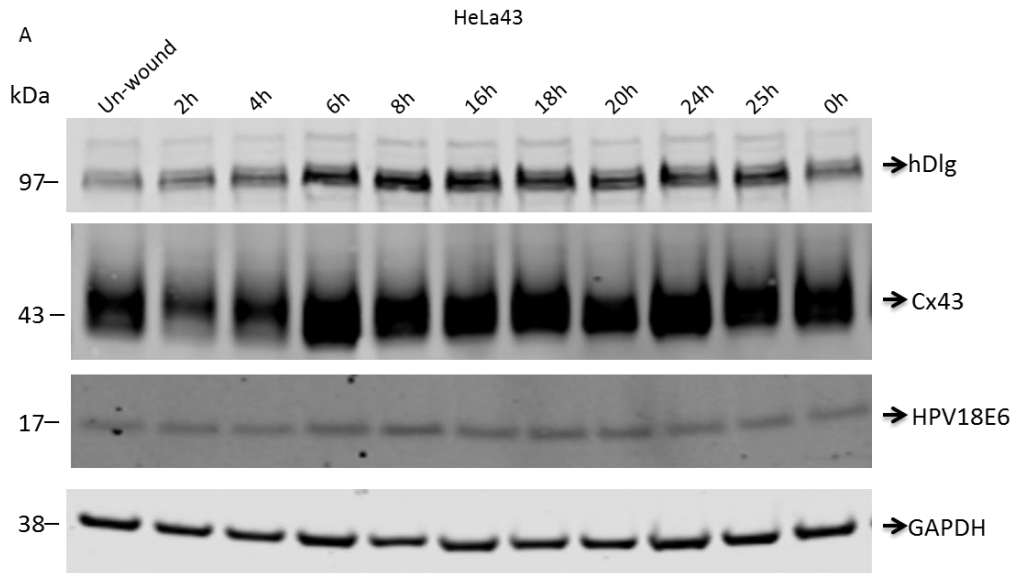


**Figure 4.16: The levels of Cx43 and hDlg in HeLa43 cells altered during the wound healing process.**

(A) Western blot showing the expression of Cx43 and hDlg in HeLa43 cell extracts according to wound healing time points. Images of hDlg and GAPDH were obtained from Licor imaging and the image of Cx43 was exposed with X-ray film. (B) Quantification of Cx43 and hDlg levels during the wound healing process. The intensity of Cx43 and hDlg bands was measure by ImageJ and normalised to un-wounded cell layers. This experiment has been repeated three times.

## 4.4 Discussion

Previously it is reported that the gap junction protein Cx43 and its binding partner, hDlg were presented on the plasma membrane in W12G cells while in tumour cells derived from them (W12GPXY cells (Aasen et al., 2003b) both proteins co-located in the cytoplasm. A significantly increased level of HPVE6 was observed in W12GPXY cells, where E6 was located in the nucleus and the cytoplasm compared to W12G cells, where E6 was mainly in the nucleus (Macdonald et al., 2012b, Sun et al., 2015). E6 siRNA depletion in W12GPXY cells resulted in Cx43 relocation from the cytoplasm back to the plasma membrane, which indicates that the increasing levels (or high levels) of HPVE6 in the cytoplasm can control Cx43 trafficking (Sun et al., 2015). A similar pattern of Cx43 trafficking to and from the membrane is known to occur during the wound healing process. In the early stages of the wound healing process, Cx43 was found to relocate from the plasma membrane into the cytoplasm in primary human keratinocytes at the leading edge of a wound (Wright et al., 2009).

Therefore, the alteration of hDlg in subcellular location and expression was investigated in response to wound repair and whether it is related to the alteration of Cx43 during the wound healing process. Table 4.1 summarizes the subcellular location of Cx43 and hDlg in HaCaT cells and NIKS cells during the wound healing process in Figure 4.1 and Figure 4.4. Cx43 was observed to traffic from plasma membrane (0h) to the cytoplasm (4h, 8h in NIKS; 4h, 8h, 16h in HaCaT) and back to the membrane (16h in NIKS; 24h in HaCaT) in HaCaT and NIKS cells during the wound healing process (Figure 4.1 & 4.4). Membrane hDlg was observed in the entire wound repairing time points in both cells. Some hDlg co-localised with Cx43 in the cytoplasm during the wound healing process (4h, 8h in NIKS; 4h, 8h, 16h in HaCaT) (Table 4.1). These data indicate the role of hDlg involved in the wound healing process.

hDlg, involved in maintaining cell polarity, is also essential for cell migration especially directed migration (Etienne-Manneville, 2008). Briefly, hDlg is targeted to the plasma membrane of the leading edges of wounding cells and regulates microtubule interaction for the plus-end of microtubules at the plasma membrane (Etienne-Manneville, 2008).

siRNA depletion of hDlg also led to the relocation of Cx43 from the plasma membrane into the cytoplasm in HaCaT cells similar to the trafficking of Cx43 at the early stages of wound healing. However, HaCaT cells with siRNA depletion of hDlg led to slow wound repair and lots of cell death during the wound healing process (Figure 4.8 & 4.10 A). This indicates the role of hDlg in maintaining cell survival in response to wounds and the expression of hDlg is required in the proper wound healing process.

However, results shown in HaCaT cells with stable depletion of hDlg (HaCaT shDlg, growth medium containing puromycin) is not consistent with the observation in HaCaT cells with siRNA depletion of hDlg, instead, faster wound closure was observed (full closure at 16h) (Figure 4.11). This might be because HaCaT shDlg cells had adjusted their growth properties to exist without hDlg (no significant cell death was observed during wound healing or culturing under the normal conditions with these cells). In this case, some other proteins might function effectively to compensate for the loss of hDlg to maintain normal cell growth and hScrib came into consideration. hScrib and hDlg both are involved in the regulation of cellular polarity and acts as tumour suppressor proteins (Thomas et al., 1997, Dow et al., 2003). Both hScrib and hDlg are targeted by High-risk HPV E6 for proteasome degradation (Nakagawa and Huibregtse, 2000, Gardiol et al., 1999). Most importantly, Bank's group, where the HaCaT shDlg came from, found that hScrib and hDlg showed complementary roles, and the higher level of hScrib was observed in HaCaT shDlg cells. Loss of hDlg in HaCaT cells did not affect the cell-cell contacts (Massimi et al., 2012). Therefore, the possible explanation of faster wound repair in HaCaT shDlg cells could be that HaCaT shDlg has adapted into the loss of hDlg by expressing more hScrib to compensate for the loss of hDlg and maintains the cell polarity. This might increase cells' ability in response to cell stress (e.g. wound healing). Stable depletion of hDlg in endometrial cancer cell line KLE enhanced the cell migration in wound healing assay (Sugihara et al., 2016). In contrast, in HaCaT with siRNA depletion of hDlg, a complementary system to cover the loss of hDlg may not be activated leading to cell stress and then cell death during wound closure. This increasing rate of closure of HaCaT shDlg cell layers might also be due to increasing levels of beta-catenin in these cells (Massimi et al., 2012). The lower amount of membranous Cx43 in HaCaT shDlg cells should no longer

prevent beta-catenin from moving into the nucleus to activate transcription of genes encoding proteins involved in cell migration.

Beta-catenin, involved in the Wnt pathway (normally activated in response to wounding), is known to be increased in response to injury, as are the levels of expression of its target genes during the proliferative phase (Houschyar et al., 2015). In the absence of Wnt signalling, beta-catenin is maintained at a low level in the cells by continuous degradation by the so-called destruction complex which includes adenomatous polyposis coli (APC) (Stamos and Weis, 2013). Wnt signalling prevents degradation of beta-catenin and stabilized beta-catenin is translocated into the nucleus to activate transcription of genes in response to cellular stresses such as wound healing (Houschyar et al., 2019). Expressing stabilized beta-catenin in NBT-II epithelial cells increased cell migration (Müller et al., 2002). Knockdown of beta-catenin in renal cell carcinoma cells (A498) significantly decreased cell migration while its overexpression in renal cell carcinoma cells (786-O and ACHN) increased cell migration (Yang et al., 2017). Therefore, increasing levels of activated beta-catenin and its nuclear location is important in wound healing. hDlg might also be involved in the regulation of beta-catenin since hDlg activates beta-catenin signals in vascular endothelial cells (EC) (Cho et al., 2019). Transfection with Dlg1 increased the signalling of beta-catenin in HEK293 cells with a knockout of hDlg (Cho et al., 2019).

Interestingly, NIKS16 cells closed the wound faster than NIKS cells (Figure 4.7). Comparing the expression of Cx43 and hDlg in NIKS and NIKS16 cells during the wound healing process, the significant difference that could be observed is that in NIKS16 cells the level of hDlg was increased between 0h and 4h followed by a reduction at 8h while in NIKS cells it was other way around. The gap area of NIKS cells at 8h was similar to that in NIKS16 cells at 4h (Figure 4.7). This indicates that the presence of the HPV16 genome increased cell proliferation and migration, perhaps due to the expression of HPV16 E6, which can induce cervical cancer cell migration (Wang et al., 2018). This is possibly due to HPVE6 induced accumulation of nuclear beta-catenin via its PDZ-binding domain (Bonilla-Delgado et al., 2012) since the nuclear accumulation of beta-catenin was only observed in transgenic mice expressing wild-type HPVE6 but not with truncated HPVE6 lacking a PDZ-binding domain (Bonilla-Delgado et al., 2012).

**Table 4.1: Summary of the location of Cx43 and hDlg in cells during the wound healing process in HaCaT and NIKS cells.**

(Cx43 is indicated in red and hDlg is indicated in black)

	0h	4h	8h	16h	24h
HaCaT	M/M	C,M/C,M	C,Pn/C,M	C/C,M	C,M/M
NIKS	C,M/M	C,Pn/C,M	C,Pn/M	M/M	M/M

M: membrane; C: cytoplasm; Pn: peri-nuclear area.

**Table 4.2: Summary of expression of Cx43 and hDlg during the wound healing process in different cell types.**

(Cx43 is indicated in red and hDlg is indicated in black)

	0h	4h	8h	16h	24h
HaCaT	-	↓ / ↓	↑ / -	↑ / ↑	↓ / ↓
NIKS	-	↑ / ↓	- / ↑	- / ↑	↓ / ↓
NIKS16	-	↑ / ↑	↓ / ↓	↑ / ↑	↓ / -
C33a	-	↓ / ↓	↑ / ↓	↓ / ↑	↓ / -
C33aE6	-	↑ / ↑	↓ / ↑	↑ / ↑	↓ / -

In cervical cancer cells with membrane Cx43 (C33a and HeLa43 cells), without membrane Cx43 (C33aE6 cells), or with HPVE6 (C33aE6 and HeLa43 cells) or without HPVE6 (C33a cells), the scrape wounds did not close (Figure 4.12 & 4.15). These data indicate that less membranous Cx43 led to better wound healing, which might be associated with nuclear beta-catenin. Cx43 is thought to interact with beta-catenin at the membrane and prevent its translocation to the nucleus. shRNA knockdown of Cx43 in PC3 human prostate cancer cells led to no significant changes in total protein levels of beta-catenin but accumulated nuclear beta-catenin was observed (Hou et al., 2019). Overexpression of Cx43 in human mammary adenocarcinoma cells (MCF-7 and MDA-MB-231) did not change the total levels of beta-catenin but increased its membrane location (Talhok et al., 2013). Also, nuclear beta-catenin could reduce the mRNA expression of GJA1 (Cx43) in HaCaT cells with infections of adenovirus (Calhoun et al., 2020). Together with the observation that HPVE6 increased the nuclear beta-catenin (Bonilla-Delgado et al., 2012), the non-closure of the wound in cervical cancer cells could be explained: for C33a cells, membranous Cx43 prevents nuclear location of beta-catenin, which leads to reduced wound closure. For C33aE6 cells, HPVE6 targets and degrades hDlg which decreases protein levels and membranous location of Cx43, resulting increasing nuclear beta-catenin and better wound closure. For HeLa43 cells, overexpression of Cx43 leads to accumulated membranous Cx43 preventing nuclear transition of beta-catenin, but HPVE6 in HeLa43 promotes nuclear beta-catenin. Thus, wound closure rate is slowest in C33a cells, and similar in C33aE6 and HeLa43 cells (Figure 4.11 and 4.15).

In conclusion, Cx43 in the cells at the wound edge traffic from the plasma membrane into the cytoplasm and back to the membrane during the wound healing process. hDlg partially trafficked together with Cx43 in this process. The role of hDlg in the wound healing process might be as a regulator of Cx43, together with regulating cell polarity involved in direct cell migration. The nuclear location of beta-catenin is important for the wound healing process and might be negatively regulated by membranous Cx43.

## 5 Chapter 5

# Mapping the interaction of Cx43 C-terminal tail with hDlg

Cx43 has a 150 amino acids long C-terminal tail (residues 232-382) (Leithe et al., 2017b). NMR (nuclear magnetic resonance) analysis of Cx43 CT residues 255-382 suggested that most of the structure of the Cx43 CT is disordered but with two regions of helical structure observed (Sorgen et al., 2004). High conservation of the amino acid sequences of Cx43 CT is observed in vertebrate species including zebrafish (Bai, 2016, Chatterjee et al., 2005). This suggests a fundamental function of Cx43 CT within these species. Cx43 CT has been thought to be involved in many biological processes, especially in the regulation of gap junction channel functions. This is mainly done by the interaction between Cx43 CT with other proteins or post-translation modification on the Cx43 CT. For example, integral membrane proteins caveolins interact with Cx43 CT in the Golgi apparatus and are then trafficked together to the plasma membrane in lipid raft in keratinocytes. A reduced level of caveolins may reduce Cx43 trafficking to the plasma membrane, which is associated with a reduced gap junction intercellular channel (GJIC) (Langlois et al., 2008). In the case of post-translational modifications, the reduced opening of hemichannels (made of six Cxs) was observed under the PKC-induced phosphorylation of Cx43 at S368 (Bao et al., 2004). Cx43 CT enhanced HeLa cell migration via the p38 MAP kinase pathway (Behrens et al., 2010) and in human glioma cells, migration was increased by Cx43 CT through inducing regeneration of the actin cytoskeleton (Crespin et al., 2010).

Cx43 can interact with a large number of proteins mainly through its C-terminal tail. These interactions serve in the regulation of Cx43, gap junction assembly, or even cell cycle control. The Cx43 CT sequences which interact with some binding partners have been listed in Figure 5.1. Cx43 CT binds to 14-3-3 theta at the 14-3-3-binding motif (370-376), which requires Akt-induced phosphorylation of Cx43 CT-S373 (Park et al., 2006, Park et al., 2009). Caveolin-1 directly binds to Cx43 CT via its caveolin-scaffolding domain (residues 82-101) and the C-terminal domain (135-178) (Schubert et al., 2002). The specific binding region of caveolin-1 on Cx43 CT remains unclear. CIP75 (Cx43-interacting protein of 75kDa) binds to Cx43 CT with its C-terminal UBA (ubiquitin-associated) domain. The

Cx43-CIP75 interaction region was between 264 and 302 within Cx43 CT (Li et al., 2008). NEDD4 (neural precursor cell-expressed developmentally downregulated gene 4) binds to the PY motif (XPPXY, where P is proline, X is any amino acid, and Y is tyrosine) on the Cx43 CT specifically at 283-286 (Spagnol et al., 2016). Membrane-associated guanylate kinase protein ZO-1 is found to directly bind to the last five amino acids of Cx43 CT via its middle PDZ domain (Toyofuku et al., 1998, Giepmans and Moolenaar, 1998).

In this chapter, the binding of hDlg to the Cx43 CT was investigated, and attempted to map for the first time the Cx43 CT-hDlg interaction, and investigate whether phosphorylation on the Cx43 CT affected the Cx43-hDlg interaction.

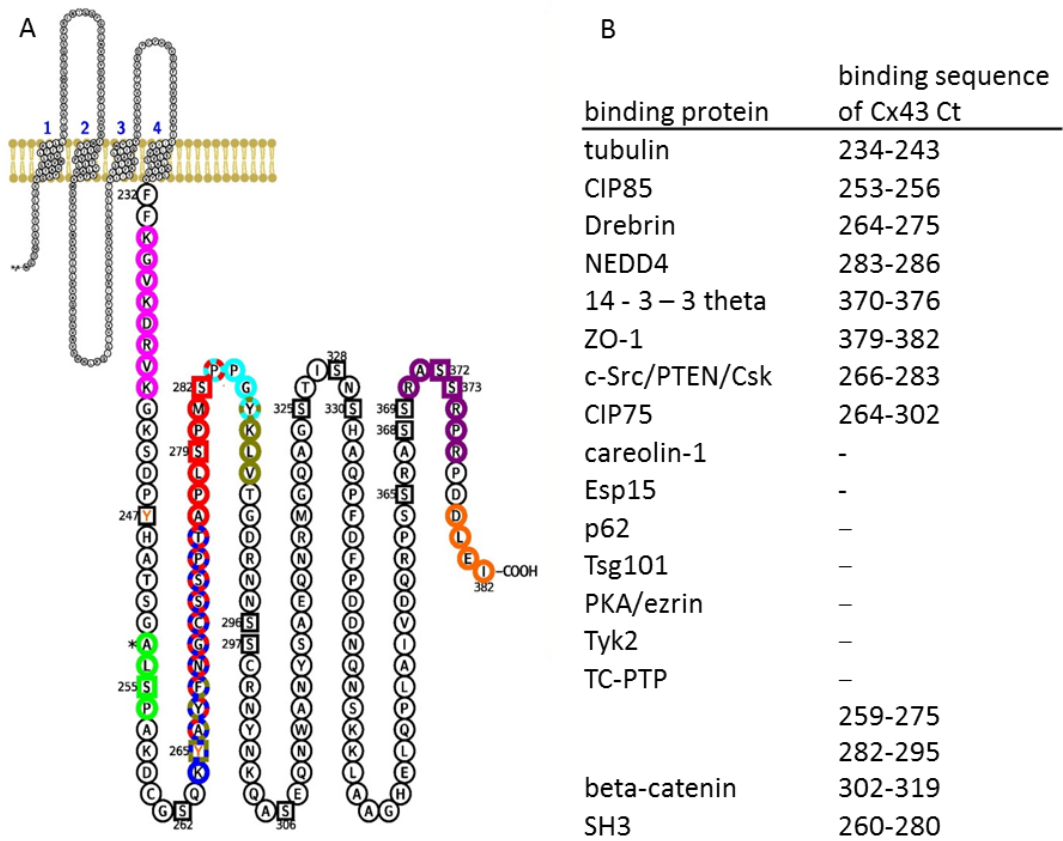


**Figure 5.1: Sequence information of Cx43 CT with some interaction partners.**

(A) Topological presentation of Cx43 CT with some protein-protein interaction domains. (B) A table listing the binding partners of Cx43 CT and potential binding sequences. The figure is taken from (Leithe et al., 2017b).

## 5.1 The region of Cx43 which binds hDlg is located in the last 33 amino acids of the Cx43 C-terminus

Like ZO-1, hDlg is a MAGUK (membrane-associated guanylate kinase) protein. It shares a similar structure with ZO-1, which includes a GUK domain, an SH3 domain, a HOOK domain, and three PDZ domains (Matsumine et al., 1996b). hDlg, with its SH3/HOOK domain, has been shown to bind to the C-terminal of another gap junction protein Cx32 (aa 209-283) (Duffy et al., 2007) and MS/MS analysis showed its potential binding affinity to the Cx43 C-terminal tail (Singh and Lampe, 2003). Previously Macdonald and co-workers utilized the HPV-positive cervical tumour cell W12 model to investigate Cx43 behaviour in the presence of oncoprotein HPVE6 during tumour progression. HPVE6 has been known to target hDlg for proteasome degradation. Therefore, a Cx43-hDlg-E6 interaction is under consideration. Co-IP experiments showed the interaction between Cx43 and hDlg in both non-transformed W12G and fully transformed W12GPXY cells, although the interaction was greatest in W12GPXY cells. The GST-pulldown assay showed that the Cx43 CT binds not to the PDZ domains (like ZO-1) but to both N-terminal and C-termini of hDlg. GST-Cx43 CT with deletion of the last five amino acids (the binding site for ZO-1) could still interact with hDlg, indicating the binding sites of Cx43 to hDlg are different from ZO-1 (Macdonald et al., 2012b).

*In vitro* direct protein-protein pull-downs showed that Cx43 and hDlg could bind directly (Macdonald et al., 2012b) (Figure 5.2). Three years later, Proximity Ligation Assays (PLA) confirmed the Cx43-hDlg interaction in cervical tumour tissues *in vivo* (Sun et al., 2015). Chapter 3 in this thesis showed that Cx43-hDlg interaction is neither HPV-dependent nor cancer cell-specific. siRNA depletion of hDlg in non-tumour cells led to a reduction in levels of Cx43 and this reduction could be rescued in the presence of lysosomal inhibitor NH<sub>4</sub>Cl, which is consistent with Macdonald et al. observations in W12GPXY cells (Macdonald et al., 2012b). The Cx43 C-terminal corresponds to amino acids 263 - 382, while the N-terminal of hDlg corresponds to amino acids 1-122, and the C-terminal of hDlg corresponds to amino acids 560-911 (Macdonald et al., 2012b).

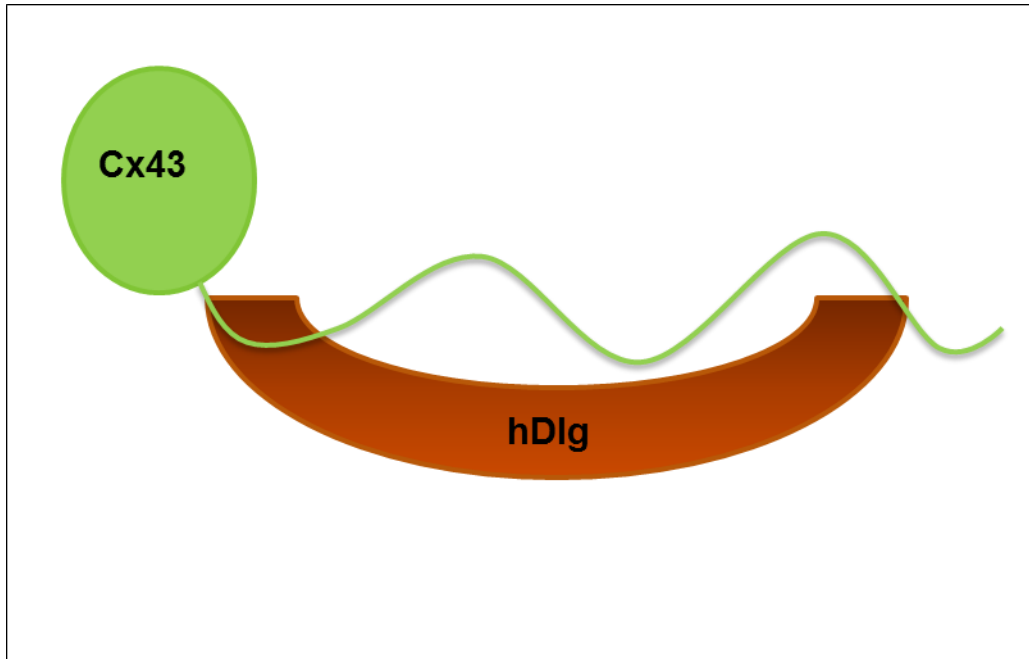


**Figure 5.2: A scheme of Cx43 interaction with hDlg.**

Specifically, the Cx43 CT correspond to amino acids 263 – 382 and the last 5 amino acids responsible for Cx43-ZO-1 interaction is not involved in Cx43-hDlg binding. The Cx43-hDlg binding regions in hDlg correspond to N-terminal (aa 1-122) and C-terminal (aa 560 -911) including SH3, HOOK and GUK domains.

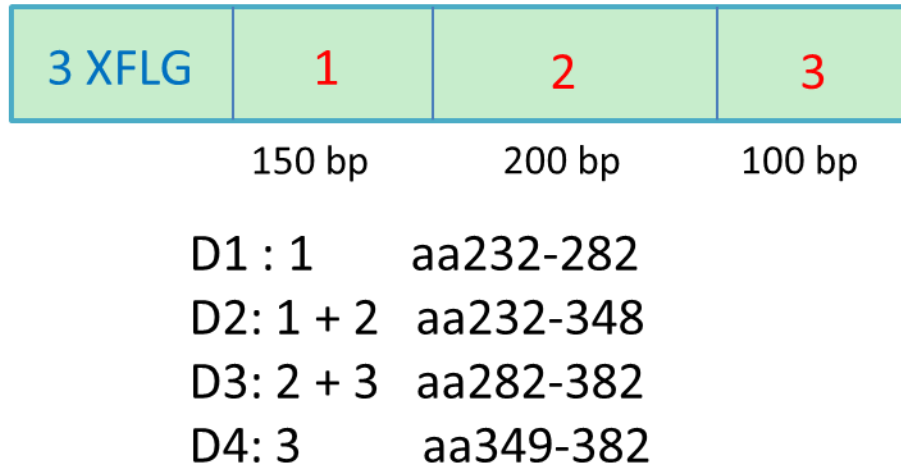
To investigate the specific region responsible for Cx43-hDlg interaction, preparing the deletion mutants of the Cx43 C-terminus is the first step. The human Cx43-containing plasmid pcDNA3-Cx43, kindly provided by Dr Dale Laird, was used as the template for PCR-mediated mutagenesis. Primers were used to generate Cx43 CT (wild-type) corresponding to amino acids 263-382 (Macdonald et al., 2012b). The plasmids of Cx43 CT deletions were generated through mutagenesis. D1 contains region 1 which correlates to amino acid 232-282. D2 contains region 1 and region 2, which correlates to amino acid 232-348. D3 contains region 2 and region 3, which correlates to amino acid 282-382. D4 contains region 3, which correlates to amino acids 349 - 382. All Cx43 deletions were fused with a 3X Flag tag so that they can be identified by anti-Flag antibody (Figure 5.3A). HEK293 cells are good cells for transfection with high expression of proteins expressed from transfected plasmids. All plasmids of Cx43 CT deletions together with wild-type Cx43 CT were transfected into HEK293 cells for 48h before harvesting cells and preparing protein extracts with NP-40 lysis buffer. Cell extracts were checked by western blot to ensure the expression of all these Cx43 deletions (Figure 5.3 B). It is clear that Cx43 CT wild-type and two deletion forms (D2 and D3) were successfully expressed. However, only very low levels of D1 were detected by western blot and no clear bands of D4 were observed (Figure 5.3B). The possible explanation for this is that D1 and D4 contain small regions of the Cx43 CT (150bp and 100bp) resulting in the expression of proteins with low molecular weight (about 8.55kDa and 6.7 kDa), which are difficult to blot successfully. Also, these small protein fragments could have been unstable. Therefore, Cx43 CT deletions (D2 and D3) were used for further experiments.

GST-fused hDlg protein preparations were carried out as described in (Macdonald et al., 2012b). Fused GST proteins were prepared for full-length hDlg (GST-hDlg) and for N-terminus of hDlg plus the first PDZ domain (GST-hDlg NT+1), both of which are known to bind Cx43 CT. Coomassie stain showed the successful induction of these GST-fused proteins upon the treatment with 1mM IPTG (Figure 5.4A, arrows). Bacterial lysates were incubated with Protein-G beads that can bind to the GST tag. Coomassie stain showed the successful binding of beads to GST-fused proteins (Figure 5.4B). This confirmed the binding ability of beads to

GST and supported the successful induction of GST-fused proteins under the IPTG treatment.

The next step was to incubate these beads with GST-fused protein and lysates of cells expressing the Cx43 CT deletions. Under incubation with Cx43 CT wt, a faint band was observed in the control GST-EV lane, but a much stronger band was observed in the lane for GST-hDlg, which indicated that Cx43 CT wt could interact with GST-hDlg (Figure 5.5A). This is in accordance with what Macdonald et. al have observed (Macdonald et al., 2012b). However, no clear bands were observed in lanes for GST-hDlg and GST-EV when incubation with Cx43 CT D2 was performed (Figure 5.5B). This indicated that Cx43 CT deletion form 2 did not bind to GST-hDlg, which further suggested the region 1 and region 2 at the Cx43 CT did not contain the regions responsible for Cx43-hDlg interaction. For Cx43 CT D3, a clear band was observed in the lane for GST-hDlg but not in the lane for control GST-EV (Figure 5.5C). That is the binding domain of Cx43-hDlg is contained in region 2 and region 3. Taken together, the binding region of Cx43-hDlg was located in region 3, which is at the last 100bp of the Cx43 CT (which containing amino acid 348 - 382). The last five amino acids on Cx43 CT, which are responsible for Cx43-ZO-1 interaction, are not involved in Cx43-hDlg interaction (Macdonald et al., 2012b). Therefore, the binding region of Cx43-hDlg is located in the Cx43 C-terminal between the amino acids 348 and 377.

A



B

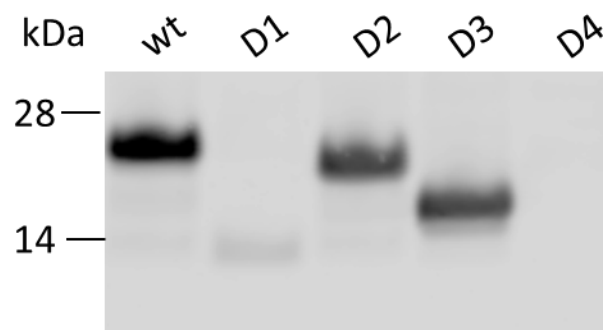


**Figure 5.3: Generating the flag tagged Cx43 CT deletions.**

(A) The diagram shows the region of Cx43 CT deletions. Region 1 is 150bp long. Region 2 is 200bp long and region 3 is 100bp long. D1 – D4 were referred to different regions. The amino acids sequence region of the Cx43 CT contained are also listed. (B) Western blot shows the successful expression of D2 and D3, wild-type is also expressed.

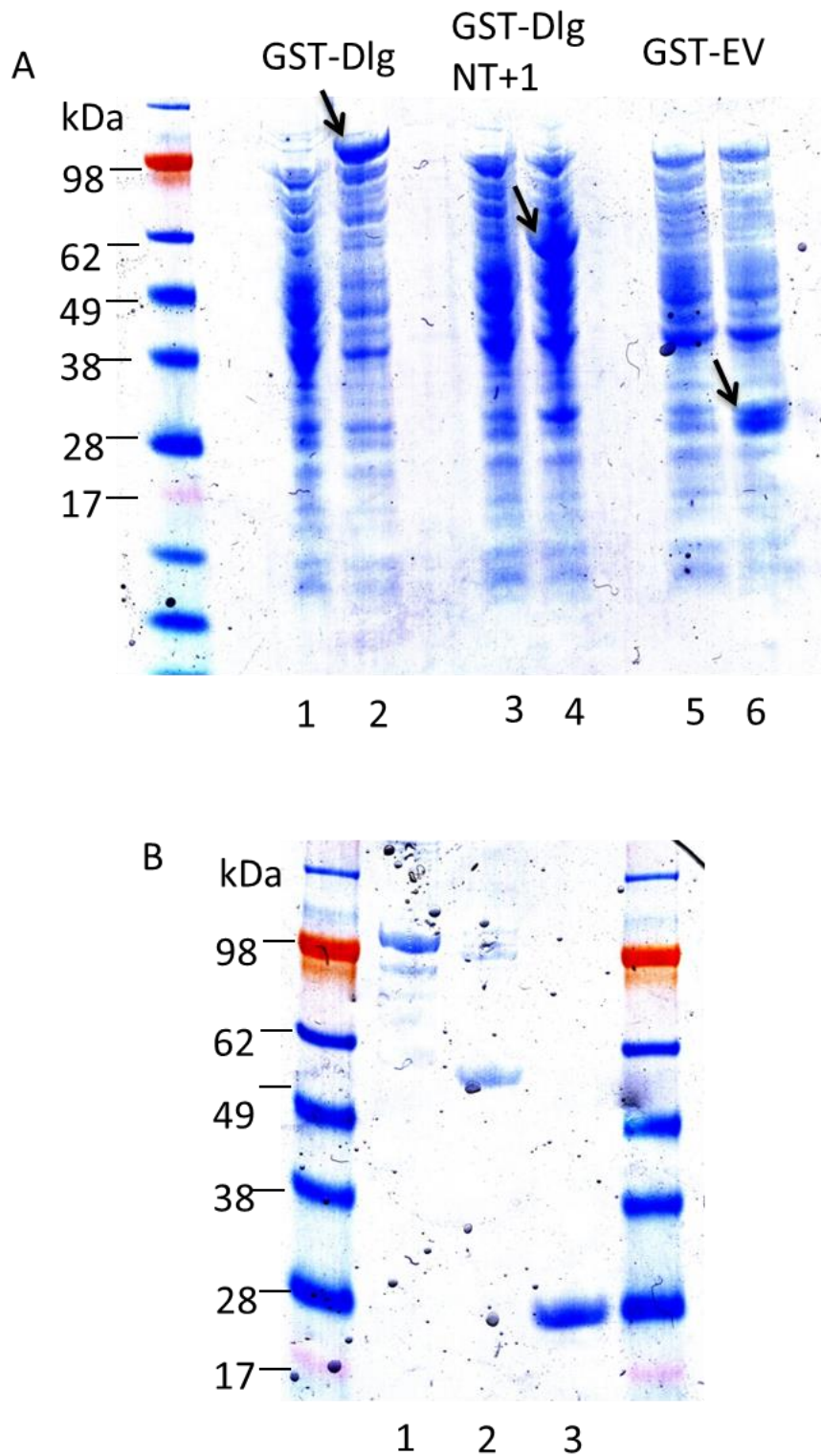


**Figure 5.4: GST-hDIg is successful induced by IPTG.**

(A) Coomassie stain shows the successful induction of GST-fused proteins. Lanes 1 and 2 are GST-hDIg without or with IPTG induction. Lanes 3 and 4 are GST-hDIg NT +1 (N-terminal and first PDZ domain) without or with IPTG induction. Lanes 5 and 6 are GST-EV (empty vector) without or with IPTG induction. The arrows indicate the location of GST-fused protein. (B) Coomassie stain of the purified GST-fused proteins. Lane 1 is GST-hDIg, lane 2 is GST-hDIg NT+1 and lane 3 is GST-EV. This indicates that GST-fused proteins bind to beads successfully and can be purified.

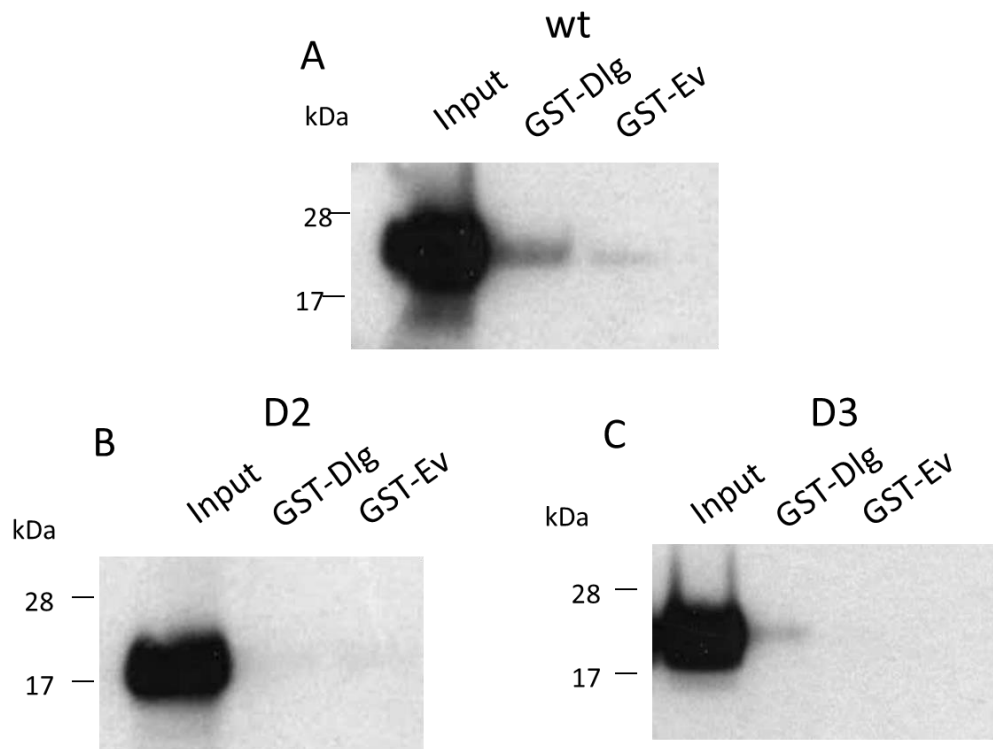


**Figure 5.5: The binding region of hDlg is located at the last 100bp of Cx43 CT.**

(A) Co-IP shows that Cx43 CT wt can bind to GST-hDlg. (B) Co-IP shows that Cx43 CT D2 cannot bind to GST-hDlg. D2 contains region 1 and region 2 of Cx43 CT. (C) Co-IP shows that Cx43 CT D3 can bind to GST-hDlg. D3 contains region 2 and region 3 of Cx43 CT. Input is one-tenth of the volume of lysate used in the Co-IP experiment.

## 5.2 Phosphorylation mutation does not affect the interaction between Cx43 and hDlg

Data from previously, and in this chapter, showed that while Cx43 binds to the central PDZ domain of ZO-1 through the very end of its C-terminus (last 5 amino acids), Cx43 bound to both the N and C-termini of hDlg through the last 33 amino acids of the C-terminal tail, and the ZO-1 binding domain was not involved (Macdonald et al., 2012b). Phosphorylation is an important bioprocess that controls the interactions between proteins, and also can control the opening and closing of gap junctions. Previous data suggested that the phosphorylated status of Cx43 is decreased in cervical tumour cells (Sun et al., 2015). These cells expressed HPV16E6, which is known to regulate cellular signalling pathways (Ganti et al., 2015). Therefore, six individual phosphorylation site mutations of the Cx43 CT domains were made to exam the effects of phosphorylation on interactions between Cx43 and hDlg (Table 5.1). These six phosphorylation sites are each phosphorylated by one of three pathways (MAPK, Akt, and PKC). These three pathways are regulated by HPV16 E6 (Chen, 2015). Site-directed mutagenesis in GST tagged plasmid pGEX2TGSTCx43 changed serine residues to alanine, which mimics the un-phosphorylated form of serine. Phosphorylation of S255, S279, and S282 is known to inhibit GJ opening. Phosphorylation of S262 and S368 can reduce the cell to cell communication of gap junctions (Johnstone et al., 2012). Batra and co-workers (Batra et al., 2014) discovered that AKT phosphorylation of Cx43-S373 is critical for the closure of Cx43 hemi-channels and for interaction with integrin  $\alpha 5$ . Cx43 CT with an S373A de-phosphorylated mimic mutant was no longer able to interact with integrin  $\alpha 5$  and was unable to inhibit the opening of hemichannels. This involved the disengagement of Cx43 from ZO-1. The phosphorylation mutation at S373 of Cx43 CT blocked its interaction with ZO-1. Other phosphorylation/dephosphorylated form mutants at S365, S368 and a phosphorylated form mutant at S373 of the Cx43 CT affected the subcellular location of the Cx43-ZO-1 complex throughout the GJ plaques, while wild-type Cx43 bound to ZO-1 at the periphery of GJ plaques (Thévenin et al., 2017). Therefore, these six phosphorylation sites at the Cx43 CT were chosen for site-directed mutagenesis.

Mutations 368 and 373 belong to region 3, which is located in the potential interaction domain of Cx43-hDlg, which was identified above. Mutations 282 and

279 belong to Cx43 CT deletion 3, which is shown to interact with GST-hDlg in the Co-IP experiments. Mutations 255 and 262 are outside this region. However, sometimes the conformational change caused by a phosphorylation event outside the interaction region will affect the binding affinity of two proteins. Therefore, plasmids expressing each of these phosphorylation site-mutations of Cx43 CT were transfected into HEK293 cells. After 48h incubation, cells were harvest and protein lysates were prepared in NP-40 lysis buffer. Successful expression of these phosphorylation site mutations was confirmed by western blot (Figure 5.6).

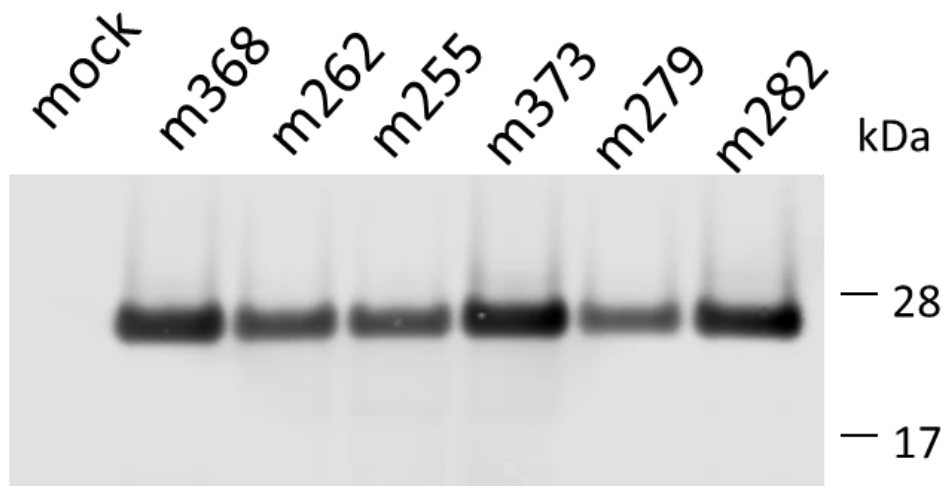
Co-IP utilized the GST fusion proteins from Figure 5.4 to investigate the effect of phosphorylation site-mutations in the interaction of Cx43-hDlg. GST pull-down with Cx43 CT wt gave a stronger band on the western blot corresponding to GST-hDlg compared to that under GST-EV (control). This indicates Cx43 CT can bind to GST-hDlg as expected. A band in the lane of GST-Dlg NT+1 was observed but is lighter than that in the lane of GST-EV, which is unable to indicate the interaction between GST-Dlg NT+1 and Cx43 CT (Figure 5.7 A) that was reported previously (Macdonald et al., 2012b). An unexpected band was observed in the lane of GST-EV, which should be a negative control (Figure 5.7 A). This might be due to the use of glutathione sepharose beads that trapped Cx43 as non-specific binding or it could be due to contamination of the protein preparation with nucleic acid (Nguyen and Goodrich, 2006). For the mutation S255A, a stronger band was observed in the lane of GST-Dlg. No bands were observed in the lane of GST-Dlg NT+1. There was a weak band in the lane of GST-EV lighter than that in the lane of GST-Dlg (Figure 5.7 B). For mutation S262A, a band was observed in the lane of GST-Dlg with a lighter band observed in the lane of GST-EV and the lane of GST-Dlg NT+1 (Figure 5.7 C). For mutation S279A, A band was observed in the lane of GST-Dlg, while no clear bands were observed in the lane of GST-Dlg NT+1 and GST-EV (Figure 5.7 D). A strong band was observed in the lane of GST-Dlg in Cx43 CT with mutated S282A. No obvious bands were observed in the lane of GST-Dlg NT+1 and GST-EV (Figure 5.7 E). All these four mutations belonging to the MAPK pathway shared similar patterns that a band was observed in the lane of GST-Dlg and no clear band was observed in the lane of GST-Dlg NT+1 and GST-EV (Figure 5.7 B - E). For mutation S368A, there was a strong band in the lane of GST-Dlg. A weak band was observed in the lane of GST-Dlg NT+1 and GST-EV (Figure 5.7 F). Similar results were observed in mutation S373A, a strong band

was observed in the lane of GST-Dlg with a weak band observed in the lane of GST-EV and a weaker band in the lane of GST-Dlg NT+1 (Figure 5.7 G).

In order to investigate the effect of these un-phosphorylated mimic mutations at different Cx43 CT sites on Cx43-hDlg interaction, the band intensities were measured by ImageJ. The band intensity was obtained utilizing the intensity measured in the lane of GST-Dlg minus the intensity measured in the lane of GST-EV in each Cx43 CT mutations and all related to the results in wild-type Cx43 CT. The results were shown in Figure 5.6 H. It was clear that apart from mutation S282A higher than wt, the band intensity of the rest mutations was lower than wt (Figure 5.7 H). This indicates that un-phosphorylated at the site S282 increases the Cx43-hDlg interaction and the rest decreases the binding of Cx43 CT to hDlg, in which mutation S255A showing the lowest binding affinity (about 23% of wt), S262A and S279A showing higher binding affinity (about 40% of wt) and S368A and S373A showing even higher binding affinity (about 60% of wt) (Figure 5.7 H). This indicates that compared with PKC and Akt pathway, phosphorylation by MAPK affects the Cx43 CT interaction with hDlg.

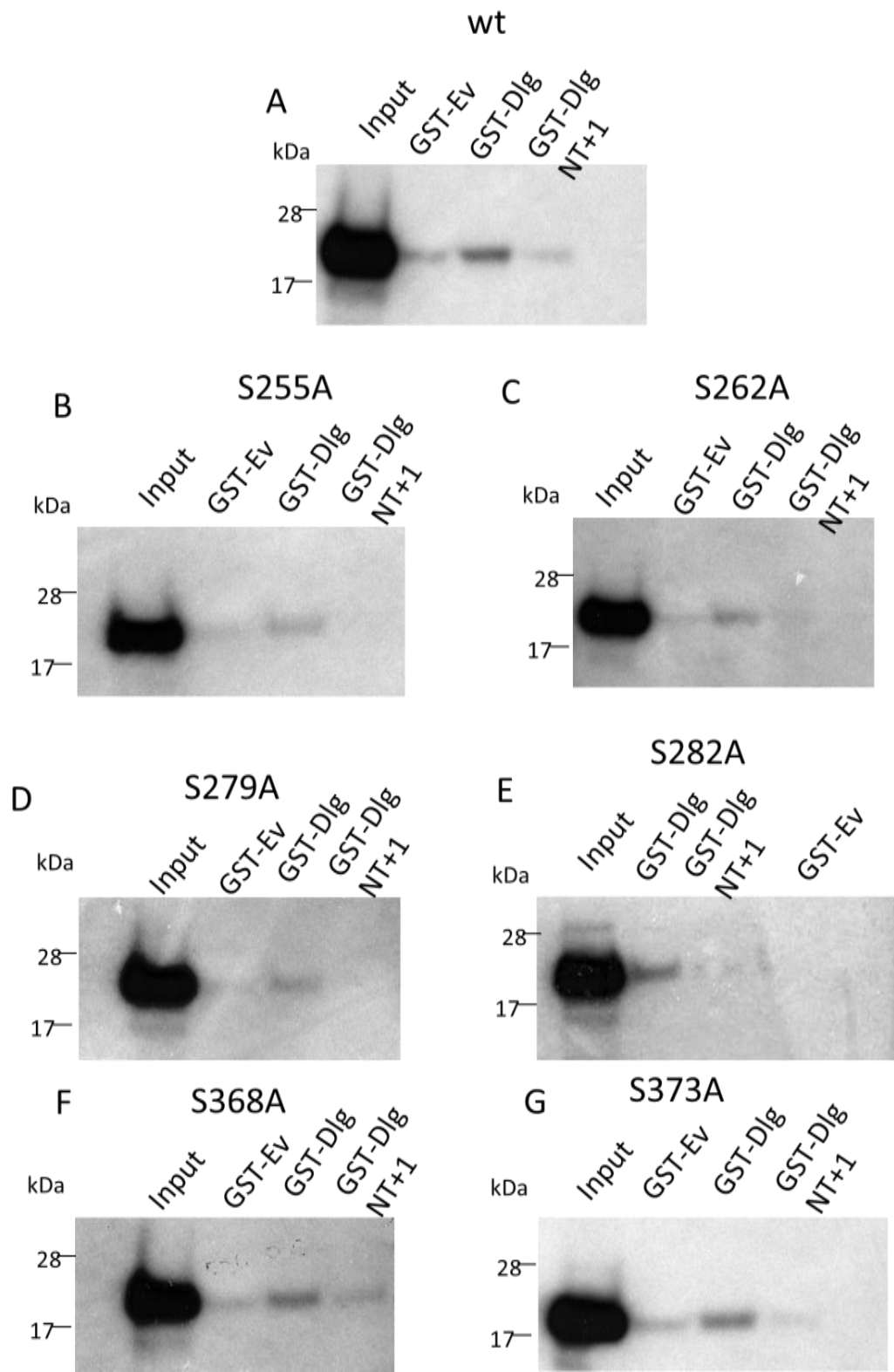
**Table 5.1: List of phosphorylation mimic site-mutation at Cx43 CT and the kinase involved in each phosphorylation site.**

<b>kinase</b>	<b>mutations</b>			
<b>MAPK</b>	S255A	S262A	S279A	S282A
<b>Akt</b>	S373A			
<b>PKC</b>	368A			



**Figure 5.6: Successful expression of all these un-phosphorylation mimic site mutations of the Cx43 CT.**

Plasmids expressing Cx43 CT with these mutations were transfected into HEK293 cells. After 48h post-transfection, cells were harvested, and western blot was carried out on protein lysates to check the expression.



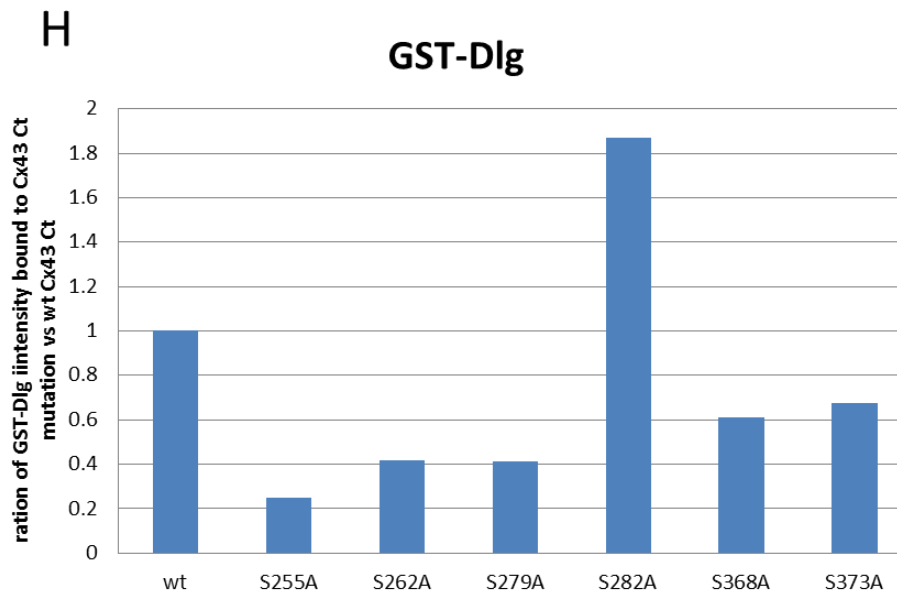


**Figure 5.7: Non-phosphorylation mimic site mutations at Cx43 CT did not affect/block the Cx43-hDlg interactions.**

(A) Co-IP shows that Cx43 CT wild-type (O'Neill et al.) can bind to GST-hDlg. Co-IP shows the Cx43 CT with the mutations at sites (B) S255A, (C) S262A, (D) S279A, (E) S282A, (F) S268A, and (G) S373A can bind to GST-Dlg. GST-Dlg indicates the full length of hDlg. GST-Dlg NT+1 indicates the N-terminal and first PDZ domain of hDlg. GST-EV indicates the empty vector, which is a negative control. (H) Related band intensity of GST-Dlg in each mutation compared with the band intensity in wt Cx43 CT. related band intensity of GST-Dlg in each mutation was achieved by the intensity of GST-Dlg minus the intensity of GST-EV. All the band intensities were measured using ImageJ.

## 5.3 Discussion

Cx43, as the most widespread Cx, has a long C-terminal tail that contains many protein-protein interaction regions. This allows Cx43 to interact with many other proteins such as binding to other Cxs (Cx26, Cx33, and Cx40), actins, and PDZ domain proteins zonula occludens -1 (ZO-1) and hDlg (Giepmans and Moolenaar, 1998, Macdonald et al., 2012b, Fiorini, 2004, He et al., 1999, Squecco et al., 2006). With interaction with other proteins, Cx43 gets involved in cell signalling pathways leading to regulation of gap junction channel abilities. Previously Macdonald and co-workers (Macdonald et al., 2012b) have shown that Cx43 binds to both the N-terminal (amino acids 1- 122) and C-terminal (amino acids 560 - 911) of hDlg via its C-terminal tail (amino acids 263 - 382). In terms of Cx43, in that experiment, the Cx43 CT was defined from amino acid 263 to 382. Studies here limited the interaction region of Cx43-hDlg to a location at the last 100bp of the Cx43 CT coding region, which is from amino acids 348 to 382. The binding region of Cx43 to hDlg is different from the binding sites of Cx43 to ZO-1, and loss of Cx43 the binding region to ZO-1 did not affect the interaction between Cx43 and hDlg (Macdonald et al., 2012b). The last 5 amino acids at the Cx43 CT are responsible for binding to ZO-1 (Giepmans and Moolenaar, 1998). Therefore, the binding region of Cx43 to hDlg is located at amino acids 348 to 377. Only the 14-3-3-theta-binding site was found previously in this region (Leithe et al., 2017b). 14-3-3 theta was identified as one of the binding partners to Cx43 utilizing a yeast two-hybrid screen of a mouse embryonic cDNA of Cx43 CT (amino acids 222 - 382) (Jin et al., 2000).

In terms of hDlg, the regions of hDlg utilized in Macdonald's experiment includes the L27 (lin-2 lin-7) binding domain at its N-terminal (amino acids 2 - 62; NCBI, [https://www.ncbi.nlm.nih.gov/protein/NP\\_001277912.1](https://www.ncbi.nlm.nih.gov/protein/NP_001277912.1)) and the C-terminal including the SH3, HOOK, and GUK domains (Macdonald et al., 2012b). hDlg with its L27 binding domain can bind to CASK, another protein that belongs to the MAGUK family (Lee et al., 2002). Co-immunoprecipitation indicated the direct interaction between CASK and Cx43 and PDZ binding domain in Cx43 CT (lack the last three amino acids) was not involved in CASK-Cx43 interaction (Marquez-Rosado et al., 2012). This indicates that Cx43 might have an L27 domain or MASK could be involved in Cx43-hDlg interaction. hDlg with its SH3/HOOK/GUK domain has been reported to bind to gap junction protein Cx32 at its C-terminal (Duffy

et al., 2007, Stauch et al., 2012). There is an SH3 binding domain located in the C-terminal of Cx43 (amino acids 253 - 256) (Solan and Lampe, 2009). However, this region is not included in the identified region (amino acids 348 - 377). It is located in region 1, which is included in Cx43 CT deletion 1 and deletion 2 (Figure 5.3). The band shown in Cx43 CT deletion 3 was weaker than that in wt (Figure 5.5) and the Cx43 CT bound to C-terminal of hDlg weakly compared to its binding to N-terminal of hDlg (Macdonald et al., 2012b). In this case, the binding between Cx43 CT SH3 binding domain and SH3 domain in hDlg might be too weak to be observed in Co-IP experiments. Another sensitive method is required. To identify the regions of Cx43-hDlg interaction more specifically, truncated experiments could be carried out. For example, the L27 region of hDlg could be truncated and pull-down with Cx43 CT.

Phosphorylation plays an important role in Gap Junction Intracellular Channels (GJIC). For example, phosphorylation at S364 increases the assembly and stability of gap junctions. There are in total 66 S/T/Y sites in Cx43 that could be phosphorylated with many kinases such as MAPK and Akt, and nearly half of them are in the CT domain (Chen et al., 2013b). Phosphorylation might cause a conformational change that alters the interaction between Cx43 and other proteins. For example, phosphorylation of Cx43 at the site of Y265 disrupts the binding between Cx43 and ZO-1 (Toyofuku et al., 2001). Interaction between Cx43 and 14-3-3 theta requires phosphorylation at S373 (Park et al., 2009). Our studies demonstrated that un-phosphorylation mimic mutations at S255, S262A, S279A, S282A, S368A, and S373A of Cx43 CT did affect the interaction between Cx43 and hDlg to some extent. Within these un-phosphorylation site-mutations, S282A increased the binding affinity of Cx43 CT to GST-hDlg reached over 1.8-fold to wt Cx43 CT (Figure 5.7 H). The mutation S255A decreased the binding affinity to about 20% of Cx43 CT wt, while mutation S262A and S279A decreased to about 40%, and S368A and S373A decrease to about 60% of Cx43 CT wt (Figure 5.7 H). Phosphorylation at these chosen sites was driven by different kinases: MAPK phosphorylated S255, S262, S279, and S282; S368 was phosphorylated by PKC, and S373 was phosphorylated by Akt. Therefore, MAPK seems to affect the Cx43-hDlg interaction stronger than PKC and Akt kinases.

However, the phosphorylation site mutation in this experiment was used as a phosphor null form of Cx43 CT and Co-IP assay. To ensure the effect of

phosphorylation of these chosen sites on Cx43-hDlg interaction, phosphor mimic mutations at the same phosphorylation sites should be investigated in their interaction with hDlg by Co-IP. Comparison of both phosphor-null and phosphor-mimic data of the same phosphorylation site in interaction with hDlg could provide better evidence of the binding affinity of Cx43-hDlg interaction affected by the phosphorylated site at Cx43 CT. Also, mimetic peptides of Cx43 CT with phosphor-null or phosphor-mimic site mutations could be generated to investigate whether phosphorylated Cx43 affect the Cx43-hDlg interactions.

PDZ domain protein hDlg normally works as a scaffold protein that provides a hub for more proteins to interact. It could also be considered that other proteins might work as hub or help in the Cx43-hDlg interactions. 14-3-3 theta might be one of the candidates, due to its ability to interact with both Cx43 and hDlg (Park et al., 2006, Nakajima et al., 2019). The interaction between Cx43 and 14-3-3 theta was associated with internalization of gap junctions, which led to subsequent phosphorylation at Ser368 in the Cx43 CT and followed by ubiquitination, which results in gap junction internalisation (Smyth et al., 2014). 14-3-3 zeta and epsilon could bind to Dlg in *Drosophila* and through these interactions, the Scrib/Dlg complex may control the orientation of the planar spindle (Nakajima et al., 2019).

Calcium/calmodulin-dependent serine kinase (CASK, also known as Lin2) is also considered since it can interact with both Cx43 and hDlg (Lee et al., 2002, Marquez-Rosado et al., 2012). CASK is expressed mainly in the cytoplasm and has limited co-localisation with Cx43. Cx43 appears on the plasma membrane in unwounded human foreskins explant tissue and extensive colocalization between Cx43 and CASK were observed on the plasma membrane after one hour in the skin experiment wound model (Márquez-Rosado et al., 2012). Co-expression of Cx43 and CASK increased the migration of Madin-Darby canine kidney (MDCK) cells (Márquez-Rosado et al., 2012). Both CASK and hDlg belong to the MAGUK family of proteins and their colocalization was observed on the epithelial cell membranes in the intestine and in neuromuscular junctions of skeletal muscles (Nix et al., 2000, Sanford et al., 2004). They might be involved in the same developmental pathway since mutations disrupting the function of hDlg or CASK in the mouse showed similar phenotypic results such as cleft palate (Caruana, 2002).

From the STRING website, where protein-protein interaction networks are deposited (<https://string-db.org/>), Cx43 and hDlg share one common interaction candidate, CTNNB1, which is beta-catenin. Beta-catenin is a critical protein involving in the Wnt signalling pathway. Beta-catenin interacts with Cx43 CT at residues 259-275, 282-295, and 302-319 by Nuclear Magnetic Resonance (NMR) and this interaction was negatively regulated by Src phosphorylation at the residues Y265 and Y313 at Cx43 CT (Spagnol et al., 2018). Beta-catenin, as part of adheren junctions, colocalized with Cx43 in cardiac myocytes in response to Wnt signalling (Ai et al., 2000). Interaction with and leading to the proteasomal degradation of hDlg might be one mechanism through which beta-catenin contributes to tumour progression (Subbaiah et al., 2012).

In conclusion, in this chapter, it is now shown that the potential binding region of hDlg is located at the last 100bp of Cx43 CT (amino acids 348 to 377). The un-phosphorylation mimic mutation at Cx43 CT that can be phosphorylated by kinase MAPK, PKC and Akt did show the ability to affect the Cx43-hDlg interactions. Cx43 binding domain to 14-3-3 theta is located in this area (amino acids 370 - 376) and Cx43 CT with a mutation at the site of 282 showed the strongest bands within all these mutations. Therefore 14-3-3 theta, CASK, and beta-catenin might act as a hub for Cx43-hDlg interactions.

## 6 Discussion, conclusion and future work

Gap junction intracellular channels (GJIC) act as a bridge between two neighbouring cells, allowing the exchange of small molecules (< 1kDa) between cells and their surrounding environment to maintain proper cellular physiological activities (Alexander and Goldberg, 2003a). It has been reported that GJIC is normally disrupted during the cancer progression pathway in many cancers. For example, the loss of GJIC is observed in HPV-related cervical cancer cells (Aasen et al., 2003b). Therefore, the role of connexins, the building block of gap junctions, involved in cancer progression is important to investigate. Both anti- and pro-tumorigenic activities of connexins are indicated depending on different types and stages of cancers (Aasen et al., 2019). Since connexins only have a short half-life of 1 - 5 h, the regulation of the connexin life cycle is important, especially in response to tumourigenesis and cellular stress such as wound healing. However, the full story of the connexin life cycle in detail still remains to be elucidated. Previously, utilizing the W12 cervical cancer cell line model, our lab found that the high-risk HPV E6 oncoprotein controls the trafficking of Cx43 to the membrane, the most spread connexin, via the interaction with hDlg, a PDZ-domain MAGUK protein (Macdonald et al., 2012b, Sun et al., 2015). This indicates the role of hDlg in controlling the trafficking of Cx43, at least in HPV-positive cervical cancer cells.

The first aim of this project was to investigate the Cx43-hDlg interaction in non-tumour epithelial cells. To test this, HEK293, HaCaT, NIKS, and HPV-positive non-tumour NIKS16 cells were used. The interaction of Cx43 and hDlg was confirmed by colocalisation on the plasma membrane in these non-tumour cells by immunofluorescence confocal microscopy and by Co-IP of the protein in lysates from these cells (Figure 3.4, 3.5, and 3.6). The Cx43-hDlg interaction was also observed on the membrane of C33a cells that are HPV-negative cervical cancer cells (Figure 3.1 A, Figure 3.2 A) and in these cells ectopically expressing HPV E6 oncoprotein (C33aE6 cells). Although in this case, the interaction was no longer at the cell membrane in C33aE6 cells but in the cytoplasm. This indicates the Cx43-hDlg interaction is neither HPVE6-dependent nor cancer cell-specific, which further indicates the role of hDlg in regulating Cx43 could be a general phenomenon. However, it is better to test Cx43-hDlg interaction in primary cells.

There is a cytoplasmic pool of Cx43 that can be used to re-build gap junctional communication (Boassa et al., 2010), and previous data together with the data reported here show that hDlg plays a role in maintaining a cytoplasmic pool of Cx43. siRNA depletion of hDlg in non-tumour cells led to a reduction in levels of Cx43 (Figure 3.7) and relocation of Cx43 from the plasma membrane into the cytoplasm in HaCaT and HEK293 cells (Figure 3.8). This reduction in levels and cytoplasmic location of Cx43 were also observed in HaCaT cells with stable depletion of hDlg (Figure 3.9). This reduction in levels of Cx43 by siRNA depletion of hDlg in HaCaT cells was reversed by endo-lysosome inhibitors NH<sub>4</sub>Cl and Chloroquine (Figure 3.12), which is consistent with the observation of MacDonald et al. in W12GPXY cervical tumour cells (Macdonald et al., 2012b).

Based on data in this thesis, it can be hypothesised that the involvement of hDlg in regulating the life cycle of Cx43 can be separated into two parts: the transport of Cx43 to the membrane and the transport of Cx43 from the membrane (Figure 6.1). For the aspect of transport to the membrane, the cytoplasmic pool of Cx43 that can be used to rebuild gap junctions must rely on hDlg as discussed above. Connexins traffic to the plasma membrane in the form of connexons. Connexons leaving the Golgi in vesicles can traffic to the membrane along the microtubules (Shaw et al., 2007). hDlg has been found to be involved in controlling the trafficking of vesicles, which requires the motor protein KIF13B (Walch, 2013). hDlg controls cell polarity and mutation of *Drosophila* Dlg resulted in disorganisation of epithelial structure and loss of cell polarity (Bilder, 2004, Roberts et al., 2012a). hDlg is also required for the proper organisation of the actin cytoskeleton (Laprise et al., 2004). Loss of Dlg protein led to disruption of proper location of actin and tubulin (Woods et al., 1996a). hDlg, as a scaffold protein, can tether many other proteins through its binding domains. For example, cytoskeletal protein protein 4.1R is reported to bind to the HOOK domain of hDlg (Hanada et al., 2003). It can also bind to tumour suppress protein APC and tumour suppressor phosphatase PTEN with its PDZ domain (Goode and Perrimon, 1997, Matsumine et al., 1996a, Valiente et al., 2005). Therefore, hDlg could bind Cx43 and allow interaction with vesicular trafficking and/or the actin cytoskeleton for transport to the membrane.

Phosphorylation at S373 in the Cx43 CT allows its binding with 14-3-3 theta protein (binding site aa 370 - 376) and this interaction is thought to facilitate the

trafficking of Cx43 to the plasma membrane (Majoul et al., 2009, Batra et al., 2013, Park et al., 2006, Park et al., 2009). Phosphorylation at S365 is required to prevent phosphorylation at S368 induced by interaction with 14-3-3 theta and led to ubiquitination and lysosome degradation. However, de-phosphorylation at S373 is required for Cx43 at the cell membrane to allow its interaction with ZO-1, which targets connexons to gap junction plaques. This de-phosphorylation at S373 prevents the interaction between Cx43 and 14-3-3 theta. hDlg can interact with 14-3-3 as well (Nakajima et al., 2019) and the Cx43-14-3-3 region is involved in the potential Cx43-hDlg interaction region (aa 348 - 382). Therefore, hDlg could replace 14-3-3 binding with Cx43 and deliver Cx43 to the plasma membrane (possibly de-phosphorylation at S373), or together with 14-3-3 theta deliver Cx43 to the plasma membrane. After reaching the plasma membrane, 14-3-3 is released from Cx43 due to de-phosphorylation at S373, which allows the Cx43-ZO-1 interaction that targets connexons to gap junction plaques. hDlg may or may not be involved in the building of gap junctions. Co-localisation of Cx43 and hDlg were observed on the plasma membrane in gap junction plaques (Figure 3.4 and 3.6) and the Cx43-hDlg interaction region is different from Cx43-ZO-1 (Macdonald et al., 2012b). Further work is required to address this question.

For the aspect of transport from the membrane, hDlg could accompany Cx43 into endosomes (Figure 6.1). hDlg was observed co-stained with Cx43 in the early-endosomes and late-endosomes in W12GPXY and C33aHPV18E6 cervical cancer cells. However, no co-staining was observed for Cx43 and early endosome marker (EEA1) in C33a (HPV-negative cervical cancer cells) and C33aHPV18mutE6 (C33a cells transfected with mutated HPV18E6 that lack PDZ binding domain) (Peng Sun, PhD thesis, 2005). After internalisation, Cx43 can be fused with the early-endosomes and sorted to the recycle-endosomes (without ubiquitination) and then back to the plasma membrane or to the late-endosomes (with ubiquitination) and further to the lysosomes for degradation. Cx43 can be mono-ubiquitinated, which is a signal for lysosome degradation. This ubiquitination process is regulated by E3 ubiquitin ligase NEDD4. Overexpression of NEDD4 in HeLa43 cells led to increased ubiquitination of Cx43 and reduced level of Cx43 (Totland et al., 2017). De-phosphorylation at S365 of Cx43 CT leads to a conformational change and is required for phosphorylation at S368, which is induced by phosphorylation at S373. These sites lie within the region of Cx43

that we have identified as the hDlg binding site. Therefore, if Cx43 is bound to hDlg, the complex could block Cx43 lysosomal degradation.

Phosphorylation at S373 of Cx43 CT, as a docking sign for Cx43 on the plasma membrane, led to disruption of the interaction between Cx43 and ZO-1, thus making Cx43 available to trafficking from the plasma membrane. The phosphorylation and ubiquitination sites involved in internalisation are within the region of Cx43-hDlg interaction (aa 348 - 382). Therefore, hDlg might maintain a cytoplasmic pool of Cx43 by preventing its ubiquitination. Cx43 molecules would then be available to be recycled to the plasma membrane instead of being degraded in the lysosomes. Phosphorylation at S373 also allows 14-3-3 binding to Cx43 CT (aa 370 -376) (Park et al., 2006, Park et al., 2009). This interaction is important in the internalization of Cx43. The un-phosphorylated mimic mutation S373A at Cx43 CT disrupts Cx43-14-3-3 interaction and stabilizes Cx43 on the plasma membrane (Smyth et al., 2014).

hDlg can also interact with 14-3-3 (Nakajima et al., 2019). High-risk HPV E6 interacts with 14-3-3 through its PDZ-binding motif (Boon and Banks, 2013). This suggests that 14-3-3 could be an essential molecule that is involved in the hDlg/E6 regulation of Cx43. It will be important in future studies to determine if 14-3-3 is part of the Cx43/hDlg complex in the cytoplasm of non-tumour and tumour cells.

The second aim of this project was to investigate the Cx43/hDlg interaction during the wound healing process. The wound healing process shares many similarities with tumour progression. Some scientists have concluded that the hallmarks of cancer are also the hallmarks for wound healing; cancer is a result of over-healing of a wound (MacCarthy-Morrogh and Martin, 2020, Sundaram et al., 2018). The key cellular behaviour for wound healing is proliferation and migration. Many growth factors, such as epidermal growth factor (EGF), are involved in the wound healing process as well as in cancer metastasis (Sundaram et al., 2018, MacCarthy-Morrogh and Martin, 2020). Results in Chapter 4 show that Cx43 relocated from the plasma membrane into the cytoplasm in the cells at the leading edge of a scrape wound in HaCaT cell monolayers during the early stage of wound healing (4h post-wound), and was relocated back to the membrane after wound closure (24h) (Figure 4.1). A similar phenomenon was

also observed in NIKS cell monolayers (Figure 4.4). This is consistent with key observations in human epidermal keratinocytes (Wright et al., 2009). Similar movement was observed for hDlg during wound healing, where it specifically co-localised with Cx43 (Figure 4.1 and 4.4). This again suggests the role of hDlg in the regulation of Cx43 trafficking. Observations of protein levels during wound healing in HaCaT cells (Figure 4.2), where Cx43 decreased at the early stage of wound healing, followed by increasing levels of the protein (peak at 16h) then recovery to un-wounded level after wound closure, are consistent with the previous observations (Wright et al., 2009). The pattern of alteration in levels of hDlg is similar to what has been observed for Cx43 levels (Figure 4.2). An upper band of Cx43, possibly ubiquitination, was observed clearly at 4h and 8h post-wounding, when the total levels of Cx43 and hDlg were decreased. If hDlg protects Cx43 from lysosomal degradation then in its absence, as discussed above, Cx43 ubiquitination could lead to lysosomal degradation of Cx43. This suggests that hDlg could inhibit Cx43 post-translational modification, possibly prevent its mono-ubiquitination which as tag delivery to lysosome for degradation and through binding with Cx43, hDlg might recycle it back to the membrane (Figure 6.1). Poly-ubiquitination leads to proteasome degradation of Cx43, which normally occurs through ERAD (endoplasmic-reticulum-associated protein degradation). Mono-ubiquitination triggers the internalisation of Cx43 from the plasma membrane. This could be tested with ubiquitination antibodies and markers for recycle-endosomes.

siRNA depletion of hDlg led to cell death during the wound healing process and loss of wound closure (Figure 4.8 and 4.9). This indicates the importance of hDlg for cells that are dividing and/or migrating to close the wound. One key inconsistency in the results is that while hDlg depletion by siRNA leads to inhibition of wound closure, in cells where hDlg expression is stably knocked down wound closure occurred faster than that in mock-treated cells (Figure 4.10). hScrib and hDlg show complementary roles and higher levels of hScrib were observed in HaCaT cells with stable depletion of hDlg by the Bank's group who supplied the HaCaT shDlg cells (Massimi et al., 2012). Endometrial cancer cells KLE with stable knockdown of hDlg increased cell migration in a wound-healing assay (Sugihara et al., 2016). Upon the stable loss of hDlg (an opposed to partial loss), leading potentially to total loss of cell polarity, hScrib could

compensate by increased activity and lead to a faster response to cellular stress such as wound healing.

It is interesting to notice that none of the cervical cancer cell lines investigated in this report was able to close scrape wounds properly either in the absence or presence of HPV E6. These data might suggest that loss of membranous Cx43 leads to better wound healing and might do so through regulation of nuclear beta-catenin. C33aE6 and HeLa43 cells containing HPV E6 that could lead to accumulated beta-catenin in the nucleus, which would allow faster wound healing than in C33a cells, which expressing just membranous Cx43 that prevents beta-catenin from transitioning to the nucleus (Figure 4.12 and 4.15).

Cx43 and hDlg roles in wound healing might be through regulating nuclear beta-catenin. In response to wounding, Wnt signalling is activated and leads to stabilization of beta-catenin, which led to the cytoplasmic location of Cx43 (Hou et al., 2019). This activation of beta-catenin also leads to the proteasomal degradation of hDlg (Subbaiah et al., 2012), which could lead to a decrease in levels of Cx43 and hDlg at early stages of wound healing (Figure 4.2 and 4.5). Also, the lower level of hDlg might lead to less membranous Cx43, which enhances nuclear beta-catenin. Thus, nuclear beta-catenin activates the expression of proteins involved in the wound healing process. After the activity of these healing-wound proteins is complete, nuclear levels of beta-catenin become reduced perhaps due to the increasing levels of Cx43 and hDlg as observed in Figures 4.2 and 4.5. When wound closure is complete, membranous Cx43 is observed, part of which might be recycled from a cytoplasmic pool maintained by hDlg.

The final aim of this project was to investigate the possible region of Cx43-hDlg interaction at the Cx43 CT and whether some phosphorylation sites at the Cx43 CT are involved in this interaction. We limited the Cx43-hDlg interaction region to within amino acid 348 - 382 at the Cx43 CT. Un-phosphorylated mimic mutation at S282 shows almost double the affinity for Cx43 binding to hDlg while other un-phosphorylated mimic mutations at Cx43 CT showed reduced Cx43-hDlg interaction (Figure 5.7). This indicates the phosphorylation site of S282 at Cx43 CT might be important in regulating the Cx43-hDlg interaction.

However, there are limitations to the study. Some of the data in this thesis are still preliminary and require further investigation. For example, Golgi tracker could be used to test whether the accumulation of Cx43 occurs in the Golgi upon the siRNA depletion of hDlg in HaCaT cells. Markers could be used to identify/measure apoptosis, as well as using trypan blue to count live or dead cells together with counting floating cells in the wound closure experiments.

Data in this thesis indicate the Cx43-hDlg interaction occurs widely in epithelial cells. However, the experiments were carried out *in vitro* in cell lines. It would be important to test their interaction *in vivo*. For example, immunofluorescence staining of Cx43 and hDlg could be used in healthy epithelial tissues, and proximity ligation assay (PLA) could be done on healthy epithelial tissue samples as previously described using epithelial tissue from patients with cervical cancer (Sun et al., 2015).

For the subcellular location alteration of Cx43 and hDlg during wound healing, it would be worth investigating this using live-cell imaging with fluorescently-tagged Cx43 and hDlg. This would give a clearer picture of the timed movement of Cx43 and hDlg during wound repair. The movement of Cx43 and hDlg during wound healing could also be done in 3D organotypic raft cultures, which are a model to mimic the multi-layers of epithelial tissue. This time-lapse trafficking model should also be carried out in primary epithelial cells.

Data in this thesis indicate the siRNA depletion of hDlg led to a reduction in levels and the cytoplasmic location of Cx43. It would be worth repeating these experiments using NIKS and NIKS16 cells to compare the subcellular location changes on Cx43 upon siDlg treatment and investigate whether the presence and expression HPV16 genome affects this process.

The effects of some un-phosphorylated mimic mutations of some of the phosphorylation sites at the Cx43 CT on Cx43-hDlg interaction have been investigated. It would be worth to also test the effects of the phosphorylated mimic mutations of the same phosphorylation sites at Cx43 CT on Cx43-hDlg interaction.

In conclusion, this thesis expanded the Cx43-hDlg interaction in a wider range of cells and showed that the interaction is not limited to cancer cells nor is dependent on the involvement of HPVE6. This study limited the Cx43-hDlg interaction region at the Cx43 CT to amino acids 348 - 382. The study also indicated the role of hDlg in the trafficking of Cx43 to the plasma membrane and maintaining the cytoplasmic pool of Cx43, which might involve 14-3-3 theta. Given that abnormal regulation of Cx43 trafficking is observed in many diseases and cancers, these findings help to picture the full story of the Cx43 life cycle and may have considerable future clinical implications. For example, designing a blocker or antisense RNA that blocks the Cx43-hDlg interaction so that membranous Cx43 is maintained in cervical cancer cells or to prevent Cx43 membrane trafficking in chronic wounds.

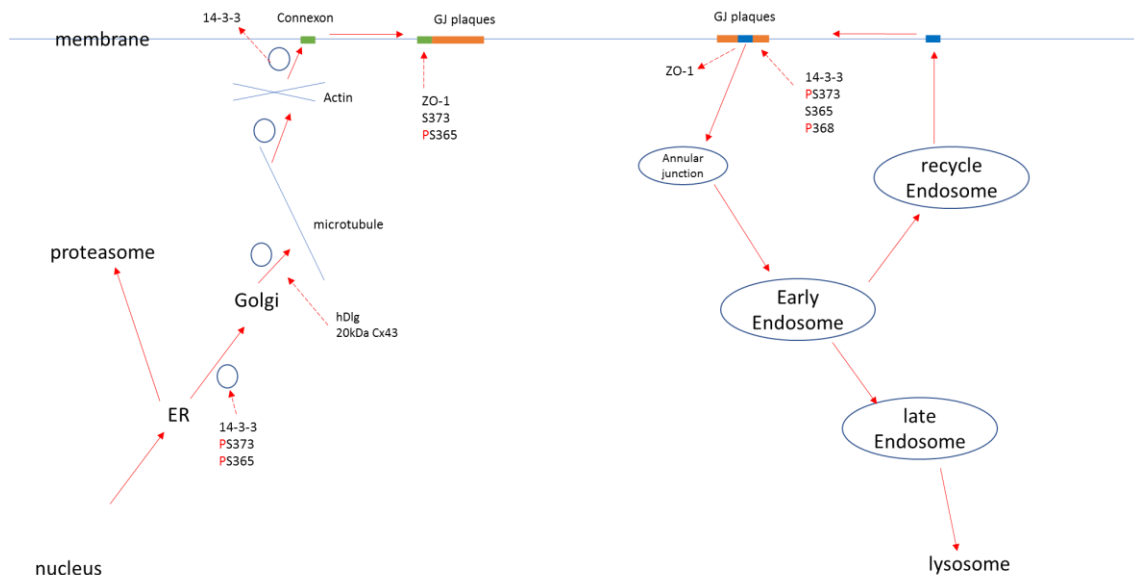


**Figure 6.1: A schematic diagram of the Cx43 life cycle and the possible stages that hDlg and ZO-1 were involved.**

From the trans-Golgi network, connexons are transported to the plasma membrane in vesicles. hDlg may be involved in this transport process. ZO-1 then interacts with Cx43 and targets it to gap junction plaques. For internalisation, connexons are released from ZO-1 and are transported to early endosomes where they are further sorted to 1) recycling endosomes (without ubiquitination) and back to the plasma membrane or to 2) late-endosomes (with ubiquitination) and further degraded in the lysosomes. hDlg may maintain a cytoplasmic pool of Cx43 and recycle it to the plasma membrane by preventing its ubiquitination by NEDD4.

## 7 Reference list

- AASEN, T., GRAHAM, S. V., EDWARD, M. & HODGINS, M. B. 2005. Reduced expression of multiple gap junction proteins is a feature of cervical dysplasia. *Mol Cancer*, 4, 31.
- AASEN, T., HODGINS, M. B., EDWARD, M. & GRAHAM, S. V. 2003a. The relationship between connexins, gap junctions, tissue architecture and tumour invasion, as studied in a novel in vitro model of HPV-16-associated cervical cancer progression. *Oncogene*, 22, 7969-7980.
- AASEN, T., HODGINS, M. B., EDWARD, M. & GRAHAM, S. V. 2003b. The relationship between connexins, gap junctions, tissue architecture and tumour invasion, as studied in a novel in vitro model of HPV-16-associated cervical cancer progression. *Oncogene*, 22, 7969-80.
- AASEN, T., LEITHE, E., GRAHAM, S. V., KAMERITSCH, P., MAYAN, M. D., MESNIL, M., POGODA, K. & TABERNERO, A. 2019. Connexins in cancer: bridging the gap to the clinic. *Oncogene*, 38, 4429-4451.
- AASEN, T., MESNIL, M., NAUS, C. C., LAMPE, P. D. & LAIRD, D. W. 2016. Erratum: Gap junctions and cancer: communicating for 50 years. *Nature Reviews Cancer*, 17, 74-74.
- AHMAD, S., MARTIN, P. E. M. & EVANS, W. H. 2001. Assembly of gap junction channels. *European Journal of Biochemistry*, 268, 4544-4552.
- AI, Z., FISCHER, A., SPRAY, D. C., BROWN, A. M. & FISHMAN, G. I. 2000. Wnt-1 regulation of connexin43 in cardiac myocytes. *The Journal of clinical investigation*, 105, 161-171.
- ALEXANDER, D. & GOLDBERG, G. 2003a. Transfer of Biologically Important Molecules Between Cells Through Gap Junction Channels. *Current Medicinal Chemistry*, 10, 2045-2058.
- ALEXANDER, D. B. & GOLDBERG, G. S. 2003b. Transfer of biologically important molecules between cells through gap junction channels. *Curr Med Chem*, 10, 2045-58.
- ALLEN-HOFFMANN, B. L., SCHLOSSER, S. J., IVARIE, C. A. R., MEISNER, L. F., O'CONNOR, S. L. & SATTLER, C. A. 2000. Normal Growth and Differentiation in a Spontaneously Immortalized Near-Diploid Human Keratinocyte Cell Line, NIKS. *Journal of Investigative Dermatology*, 114, 444-455.
- AMBROSI, C., REN, C., SPAGNOL, G., CAVIN, G., CONE, A., GRINTSEVICH, E. E., SOSINSKY, G. E. & SORGEN, P. L. 2016. Connexin43 Forms Supramolecular Complexes through Non-Overlapping Binding Sites for Drebrin, Tubulin, and ZO-1. *PLoS One*, 11, e0157073.
- ARTESI, M., KROONEN, J., BREDEL, M., NGUYEN-KHAC, M., DEPREZ, M., SCHOYSMAN, L., POULET, C., CHAKRAVARTI, A., KIM, H., SCHOLTENS, D., SEUTE, T., ROGISTER, B., BOURS, V. & ROBE, P. A. 2015. Connexin 30 expression inhibits growth of human malignant gliomas but protects them against radiation therapy. *Neuro Oncol*, 17, 392-406.
- ATKINSON, M. M., MENKO, A. S., JOHNSON, R. G., SHEPPARD, J. R. & SHERIDAN, J. D. 1981. Rapid and reversible reduction of junctional permeability in cells infected with a temperature-sensitive mutant of avian sarcoma virus. *J Cell Biol*, 91, 573-8.
- AVANZO, J. L., MESNIL, M., HERNANDEZ-BLAZQUEZ, F. J., MACKOWIAK, II, MORI, C. M., DA SILVA, T. C., OLORIS, S. C., GARATE, A. P., MASSIRONI, S. M., YAMASAKI, H. & DAGLI, M. L. 2004. Increased susceptibility to urethane-

- induced lung tumors in mice with decreased expression of connexin43. *Carcinogenesis*, 25, 1973-82.
- BAI, D. 2016. Structural analysis of key gap junction domains--Lessons from genome data and disease-linked mutants. *Semin Cell Dev Biol*, 50, 74-82.
- BAI, D., YUE, B. & AOYAMA, H. 2018. Crucial motifs and residues in the extracellular loops influence the formation and specificity of connexin docking. *Biochim Biophys Acta Biomembr*, 1860, 9-21.
- BAKIRTZIS, G., JAMIESON, S., AASEN, T., BRYSON, S., FORROW, S., TETLEY, L., FINBOW, M., GREENHALGH, D. & HODGINS, M. 2003. The Effects of a Mutant Connexin 26 on Epidermal Differentiation. *Cell Communication & Adhesion*, 10, 359-364.
- BALDWIN, P., LASKEY, R. & COLEMAN, N. 2003. Translational approaches to improving cervical screening. *Nature Reviews Cancer*, 3, 217-226.
- BAO, X., REUSS, L. & ALTENBERG, G. A. 2004. Regulation of Purified and Reconstituted Connexin 43 Hemichannels by Protein Kinase C-mediated Phosphorylation of Serine 368. *Journal of Biological Chemistry*, 279, 20058-20066.
- BATRA, N., RIQUELME, M. A., BURRA, S. & JIANG, J. X. 2013. 14-3-3 facilitates plasma membrane delivery and function of mechanosensitive connexin 43 hemichannels. *Journal of Cell Science*, 127, 137-146.
- BATRA, N., RIQUELME, M. A., BURRA, S., KAR, R., GU, S. & JIANG, J. X. 2014. Direct Regulation of Osteocytic Connexin 43 Hemichannels through AKT Kinase Activated by Mechanical Stimulation. *Journal of Biological Chemistry*, 289, 10582-10591.
- BATZER, A. T., MARSH, C. & KIRSNER, R. S. 2016. The use of keratin-based wound products on refractory wounds. *International Wound Journal*, 13, 110-115.
- BECKER, D. L., THRASIVOULOU, C. & PHILLIPS, A. R. 2012. Connexins in wound healing; perspectives in diabetic patients. *Biochim Biophys Acta*, 1818, 2068-75.
- BEHRENS, J., KAMERITSCH, P., WALLNER, S., POHL, U. & POGODA, K. 2010. The carboxyl tail of Cx43 augments p38 mediated cell migration in a gap junction-independent manner. *European Journal of Cell Biology*, 89, 828-838.
- BERGOFFEN, J., SCHERER, S. S., WANG, S., SCOTT, M. O., BONE, L. J., PAUL, D. L., CHEN, K., LENSCH, M. W., CHANCE, P. F. & FISCHBECK, K. H. 1993. Connexin mutations in X-linked Charcot-Marie-Tooth disease. *Science*, 262, 2039-42.
- BERNARD, H.-U. 2013. Regulatory elements in the viral genome. *Virology*, 445, 197-204.
- BERNARD, H.-U., BURK, R. D., CHEN, Z., VAN DOORSLAER, K., HAUSEN, H. Z. & DE VILLIERS, E.-M. 2010. Classification of papillomaviruses (PVs) based on 189 PV types and proposal of taxonomic amendments. *Virology*, 401, 70-79.
- BEYER, E. C., PAUL, D. L. & GOODENOUGH, D. A. 1987. Connexin43: a protein from rat heart homologous to a gap junction protein from liver. *Journal of Cell Biology*, 105, 2621-2629.
- BILDER, D. 2004. Epithelial polarity and proliferation control: links from the Drosophila neoplastic tumor suppressors. *Genes & Development*, 18, 1909-1925.
- BOASSA, D., SOLAN, J. L., PAPAS, A., THORNTON, P., LAMPE, P. D. & SOSINSKY, G. E. 2010. Trafficking and Recycling of the Connexin43 Gap Junction Protein during Mitosis. *Traffic*, 11, 1471-1486.

- BODNAR, A. G. 1998. Extension of Life-Span by Introduction of Telomerase into Normal Human Cells. *Science*, 279, 349-352.
- BONILLA-DELGADO, J., BULUT, G., LIU, X., CORT S-MALAG N, E. M., SCHLEGEL, R., FLORES-MALDONADO, C., CONTRERAS, R. G., CHUNG, S. H., LAMBERT, P. F., UREN, A. & GARIGLIO, P. 2012. The E6 oncoprotein from HPV16 enhances the canonical Wnt/ $\beta$ -catenin pathway in skin epidermis in vivo. *Mol Cancer Res*, 10, 250-8.
- BOON, S. S. & BANKS, L. 2013. High-Risk Human Papillomavirus E6 Oncoproteins Interact with 14-3-3 $\zeta$  in a PDZ Binding Motif-Dependent Manner. *Journal of Virology*, 87, 1586-1595.
- BOSHART, M., GISSMANN, L., IKENBERG, H., KLEINHEINZ, A., SCHEURLLEN, W. & ZUR HAUSEN, H. 1984. A new type of papillomavirus DNA, its presence in genital cancer biopsies and in cell lines derived from cervical cancer. *The EMBO journal*, 3, 1151-1157.
- BOUKAMP, P., PETRUSSEVSKA, R. T., BREITKREUTZ, D., HORNING, J., MARKHAM, A. & FUSENIG, N. E. 1988. Normal keratinization in a spontaneously immortalized aneuploid human keratinocyte cell line. *The Journal of Cell Biology*, 106, 761-771.
- BRANDNER, J. M., HOUDEK, P., H SING, B., KAISER, C. & MOLL, I. 2004. Connexins 26, 30, and 43: Differences Among Spontaneous, Chronic, and Accelerated Human Wound Healing. *Journal of Investigative Dermatology*, 122, 1310-1320.
- BRAY, F., FERLAY, J., SOERJOMATARAM, I., SIEGEL, R. L., TORRE, L. A. & JEMAL, A. 2018. Global cancer statistics 2018: GLOBOCAN estimates of incidence and mortality worldwide for 36 cancers in 185 countries. *CA: A Cancer Journal for Clinicians*, 68, 394-424.
- BUCK, C. B. & TRUS, B. L. 2012. The papillomavirus virion: a machine built to hide molecular Achilles' heels. *Viral Molecular Machines*. Springer.
- BURD, E. M. 2003. Human Papillomavirus and Cervical Cancer. *Clinical Microbiology Reviews*, 16, 1-17.
- BURD, E. M. & DEAN, C. L. 2016. Human Papillomavirus. *Microbiology Spectrum*, 4.
- BUTZ, S., OKAMOTO, M. & S DHOF, T. C. 1998. A Tripartite Protein Complex with the Potential to Couple Synaptic Vesicle Exocytosis to Cell Adhesion in Brain. *Cell*, 94, 773-782.
- CABRAL, J. H. M., PETOSA, C., SUTCLIFFE, M. J., RAZA, S., BYRON, O., POY, F., MARFATIA, S. M., CHISHTI, A. H. & LIDDINGTON, R. C. 1996. Crystal structure of a PDZ domain. *Nature*, 382, 649-652.
- CALHOUN, P. J., PHAN, A. V., TAYLOR, J. D., JAMES, C. C., PADGET, R. L., ZEITZ, M. J. & SMYTH, J. W. 2020. Adenovirus targets transcriptional and posttranslational mechanisms to limit gap junction function. *Faseb j*, 34, 9694-9712.
- CARUANA, G. 2002. Genetic studies define MAGUK proteins as regulators of epithelial cell polarity. *Int J Dev Biol*, 46, 511-8.
- CHATTERJEE, B., CHIN, A. J., VALDIMARSSON, G., FINIS, C., SONNTAG, J. M., CHOI, B. Y., TAO, L., BALASUBRAMANIAN, K., BELL, C., KRUFKA, A., KOZLOWSKI, D. J., JOHNSON, R. G. & LO, C. W. 2005. Developmental regulation and expression of the zebrafish connexin43 gene. *Developmental Dynamics*, 233, 890-906.
- CHEN, J. 2015. Signaling pathways in HPV-associated cancers and therapeutic implications. *Reviews in Medical Virology*, 25, 24-53.

- CHEN, J., PAN, L., WEI, Z., ZHAO, Y. & ZHANG, M. 2008. Domain-swapped dimerization of ZO-1 PDZ2 generates specific and regulatory connexin43-binding sites. *EMBO J*, 27, 2113-23.
- CHEN, Q., BOIRE, A., JIN, X., VALIENTE, M., ER, E. E., LOPEZ-SOTO, A., JACOB, L., PATWA, R., SHAH, H., XU, K., CROSS, J. R. & MASSAGUE, J. 2016. Carcinoma-astrocyte gap junctions promote brain metastasis by cGAMP transfer. *Nature*, 533, 493-498.
- CHEN, V. C., GOUW, J. W., NAUS, C. C. & FOSTER, L. J. 2013a. Connexin multi-site phosphorylation: Mass spectrometry-based proteomics fills the gap. *Biochimica et Biophysica Acta (BBA) - Biomembranes*, 1828, 23-34.
- CHEN, V. C., GOUW, J. W., NAUS, C. C. & FOSTER, L. J. 2013b. Connexin multi-site phosphorylation: mass spectrometry-based proteomics fills the gap. *Biochimica et Biophysica Acta (BBA)-Biomembranes*, 1828, 23-34.
- CHO, C., WANG, Y., SMALLWOOD, P. M., WILLIAMS, J. & NATHANS, J. 2019. Dlg1 activates beta-catenin signaling to regulate retinal angiogenesis and the blood-retina and blood-brain barriers. 8.
- COMMON, J. E. A., BITNER-GLINDZICZ, M., O'TOOLE, E. A., BARNES, M. R., JENKINS, L., FORGE, A. & KELSELL, D. P. 2005. Specific loss of connexin 26 expression in ductal sweat gland epithelium associated with the deletion mutation del(GJB6-D13S1830). *Clinical and Experimental Dermatology*, 30, 688-693.
- CONTRERAS, J. E., SANCHEZ, H. A., EUGEN N, E. A., SPEIDEL, D., THEIS, M., WILLECKE, K., BUKAUSKAS, F. F., BENNETT, M. V. & SEZ, J. C. 2002. Metabolic inhibition induces opening of unapposed connexin 43 gap junction hemichannels and reduces gap junctional communication in cortical astrocytes in culture. *Proceedings of the National Academy of Sciences*, 99, 495-500.
- COUTINHO, P. 2003. Dynamic changes in connexin expression correlate with key events in the wound healing process. *Cell Biology International*, 27, 525-541.
- COUTINHO, P., QIU, C., FRANK, S., TAMBER, K. & BECKER, D. 2003. Dynamic changes in connexin expression correlate with key events in the wound healing process. *Cell Biology International*, 27, 525-541.
- CRESPIN, S., BECHBERGER, J., MESNIL, M., NAUS, C. C. & SIN, W. C. 2010. The carboxy-terminal tail of connexin43 gap junction protein is sufficient to mediate cytoskeleton changes in human glioma cells. *J Cell Biochem*, 110, 589-97.
- CROOK T, W. D., VOUSDEN KH 1991. p53 point mutation in HPV negative human cervical carcinoma cell lines. *oncogene*, 6, 873-5.
- CROSBIE, E. J., EINSTEIN, M. H., FRANCESCHI, S. & KITCHENER, H. C. 2013. Human papillomavirus and cervical cancer. *The Lancet*, 382, 889-899.
- DANIELSON, E., ZHANG, N., METALLO, J., KALEKA, K., SHIN, S. M., GERGES, N. & LEE, S. H. 2012. S-SCAM/MAGI-2 Is an Essential Synaptic Scaffolding Molecule for the GluA2-Containing Maintenance Pool of AMPA Receptors. *Journal of Neuroscience*, 32, 6967-6980.
- DAS, S., SMITH, T. D., SARMA, J. D., RITZENTHALER, J. D., MAZA, J., KAPLAN, B. E., CUNNINGHAM, L. A., SUAUD, L., HUBBARD, M. J., RUBENSTEIN, R. C., KOVAL, M. & BRODSKY, J. L. 2009. ERp29 Restricts Connexin43 Oligomerization in the Endoplasmic Reticulum. *Molecular Biology of the Cell*, 20, 2593-2604.
- DE MENDOZA, A., SUGA, H. & RUIZ-TRILLO, I. 2010. Evolution of the MAGUK protein gene family in premetazoan lineages. *BMC Evolutionary Biology*, 10, 93.

- DE VILLIERS, E.-M. 2013. Cross-roads in the classification of papillomaviruses. *Virology*, 445, 2-10.
- DE VILLIERS, E.-M., FAUQUET, C., BROKER, T. R., BERNARD, H.-U. & ZUR HAUSEN, H. 2004. Classification of papillomaviruses. *Virology*, 324, 17-27.
- DE VUYST, E., DECROCK, E., DE BOCK, M., YAMASAKI, H., NAUS, C. C., EVANS, W. H. & LEYBAERT, L. 2007. Connexin hemichannels and gap junction channels are differentially influenced by lipopolysaccharide and basic fibroblast growth factor. *Molecular biology of the cell*, 18, 34-46.
- DEPIANTO, D. & COULOMBE, P. A. 2004. Intermediate filaments and tissue repair. *Experimental Cell Research*, 301, 68-76.
- DEWEY, M. M. & BARR, L. 1962. Intercellular Connection between Smooth Muscle Cells: the Nexus. *Science*, 137, 670-2.
- DIEZ, J. A., AHMAD, S. & EVANS, W. H. 1999. Assembly of heteromeric connexons in guinea-pig liver en route to the Golgi apparatus, plasma membrane and gap junctions. *European Journal of Biochemistry*, 262, 142-148.
- DIMITRATOS, S. D., WOODS, D. F., STATHAKIS, D. G. & BRYANT, P. J. 1999. Signaling pathways are focused at specialized regions of the plasma membrane by scaffolding proteins of the MAGUK family. *BioEssays*, 21, 912-921.
- DOERKS, T., BORK, P., KAMBEROV, E., MAKAROVA, O., MUECKE, S. & MARGOLIS, B. 2000. L27, a novel heterodimerization domain in receptor targeting proteins Lin-2 and Lin-7. *Trends in Biochemical Sciences*, 25, 317-318.
- DOORBAR, J. 2005. The papillomavirus life cycle. *Journal of Clinical Virology*, 32, 7-15.
- DOORBAR, J., EGAWA, N., GRIFFIN, H., KRANJEC, C. & MURAKAMI, I. 2015. Human papillomavirus molecular biology and disease association. *Reviews in Medical Virology*, 25, 2-23.
- DOW, L. E., BRUMBY, A. M., MURATORE, R., COOMBE, M. L., SEDELIES, K. A., TRAPANI, J. A., RUSSELL, S. M., RICHARDSON, H. E. & HUMBERT, P. O. 2003. hScrib is a functional homologue of the Drosophila tumour suppressor Scribble. *Oncogene*, 22, 9225-9230.
- DOYLE, D. A., LEE, A., LEWIS, J., KIM, E., SHENG, M. & MACKINNON, R. 1996. Crystal Structures of a Complexed and Peptide-Free Membrane Protein-Binding Domain: Molecular Basis of Peptide Recognition by PDZ. *Cell*, 85, 1067-1076.
- DUDOK, J. J., SANZ, A. S., LUNDTVIG, D. M. S. & WIJNHOLDS, J. 2013. MPP3 Is Required for Maintenance of the Apical Junctional Complex, Neuronal Migration, and Stratification in the Developing Cortex. *Journal of Neuroscience*, 33, 8518-8527.
- DUFFY, H. S., IACOBAS, I., HOTCHKISS, K., HIRST-JENSEN, B. J., BOSCO, A., DANDACHI, N., DERMETZEL, R., SORGEN, P. L. & SPRAY, D. C. 2007. The Gap Junction Protein Connexin32 Interacts with the Src Homology 3/Hook Domain of Discs Large Homolog 1. *Journal of Biological Chemistry*, 282, 9789-9796.
- DUNN, C. A. & LAMPE, P. D. 2014. Injury-triggered Akt phosphorylation of Cx43: a ZO-1-driven molecular switch that regulates gap junction size. *Journal of cell science*, 127, 455-464.
- DURST, M., GISSMANN, L., IKENBERG, H. & ZUR HAUSEN, H. 1983. A papillomavirus DNA from a cervical carcinoma and its prevalence in cancer biopsy samples from different geographic regions. *Proceedings of the National Academy of Sciences*, 80, 3812-3815.

- E., M. P., G. B., S. A., RJ, E. & WH, E. 2001. Multiple pathways in the trafficking and assembly of connexin 26, 32 and 43 into gap junction intercellular communication channels. *Cell Science*, 3845-3855.
- EL-SABBAN, M. E., ABI-MOSLEH, L. F. & TALHOUK, R. S. 2003. Developmental regulation of gap junctions and their role in mammary epithelial cell differentiation. *J Mammary Gland Biol Neoplasia*, 8, 463-73.
- EL-SABBAN, M. E. & PAULI, B. U. 1991. Cytoplasmic dye transfer between metastatic tumor cells and vascular endothelium. *J Cell Biol*, 115, 1375-82.
- ELIAS, G. M. & NICOLL, R. A. 2007. Synaptic trafficking of glutamate receptors by MAGUK scaffolding proteins. *Trends in Cell Biology*, 17, 343-352.
- ELZARRAD, M. K., HAROON, A., WILLECKE, K., DOBROWOLSKI, R., GILLESPIE, M. N. & AL-MEHDI, A. B. 2008. Connexin-43 upregulation in micrometastases and tumor vasculature and its role in tumor cell attachment to pulmonary endothelium. *BMC Med*, 6, 20.
- EMING, S. A., KRIEG, T. & DAVIDSON, J. M. 2007. Inflammation in Wound Repair: Molecular and Cellular Mechanisms. *Journal of Investigative Dermatology*, 127, 514-525.
- EPIFANTSEVA, I. & SHAW, R. M. 2017. Intracellular trafficking pathways of Cx43 gap junction channels. *Biochim Biophys Acta Biomembr*, 1860, 40-47.
- ETIENNE-MANNEVILLE, S. 2008. Polarity proteins in migration and invasion. *Oncogene*, 27, 6970-80.
- EVANS, W. H. & MARTIN, P. E. 2002. Gap junctions: structure and function (Review). *Mol Membr Biol*, 19, 121-36.
- EZUMI, K., YAMAMOTO, H., MURATA, K., HIGASHIYAMA, M., DAMDINSUREN, B., NAKAMURA, Y., KYO, N., OKAMI, J., NGAN, C. Y., TAKEMASA, I., IKEDA, M., SEKIMOTO, M., MATSUURA, N., NOJIMA, H. & MONDEN, M. 2008. Aberrant expression of connexin 26 is associated with lung metastasis of colorectal cancer. *Clin Cancer Res*, 14, 677-84.
- FAUQUET, C. & MAYO, M. A. 2001. The 7th ICTV report. *Archives of virology*, 146, 189-94.
- FAUQUET, C., MAYO, M. A., MANILOFF, J., DESSELBERGER, U. & BALL, L. A. 2005. Virus taxonomy - eighth report of the International Committee on the taxonomy of viruses. *The Viruses*, 83, 988-992.
- FIORINI, C. 2004. Dominant negative effect of connexin33 on gap junctional communication is mediated by connexin43 sequestration. *Journal of Cell Science*, 117, 4665-4672.
- FISHMAN, G. I., EDDY, R. L., SHOWS, T. B., ROSENTHAL, L. & LEINWAND, L. A. 1991. The human connexin gene family of gap junction proteins: distinct chromosomal locations but similar structures. *Genomics*, 10, 250-6.
- FU, C. T., BECHBERGER, J. F., OZOG, M. A., PERBAL, B. & NAUS, C. C. 2004. CCN3 (NOV) interacts with connexin43 in C6 glioma cells: possible mechanism of connexin-mediated growth suppression. *J Biol Chem*, 279, 36943-50.
- FUJA, T. J., LIN, F., OSANN, K. E. & BRYANT, P. J. 2004. Somatic Mutations and Altered Expression of the Candidate Tumor Suppressors CSNK1 $\epsilon$ , DLG1, and EDD/hHYD in Mammary Ductal Carcinoma. *Cancer Research*, 64, 942-951.
- GAIETTA, G., DEERINCK, T. J., ADAMS, S. R., BOUWER, J., TOUR, O., LAIRD, D. W., SOSINSKY, G. E., TSIEN, R. Y. & ELLISMAN, M. H. 2002. Multicolor and electron microscopic imaging of connexin trafficking. *Science*, 296, 503-7.
- GANTI, K., BRONIARCZYK, J., MANOUBI, W., MASSIMI, P., MITTAL, S., PIM, D., SZALMAS, A., THATTE, J., THOMAS, M., TOMAIĆ, V. & BANKS, L. 2015. The

- Human Papillomavirus E6 PDZ Binding Motif: From Life Cycle to Malignancy. *Viruses*, 7, 3530-3551.
- GANTWERKER, E. A. & HOM, D. B. 2011. Skin: histology and physiology of wound healing. *Facial Plast Surg Clin North Am*, 19, 441-53.
- GARDIOL, D., K HNE, C., GLAUNSINGER, B., LEE, S. S., JAVIER, R. & BANKS, L. 1999. Oncogenic human papillomavirus E6 proteins target the discs large tumour suppressor for proteasome-mediated degradation. *Oncogene*, 18, 5487-5496.
- GARDIOL, D., ZACCHI, A., PETRERA, F., STANTA, G. & BANKS, L. 2006. Human discs large and scrib are localized at the same regions in colon mucosa and changes in their expression patterns are correlated with loss of tissue architecture during malignant progression. *Int J Cancer*, 119, 1285-90.
- GEORGE, C. H., KENDALL, J. M. & EVANS, W. H. 1999. Intracellular trafficking pathways in the assembly of connexins into gap junctions. *J Biol Chem*, 274, 8678-85.
- GEWIN, L. 2004. Identification of a novel telomerase repressor that interacts with the human papillomavirus type-16 E6/E6-AP complex. *Genes & Development*, 18, 2269-2282.
- GIEPMANS, B. N. & MOOLENAAR, W. H. 1998. The gap junction protein connexin43 interacts with the second PDZ domain of the zona occludens-1 protein. *Curr Biol*, 8, 931-4.
- GIEPMANS, B. N., VERLAAN, I., HENGEVELD, T., JANSSEN, H., CALAFAT, J., FALK, M. M. & MOOLENAAR, W. H. 2001a. Gap junction protein connexin-43 interacts directly with microtubules. *Curr Biol*, 11, 1364-8.
- GIEPMANS, B. N., VERLAAN, I. & MOOLENAAR, W. H. 2001b. Connexin-43 interactions with ZO-1 and alpha- and beta-tubulin. *Cell Commun Adhes*, 8, 219-23.
- GILULA, N. B., REEVES, O. R. & STEINBACH, A. 1972. Metabolic coupling, ionic coupling and cell contacts. *Nature*, 235, 262-5.
- GISSMANN, L. & HAUSEN, H. Z. 1976. Human papilloma virus DNA: physical mapping and genetic heterogeneity. *Proceedings of the National Academy of Sciences*, 73, 1310-1313.
- GISSMANN, L., PFISTER, H. & ZUR HAUSEN, H. 1977. Human papilloma viruses (HPV): Characterization of four different isolates. *Virology*, 76, 569-580.
- GONZ LEZ-MARISCAL, L., BETANZOS, A. & ÁVILA-FLORES, A. 2000. MAGUK proteins: structure and role in the tight junction. *Seminars in Cell & Developmental Biology*, 11, 315-324.
- GONZALEZ, A. C. D. O., COSTA, T. F., ANDRADE, Z. D. A. & MEDRADO, A. R. A. P. 2016. Wound healing - A literature review. *Anais Brasileiros de Dermatologia*, 91, 614-620.
- GOODE, S. & PERRIMON, N. 1997. Inhibition of patterned cell shape change and cell invasion by Discs large during Drosophila oogenesis. *Genes & Development*, 11, 2532-2544.
- GOODENOUGH, D. A. 1974. Bulk isolation of mouse hepatocyte gap junctions. Characterization of the principal protein, connexin. *J Cell Biol*, 61, 557-63.
- GOODENOUGH, D. A. & STOECKENIUS, W. 1972. The isolation of mouse hepatocyte gap junctions. Preliminary chemical characterization and x-ray diffraction. *J Cell Biol*, 54, 646-56.
- GOODRIDGE, D., TREPAN, E. & EMBIL, J. M. 2005. Health-Related Quality of Life in Diabetic Patients With Foot Ulcers. *Journal of Wound, Ostomy and Continence Nursing*, 32, 368-377.

- GRAHAM, SHEILA V. 2017. The human papillomavirus replication cycle, and its links to cancer progression: a comprehensive review. *Clinical Science*, 131, 2201-2221.
- GRM, H. S. & BANKS, L. 2004. Degradation of hDlg and MAGIs by human papillomavirus E6 is E6-AP-independent. *Journal of General Virology*, 85, 2815-2819.
- GUPTA, S. M. & MANIA-PRAMANIK, J. 2019. RETRACTED ARTICLE: Molecular mechanisms in progression of HPV-associated cervical carcinogenesis. *Journal of Biomedical Science*, 26.
- H, S.-S., RR, B. & JD, P. 1969. Metabolic co-operation between biochemically marked mammalian cells in tissue culture. *Cell Science*, 4, 353-367.
- HANADA, T., TAKEUCHI, A., SONDARVA, G. & CHISHTI, A. H. 2003. Protein 4.1-mediated Membrane Targeting of Human Discs Large in Epithelial Cells. *Journal of Biological Chemistry*, 278, 34445-34450.
- HANAHAN, D. & WEINBERG, ROBERT A. 2011. Hallmarks of Cancer: The Next Generation. *Cell*, 144, 646-674.
- HARPER, D. M. & DEMARS, L. R. 2017. HPV vaccines - A review of the first decade. *Gynecol Oncol*, 146, 196-204.
- HE, D. S., JIANG, J. X., TAFFET, S. M. & BURT, J. M. 1999. Formation of heteromeric gap junction channels by connexins 40 and 43 in vascular smooth muscle cells. *Proceedings of the National Academy of Sciences*, 96, 6495-6500.
- HENDRIX, E. M., MAO, S. J. T., EVERSON, W. & LARSEN, W. J. 1992. Myometrial connexin 43 trafficking and gap junction assembly at term and in preterm labor. *Molecular Reproduction and Development*, 33, 27-38.
- HILGERT, N., SMITH, R. & CAMP, G. 2009. Function and Expression Pattern of Nonsyndromic Deafness Genes. *Current Molecular Medicine*, 9, 546-564.
- HONG, H.-M., YANG, J.-J., SHIEH, J.-C., LI, M.-L. & LI, S.-Y. 2010. Novel mutations in the connexin43 (GJA1) and GJA1 pseudogene may contribute to nonsyndromic hearing loss. *Human Genetics*, 127, 545-551.
- HOU, X., KHAN, M. R. A., TURMAINE, M., THRASIVOULOU, C., BECKER, D. L. & AHMED, A. 2019. Wnt signaling regulates cytosolic translocation of connexin 43. *American Journal of Physiology-Regulatory, Integrative and Comparative Physiology*, 317, R248-R261.
- HOUGH, C. D., WOODS, D. F., PARK, S. & BRYANT, P. J. 1997. Organizing a functional junctional complex requires specific domains of the Drosophila MAGUK Discs large. *Genes & Development*, 11, 3242-3253.
- HOUSCHYAR, K. S., DUSCHER, D., REIN, S., MAAN, Z. N., CHELLIAH, M. P., CHA, J. Y., WEISSENBERG, K. & SIEMERS, F. 2019. Wnt Signaling During Cutaneous Wound Healing. In: DUSCHER, D. & SHIFFMAN, M. A. (eds.) *Regenerative Medicine and Plastic Surgery: Skin and Soft Tissue, Bone, Cartilage, Muscle, Tendon and Nerves*. Cham: Springer International Publishing.
- HOUSCHYAR, K. S., MOMENI, A., PYLES, M. N., MAAN, Z. N., WHITTAM, A. J. & SIEMERS, F. 2015. Wnt signaling induces epithelial differentiation during cutaneous wound healing. *Organogenesis*, 11, 95-104.
- HUMBERT, P. O., GRZESCHIK, N. A., BRUMBY, A. M., GALEA, R., ELSUM, I. & RICHARDSON, H. E. 2008. Control of tumourigenesis by the Scribble/Dlg/Lgl polarity module. *Oncogene*, 27, 6888-6907.
- HUNTER, A. W., BARKER, R. J., ZHU, C. & GOURDIE, R. G. 2005. Zonula occludens-1 alters connexin43 gap junction size and organization by influencing channel accretion. *Molecular biology of the cell*, 16, 5686-5698.

- ISAACSON WECHSLER, E., WANG, Q., ROBERTS, I., PAGLIARULO, E., JACKSON, D., UNTERSPEGER, C., COLEMAN, N., GRIFFIN, H. & DOORBAR, J. 2012. Reconstruction of Human Papillomavirus Type 16-Mediated Early-Stage Neoplasia Implicates E6/E7 Deregulation and the Loss of Contact Inhibition in Neoplastic Progression. *Journal of Virology*, 86, 6358-6364.
- ISHIDATE, T., MATSUMINE, A., TOYOSHIMA, K. & AKIYAMA, T. 2000. The APC-hDLG complex negatively regulates cell cycle progression from the G0/G1 to S phase. *Oncogene*, 19, 365-372.
- J.KING, T., H.FUKUSHIMA, L., A.DONLON, T., HIEBER, A. D., A.SHIMABUKURO, K. & S.BERTRAM, J. 2000. Correlation between growth control, neoplastic potential and endogenous connexin43 expression in HeLa cell lines: implications for tumor progression. *Carcinogenesis*, 21, 311-315.
- JAMAKOSMANOVIC, A. & LOEWENSTEIN, W. R. 1968. Intercellular communication and tissue growth. 3. Thyroid cancer. *J Cell Biol*, 38, 556-61.
- JIN, C., LAU, A. F. & MARTYN, K. D. 2000. Identification of Connexin-Interacting Proteins: Application of the Yeast Two-Hybrid Screen. *Methods*, 20, 219-231.
- JOHN, S. A. & REVEL, J.-P. 1991. Connexon integrity is maintained by non-covalent bonds: Intramolecular disulfide bonds link the extracellular domains in rat connexin-43. *Biochemical and Biophysical Research Communications*, 178, 1312-1318.
- JOHNSTONE, S. R., BEST, A. K., WRIGHT, C. S., ISAKSON, B. E., ERRINGTON, R. J. & MARTIN, P. E. 2010. Enhanced connexin 43 expression delays intramitotic duration and cell cycle traverse independently of gap junction channel function. *Journal of Cellular Biochemistry*, 110, 772-782.
- JOHNSTONE, S. R., BILLAUD, M., LOHMAN, A. W., TADDEO, E. P. & ISAKSON, B. E. 2012. Posttranslational modifications in connexins and pannexins. *The Journal of membrane biology*, 245, 319-332.
- K LSCH, A., WINDOFFER, R. & LEUBE, R. E. 2009. Actin-dependent dynamics of keratin filament precursors. *Cell Motil Cytoskeleton*, 66, 976-85.
- KALIMI, G. H. & SIRSAT, S. M. 1984. Phorbol ester tumor promoter affects the mouse epidermal gap junctions. *Cancer Lett*, 22, 343-50.
- KAMERITSCH, P., POGODA, K. & POHL, U. 2012. Channel-independent influence of connexin 43 on cell migration. *Biochim Biophys Acta*, 1818, 1993-2001.
- KANCZUGA-KODA, L., SULKOWSKI, S., LENCZEWSKI, A., KODA, M., WINCEWICZ, A., BALTAZIAK, M. & SULKOWSKA, M. 2006. Increased expression of connexins 26 and 43 in lymph node metastases of breast cancer. *J Clin Pathol*, 59, 429-33.
- KANDA, T., WATANABE, S., ZANMA, S., SATO, H., FURUNO, A. & YOSHIKE, K. 1991. Human papillomavirus type 16 E6 proteins with glycine substitution for cysteine in the metal-binding motif. *Virology*, 185, 536-543.
- KARRER, H. E. 1960. The striated musculature of blood vessels. II. Cell interconnections and cell surface. *J Biophys Biochem Cytol*, 8, 135-50.
- KELLY, J. J., SIMEK, J. & LAIRD, D. W. 2014. Mechanisms linking connexin mutations to human diseases. *Cell Tissue Res*, 360, 701-21.
- KIM, E., NIETHAMMER, M., ROTHSCCHILD, A., NUNG JAN, Y. & SHENG, M. 1995. Clustering of Shaker-type K<sup>+</sup> channels by interaction with a family of membrane-associated guanylate kinases. *Nature*, 378, 85-88.
- KING, T. J., FUKUSHIMA, L. H., HIEBER, A. D., SHIMABUKURO, K. A., SAKR, W. A. & BERTRAM, J. S. 2000. Reduced levels of connexin43 in cervical dysplasia: inducible expression in a cervical carcinoma cell line decreases neoplastic potential with implications for tumor progression. *Carcinogenesis*, 21, 1097-1109.

- KING, T. J. & LAMPE, P. D. 2004. Mice deficient for the gap junction protein Connexin32 exhibit increased radiation-induced tumorigenesis associated with elevated mitogen-activated protein kinase (p44/Erk1, p42/Erk2) activation. *Carcinogenesis*, 25, 669-680.
- KLEOPA, K. A., ABRAMS, C. K. & SCHERER, S. S. 2012. How do mutations in GJB1 cause X-linked Charcot-Marie-Tooth disease? *Brain Res*, 1487, 198-205.
- KLINGELHUTZ, A. J., FOSTER, S. A. & MCDOUGALL, J. K. 1996. Telomerase activation by the E6 gene product of human papillomavirus type 16. *Nature*, 380, 79-82.
- KOTINI, M. & MAYOR, R. 2015. Connexins in migration during development and cancer. *Dev Biol*, 401, 143-51.
- KOVAL, M., HARLEY, J. E., HICK, E. & STEINBERG, T. H. 1997. Connexin46 Is Retained as Monomers in a trans-Golgi Compartment of Osteoblastic Cells. *Journal of Cell Biology*, 137, 847-857.
- KRANJEC, C. & BANKS, L. 2010. A Systematic Analysis of Human Papillomavirus (HPV) E6 PDZ Substrates Identifies MAGI-1 as a Major Target of HPV Type 16 (HPV-16) and HPV-18 Whose Loss Accompanies Disruption of Tight Junctions. *Journal of Virology*, 85, 1757-1764.
- KRETZ, M. 2003. Altered connexin expression and wound healing in the epidermis of connexin-deficient mice. *Journal of Cell Science*, 116, 3443-3452.
- KRUTOVSKIKH, V., MAZZOLENI, G., MIRONOV, N., OMORI, Y., AGUELON, A. M., MESNIL, M., BERGER, F., PARTENSKY, C. & YAMASAKI, H. 1994. Altered homologous and heterologous gap-junctional intercellular communication in primary human liver tumors associated with aberrant protein localization but not gene mutation of connexin 32. *Int J Cancer*, 56, 87-94.
- KULAR, J., SCHEER, KAITLIN G., PYNE, NATASHA T., ALLAM, AMR H., POLLARD, ANTHONY N., MAGENAU, A., WRIGHT, REBECCA L., KOLESNIKOFF, N., MORETTI, PAUL A., WULLKOPF, L., STOMSKI, FRANK C., COWIN, ALLISON J., WOODCOCK, JOANNA M., GRIMBALDESTON, MICHELE A., PITSON, STUART M., TIMPSON, P., RAMSHAW, HAYLEY S., LOPEZ, ANGEL F. & SAMUEL, MICHAEL S. 2015. A Negative Regulatory Mechanism Involving 14-3-3ζ Limits Signaling Downstream of ROCK to Regulate Tissue Stiffness in Epidermal Homeostasis. *Developmental Cell*, 35, 759-774.
- KUMAR, N. M., FRIEND, D. S. & GILULA, N. B. 1995. Synthesis and assembly of human beta 1 gap junctions in BHK cells by DNA transfection with the human beta 1 cDNA. *Journal of Cell Science*, 108, 3725-3734.
- KUROCHKINA, N. & GUHA, U. 2012. SH3 domains: modules of protein-protein interactions. *Biophysical Reviews*, 5, 29-39.
- KYO, N., YAMAMOTO, H., TAKEDA, Y., EZUMI, K., NGAN, C. Y., TERAYAMA, M., MIYAKE, M., TAKEMASA, I., IKEDA, M., DOKI, Y., DONO, K., SEKIMOTO, M., NOJIMA, H. & MONDEN, M. 2008. Overexpression of connexin 26 in carcinoma of the pancreas. *Oncol Rep*, 19, 627-31.
- LAIRD, DALE W. 2006. Life cycle of connexins in health and disease. *Biochemical Journal*, 394, 527-543.
- LAIRD, D. W. 2010. The gap junction proteome and its relationship to disease. *Trends in cell biology*, 20, 92-101.
- LAIRD, D. W. 2014. Syndromic and non-syndromic disease-linked Cx43 mutations. *FEBS Letters*, 588, 1339-1348.
- LAL, A., HAYNES, S. R. & GOROSPE, M. 2005. Clean western blot signals from immunoprecipitated samples. *Molecular and Cellular Probes*, 19, 385-388.
- LAMPE, P. D. & LAU, A. F. 2004. The effects of connexin phosphorylation on gap junctional communication. *The international journal of biochemistry & cell biology*, 36, 1171-1186.

- LAMPE, P. D., TENBROEK, E. M., BURT, J. M., KURATA, W. E., JOHNSON, R. G. & LAU, A. F. 2000. Phosphorylation of connexin43 on serine368 by protein kinase C regulates gap junctional communication. *The Journal of cell biology*, 149, 1503-1512.
- LANGLOIS, S., COWAN, K. N., SHAO, Q., COWAN, B. J., LAIRD, D. W. & PARTON, R. 2008. Caveolin-1 and -2 Interact with Connexin43 and Regulate Gap Junctional Intercellular Communication in Keratinocytes. *Molecular Biology of the Cell*, 19, 912-928.
- LAPRISE, P., VIEL, A. & RIVARD, N. 2004. Human Homolog of Disc-large Is Required for Adherens Junction Assembly and Differentiation of Human Intestinal Epithelial Cells. *Journal of Biological Chemistry*, 279, 10157-10166.
- LEE, S., FAN, S., MAKAROVA, O., STRAIGHT, S. & MARGOLIS, B. 2002. A Novel and Conserved Protein-Protein Interaction Domain of Mammalian Lin-2/CASK Binds and Recruits SAP97 to the Lateral Surface of Epithelia. *Molecular and Cellular Biology*, 22, 1778-1791.
- LEE, S. S., WEISS, R. S. & JAVIER, R. T. 1997. Binding of human virus oncoproteins to hDlg/SAP97, a mammalian homolog of the Drosophila discs large tumor suppressor protein. *Proceedings of the National Academy of Sciences*, 94, 6670-6675.
- LEITHE, E., MESNIL, M. & AASEN, T. 2017a. The connexin 43 C-terminus: A tail of many tales. *Biochimica et Biophysica Acta (BBA)-Biomembranes*.
- LEITHE, E., MESNIL, M. & AASEN, T. 2017b. The connexin 43 C-terminus: A tail of many tales. *Biochimica et Biophysica Acta (BBA) - Biomembranes*, 1860, 48-64.
- LEITHE, E., MESNIL, M. & AASEN, T. 2018. The connexin 43 C-terminus: A tail of many tales. *Biochimica et Biophysica Acta (BBA) - Biomembranes*, 1860, 48-64.
- LI, X., SU, V., KURATA, W. E., JIN, C. & LAU, A. F. 2008. A Novel Connexin43-interacting Protein, CIP75, Which Belongs to the UbL-UBA Protein Family, Regulates the Turnover of Connexin43. *Journal of Biological Chemistry*, 283, 5748-5759.
- LI, X., SU, Y., PAN, J., ZHOU, Z., SONG, B., XIONG, E. & CHEN, Z. 2013. Connexin 26 is down-regulated by KDM5B in the progression of bladder cancer. *Int J Mol Sci*, 14, 7866-79.
- LIU, Y., CHEN, J. J., GAO, Q., DALAL, S., HONG, Y., MANSUR, C. P., BAND, V. & ANDROPHY, E. J. 1999. Multiple Functions of Human Papillomavirus Type 16 E6 Contribute to the Immortalization of Mammary Epithelial Cells. *Journal of Virology*, 73, 7297-7307.
- LIU, Y., HENRY, G. D., HEGDE, R. S. & BALEJA, J. D. 2007. Solution Structure of the hDlg/SAP97 PDZ2 Domain and Its Mechanism of Interaction with HPV-18 Papillomavirus E6 Protein†,‡. *Biochemistry*, 46, 10864-10874.
- LOEWENSTEIN, W. R. & KANNO, Y. 1966. Intercellular communication and the control of tissue growth: lack of communication between cancer cells. *Nature*, 209, 1248-9.
- LOEWENSTEIN, W. R. & KANNO, Y. 1967. Intercellular communication and tissue growth. I. Cancerous growth. *J Cell Biol*, 33, 225-34.
- LORRAINE, C., WRIGHT, C. S. & MARTIN, P. E. 2015. Connexin43 plays diverse roles in co-ordinating cell migration and wound closure events. *Biochem Soc Trans*, 43, 482-8.
- LURTZ, M. M. & LOUIS, C. F. 2007. Intracellular calcium regulation of connexin43. *American Journal of Physiology-Cell Physiology*, 293, C1806-C1813.

- M LLER, T., BAIN, G., WANG, X. & PAPKOFF, J. 2002. Regulation of epithelial cell migration and tumor formation by beta-catenin signaling. *Exp Cell Res*, 280, 119-33.
- M NGER, K. & HOWLEY, P. M. 2002. Human papillomavirus immortalization and transformation functions. *Virus Research*, 89, 213-228.
- M RQUEZ-ROSADO, L., SINGH, D., RINC N-ARANO, H., SOLAN, J. L. & LAMPE, P. D. 2012. CASK (LIN2) interacts with Cx43 in wounded skin and their coexpression affects cell migration. *Journal of cell science*, 125, 695-702.
- MACCARTHY-MORROGH, L. & MARTIN, P. 2020. The hallmarks of cancer are also the hallmarks of wound healing. *Science Signaling*, 13, eaay8690.
- MACDONALD, A. I., SUN, P., HERNANDEZ-LOPEZ, H., AASEN, T., HODGINS, M. B., EDWARD, M., ROBERTS, S., MASSIMI, P., THOMAS, M. & BANKS, L. 2012a. A functional interaction between the MAGUK protein hDlg and the gap junction protein connexin 43 in cervical tumour cells. *Biochemical Journal*, 446, 9-21.
- MACDONALD, A. I., SUN, P., HERNANDEZ-LOPEZ, H., AASEN, T., HODGINS, M. B., EDWARD, M., ROBERTS, S., MASSIMI, P., THOMAS, M., BANKS, L. & GRAHAM, S. V. 2012b. A functional interaction between the MAGUK protein hDlg and the gap junction protein connexin 43 in cervical tumour cells. *Biochem J*, 446, 9-21.
- MAJOU, I. V., ONICHTCHOUK, D., BUTKEVICH, E., WENZEL, D., CHAILAKHYAN, L. M. & DUDEN, R. 2009. Limiting transport steps and novel interactions of Connexin-43 along the secretory pathway. *Histochemistry and Cell Biology*, 132, 263-280.
- MANTOVANI, F. & BANKS, L. 1999. Inhibition of E6 induced degradation of p53 is not sufficient for stabilization of p53 protein in cervical tumour derived cell lines. *Oncogene*, 18, 3309-3315.
- MANTOVANI, F. & BANKS, L. 2001. The Human Papillomavirus E6 protein and its contribution to malignant progression. *Oncogene*, 20, 7874-7887.
- MANTOVANI, F., MASSIMI, P. & BANKS, L. 2001. Proteasome-mediated regulation of the hDlg tumour suppressor protein. *Journal of Cell Science*, 114, 4285-4292.
- MARQUEZ-ROSADO, L., SINGH, D., RINCON-ARANO, H., SOLAN, J. L. & LAMPE, P. D. 2012. CASK (LIN2) interacts with Cx43 in wounded skin and their coexpression affects cell migration. *Journal of Cell Science*, 125, 695-702.
- MARTIN, P. E., BLUNDELL, G., AHMAD, S., ERRINGTON, R. J. & EVANS, W. H. 2001. Multiple pathways in the trafficking and assembly of connexin 26, 32 and 43 into gap junction intercellular communication channels. *J Cell Sci*, 114, 3845-55.
- MARTIN, P. E., EASTON, J. A., HODGINS, M. B. & WRIGHT, C. S. 2014. Connexins: sensors of epidermal integrity that are therapeutic targets. *FEBS Lett*, 588, 1304-14.
- MARTIN, P. E., MAMBETISAEVA, E. T., ARCHER, D. A., GEORGE, C. H. & EVANS, W. H. 2000. Analysis of gap junction assembly using mutated connexins detected in Charcot-Marie-Tooth X-linked disease. *J Neurochem*, 74, 711-20.
- MARTINEZ-ZAPIEN, D., RUIZ, F. X., POIRSON, J., MITSCHLER, A., RAMIREZ, J., FORSTER, A., COUSIDO-SIAH, A., MASSON, M., POL, S. V., PODJARNY, A., TRAV, G. & ZANIER, K. 2016. Structure of the E6/E6AP/p53 complex required for HPV-mediated degradation of p53. *Nature*, 529, 541-545.
- MARZIANO, N. K. 2003. Mutations in the gene for connexin 26 (GJB2) that cause hearing loss have a dominant negative effect on connexin 30. *Human Molecular Genetics*, 12, 805-812.

- MASSIMI, P., GAMMOH, N., THOMAS, M. & BANKS, L. 2004. HPV E6 specifically targets different cellular pools of its PDZ domain-containing tumour suppressor substrates for proteasome-mediated degradation. *Oncogene*, 23, 8033-8039.
- MASSIMI, P., ZORI, P., ROBERTS, S. & BANKS, L. 2012. Differential regulation of cell-cell contact, invasion and anoikis by hScrib and hDlg in keratinocytes. *PLoS One*, 7, e40279.
- MATSUMINE, A., OGAI, A., SENDA, T. & OKUMURA, N. 1996a. Binding of APC to the human homolog of the Drosophila discs large tumor suppressor protein. *Science*, 272, 1020.
- MATSUMINE, A., OGAI, A., SENDA, T., OKUMURA, N., SATOH, K., BAEG, G. H., KAWAHARA, T., KOBAYASHI, S., OKADA, M., TOYOSHIMA, K. & AKIYAMA, T. 1996b. Binding of APC to the Human Homolog of the Drosophila Discs Large Tumor Suppressor Protein. *Science*, 272, 1020-1023.
- MATSUMOTO, Y., NAKAGAWA, S., YANO, T., TAKIZAWA, S., NAGASAKA, K., NAKAGAWA, K., MINAGUCHI, T., WADA, O., OOISHI, H., MATSUMOTO, K., YASUGI, T., KANDA, T., HUIBREGTSE, J. M. & TAKETANI, Y. 2006. Involvement of a cellular ubiquitin-protein ligase E6AP in the ubiquitin-mediated degradation of extensive substrates of high-risk human papillomavirus E6. *Journal of Medical Virology*, 78, 501-507.
- MCBRIDE, A. A. 2013. The papillomavirus E2 proteins. *Virology*, 445, 57-79.
- MCGEE, A. W., DAKOJI, S. R., OLSEN, O., BREDDT, D. S., LIM, W. A. & PREHODA, K. E. 2001. Structure of the SH3-Guanylate Kinase Module from PSD-95 Suggests a Mechanism for Regulated Assembly of MAGUK Scaffolding Proteins. *Molecular Cell*, 8, 1291-1301.
- MCMURRAY, H. R. & MCCANCE, D. J. 2003. Human Papillomavirus Type 16 E6 Activates TERT Gene Transcription through Induction of c-Myc and Release of USF-Mediated Repression. *Journal of Virology*, 77, 9852-9861.
- MCNUTT, N. S., HERSHBERG, R. A. & WEINSTEIN, R. S. 1971. FURTHER OBSERVATIONS ON THE OCCURRENCE OF NEXUSES IN BENIGN AND MALIGNANT HUMAN CERVICAL EPITHELIUM. *Journal of Cell Biology*, 51, 805-825.
- MCNUTT, N. S. & WEINSTEIN, R. S. 1969a. Carcinoma of the cervix: deficiency of nexus intercellular junctions. *Science*, 165, 597-9.
- MCNUTT, N. S. & WEINSTEIN, R. S. 1969b. Carcinoma of the Cervix: Deficiency of Nexus Intercellular Junctions. *Science*, 165, 597-598.
- MEHTA, P. P., HOTZ-WAGENBLATT, A., ROSE, B., SHALLOWAY, D. & LOEWENSTEIN, W. R. 1991. Incorporation of the gene for a cell-cell channel protein into transformed cells leads to normalization of growth. *J Membr Biol*, 124, 207-25.
- MOLL, R., DIVO, M. & LANGBEIN, L. 2008. The human keratins: biology and pathology. *Histochemistry and cell biology*, 129, 705-733.
- MONTGOMERY, J., GHATNEKAR, G. S., GREK, C. L., MOYER, K. E. & GOURDIE, R. G. 2018a. Connexin 43-Based Therapeutics for Dermal Wound Healing. *International journal of molecular sciences*, 19, 1778.
- MONTGOMERY, J., GHATNEKAR, G. S., GREK, C. L., MOYER, K. E. & GOURDIE, R. G. 2018b. Connexin 43-Based Therapeutics for Dermal Wound Healing. *Int J Mol Sci*, 19.
- MOORBY, C. & PATEL, M. 2001. Dual Functions for Connexins: Cx43 Regulates Growth Independently of Gap Junction Formation. *Experimental Cell Research*, 271, 238-248.
- MOREIRA, J. M. A., SHEN, T., OHLSSON, G., GROMOV, P., GROMOVA, I. & CELIS, J. E. 2008. A Combined Proteome and Ultrastructural Localization Analysis

- of 14-3-3 Proteins in Transformed Human Amnion (AMA) Cells: Definition of A Framework to Study Isoform-Specific Differences. *Molecular & Cellular Proteomics*, 7, 1225-1240.
- MORI, R., POWER, K. T., WANG, C. M., MARTIN, P. & BECKER, D. L. 2006. Acute downregulation of connexin43 at wound sites leads to a reduced inflammatory response, enhanced keratinocyte proliferation and wound fibroblast migration. *Journal of Cell Science*, 119, 5193-5203.
- MUNOZ, J. L., RODRIGUEZ-CRUZ, V., GRECO, S. J., RAMKISSOON, S. H., LIGON, K. L. & RAMESHWAR, P. 2014. Temozolomide resistance in glioblastoma cells occurs partly through epidermal growth factor receptor-mediated induction of connexin 43. *Cell Death Dis*, 5, e1145.
- MURRAY, A. W. & FITZGERALD, D. J. 1979. Tumor promoters inhibit metabolic cooperation in cocultures of epidermal and 3T3 cells. *Biochem Biophys Res Commun*, 91, 395-401.
- MUSIL, L. S. & GOODENOUGH, D. A. 1993. Multisubunit assembly of an integral plasma membrane channel protein, gap junction connexin43, occurs after exit from the ER. *Cell*, 74, 1065-1077.
- NAGASAKA, K., KAWANA, K., OSUGA, Y. & FUJII, T. 2013a. PDZ Domains and Viral Infection: Versatile Potentials of HPV-PDZ Interactions in relation to Malignancy. *BioMed Research International*, 2013, 1-9.
- NAGASAKA, K., KAWANA, K., OSUGA, Y. & FUJII, T. 2013b. PDZ domains and viral infection: versatile potentials of HPV-PDZ interactions in relation to malignancy. *BioMed research international*, 2013.
- NAGASHIMA, S., KODAKA, M., IWASA, H. & HATA, Y. 2015. MAGI2/S-SCAM outside brain. *Journal of Biochemistry*, 157, 177-184.
- NAKAGAWA, S. & HUIBREGTSE, J. M. 2000. Human Scribble (Vartul) Is Targeted for Ubiquitin-Mediated Degradation by the High-Risk Papillomavirus E6 Proteins and the E6AP Ubiquitin-Protein Ligase. *Molecular and Cellular Biology*, 20, 8244-8253.
- NAKAJIMA, Y.-I., LEE, Z. T., MCKINNEY, S. A., SWANSON, S. K., FLORENS, L. & GIBSON, M. C. 2019. Junctional tumor suppressors interact with 14-3-3 proteins to control planar spindle alignment. *Journal of Cell Biology*, 218, 1824-1838.
- NAOI, Y., MIYOSHI, Y., TAGUCHI, T., KIM, S. J., ARAI, T., TAMAKI, Y. & NOGUCHI, S. 2007. Connexin26 expression is associated with lymphatic vessel invasion and poor prognosis in human breast cancer. *Breast Cancer Res Treat*, 106, 11-7.
- NARISAWA-SAITO, M. & KIYONO, T. 2007. Basic mechanisms of high-risk human papillomavirus-induced carcinogenesis: Roles of E6 and E7 proteins. *Cancer Science*, 98, 1505-1511.
- NAUS, C. C., ELISEVICH, K., ZHU, D., BELLIVEAU, D. J. & DEL MAESTRO, R. F. 1992. In vivo growth of C6 glioma cells transfected with connexin43 cDNA. *Cancer Res*, 52, 4208-13.
- NAUS, C. C. G., HEARN, S., ZHU, D., NICHOLSON, B. J. & SHIVERS, R. R. 1993. Ultrastructural Analysis of Gap Junctions in C6 Glioma Cells Transfected with Connexin43 cDNA. *Experimental Cell Research*, 206, 72-84.
- NGUYEN, M. L., NGUYEN, M. M., LEE, D., GRIEP, A. E. & LAMBERT, P. F. 2003. The PDZ Ligand Domain of the Human Papillomavirus Type 16 E6 Protein Is Required for E6's Induction of Epithelial Hyperplasia In Vivo. *Journal of Virology*, 77, 6957-6964.
- NGUYEN, T. N. & GOODRICH, J. A. 2006. Protein-protein interaction assays: eliminating false positive interactions. *Nature methods*, 3, 135-139.

- NICHOLSON, B. J. 2003. Gap junctions - from cell to molecule. *J Cell Sci*, 116, 4479-81.
- NICOLAS, J. F., JAKOB, H. & JACOB, F. 1978. Metabolic cooperation between mouse embryonal carcinoma cells and their differentiated derivatives. *Proc Natl Acad Sci U S A*, 75, 3292-6.
- NIELSEN, M. S., AXELSEN, L. N., SORGEN, P. L., VERMA, V., DELMAR, M. & HOLSTEIN-RATHLOU, N.-H. 2012a. Gap junctions. *Comprehensive Physiology*, 2, 1981-2035.
- NIELSEN, M. S., AXELSEN, L. N., SORGEN, P. L., VERMA, V., DELMAR, M. & HOLSTEIN-RATHLOU, N. H. 2012b. Gap junctions. *Compr Physiol*, 2, 1981-2035.
- NITHIANANTHARAJAH, J., KOMIYAMA, N. H., MCKECHANIE, A., JOHNSTONE, M., BLACKWOOD, D. H., CLAIR, D. S., EMES, R. D., VAN DE LAGEMAAT, L. N., SAKSIDA, L. M., BUSSEY, T. J. & GRANT, S. G. N. 2012. Synaptic scaffold evolution generated components of vertebrate cognitive complexity. *Nature Neuroscience*, 16, 16-24.
- NIX, S. L., CHISHTI, A. H., ANDERSON, J. M. & WALTHER, Z. 2000. hCASK and hDlg Associate in Epithelia, and Their Src Homology 3 and Guanylate Kinase Domains Participate in Both Intramolecular and Intermolecular Interactions\*. *Journal of Biological Chemistry*, 275, 41192-41200.
- NOOH, M. M., KALE, A. & BAHOUTH, S. W. 2019. Involvement of PDZ-SAP97 interactions in regulating AQP2 translocation in response to vasopressin in LLC-PK1 cells. *American Journal of Physiology-Renal Physiology*, 317, F375-F387.
- O'NEILL, A. K., GALLEGOS, L. L., JUSTILIEN, V., GARCIA, E. L., LEITGES, M., FIELDS, A. P., HALL, R. A. & NEWTON, A. C. 2011. Protein Kinase Ca Promotes Cell Migration through a PDZ-Dependent Interaction with its Novel Substrate Discs Large Homolog 1 (DLG1). *Journal of Biological Chemistry*, 286, 43559-43568.
- OH, S. T., KYO, S. & LAIMINS, L. A. 2001. Telomerase Activation by Human Papillomavirus Type 16 E6 Protein: Induction of Human Telomerase Reverse Transcriptase Expression through Myc and GC-Rich Sp1 Binding Sites. *Journal of Virology*, 75, 5559-5566.
- OLSEN, O. & BREDET, D. S. 2003. Functional Analysis of the Nucleotide Binding Domain of Membrane-associated Guanylate Kinases. *Journal of Biological Chemistry*, 278, 6873-6878.
- OSSWALD, M., JUNG, E., SAHM, F., SOLECKI, G., VENKATARAMANI, V., BLAES, J., WEIL, S., HORSTMANN, H., WIESTLER, B., SYED, M., HUANG, L., RATLIFF, M., KARIMIAN JAZI, K., KURZ, F. T., SCHMENGER, T., LEMKE, D., GOMMEL, M., PAULI, M., LIAO, Y., HARING, P., PUSCH, S., HERL, V., STEINHAUSER, C., KRUNIC, D., JARAHIAN, M., MILETIC, H., BERGHOFF, A. S., GRIESBECK, O., KALAMAKIS, G., GARASCHUK, O., PREUSSER, M., WEISS, S., LIU, H., HEILAND, S., PLATTEN, M., HUBER, P. E., KUNER, T., VON DEIMLING, A., WICK, W. & WINKLER, F. 2015. Brain tumour cells interconnect to a functional and resistant network. *Nature*, 528, 93-8.
- OYAMADA, M., OYAMADA, Y. & TAKAMATSU, T. 2005. Regulation of connexin expression. *Biochim Biophys Acta*, 1719, 6-23.
- OZAKI, T. & NAKAGAWARA, A. 2011. Role of p53 in Cell Death and Human Cancers. *Cancers*, 3, 994-1013.
- PAL, J. D., LIU, X., MACKAY, D., SHIELS, A., BERTHOUD, V. M., BEYER, E. C. & EBIHARA, L. 2000. Connexin46 mutations linked to congenital cataract show loss of gap junction channel function. *American Journal of Physiology-Cell Physiology*, 279, C596-C602.

- PALADINI, R. D., TAKAHASHI, K., BRAVO, N. S. & COULOMBE, P. A. 1996. Onset of re-epithelialization after skin injury correlates with a reorganization of keratin filaments in wound edge keratinocytes: defining a potential role for keratin 16. *The Journal of cell biology*, 132, 381-397.
- PALATINUS, J. A., RHETT, J. M. & GOURDIE, R. G. 2011. Enhanced PKCepsilon mediated phosphorylation of connexin43 at serine 368 by a carboxyl-terminal mimetic peptide is dependent on injury. *Channels (Austin)*, 5, 236-40.
- PALATINUS, J. A., RHETT, J. M. & GOURDIE, R. G. 2012. The connexin43 carboxyl terminus and cardiac gap junction organization. *Biochim Biophys Acta*, 1818, 1831-43.
- PALMER, T., WALLACE, L., POLLOCK, K. G., CUSCHIERI, K., ROBERTSON, C., KAVANAGH, K. & CRUICKSHANK, M. 2019. Prevalence of cervical disease at age 20 after immunisation with bivalent HPV vaccine at age 12-13 in Scotland: retrospective population study. *Bmj*, 365, l1161.
- PARK, D. J., FREITAS, T. A., WALLICK, C. J., GUYETTE, C. V. & WARN-CRAMER, B. J. 2006. Molecular dynamics and in vitro analysis of Connexin43: A new 14-3-3 mode-1 interacting protein. *Protein Science*, 15, 2344-2355.
- PARK, D. J., WALLICK, C. J., MARTYN, K. D., LAU, A. F., JIN, C. & WARN-CRAMER, B. J. 2009. Akt Phosphorylates Connexin43 on Ser373, a "Mode-1" Binding Site for 14-3-3. *Cell Communication & Adhesion*, 14, 211-226.
- PAYTON, B. W., BENNETT, M. V. & PAPPAS, G. D. 1969. Permeability and structure of junctional membranes at an electrotonic synapse. *Science*, 166, 1641-3.
- PAZNEKAS, W. A., BOYADJIEV, S. A., SHAPIRO, R. E., DANIELS, O., WOLLNIK, B., KEEGAN, C. E., INNIS, J. W., DINULOS, M. B., CHRISTIAN, C., HANNIBAL, M. C. & JABS, E. W. 2003. Connexin 43 (GJA1) Mutations Cause the Pleiotropic Phenotype of Oculodentodigital Dysplasia. *The American Journal of Human Genetics*, 72, 408-418.
- PENDINO, F., TARKANYI, I., DUDOGNON, C., HILLION, J., LANOTTE, M., ARADI, J. & SEGAL-BENDIRDJIAN, E. 2006. Telomeres and Telomerase: Pharmacological Targets for New Anticancer Strategies? *Current Cancer Drug Targets*, 6, 147-180.
- PHILLIPS, S. L., WILLIAMS, C. B., ZAMBRANO, J. N., WILLIAMS, C. J. & YEH, E. S. 2017. Connexin 43 in the development and progression of breast cancer: What's the connection? (Review). *Int J Oncol*, 51, 1005-1013.
- PIECHOCKI, M. P., BURK, R. D. & RUCH, R. J. 1999. Regulation of connexin32 and connexin43 gene expression by DNA methylation in rat liver cells. *Carcinogenesis*, 20, 401-406.
- PIETSCH, E. C. & MURPHY, M. E. 2014. Low risk HPV-E6 traps p53 in the cytoplasm and induces p53-dependent apoptosis. *Cancer Biology & Therapy*, 7, 1916-1918.
- PIM, D., THOMAS, M., JAVIER, R., GARDIOL, D. & BANKS, L. 2000. HPV E6 targeted degradation of the discs large protein: evidence for the involvement of a novel ubiquitin ligase. *Oncogene*, 19, 719-725.
- POL, S. B. V. & KLINGELHUTZ, A. J. 2013. Papillomavirus E6 oncoproteins. *Virology*, 445, 115-137.
- POLLMANN, M. A., SHAO, Q., LAIRD, D. W. & SANDIG, M. 2005. Connexin 43 mediated gap junctional communication enhances breast tumor cell diapedesis in culture. *Breast Cancer Res*, 7, R522-34.
- PONTING, C. P., PHILLIPS, C., DAVIES, K. E. & BLAKE, D. J. 1997. PDZ Domains: Targeting signalling molecules to sub-membranous sites. *BioEssays*, 19, 469-479.

- QIN, H., SHAO, Q., IGDOURA, S. A., ALAOUI-JAMALI, M. A. & LAIRD, D. W. 2003. Lysosomal and Proteasomal Degradation Play Distinct Roles in the Life Cycle of Cx43 in Gap Junctional Intercellular Communication-deficient and -competent Breast Tumor Cells. *Journal of Biological Chemistry*, 278, 30005-30014.
- QIU, C., COUTINHO, P., FRANK, S., FRANKE, S., LAW, L.-Y., MARTIN, P., GREEN, C. R. & BECKER, D. L. 2003. Targeting Connexin43 Expression Accelerates the Rate of Wound Repair. *Current Biology*, 13, 1697-1703.
- QU, C., GARDNER, P. & SCHRIJVER, I. 2009. The role of the cytoskeleton in the formation of gap junctions by Connexin 30. *Experimental Cell Research*, 315, 1683-1692.
- RAHMAN, S. & EVANS, W. H. 1991. Topography of connexin32 in rat liver gap junctions. Evidence for an intramolecular disulphide linkage connecting the two extracellular peptide loops. *Journal of Cell Science*, 100, 567-578.
- REAUME, A. G., DE SOUSA, P. A., KULKARNI, S., LANGILLE, B. L., ZHU, D., DAVIES, T. C., JUNEJA, S. C., KIDDER, G. M. & ROSSANT, J. 1995. Cardiac malformation in neonatal mice lacking connexin43. *Science*, 267, 1831-4.
- REUVER, S. M. & GARNER, C. C. 1998. E-cadherin mediated cell adhesion recruits SAP97 into the cortical cytoskeleton. *Journal of Cell Science*, 111, 1071-1080.
- REVEL, J. P. & KARNOVSKY, M. J. 1967. Hexagonal array of subunits in intercellular junctions of the mouse heart and liver. *J Cell Biol*, 33, C7-C12.
- RICHARD, G. 2003. Connexin gene pathology. *Clinical and Experimental Dermatology*, 28, 397-409.
- RICHARD, G., SMITH, L. E., BAILEY, R. A., ITIN, P., HOHL, D., EPSTEIN, E. H., DIGIOVANNA, J. J., COMPTON, J. G. & BALE, S. J. 1998. Mutations in the human connexin gene GJB3 cause erythrokeratoderma variabilis. *Nature Genetics*, 20, 366-369.
- RICHARDS, T. S., DUNN, C. A., CARTER, W. G., USUI, M. L., OLERUD, J. E. & LAMPE, P. D. 2004. Protein kinase C spatially and temporally regulates gap junctional communication during human wound repair via phosphorylation of connexin43 on serine368. *The Journal of cell biology*, 167, 555-562.
- RISEK, B. & GILULA, N. B. 1996. Gap Junction Regulation during Preterm Labor in the Rat: Multiple Effects of the Antiprogestone RU4861. *Biology of Reproduction*, 55, 525-535.
- ROBERTS, S., DELURY, C. & MARSH, E. 2012a. The PDZ protein discs-large (DLG): the 'Jekyll and Hyde' of the epithelial polarity proteins. *The FEBS Journal*, 279, 3549-3558.
- ROBERTS, S., DELURY, C. & MARSH, E. 2012b. The PDZ protein discs - large (DLG): the 'Jekyll and Hyde' of the epithelial polarity proteins. *FEBS Journal*, 279, 3549-3558.
- ROMAN, A. & MUNGER, K. 2013. The papillomavirus E7 proteins. *Virology*, 445, 138-168.
- SANCHEZ, O. F., RODRIGUEZ, A. V., VELASCO-ESPANA, J. M., MURILLO, L. C., SUTACHAN, J.-J. & ALBARRACIN, S.-L. 2020. Role of Connexins 30, 36, and 43 in Brain Tumors, Neurodegenerative Diseases, and Neuroprotection. *Cells*, 9, 846.
- SAEZ, J. C., BERTHOUD, V. M., BRANES, M. C., MARTINEZ, A. D. & BEYER, E. C. 2003. Plasma membrane channels formed by connexins: their regulation and functions. *Physiol Rev*, 83, 1359-400.

- SAHA, S. K., CHOI, H. Y., KIM, B. W., DAYEM, A. A., YANG, G. M., KIM, K. S., YIN, Y. F. & CHO, S. G. 2017. KRT19 directly interacts with B-catenin/RAC1 complex to regulate NUMB-dependent NOTCH signaling pathway and breast cancer properties. *Oncogene*, 36, 332-349.
- SAIDI BRIKCI-NIGASSA, A., CLEMENT, M. J., HA-DUONG, T., ADJADJ, E., ZIANI, L., PASTRE, D., CURMI, P. A. & SAVARIN, P. 2012. Phosphorylation controls the interaction of the connexin43 C-terminal domain with tubulin and microtubules. *Biochemistry*, 51, 4331-42.
- SAITO-KATSURAGI, M., ASADA, H., NIIZEKI, H., KATOH, F., MASUZAWA, M., TSUTSUMI, M., KUNIASU, H., ITO, A., NOJIMA, H. & MIYAGAWA, S. 2007. Role for connexin 26 in metastasis of human malignant melanoma: communication between melanoma and endothelial cells via connexin 26. *Cancer*, 110, 1162-72.
- SANFORD, J. L., MAYS, T. A. & RAFAEL-FORTNEY, J. A. 2004. CASK and Dlg form a PDZ protein complex at the mammalian neuromuscular junction. *Muscle & Nerve*, 30, 164-171.
- SARGIANNIDOU, I., VAVLITOU, N., ARISTODEMOU, S., HADJISAVVAS, A., KYRIACOU, K., SCHERER, S. S. & KLEOPA, K. A. 2009. Connexin32 mutations cause loss of function in Schwann cells and oligodendrocytes leading to PNS and CNS myelination defects. *J Neurosci*, 29, 4736-49.
- SCHUBERT, A.-L., SCHUBERT, W., SPRAY, D. C. & LISANTI, M. P. 2002. Connexin Family Members Target to Lipid Raft Domains and Interact with Caveolin-1†. *Biochemistry*, 41, 5754-5764.
- SCHWARZ, T. F., KOCKEN, M., PET J, T., EINSTEIN, M. H., SPACZYNSKI, M., LOUWERS, J. A., PEDERSEN, C., LEVIN, M., ZAHAF, T., PONCELET, S., HARDT, K., DESCAMPS, D. & DUBIN, G. 2010. Correlation between levels of human papillomavirus (HPV)-16 and 18 antibodies in serum and cervicovaginal secretions in girls and women vaccinated with the HPV-16/18 AS04-adjuvanted vaccine. *Hum Vaccin*, 6, 1054-61.
- SCOTT, CLAIRE A. & KELSELL, DAVID P. 2011. Key functions for gap junctions in skin and hearing. *Biochemical Journal*, 438, 245-254.
- SHAO, Q., WANG, H., MCLACHLAN, E., VEITCH, G. I. & LAIRD, D. W. 2005. Down-regulation of Cx43 by retroviral delivery of small interfering RNA promotes an aggressive breast cancer cell phenotype. *Cancer Res*, 65, 2705-11.
- SHAW, R. M., FAY, A. J., PUTHENVEEDU, M. A., VON ZASTROW, M., JAN, Y. N. & JAN, L. Y. 2007. Microtubule plus-end-tracking proteins target gap junctions directly from the cell interior to adherens junctions. *Cell*, 128, 547-60.
- SHAW, T. J. & MARTIN, P. 2009. Wound repair at a glance. *Journal of Cell Science*, 122, 3209-3213.
- SHENG, M., WEINBERG, R. J., COHEN, A. R., NAISBITT, S., KHARAZIA, V., YANG, F.-C. & HSUEH, Y.-P. 1998. Direct Interaction of CASK/LIN-2 and Syndecan Heparan Sulfate Proteoglycan and Their Overlapping Distribution in Neuronal Synapses. *Journal of Cell Biology*, 142, 139-151.
- SINGH, D. & LAMPE, P. D. 2003. Identification of connexin-43 interacting proteins. *Cell Commun Adhes*, 10, 215-20.
- SINGH, D. & LAMPE, P. D. 2009. Identification of Connexin-43 Interacting Proteins. *Cell Communication & Adhesion*, 10, 215-220.
- SIRNES, S., LIND, G. E., BRUUN, J., FYKERUD, T. A., MESNIL, M., LOTHE, R. A., RIVEDAL, E., KOLBERG, M. & LEITHE, E. 2015. Connexins in colorectal cancer pathogenesis. *Int J Cancer*, 137, 1-11.

- SJOSTRAND, F. S., ANDERSSON-CEDERGREN, E. & DEWEY, M. M. 1958. The ultrastructure of the intercalated discs of frog, mouse and guinea pig cardiac muscle. *J Ultrastruct Res*, 1, 271-87.
- SKERRETT, I. M., ARONOWITZ, J., SHIN, J. H., CYMES, G., KASPEREK, E., CAO, F. L. & NICHOLSON, B. J. 2002. Identification of amino acid residues lining the pore of a gap junction channel. *Journal of Cell Biology*, 159, 349-360.
- SMYTH, JAMES W. & SHAW, ROBIN M. 2013. Autoregulation of Connexin43 Gap Junction Formation by Internally Translated Isoforms. *Cell Reports*, 5, 611-618.
- SMYTH, J. W., ZHANG, S.-S., SANCHEZ, J. M., LAMOUILLE, S., VOGAN, J. M., HESKETH, G. G., HONG, T., TOMASELLI, G. F. & SHAW, R. M. 2014. A 14-3-3 Mode-1 Binding Motif Initiates Gap Junction Internalization During Acute Cardiac Ischemia. *Traffic*, 15, 684-699.
- SOLAN, JOELL L. & LAMPE, PAUL D. 2009. Connexin43 phosphorylation: structural changes and biological effects. *Biochemical Journal*, 419, 261-272.
- SOLAN, J. L. & LAMPE, P. D. 2014. Specific Cx43 phosphorylation events regulate gap junction turnover in vivo. *FEBS Letters*, 588, 1423-1429.
- SOLAN, J. L. & LAMPE, P. D. 2016. Kinase programs spatiotemporally regulate gap junction assembly and disassembly: Effects on wound repair. *Semin Cell Dev Biol*, 50, 40-8.
- SONGYANG, Z. 1997. Recognition of Unique Carboxyl-Terminal Motifs by Distinct PDZ Domains. *Science*, 275, 73-77.
- SORGEN, P. L., DUFFY, H. S., SAHOO, P., COOMBS, W., DELMAR, M. & SPRAY, D. C. 2004. Structural Changes in the Carboxyl Terminus of the Gap Junction Protein Connexin43 Indicates Signaling between Binding Domains for c-Src and Zonula Occludens-1. *Journal of Biological Chemistry*, 279, 54695-54701.
- SPAGNOL, G., KIEKEN, F., KOPANIC, J. L., LI, H., ZACH, S., STAUCH, K. L., GROSELY, R. & SORGEN, P. L. 2016. Structural Studies of the Nedd4 WW Domains and Their Selectivity for the Connexin43 (Cx43) Carboxyl Terminus. *J Biol Chem*, 291, 7637-50.
- SPAGNOL, G., TREASE, A. J., ZHENG, L., GUTIERREZ, M., BASU, I., SARMIENTO, C., MOORE, G., CERVANTES, M. & SORGEN, P. L. 2018. Connexin43 Carboxyl-Terminal Domain Directly Interacts with beta-Catenin. *Int J Mol Sci*, 19.
- SQUECCO, R., SASSOLI, C., NUTI, F., MARTINESI, M., CHELLINI, F., NOSI, D., ZECCHI-ORLANDINI, S., FRANCINI, F., FORMIGLI, L., MEACCI, E. & NUSRAT, A. 2006. Sphingosine 1-Phosphate Induces Myoblast Differentiation through Cx43 Protein Expression: A Role for a Gap Junction-dependent and -independent Function. *Molecular Biology of the Cell*, 17, 4896-4910.
- STAMOS, J. L. & WEIS, W. I. 2013. The  $\beta$ -catenin destruction complex. *Cold Spring Harb Perspect Biol*, 5, a007898.
- STANLEY, M. 2010. Pathology and epidemiology of HPV infection in females. *Gynecologic Oncology*, 117, S5-S10.
- STANLEY, M. A. 2012. Epithelial cell responses to infection with human papillomavirus. *Clinical microbiology reviews*, 25, 215-222.
- STAUCH, K., KIEKEN, F. & SORGEN, P. 2012. Characterization of the Structure and Intermolecular Interactions between the Connexin 32 Carboxyl-terminal Domain and the Protein Partners Synapse-associated Protein 97 and Calmodulin. *Journal of Biological Chemistry*, 287, 27771-27788.
- STEPHENS, R., LIM, K., PORTELA, M., KVANSAKUL, M., HUMBERT, P. O. & RICHARDSON, H. E. 2018. The Scribble Cell Polarity Module in the

- Regulation of Cell Signaling in Tissue Development and Tumorigenesis. *Journal of Molecular Biology*, 430, 3585-3612.
- STERGIOPOULOS, K., ALVARADO, J. L., MASTROIANNI, M., EK-VITORIN, J. F., TAFFET, S. M. & DELMAR, M. 1999. Hetero-Domain Interactions as a Mechanism for the Regulation of Connexin Channels. *Circulation Research*, 84, 1144-1155.
- STEVENSON, B. R., SILICIANO, J. D., MOOSEKER, M. S. & GOODENOUGH, D. A. 1986. Identification of ZO-1: a high molecular weight polypeptide associated with the tight junction (zonula occludens) in a variety of epithelia. *J Cell Biol*, 103, 755-66.
- STOLETOV, K., STRNADEL, J., ZARDOUZIAN, E., MOMIYAMA, M., PARK, F. D., KELBER, J. A., PIZZO, D. P., HOFFMAN, R., VANDENBERG, S. R. & KLEMKE, R. L. 2013. Role of connexins in metastatic breast cancer and melanoma brain colonization. *J Cell Sci*, 126, 904-13.
- SUBBAIAH, V. K., KRANJEC, C., THOMAS, M. & BANKS, L. 2011. PDZ domains: the building blocks regulating tumorigenesis. *Biochemical Journal*, 439, 195-205.
- SUBBAIAH, V. K., NARAYAN, N., MASSIMI, P. & BANKS, L. 2012. Regulation of the DLG tumor suppressor by  $\beta$ -catenin. *International Journal of Cancer*, 131, 2223-2233.
- SUGIHARA, T., NAKAGAWA, S., SASAJIMA, Y., ICHINOSE, T., HIRAIKE, H., KONDO, F., UOZAKI, H., FUKUSATO, T. & AYABE, T. 2016. Loss of the cell polarity determinant human Discs-large is a novel molecular marker of nodal involvement and poor prognosis in endometrial cancer. *British Journal of Cancer*, 114, 1012-1018.
- SULLIVAN, R., RUANGVORAVAT, C., JOO, D., MORGAN, J., WANG, B. L., WANG, X. K. & LO, C. W. 1993. Structure, sequence and expression of the mouse Cx43 gene encoding connexin 43. *Gene*, 130, 191-9.
- SUN, P., DONG, L., MACDONALD, A., AKBARI, S., EDWARD, M., HODGINS, M., JOHNSTONE, S. & GRAHAM, S. 2015. HPV16 E6 Controls the Gap Junction Protein Cx43 in Cervical Tumour Cells. *Viruses*, 7, 5243-5256.
- SUNDARAM, G. M., QUAH, S. & SAMPATH, P. 2018. Cancer: the dark side of wound healing. *The FEBS Journal*, 285, 4516-4534.
- SUTCLIFFE, J. E., CHIN, K. Y., THRASIVOULOU, C., SERENA, T. E., O'NEIL, S., HU, R., WHITE, A. M., MADDEN, L., RICHARDS, T., PHILLIPS, A. R. & BECKER, D. L. 2015. Abnormal connexin expression in human chronic wounds. *Br J Dermatol*, 173, 1205-15.
- SUZUKI, T., OHSUGI, Y., UCHIDA-TOITA, M., AKIYAMA, T. & YOSHIDA, M. 1999. Tax oncoprotein of HTLV-1 binds to the human homologue of Drosophila discs large tumor suppressor protein, hDLG, and perturbs its function in cell growth control. *Oncogene*, 18, 5967-5972.
- TALHOUK, R. S., FARES, M.-B., RAHME, G. J., HARIRI, H. H., RAYESS, T., DBOUK, H. A., BAZZOUN, D., AL-LABBAN, D. & EL-SABBAN, M. E. 2013. Context dependent reversion of tumor phenotype by connexin-43 expression in MDA-MB231 cells and MCF-7 cells: Role of  $\beta$ -catenin/connexin43 association. *Experimental Cell Research*, 319, 3065-3080.
- TEMME, A., BUCHMANN, A., GABRIEL, H. D., NELLES, E., SCHWARZ, M. & WILLECKE, K. 1997. High incidence of spontaneous and chemically induced liver tumors in mice deficient for connexin32. *Curr Biol*, 7, 713-6.
- TH VENIN, A. F., MARGRAF, R. A., FISHER, C. G., KELLS-ANDREWS, R. M., FALK, M. M. & YAP, A. 2017. Phosphorylation regulates connexin43/ZO-1 binding and release, an important step in gap junction turnover. *Molecular Biology of the Cell*, 28, 3595-3608.

- THEISS, C. 2002. Microinjected Anti-actin Antibodies Decrease Gap Junctional Intercellular Communication in Cultured Astrocytes. *Experimental Cell Research*, 281, 197-204.
- THOMAS, M., MASSIMI, P., NAVARRO, C., BORG, J.-P. & BANKS, L. 2005. The hScrib/Dlg apico-basal control complex is differentially targeted by HPV-16 and HPV-18 E6 proteins. *Oncogene*, 24, 6222-6230.
- THOMAS, M., NARAYAN, N., PIM, D., TOMAIĆ, V., MASSIMI, P., NAGASAKA, K., KRANJEC, C., GAMMOH, N. & BANKS, L. 2008. Human papillomaviruses, cervical cancer and cell polarity. *Oncogene*, 27, 7018-7030.
- THOMAS, T., JORDAN, K. & LAIRD, D. W. 2001. Role of Cytoskeletal Elements in the Recruitment of Cx43-GFP and Cx26-YFP into Gap Junctions. *Cell Communication & Adhesion*, 8, 231-236.
- THOMAS, U., PHANNAVONG, B., MILLER, B., GARNER, C. C. & GUNDELFINGER, E. D. 1997. Functional expression of rat synapse-associated proteins SAP97 and SAP102 in *Drosophila* dlg-1 mutants: effects on tumor suppression and synaptic bouton structure. *Mechanisms of Development*, 62, 161-174.
- TJ, K., LH, F., AD, H., KA, S., WA, S. & JS, B. 2000. Reduced levels of connexin43 in cervical dysplasia: inducible expression in a cervical carcinoma cell line decreases neoplastic potential with implications for tumor progression. *Carcinogenesis*, 21, 1097-1099.
- TOROK, K., STAUFFER, K. & EVANS, W. H. 1997. Connexin 32 of gap junctions contains two cytoplasmic calmodulin-binding domains. *Biochem J*, 326 ( Pt 2), 479-83.
- TOTLAND, M. Z., BERGSLAND, C. H., FYKERUD, T. A., KNUDSEN, L. M., RASMUSSEN, N. L., EIDE, P. W., YOHANNES, Z., S RENSEN, V., BRECH, A., LOTHE, R. A. & LEITHE, E. 2017. The E3 ubiquitin ligase NEDD4 induces endocytosis and lysosomal sorting of connexin 43 to promote loss of gap junctions. *Journal of Cell Science*, 130, 2867-2882.
- TOYOFUKU, T., AKAMATSU, Y., ZHANG, H., KUZUYA, T., TADA, M. & HORI, M. 2001. c-Src Regulates the Interaction between Connexin-43 and ZO-1 in Cardiac Myocytes. *Journal of Biological Chemistry*, 276, 1780-1788.
- TOYOFUKU, T., YABUKI, M., OTSU, K., KUZUYA, T., HORI, M. & TADA, M. 1998. Direct association of the gap junction protein connexin-43 with ZO-1 in cardiac myocytes. *J Biol Chem*, 273, 12725-31.
- VALIENTE, M., ANDRÉS-PONS, A., GOMAR, B., TORRES, J., GIL, A., TAPPAREL, C., ANTONARAKIS, S. E. & PULIDO, R. 2005. Binding of PTEN to Specific PDZ Domains Contributes to PTEN Protein Stability and Phosphorylation by Microtubule-associated Serine/Threonine Kinases. *Journal of Biological Chemistry*, 280, 28936-28943.
- VAN DOORSLAER, K. 2013. Evolution of the Papillomaviridae. *Virology*, 445, 11-20.
- VAN ITALLIE, C. M. & ANDERSON, J. M. 2014. Architecture of tight junctions and principles of molecular composition. *Semin Cell Dev Biol*, 36, 157-65.
- VAN DOORSLAER, K., LI, Z., XIRASAGAR, S., MAES, P., KAMINSKY, D., LIOU, D., SUN, Q., KAUR, R., HUYEN, Y. & MCBRIDE, A. A. 2017. The Papillomavirus Episteme: a major update to the papillomavirus sequence database. *Nucleic Acids Research*, 45, D499-D506.
- VANDERPUYE, O. A., BELL, C. L. & MURRAY, S. A. 2016. Redistribution of connexin 43 during cell division. *Cell Biology International*, 40, 387-396.
- VANSLYKE, J. K., NAUS, C. C., MUSIL, L. S. & BRODSKY, J. L. 2009. Conformational Maturation and Post-ER Multisubunit Assembly of Gap Junction Proteins. *Molecular Biology of the Cell*, 20, 2451-2463.

- VELDMAN, T., LIU, X., YUAN, H. & SCHLEGEL, R. 2003. Human papillomavirus E6 and Myc proteins associate in vivo and bind to and cooperatively activate the telomerase reverse transcriptase promoter. *Proceedings of the National Academy of Sciences*, 100, 8211-8216.
- VINKEN, M., VANHAECKE, T., PAPELEU, P., SNYKERS, S., HENKENS, T. & ROGIERS, V. 2006. Connexins and their channels in cell growth and cell death. *Cell Signal*, 18, 592-600.
- WALCH, L. 2013. Emerging role of the scaffolding protein Dlg1 in vesicle trafficking. *Traffic*, 14, 964-73.
- WANG, Q., SONG, R., ZHAO, C., LIU, H., YANG, Y., GU, S., FENG, D. & HE, J. 2018. HPV16 E6 promotes cervical cancer cell migration and invasion by downregulation of NHERF1. *International Journal of Cancer*, 144, 1619-1632.
- WANG, R., PAN, W., JIN, L., HUANG, W., LI, Y., WU, D., GAO, C., MA, D. & LIAO, S. 2020. Human papillomavirus vaccine against cervical cancer: Opportunity and challenge. *Cancer Lett*, 471, 88-102.
- WANG, Y. & YIN, F. 2016. A Review of X-linked Charcot-Marie-Tooth Disease. *J Child Neurol*, 31, 761-72.
- WATSON, R. A. 2002. Changes in expression of the human homologue of the Drosophila discs large tumour suppressor protein in high-grade premalignant cervical neoplasias. *Carcinogenesis*, 23, 1791-1796.
- WAYAKANON, P., BHATTACHARJEE, R., NAKAHAMA, K.-I. & MORITA, I. 2012. The role of the Cx43 C-terminus in GJ plaque formation and internalization. *Biochemical and Biophysical Research Communications*, 420, 456-461.
- WERNER, S., KRIEG, T. & SMOLA, H. 2007. Keratinocyte-fibroblast interactions in wound healing. *J Invest Dermatol*, 127, 998-1008.
- WOJCIK, S. M., BUNDMAN, D. S. & ROOP, D. R. 2000. Delayed wound healing in keratin 6a knockout mice. *Molecular and cellular biology*, 20, 5248-5255.
- WOODS, D. F. & BRYANT, P. J. 1993. Apical junctions and cell signalling in epithelia. *Journal of Cell Science*, 1993, 171-181.
- WOODS, D. F., HOUGH, C., PEEL, D., CALLAINI, G. & BRYANT, P. J. 1996a. Dlg protein is required for junction structure, cell polarity, and proliferation control in Drosophila epithelia. *The Journal of Cell Biology*, 134, 1469-1482.
- WOODS, D. F., HOUGH, C., PEEL, D., CALLAINI, G. & BRYANT, P. J. 1996b. Dlg protein is required for junction structure, cell polarity, and proliferation control in Drosophila epithelia. *Journal of Cell Biology*, 134, 1469-1482.
- WRIGHT, C. S., VAN STEENSEL, M. A. M., HODGINS, M. B. & MARTIN, P. E. M. 2009. Connexin mimetic peptides improve cell migration rates of human epidermal keratinocytes and dermal fibroblasts in vitro. *Wound Repair and Regeneration*, 17, 240-249.
- WU, H., REUVER, S. M., KUHLENDahl, S., CHUNG, W. J. & GARNER, C. C. 1998. Subcellular targeting and cytoskeletal attachment of SAP97 to the epithelial lateral membrane. *Journal of Cell Science*, 111, 2365-2376.
- XIAO, Y., LIN, V. Y., KE, S., LIN, G. E., LIN, F.-T. & LIN, W.-C. 2014. 14-3-3 $\tau$  promotes breast cancer invasion and metastasis by inhibiting RhoGDI $\alpha$ . *Molecular and cellular biology*, 34, 2635-2649.
- XU, J. & NICHOLSON, B. J. 2013. The role of connexins in ear and skin physiology – Functional insights from disease-associated mutations. *Biochimica et Biophysica Acta (BBA) - Biomembranes*, 1828, 167-178.
- YANG, C.-M., JI, S., LI, Y., FU, L.-Y., JIANG, T. & MENG, F.-D. 2017. B-Catenin promotes cell proliferation, migration, and invasion but induces apoptosis in renal cell carcinoma. *Oncotargets and therapy*, 10, 711-724.

- YE, F., ZENG, M. & ZHANG, M. 2018. Mechanisms of MAGUK-mediated cellular junctional complex organization. *Curr Opin Struct Biol*, 48, 6-15.
- YOON, S. & LEUBE, RUDOLF E. 2019. Keratin intermediate filaments: intermediaries of epithelial cell migration. *Essays in Biochemistry*, 63, 521-533.
- YOTTI, L. P., CHANG, C. C. & TROSKO, J. E. 1979. Elimination of metabolic cooperation in Chinese hamster cells by a tumor promoter. *Science*, 206, 1089-91.
- YU, J., BERGA, S. L., ZOU, W., SUN, H. Y., JOHNSTON-MACANANNY, E., YALCINKAYA, T., SIDELL, N., BAGCHI, I. C., BAGCHI, M. K. & TAYLOR, R. N. 2014. Gap junction blockade induces apoptosis in human endometrial stromal cells. *Mol Reprod Dev*, 81, 666-75.
- YUM, S. W., KLEOPA, K. A., SHUMAS, S. & SCHERER, S. S. 2002. Diverse Trafficking Abnormalities of Connexin32 Mutants Causing CMTX. *Neurobiology of Disease*, 11, 43-52.
- ZHANG, J. T., CHEN, M., FOOTE, C. I. & NICHOLSON, B. J. 1996. Membrane integration of in vitro-translated gap junctional proteins: co- and post-translational mechanisms. *Mol Biol Cell*, 7, 471-82.
- ZHOU, Y., YANG, W., LURTZ, M. M., YE, Y., HUANG, Y., LEE, H. W., CHEN, Y., LOUIS, C. F. & YANG, J. J. 2007. Identification of the calmodulin binding domain of connexin 43. *J Biol Chem*, 282, 35005-17.
- ZHU, D., CAVENEY, S., KIDDER, G. M. & NAUS, C. C. 1991. Transfection of C6 glioma cells with connexin 43 cDNA: analysis of expression, intercellular coupling, and cell proliferation. *Proc Natl Acad Sci U S A*, 88, 1883-7.
- ZHU, J., SHANG, Y., XIA, C., WANG, W., WEN, W. & ZHANG, M. 2011. Guanylate kinase domains of the MAGUK family scaffold proteins as specific phospho-protein-binding modules. *The EMBO Journal*, 30, 4986-4997.
- ZUR HAUSEN, H., GISSMANN, L., STEINER, W., DIPPOLD, W. & DREGER, I. 1976. Human Papilloma Viruses and Cancer1. 43, 569-571.